Atlas of Lymphatic Anatomy in the Head, Neck, Chest and Limbs

Wei-Ren Pan

PEOPLE'S MEDICAL PUBLISHING HOUSE

Springer

Atlas of Lymphatic Anatomy in the Head, Neck, Chest and Limbs

Wei-Ren Pan

Atlas of Lymphatic Anatomy in the Head, Neck, Chest and Limbs

PEOPLE'S MEDICAL PUBLISHING HOUSE

Springer

Wei-Ren Pan
Department of Anatomy
Xuzhou Medical College
Xuzhou
Jiangsu
China

ISBN 978-981-10-3748-1 ISBN 978-981-10-3749-8 (eBook)
DOI 10.1007/978-981-10-3749-8

Library of Congress Control Number: 2017936661

Printed on acid-free paper

This Springer imprint is published by Springer Nature
The registered company is Springer Nature Singapore Pte Ltd.
The registered company address is: 152 Beach Road, #21-01/04 Gateway East, Singapore 189721, Singapore

Acknowledgements

The experimental work was done in the Department of Anatomy, Xuzhou Medical College, China, and the Reconstructive Plastic Surgery Research Unit, Department of Anatomy and Cell Biology, Melbourne University, Australia. I hereby acknowledge with thanks to everyone who provided support and premises for this book.

I would like to acknowledge with thanks to National Natural Science Foundation of China (NSFC Founding No: 31671253) and National Health and Medical Research Council, Australia (NHMRC Founding No: 350222; 566549), Xuzhou Medical University President Special Fund (No: 53051116) and the foreign experts special fund of Department of International Cooperation and Exchange (No: 537101) for their supporting.

I would like to express a special thanks to Professor G. I. Taylor AO, Professor H. Suami, Doctor S. Dhar, colleagues and friends for their support, collaboration and encouragement.

Finally, I wish to thank my wife, Cherry Hao Chen, and my son, Philip Chen, for their unconditional support, which allowed me to achieve my professional dreams. I dedicate this book to them.

Xuzhou, Jiangsu, China Wei-Ren Pan

Contents

Chapter 1
Components of the Lymphatic System

The lymphatic system consists of the lymphatic vessels (capillary plexus, precollecting and collecting lymph vessels including lymphatic ampullae and diverticulum and lymphatic trunks and ducts), organs (lymph nodes, spleen, thymus and tonsils), tissue (Peyer's patch), etc. Relevant terminology regarding the components of the lymphatic system and newly discovered structures is listed and described in this chapter (Figs. 1.1 and 1.2).

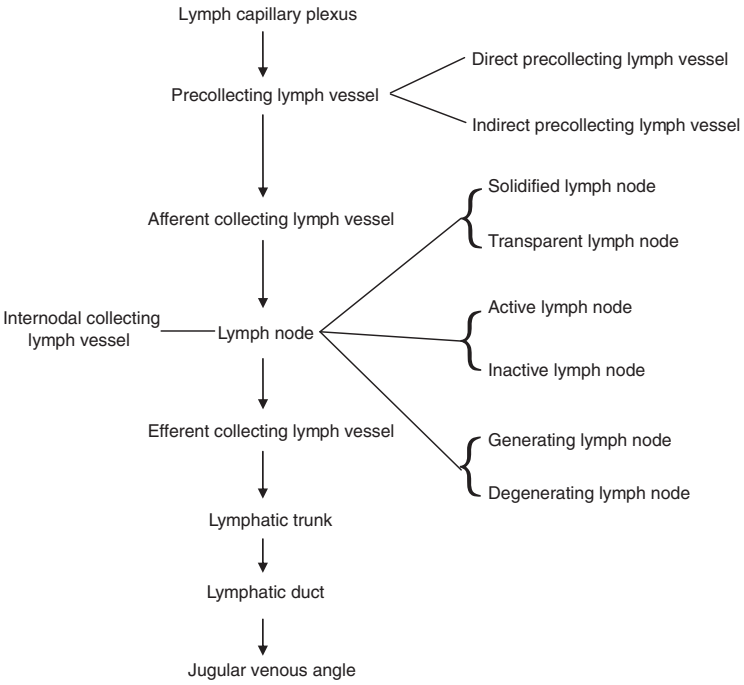

Fig. 1.1 Components and reflux of the lymphatic pathway

W.-R. Pan, *Atlas of Lymphatic Anatomy in the Head, Neck, Chest and Limbs*,
DOI 10.1007/978-981-10-3749-8_1

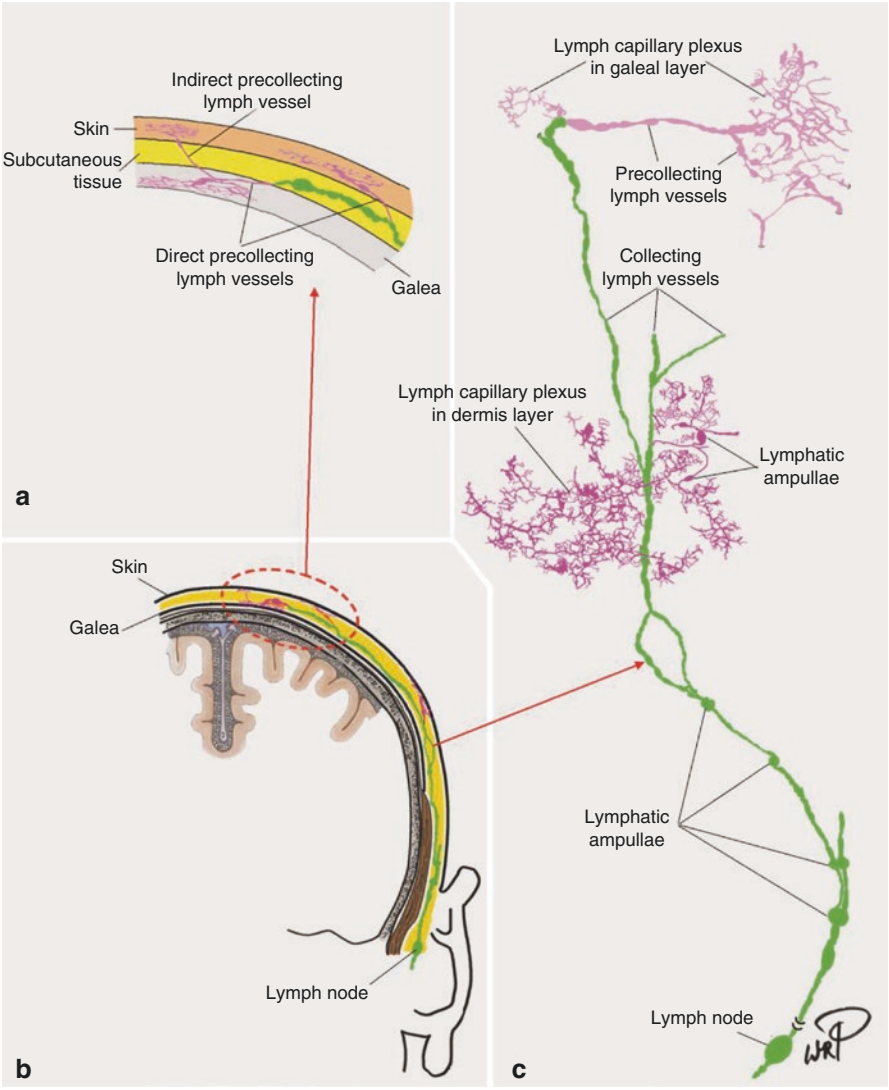

Fig. 1.2 A sketch map of the basic lymphatic pathway in the scalp. (**a**) Lymph capillary plexus originates from both the dermis and galeal layer to unite a precollecting lymph vessel that runs either directly or indirectly for a short distance before entering a collecting vessel in the subcutaneous tissue. (**b**) The basic lymphatic pathway in the scalp. (**c**) A magnified view of the basic lymphatic pathway in the scalp, showing the relationship among the lymph capillary plexus, precollecting and collecting lymph vessels, lymphatic ampullae, and lymph nodes

1 Lymph Capillary Plexus

Originating with the blind ends, two layers of the lymph capillaries have been observed, one on shallow and one on deeper parts in the dermis (Fig. 1.3) and mucosa (Fig. 2.64). They are connected to form a three-dimensional network – the lymph capillary plexus. They are also named as the initial lymphatics in some literatures (Földi et al. 2003; Shayan et al.2006).

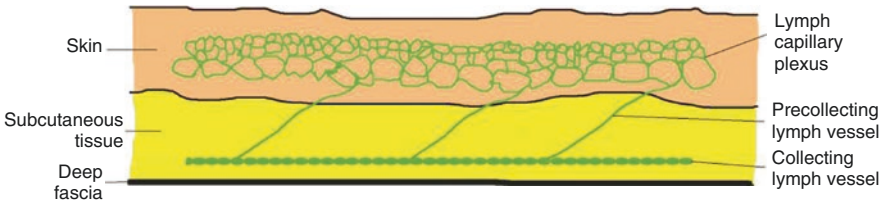

Fig. 1.3 A schematic diagram of connections among the capillary lymphatic plexus and precollecting and collecting lymphatic vessels in the skin

2 Precollecting Lymph Vessel

Precollecting lymph vessels connect the lymph capillary plexus and collecting lymph vessels. They arise from the deep side of the dermis, mucosal and the galeal layer, etc., travel from the superficial to deeper layer of the subcutaneous tissue in different directions and then drain to the collecting lymph vessels (Figs. 1.2 and 1.3).

In the scalp, two types of precollecting pathways were found, "direct" and "indirect" (or bridge) precollecting lymph vessels. The former arose from the lymph capillary plexus in the dermis or galea and directly drained to the collecting lymph vessel in the subcutaneous tissue. The latter arose from the lymph capillary plexus in the dermis and crossed the subcutaneous tissue, bypassed collecting vessels to reach the galeal layer when merging with the other precollecting lymph vessels and then travelled to the subcutaneous tissue again to link the collecting lymph vessel, which communicate the lymphatic drainage between the dermis and the galeal layer in the scalp (Fig. 1.2).

3 Collecting Lymph Vessel

With numerous valves in the lumen, collecting lymph vessels were seen to connect precollecting lymph vessels and lymphatic trunks, running tortuously in the subcutaneous and submucosal tissues. During their centripetal courses, vessels branched or diverged, converged and sometimes anastomosed with or crossed over neighbouring vessels (Figs. 1.1 and 1.2). Vessels were known as the afferent, the internodal and the efferent lymph vessels according to their relation with lymph nodes (Figs. 1.4 and 1.5):

1. The afferent collecting lymph vessels carry lymph into the lymph node.
2. The efferent collecting lymph vessels drain lymph away from the lymph node.
3. The internodal collecting lymph vessels can be the efferent vessel of the distal node or the afferent vessel of the proximal node.

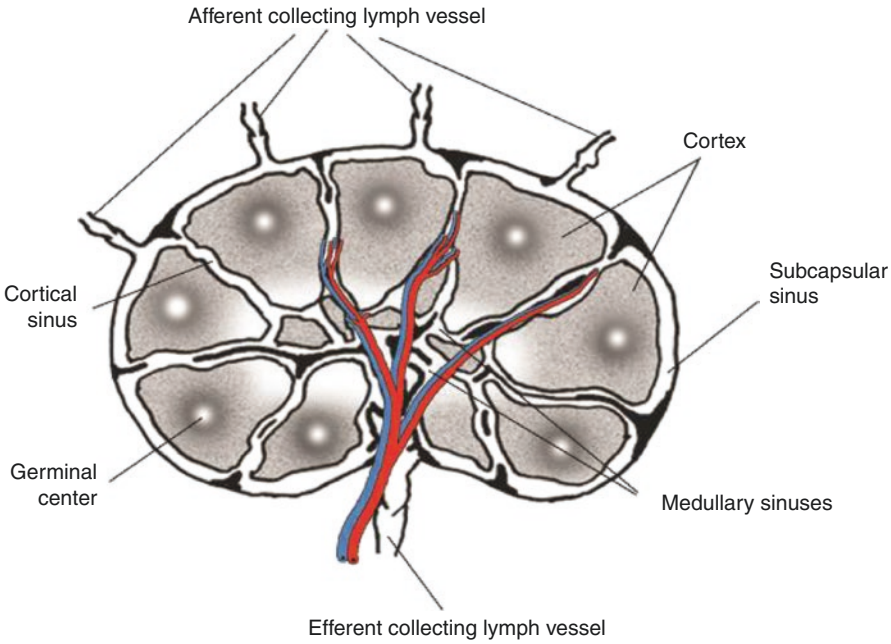

Fig. 1.4 A schematic diagram of relationship between collecting lymphatic vessels and the lymph node

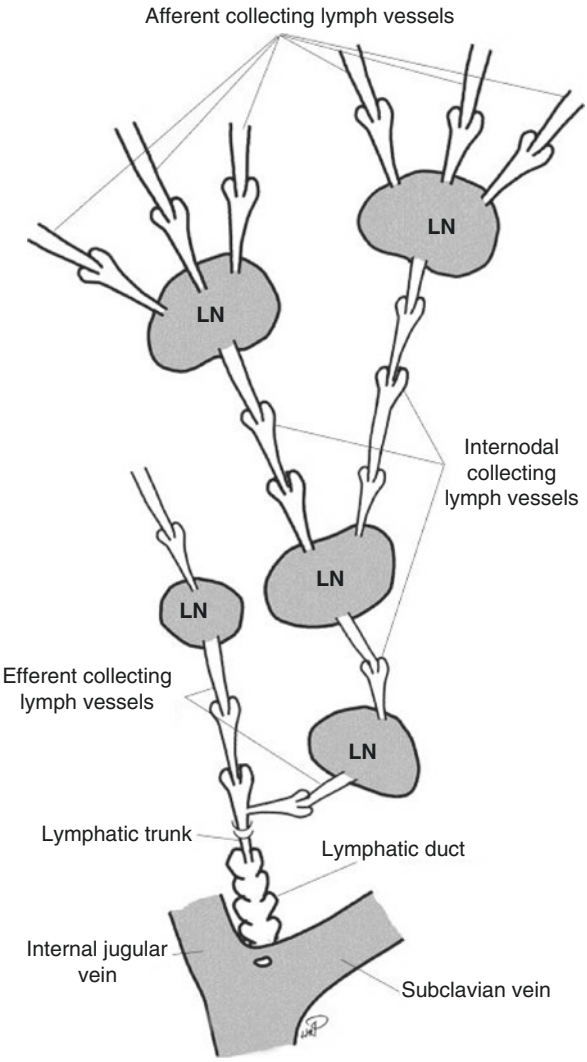

Fig. 1.5 A schematic diagram of relationship among collecting lymphatic vessels, the lymph node and the vein

4 Lymph Node

According to the morphological structure and function of lymph nodes, they can be classified into different types (Figs. 1.4 and 1.6). Details will be explained in Sect. 8 of Chap. 2.

1. The solidified lymph node: The node has a solid three-dimensional nature in different sizes and shapes. Usually it can be seen with the naked eye and often palpable.
2. The transparent lymph node: The node has a transparent nature in many different sizes and shapes. It can be seen under a microscope using hydrogen peroxide and/or after radiopaque/dye injection.
3. The active lymph node: The node contains lymphoid tissue and still provides full or partial function.
4. The inactive lymph node: The lymph node contains no lymphoid tissue and has lost its functions. It is also known as a degenerated lymph node.
5. The generating lymph node: This lymph node is a node in any generating stage.
6. The degenerating lymph node: This lymph node is a node in any degenerating stage.

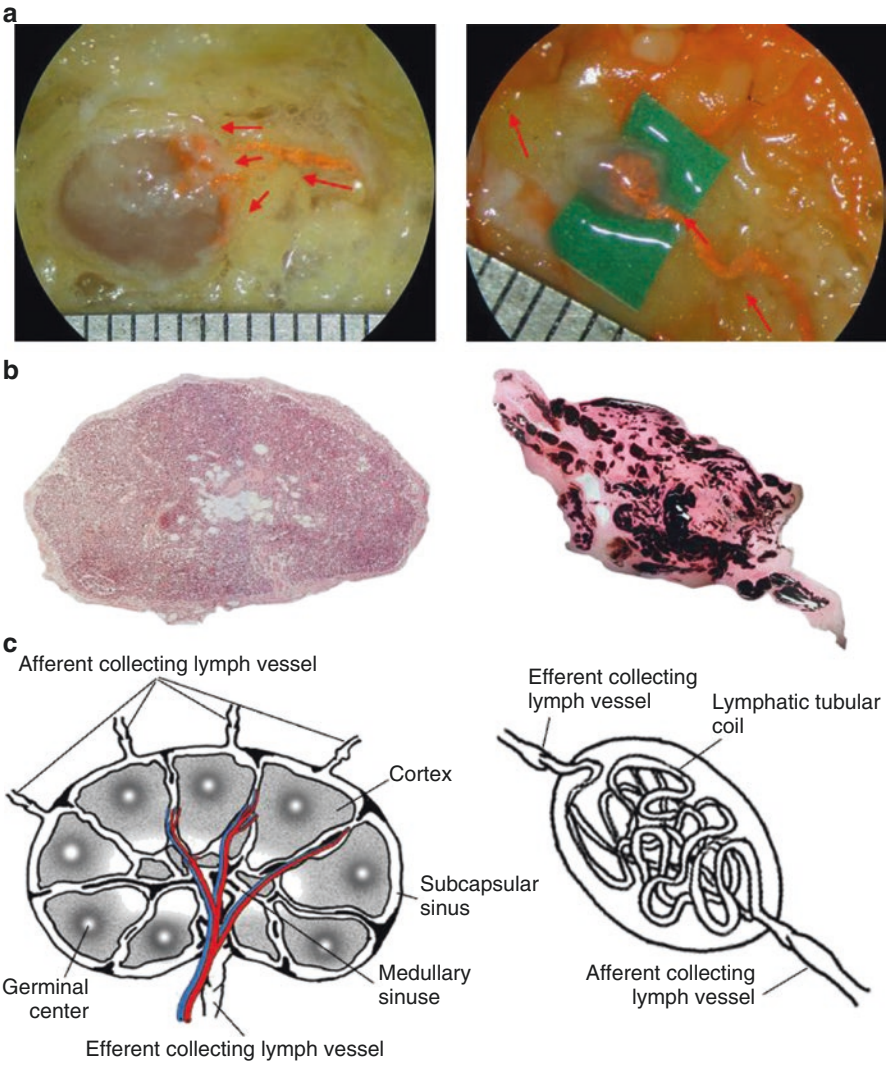

Fig. 1.6 Comparison chart of the solidified and the transparent lymph node. (**a**) Appearance of lymph nodes; (**b**) histological sections (H&E staining); (**c**) schematic structure of the lymph nodes

5 Lymphatic Trunk

Derived from the efferent collecting lymph vessels, the lymphatic trunks link to the lymphatic ducts (the right lymphatic duct and the thoracic duct) (Fig. 1.5).

6 Lymphatic Duct

Lymphatic ducts are the largest lymph vessels. The thoracic duct links to the vein in the left jugular venous angle while the right lymphatic duct to the right jugular venous angle (Fig. 1.5).

Chapter 2
Components and Morphology of the Lymphatic System

1 Lymphatic Valves

Since lymphatic vessels in the mesentery of the postprandial dog were originally discovered by Aselli(1627), the lymphatic valves were identified and their morphology and function were described by Ruysch (1665) and Lord (1967).

An existence of abundant lymphatic valves in most lymphatic vessels was confirmed by Cruikshank (1786), Mascagni (1787), Cooper (1840), and Sappey (1874) et al., prior to the discovery of X-rays in 1895 using a mercury injection, which was then recorded by a series of drawings.

After a new technique was established (Suami et al. 2005a), lymphatic valves could be observed under a surgical microscopy in human cadaver tissue and recorded by photographs and radiographs (Pan et al. 2010a, b and c).

1.1 Structure of Valves

The size of paired valves varied according to the calibre of the vessels, small in precollecting lymph vessels and large in lymphatic ducts. Each vessel segment (inter-valvular section) between valves formed a peanut-like fragment, the cusp (valves) of the distal side of the fragment inserted and opened into the blunt end of the proximal side of the segment, which formed a constrictive ring on the vessel wall (Fig. 2.1).

W.-R. Pan, *Atlas of Lymphatic Anatomy in the Head, Neck, Chest and Limbs*,
DOI 10.1007/978-981-10-3749-8_2

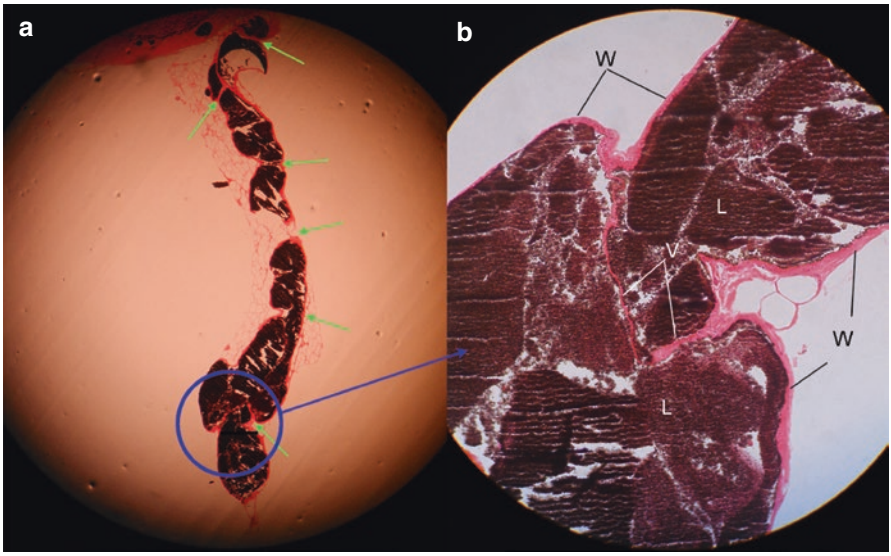

Fig. 2.1 (**a**) A longitudinal section of an afferent lymph vessel filled with lead oxide mixture showing the inner structure of the vessel. (**b**) The structures in the *blue-circled area* have been magnified showing the vessel walls (*W*) and valves (*V*) and the lumen of the vessel filled by lead oxide mixture (*L*). *Green arrows* indicate valves

1.2 Appearance of Valves

Multiple valves were present in the lumen of the precollecting and collecting lymph vessels, lymphatic trunks and lymphatic ducts. There were numerous valves in lymph-collecting vessels and trunks and sparse in lymph-precollecting vessels. Vessels looked like a string of beads or a bamboo trunk (Figs. 2.2, 2.3, 2.4, 2.5, 2.6, 2.7 and 2.8) depending on the ratio between the diameter of vessels and the interval length of the vessel in valves. Valves occurred at intervals averaging 2 mm (ranging from 1 to 3 mm) in the collecting lymph vessels and the lymphatic trunks. The diameter of the collecting lymph vessels averaged 0.2 mm (Figs. 2.2 and 2.4). The ratio of the diameter of the vessel and the interval length of valves is ≤0.1. Thus, most collecting lymph vessels resembled bamboo trunks (Fig. 2.7a, c). The diameter of the lymphatic trunks averaged 2 mm (Fig. 2.6). The ratio of the diameter of the vessels and the interval length of valves is ≥1; therefore, most lymphatic trunks look like a string of beads (Fig. 2.7b, d).

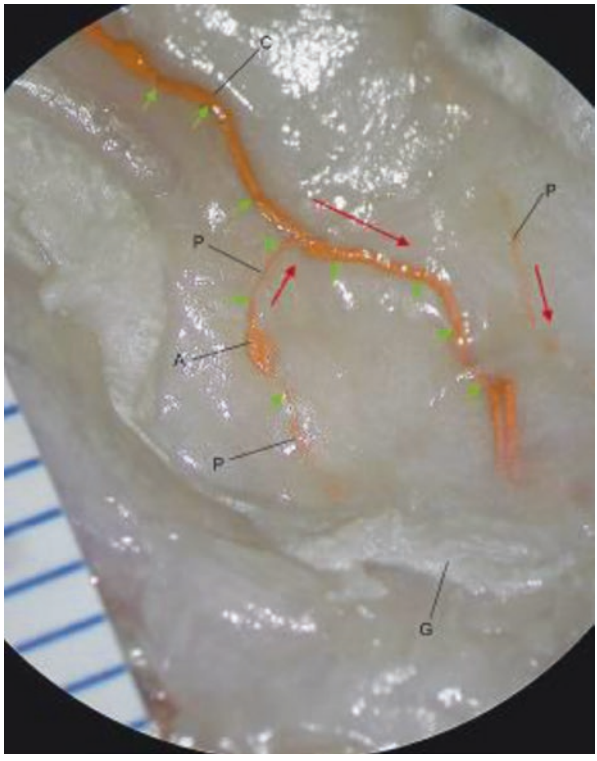

Fig. 2.2 An image showing precollecting (*P*) and collecting (*C*) lymph vessels filled with lead oxide mixture lying in the galea layer (*G*) of the parietal region. *Green arrows* indicate valves and *red arrows* indicate the direction of lymph flow. A single small ampulla (*A*) was presented

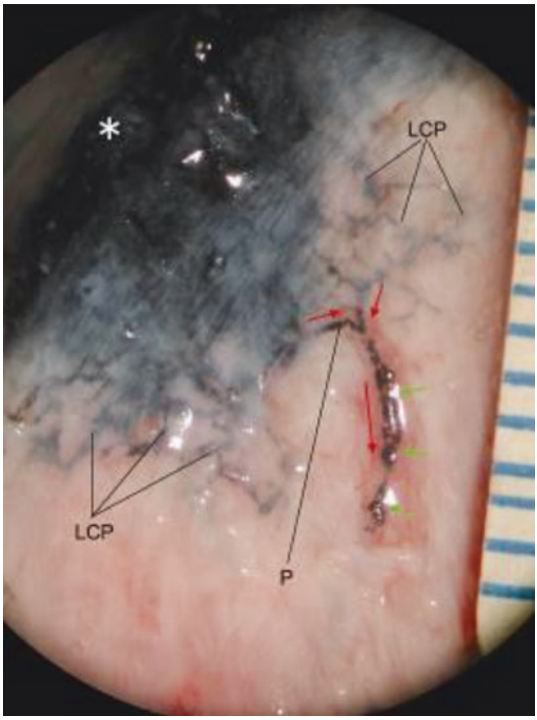

Fig. 2.3 An image showing the lymphatic capillary plexus (*LCP*) and precollecting lymph vessels (*P*) filled with India ink mixture lying in the galea layer of the occipital region. *Green arrows* indicate valves and *red arrows* indicate the direction of lymph flow

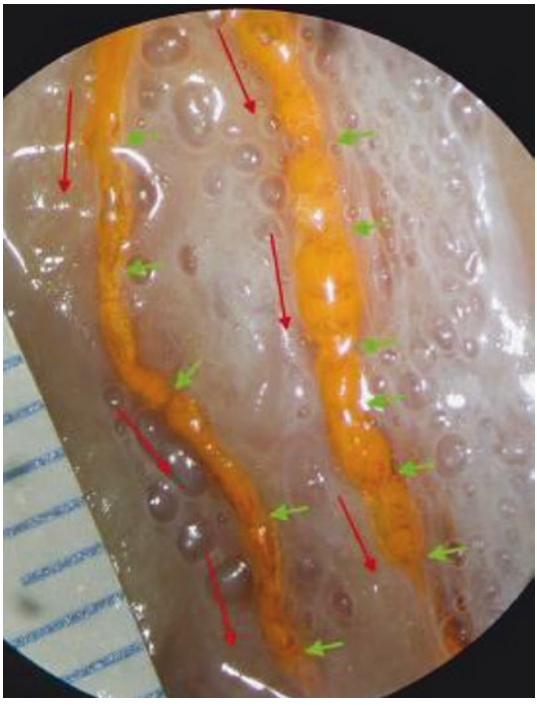

Fig. 2.4 Two collecting lymph vessels filled with lead oxide mixture in the preauricular area, different calibre and valves indicated by *green arrows*. *Red arrows* indicate the direction of lymph flow

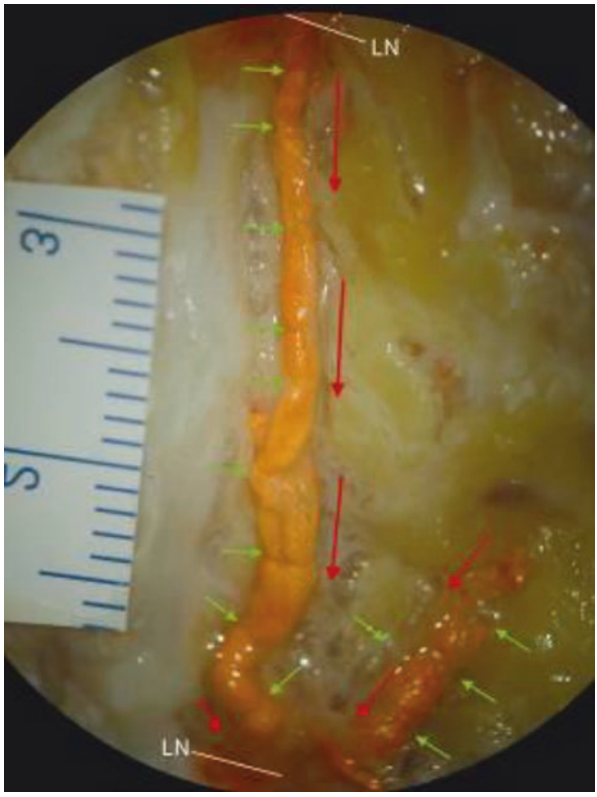

Fig. 2.5 An internodal vessels filled with lead oxide mixture showing their calibre, number of valves (indicated by *green arrows*) and appearance. *Red arrows* indicate the direction of lymph flow. *LN* lymph node

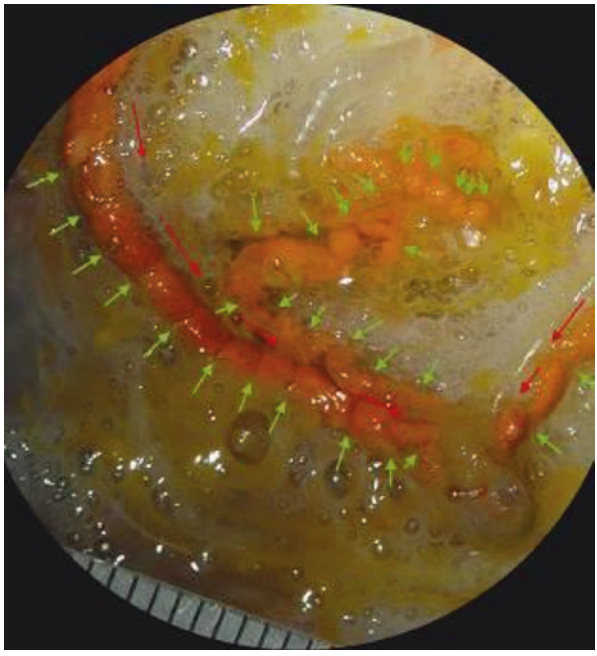

Fig. 2.6 Lymphatic trunks in the supraclavicular region filled with lead oxide mixture showing calibre, valves and appearance. Valves were so numerous that this specimen resembled a "string of beads". *Green arrows* indicate valves and *red arrows* indicate the direction of lymph flow

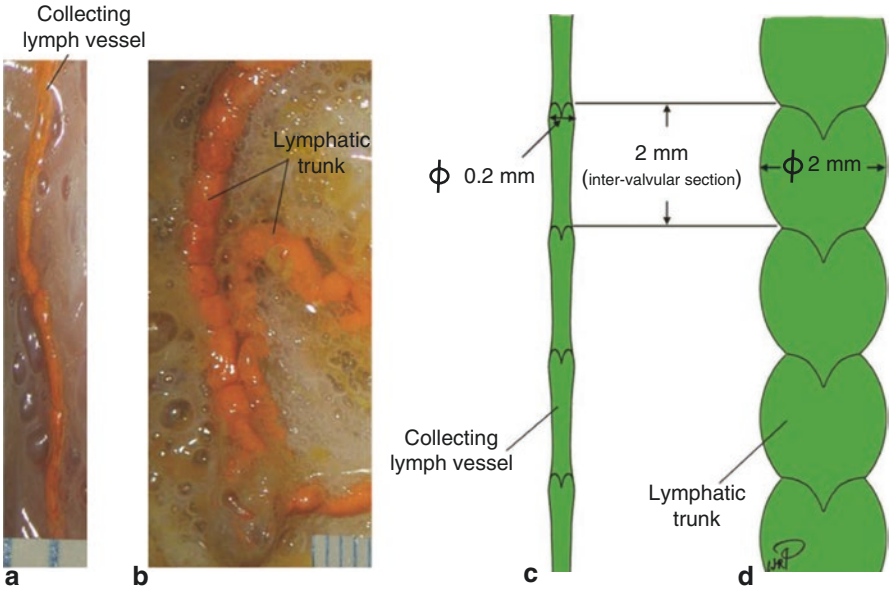

Fig. 2.7 Comparison of the appearance, calibre and inter-valvular section in the collecting lymph vessel and lymphatic trunk. Phtographs of the collecting lymph vessel (**a**) and the lymphatic trunks (**b**); Line drawings of the collecting lymph vessel (**c**) and lymphatic trunk (**d**)

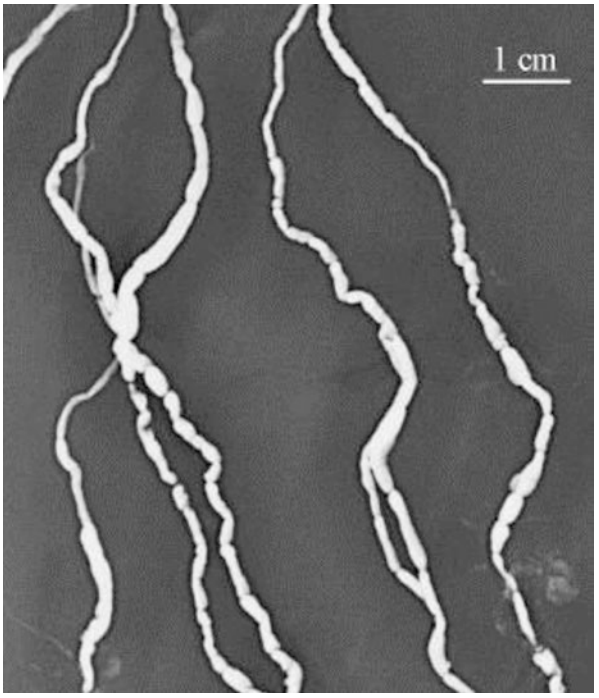

Fig. 2.8 Radiological manifestations of valves of collecting lymph vessels in the subcutaneous of the thigh

1.3 Abnormal Valves

Usually lymphatic valves were presented in pairs in the lumen of the lymph vessels, but abnormal valves were found occasionally (Figs. 2.9 and 2.10).

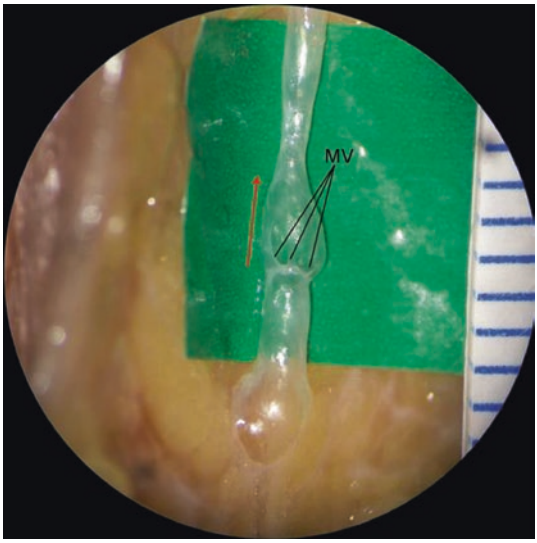

Fig. 2.9 Multiple lymphatic valves (*MV*)

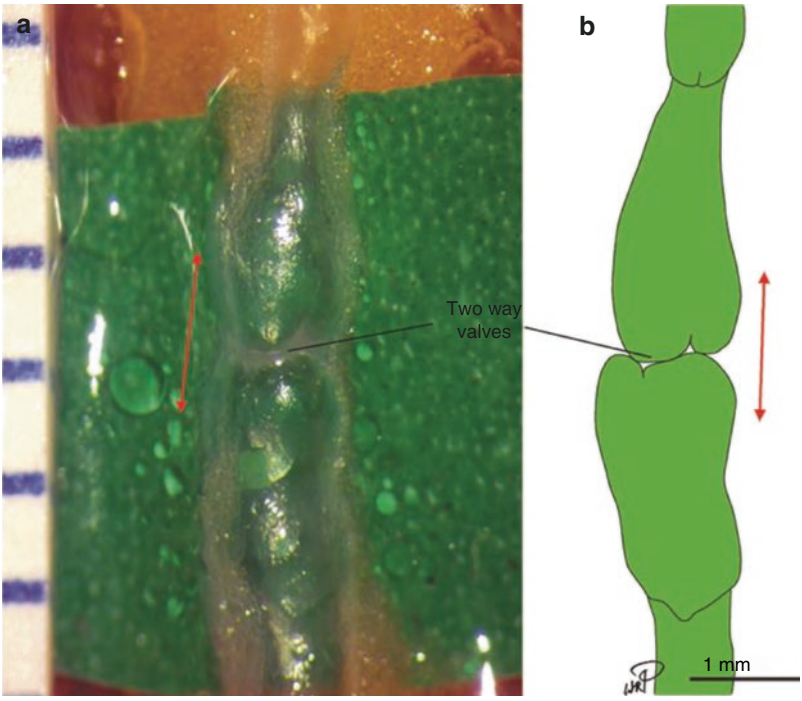

Fig. 2.10 Two-way lymphatic valves. A photograph of the collecting lymph vessel (**a**) and a line drawing of the same vessel (**b**)

Clinical Implication

The characteristic appearances of a string of beads or a bamboo trunk of the lymphatic vessels were related to the vessels' calibre and inter-valvular section in the collecting lymph vessel (and lymphatic trunk). These descriptions may help surgeons distinguish the lymphatic vessels from the venula during lymphaticovenous anastomoses when treating secondary lymphoedema.

The lymphatic flap (pedicle or free) transfer is a surgical procedure to treat secondary lymphoedema (Becker and Hidden 1988). Due to lymphatic valves opened centripetally, the direction of lymph flow in the flap and the recipient site should be consistent during the procedure (Gillies 1935).

In recent years, techniques of tissue engineering and 3D tissue bionic print have been initiated (Mironov et al. 2003; Lovett et al. 2009). Detailed information of the human lymphatic anatomy will provide the theoretical foundation for these techniques.

2 Lymphatic Ampullae and Diverticula

Different sizes and shapes of dilated vascular structures, lymphatic ampullae (Figs. 2.2, 2.11, 2.12, 2.13, 2.14, 2.15, 2.16, 2.17, 2.18, 2.19, 2.20, 2.21, 2.22, 2.23, 2.24, 2.25, 2.26, 2.27, 2.28, 2.29, 2.30 and 2.31) and diverticula (Figs. 2.32, 2.33, 2.34, 2.35, 2.36, 2.37, 2.38, 2.39, 2.40, 2.41, 2.42, 2.43, 2.44, 2.45 and 2.46) were found along the lymphatic pathway. They appeared singularly or in paired structures and circular or irregular in shape. Histological analysis confirmed that these structures had hollow centres filled with lead oxide (Fig. 2.13). Their origin and purpose are unknown.

2.1 Lymphatic Ampullae

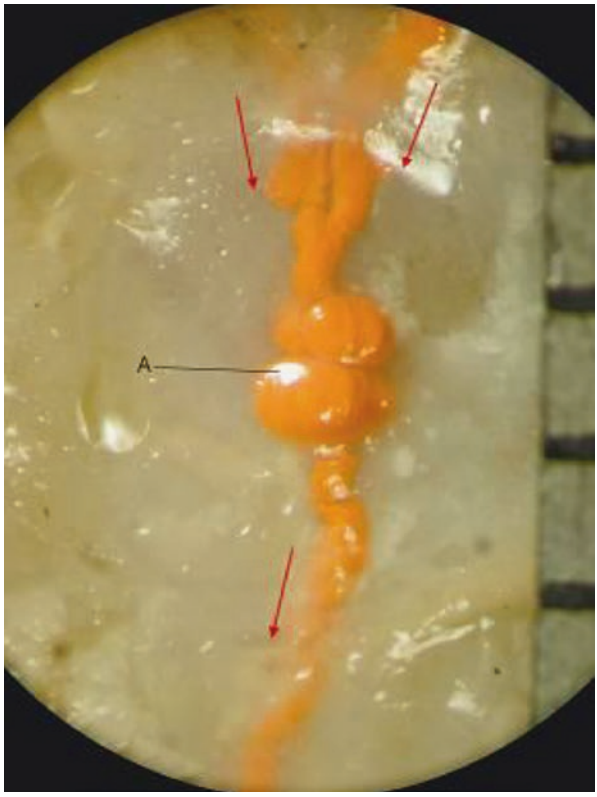

Fig. 2.11 Gourd-shaped lymphatic ampulla structures (*A*), filled with lead oxide mixture, found in a collecting lymph vessel in the occipital region. *Red arrows* indicated the direction of lymphatic flow

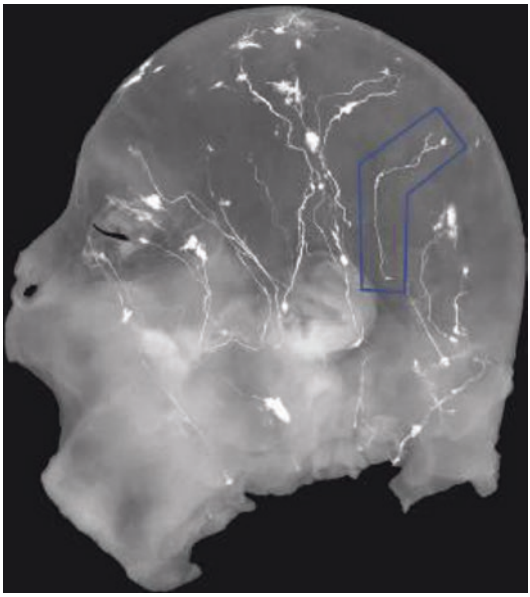

Fig. 2.12 A radiograph showing the lymphatic vessels in the integument of the head and neck after lead oxide mixture injection. The *area boxed blue* is the site of vessels with ampulla structures. A magnified image of the *area boxed blue* showed in Fig. 2.13

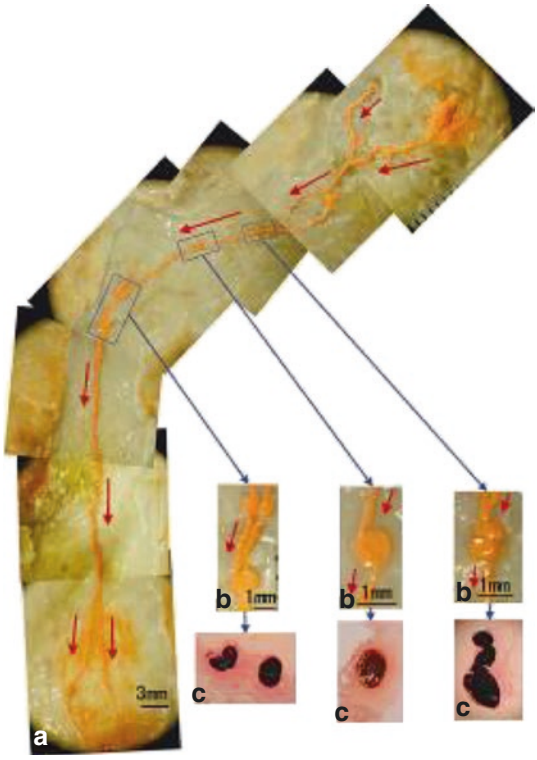

Fig. 2.13 (**a**) Magnified vessel from Fig. 2.12. (**b**) Magnified lymphatic ampullae filled with lead oxide mixture and (**c**) histological sections of each type found on this vessel

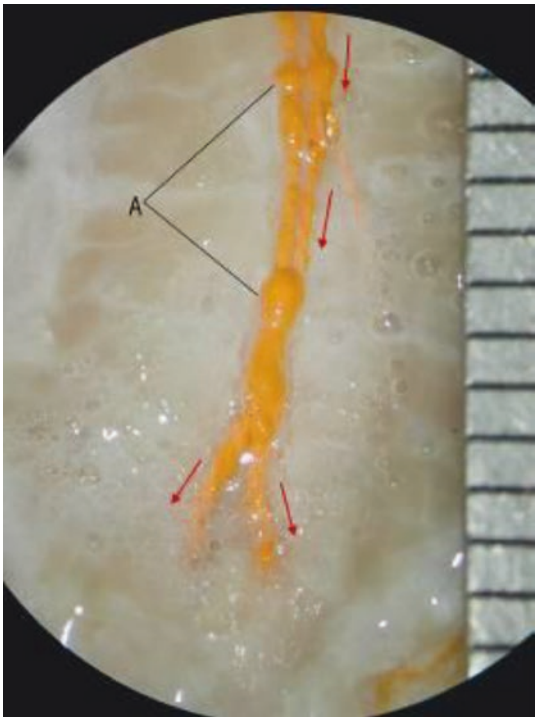

Fig. 2.14 Different sized and shaped lymphatic ampulla structures (*A*) filled with lead oxide mixture in the retroauricular region. *Red arrows* indicate the direction of lymphatic flow

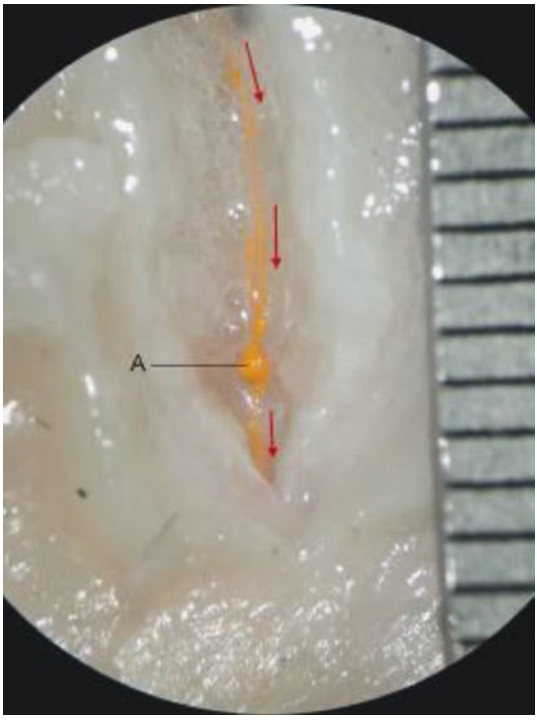

Fig. 2.15 A single ball-shaped lymphatic ampulla (*A*) filled with lead oxide mixture found in a lymphatic vessel of the cheek

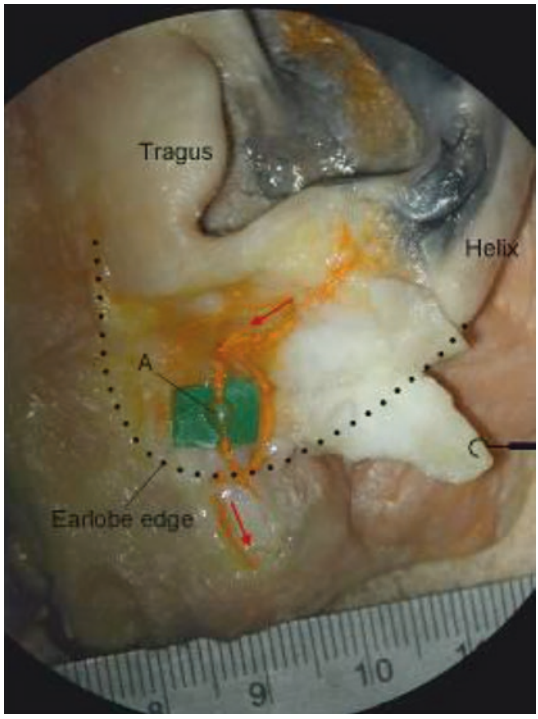

Fig. 2.16 A single ball-shaped lymphatic ampulla (*A*) found in a lymphatic vessel of the earlobe

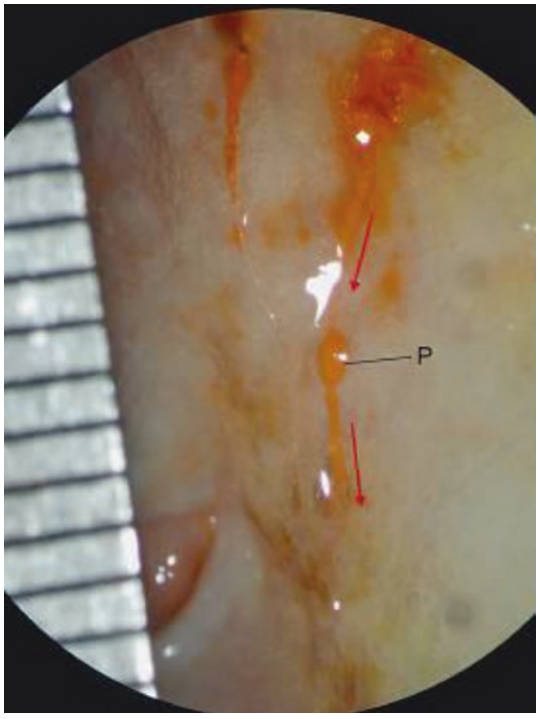

Fig. 2.17 A single oval-shaped lymphatic ampulla (*A*) seen in a collecting lymph vessel found in the preauricular area

Fig. 2.18 A single oval-shaped lymphatic ampulla (*A*) seen in a collecting lymph vessel found in the subauricular region

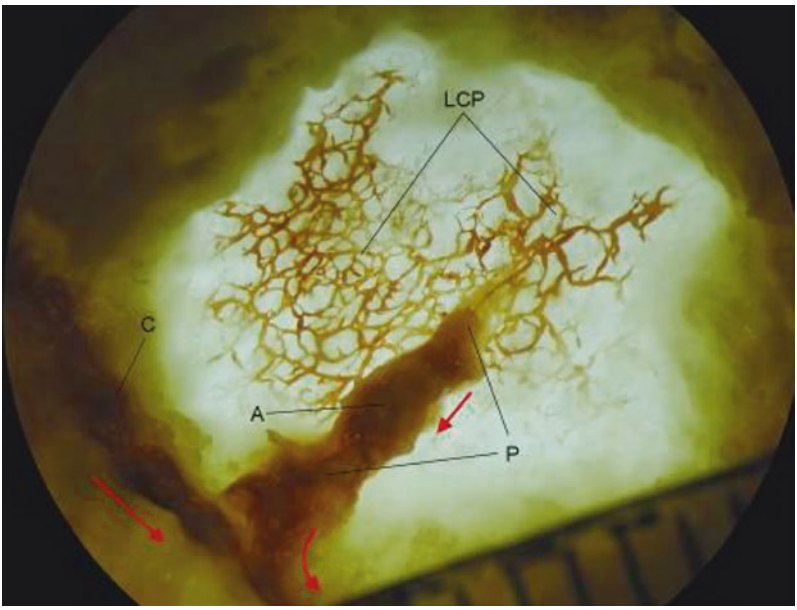

Fig. 2.19 A lymphatic ampulla (*A*) seen in the precollecting lymph vessel (*P*) filled with lead oxide mixture in the scalp. *LCP* lymph capillary plexus, *C* collecting lymph vessel

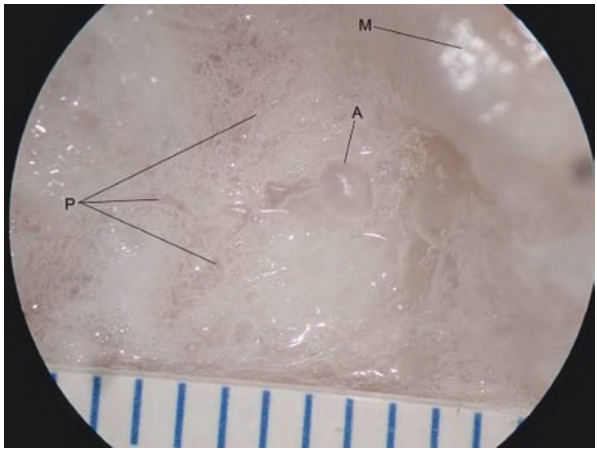

Fig. 2.20 A lymphatic ampulla (*A*) and precollecting lymph vessels (*P*) distended with hydrogen peroxide in the mucosa (*M*) of the root of the tongue

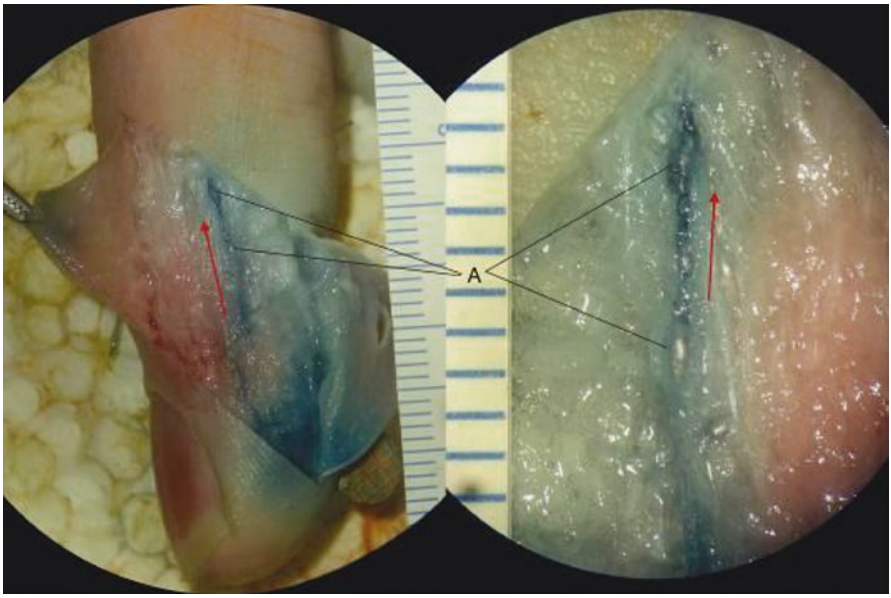

Fig. 2.21 Two lymphatic ampullae (*A*) seen in collecting lymph vessels distended by hydrogen peroxide mixed with ink in the lateral side of the index finger

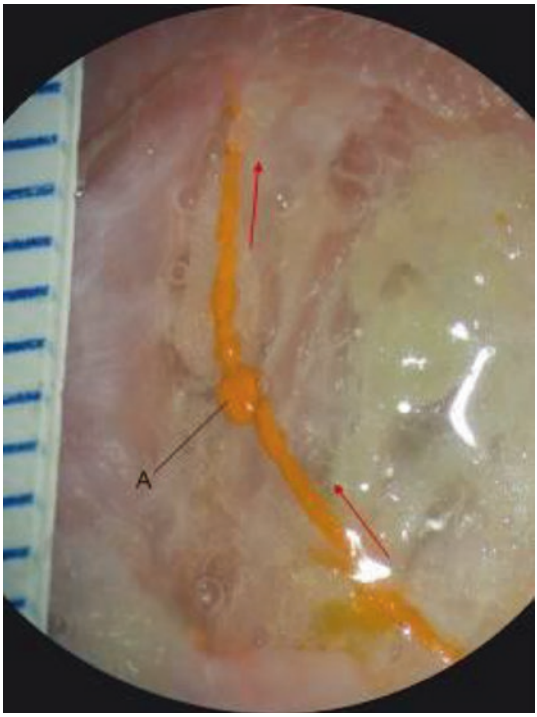

Fig. 2.22 A lymphatic ampulla (*A*) seen in the collecting lymph vessel filled with lead oxide mixture in the dorsum of the hand

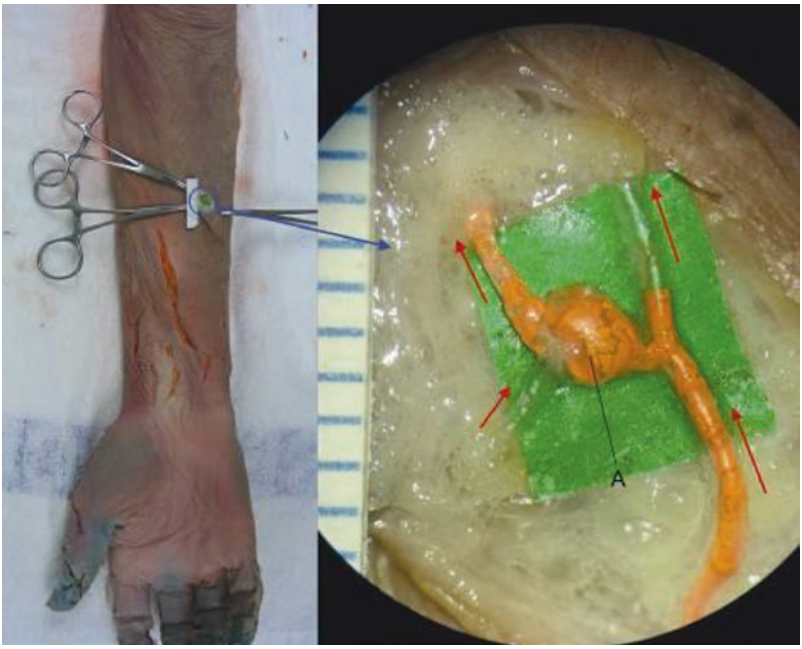

Fig. 2.23 A lymphatic ampulla (*A*) seen in collecting lymph vessels filled with lead oxide mixture in the ventral forearm

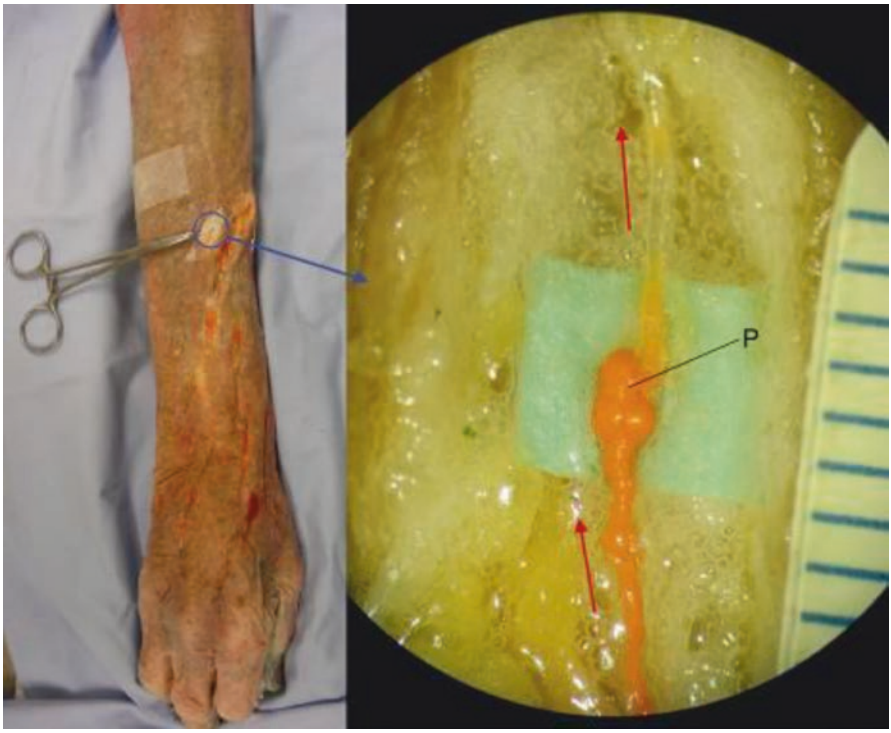

Fig. 2.24 A lymphatic ampulla (*A*) seen in the collecting lymph vessel filled with lead oxide mixture in the dorsal forearm

Fig. 2.25 Two lymphatic ampullae (*A*) seen in collecting lymph vessels filled with lead oxide mixture in the medial side of the ankle

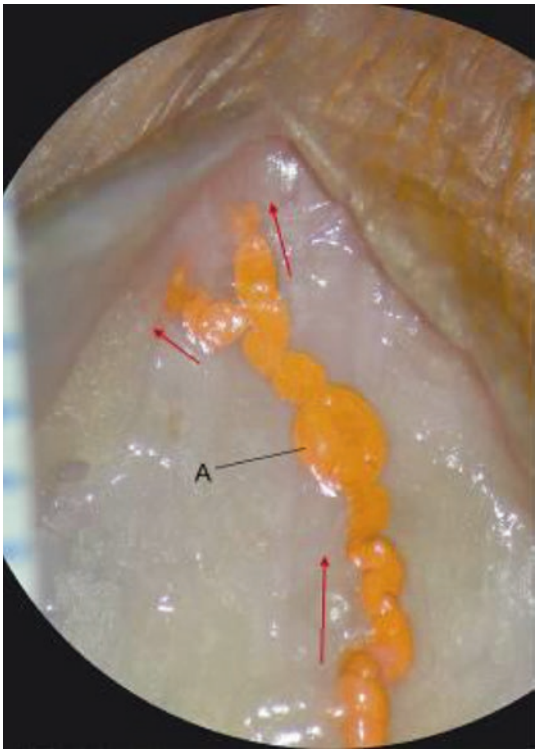

Fig. 2.26 A lymphatic ampulla (*A*) seen in a collecting lymph vessel on the medial side of the right foot

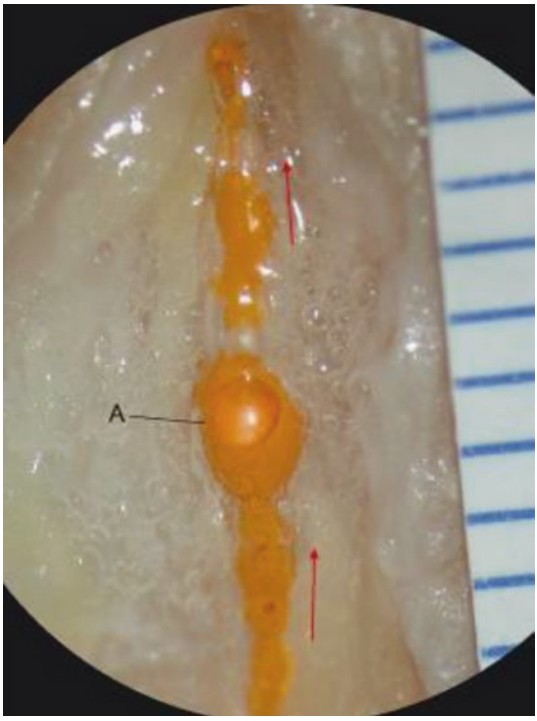

Fig. 2.27 A single oval-shaped lymphatic ampulla (*A*) seen in a collecting lymph vessel on the dorsum of the foot

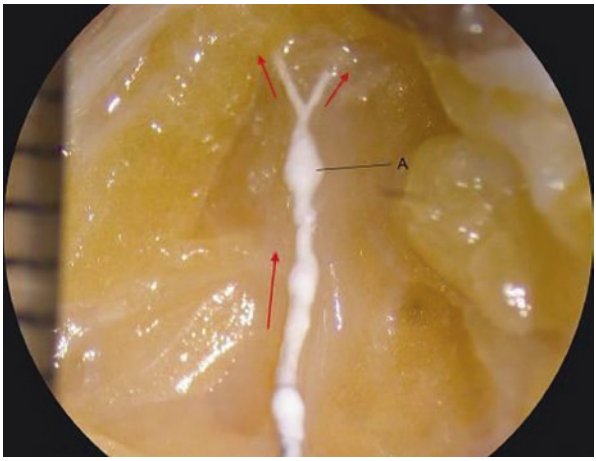

Fig. 2.28 A lymphatic ampulla (*A*) seen in a collecting lymph vessel on lateral side of the foot

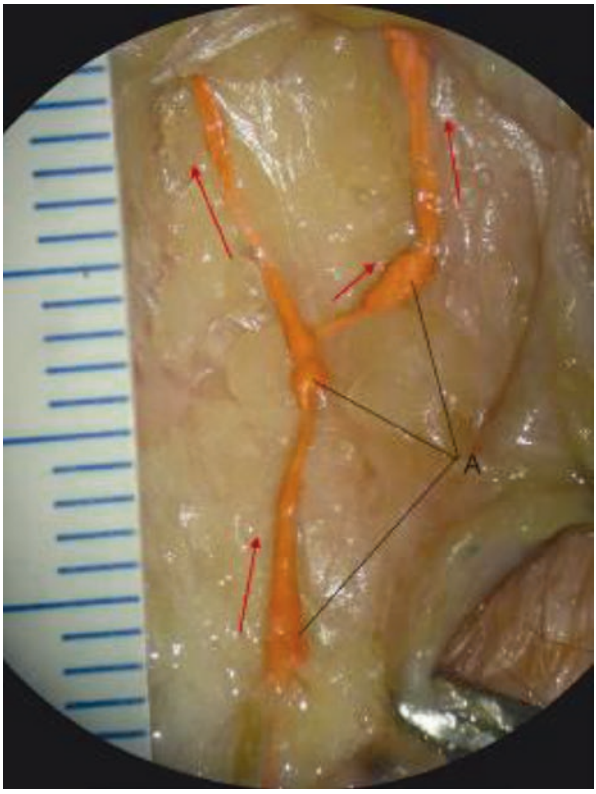

Fig. 2.29 Lymphatic ampullae (*A*) seen in collecting lymph vessels on the medial side of the left leg

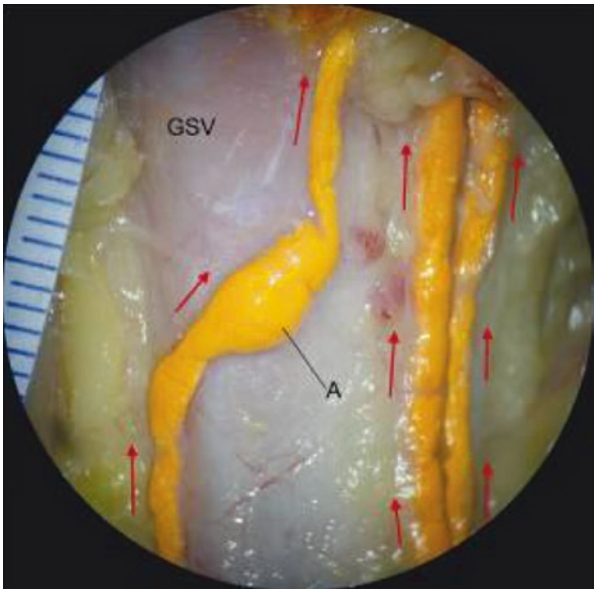

Fig. 2.30 A lymphatic ampulla (*A*) seen in a collecting lymph vessel on the medial side of the left thigh. *GSV* great saphenous vein

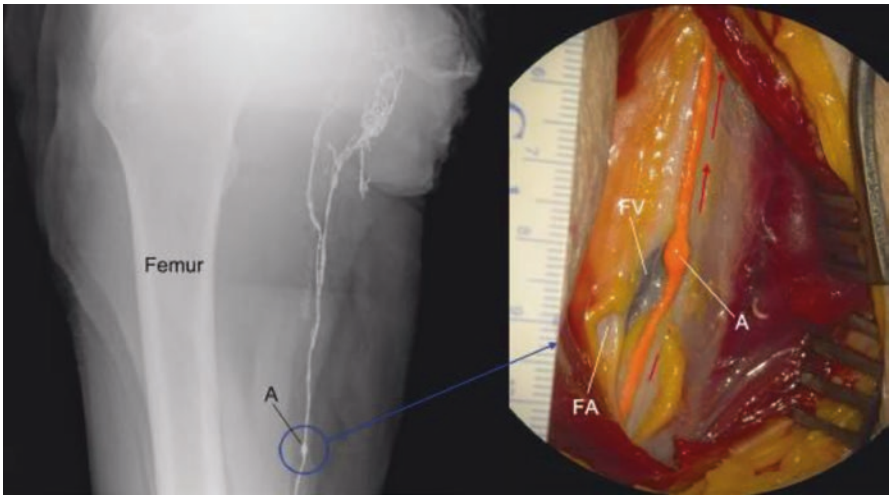

Fig. 2.31 Lymphatic ampulla (*A*) seen in a collecting lymph vessel on the medial side of the right thigh. *FA* femoral artery, *FV* femoral vein

2.2 *Lymphatic Diverticula*

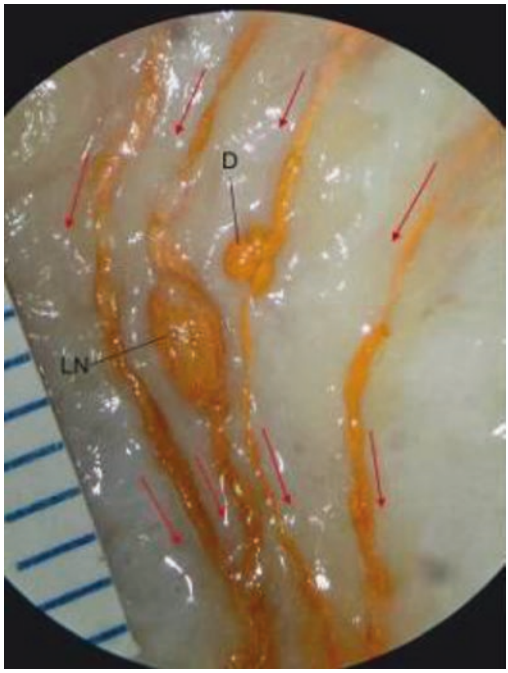

Fig. 2.32 A lymphatic diverticulum (*D*) and a lymph node (*LN*) seen in multiple collecting lymph vessels in the retroauricular region. *Red arrows* indicate the direction of the lymph flow

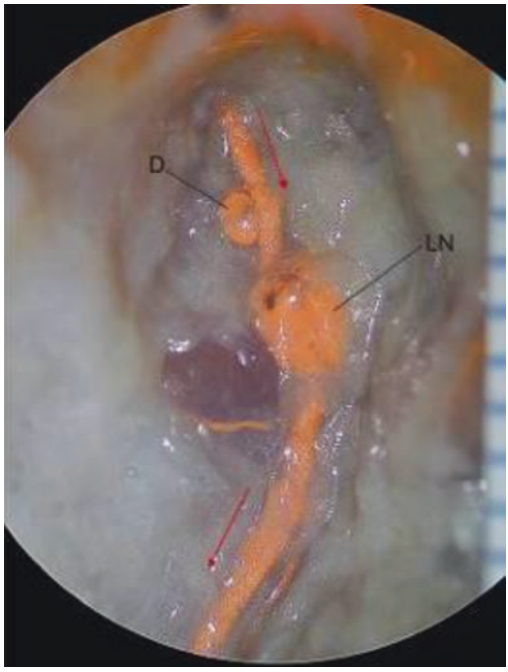

Fig. 2.33 A single diverticulum (*D*) situated on the wall of the afferent vessel near to the lymph node (*LN*) in the occipital region

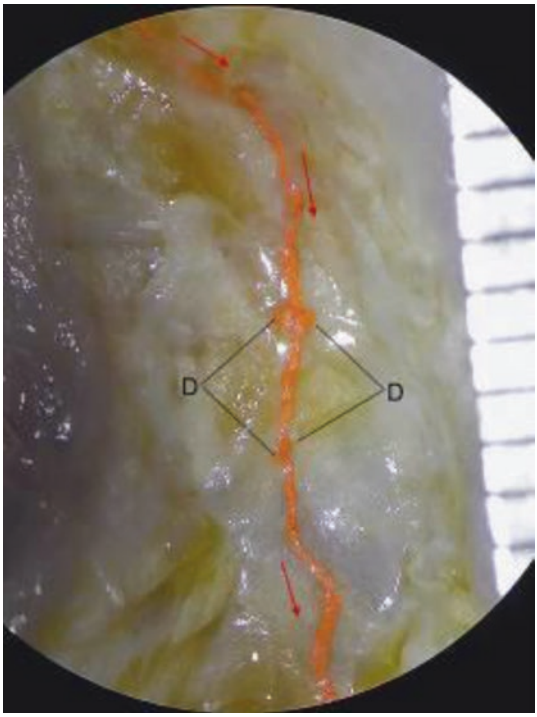

Fig. 2.34 Two pairs of different size of diverticula (*D*) filled with lead oxide mixture in the submental area. *Red arrows* indicate the direction of the lymph flow

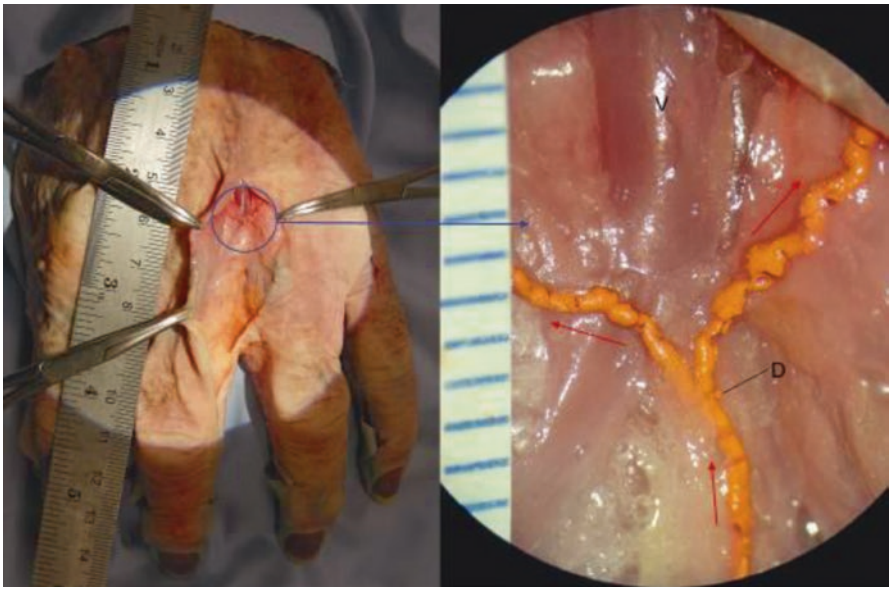

Fig. 2.35 A diverticulum (*D*) filled with lead oxide mixture in the dorsum of the left hand. *Red arrows* indicate the direction of the lymph flow. *V* metacarpal vein

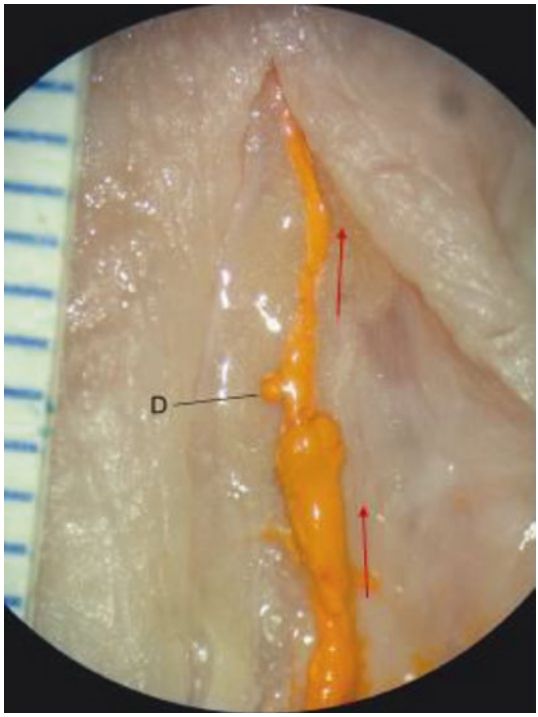

Fig. 2.36 A lymphatic diverticulum (*D*) seen on the collecting lymph vessel in the dorsoulnar aspect of the hand. *Red arrows* indicate the direction of the lymph flow

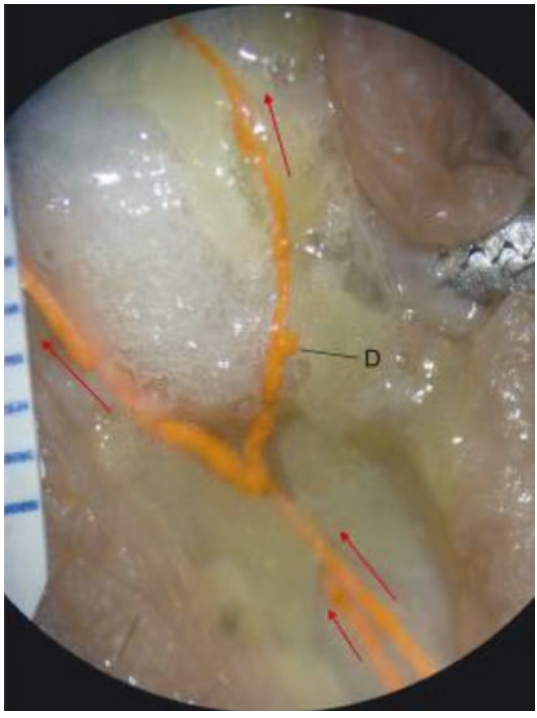

Fig. 2.37 A single diverticulum (*D*) situated on the wall of the collecting vessel in the ventral forearm

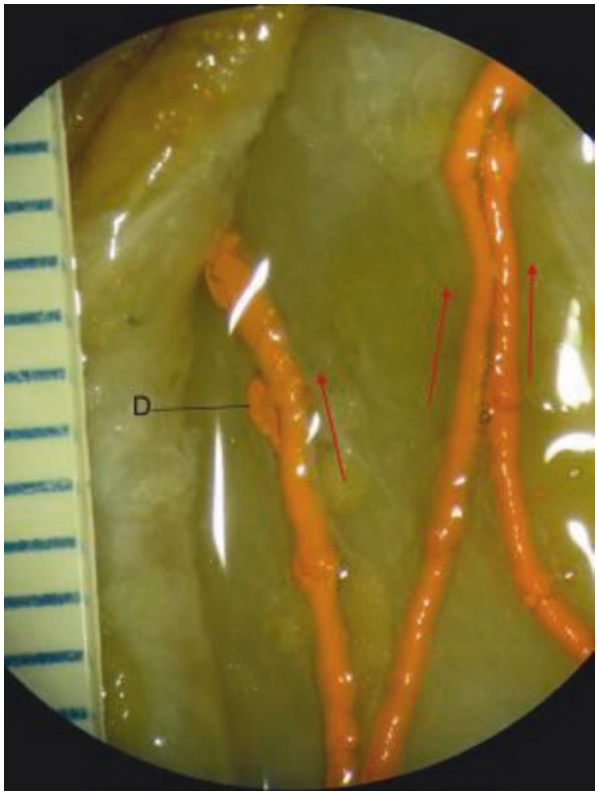

Fig. 2.38 A diverticulum (*D*) situated on the wall of the collecting vessel in the subcutaneous of the dorsal forearm

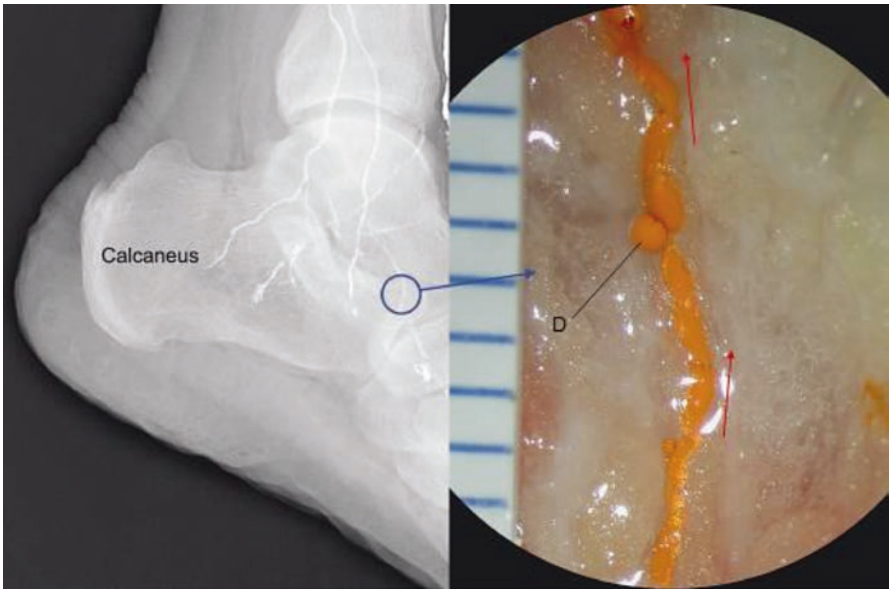

Fig. 2.39 A diverticulum (*D*) situated on the wall of the collecting vessel in the subcutaneous of the medial dorsum of the foot

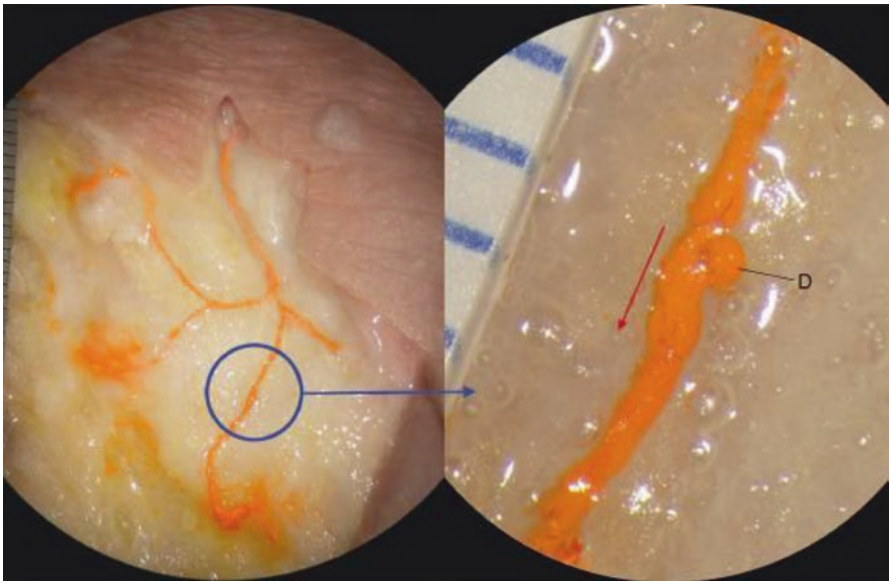

Fig. 2.40 A diverticulum (*D*) situated on the wall of the collecting vessel in the subcutaneous tissue below the medial malleolus area

Fig. 2.41 A diverticulum (*D*) situated on the wall of the collecting vessel in the subcutaneous tissue of the anterior aspect of the leg

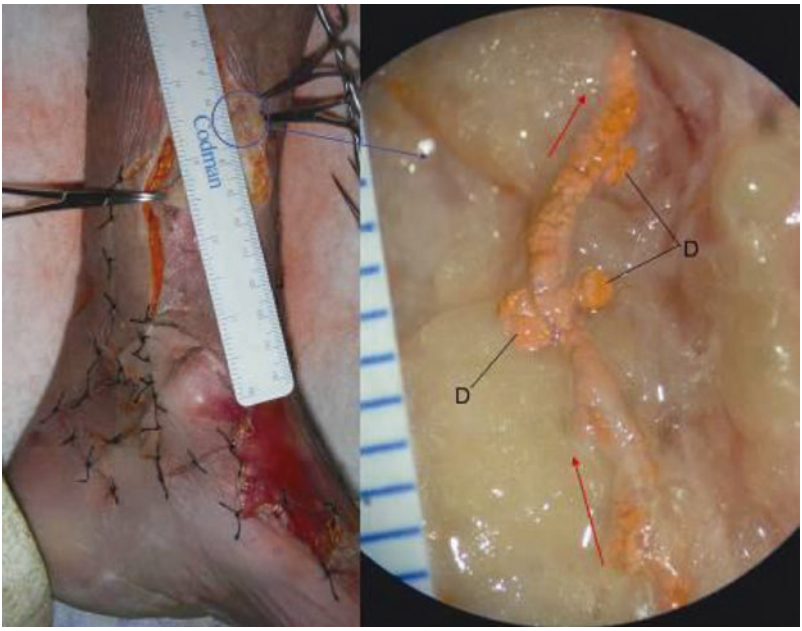

Fig. 2.42 Multiple diverticula (*D*) situated on the wall of the collecting vessel in the subcutaneous tissue of the anteromedial aspect of the leg

Fig. 2.43 Two diverticula (*D*) situated on the wall of the collecting vessel in the subcutaneous tissue of the medial aspect of the leg

Fig. 2.44 A diverticulum (*D*) situated on the wall of the collecting vessel in the subcutaneous tissue of the medial aspect of the leg

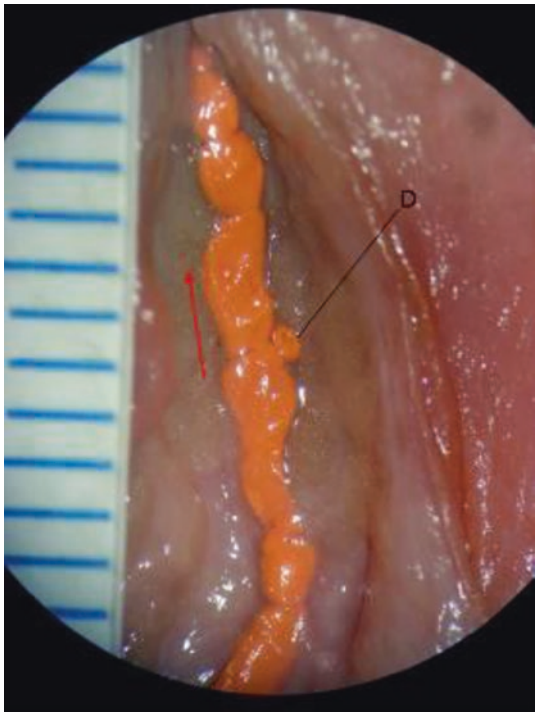

Fig. 2.45 A diverticulum (*D*) situated on the wall of the collecting vessel in the subcutaneous tissue of the lateral aspect of the leg

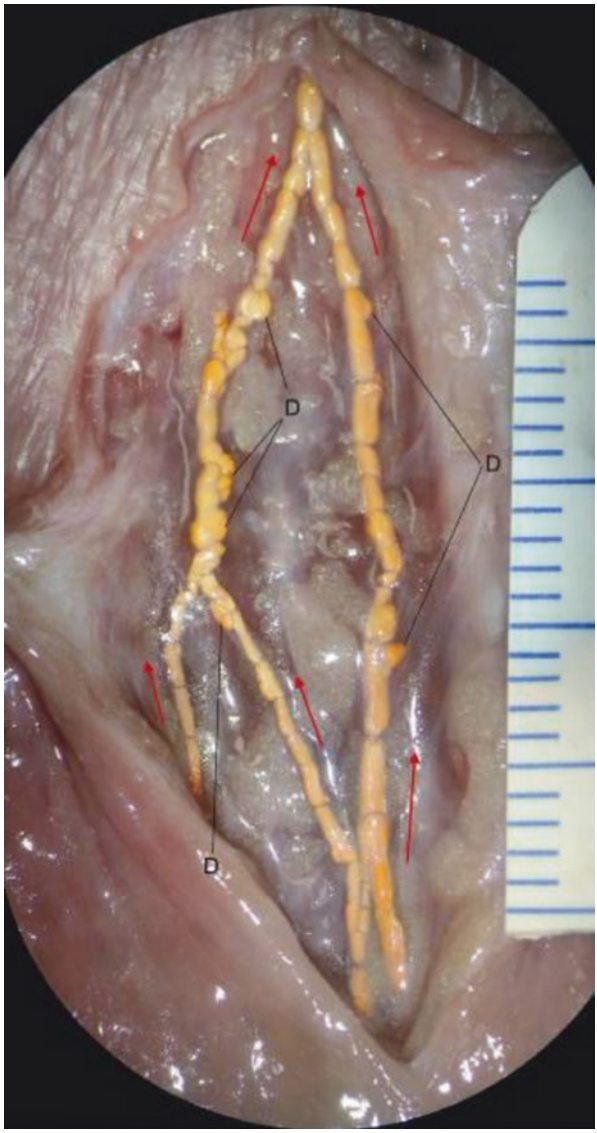

Fig. 2.46 Multiple diverticula (*D*) situated on the wall of the collecting vessel in the subcutaneous tissue of the posterolateral aspect of the leg

Note
Ampullae and diverticula were found in all subjects at various stages of the lymphatic pathway, either in precollecting or collecting lymph vessels. Their origin and purpose are unknown.

3 Lymph Capillary Plexus

The lymph capillaries have been described in many textbooks to exist in most tissues and organs of the body except the epithelia, cartilage, cornea, etc. Those originating from the dermis and the mucous membranes have an important role in the immune defence mechanism, which has been well described (Drinker and Yoffey 1941; Cowdry 1950). Those found in the galea layer (Pan et al. 2008a, b) may have a similar role to those in the skin of the scalp, as the scalp is a common site of trauma.

It has been noticed that there are two layers of lymph capillaries, one superficial and one deeper, in the dermis (Fig. 1.3) (Hudack and McMaster 1933) and mucosa (Fig. 2.64). They connect to each other to form a three-dimensional network – the lymph capillary plexus. The diameter of these vessels varies; they are tiny in the superficial layer (less than 0.02 mm) and slightly larger in the deeper layer. Sometimes larger vessels, diameter greater than 0.2 mm, could be seen in the galea layer and mucosa (Figs. 2.52, 2.63 and 2.64).

These vessels were thin walled, irregularly shaped and very fragile. Sometimes they appeared constricted and at other times dilated. They branch abundantly and undergo anastomosis freely to form a rich avalvular plexus. The micromorphology of these vessels varied in different regions (Figs. 2.47, 2.48, 2.49, 2.50, 2.51, 2.52, 2.53, 2.54, 2.55, 2.56, 2.57, 2.58, 2.59, 2.60, 2.61, 2.62, 2.63, 2.64 and 2.65).

3.1 Lymph Capillary Plexus in the Skin (Dermis) of the Scalp

Lymph capillary vessels were seen without valves in the skin (dermis) of the scalp. They form a very fine three-dimensional, polygonal network. The calibre of the vessels varied from as small as 0.02 to 0.15 mm, tiny in the superficial layer and slightly larger in the deeper (Figs. 2.19, 2.47, 2.48, 2.49, 2.50 and 2.51).

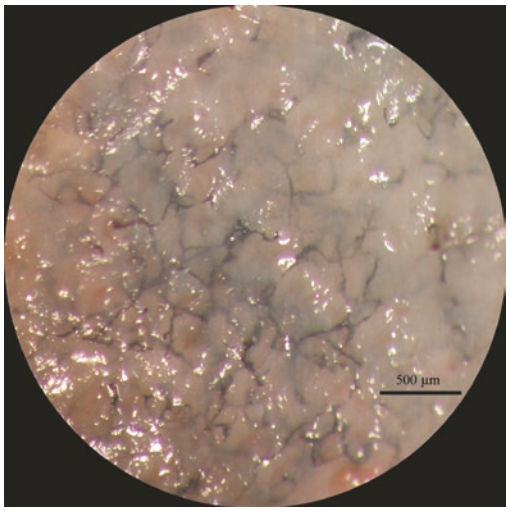

Fig. 2.47 The lymph capillary plexus in the dermis of the scalp filled with India ink and hydrogen peroxide mixture

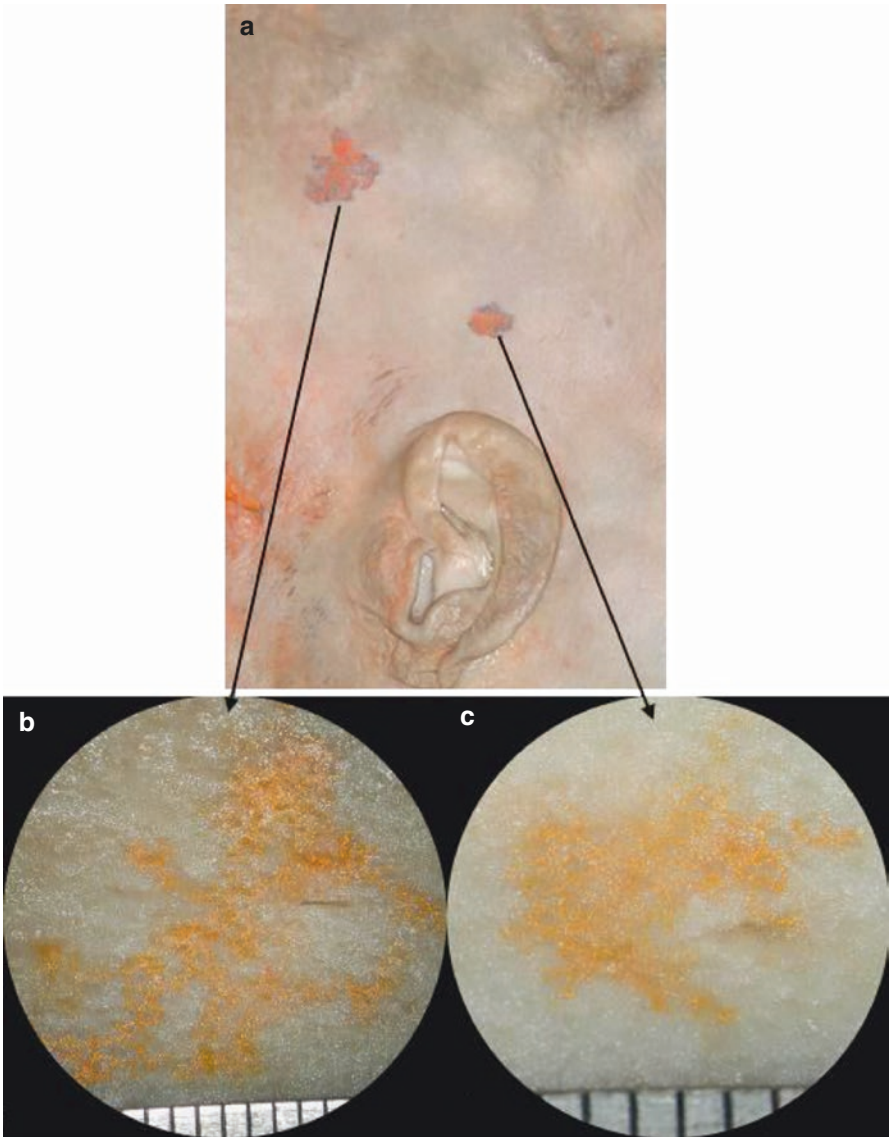

Fig. 2.48 (**a**) Two patches of the lymph capillary plexus in the dermis of the scalp retrogradely filled with lead oxide mixture. (**b**, **c**) Magnified views of patches from (**a**)

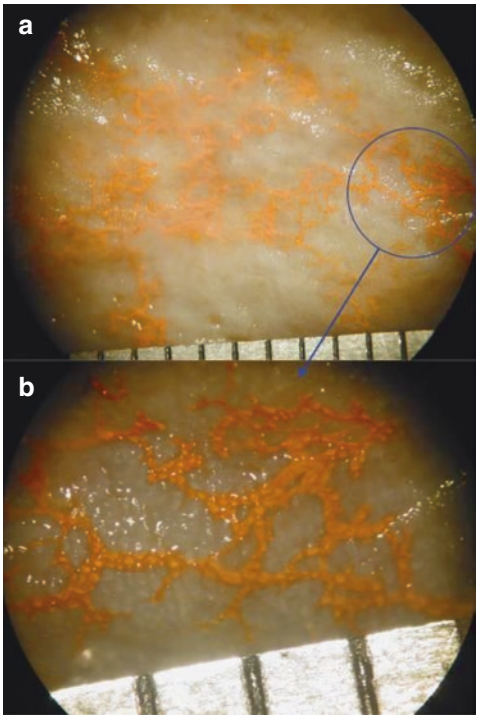

Fig. 2.49 (**a**) The lymph capillary plexus in the dermis of the scalp retrogradely filled with lead oxide mixture. Viewed skin side up. (**b**) Magnified image of the *area circled* above, showing different sized vessels, irregular and jagged walls

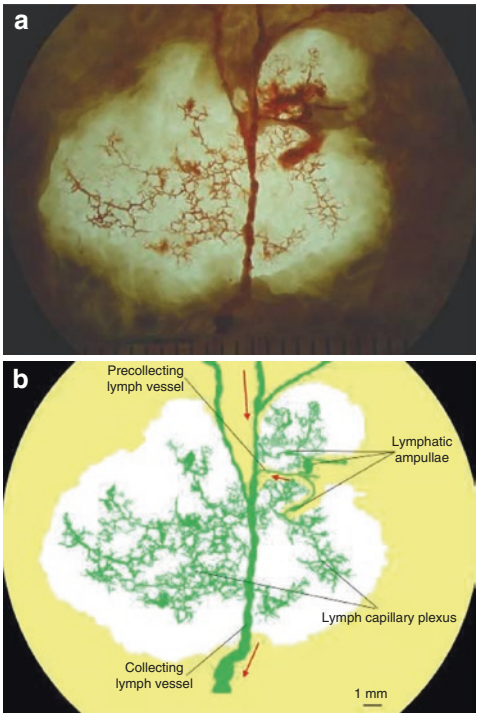

Fig. 2.50 (**a**) Transilluminated view of the injected lymphatics from the inner surface of the scalp. (**b**) The diagram is traced from the image above. *Note*: The lymph capillary plexus links to the precollecting lymph vessels that drain to collecting lymph vessels. Swollen structures on the precollecting vessels have been named as "ampullae". *Red arrows* indicate the direction of the lymph flow

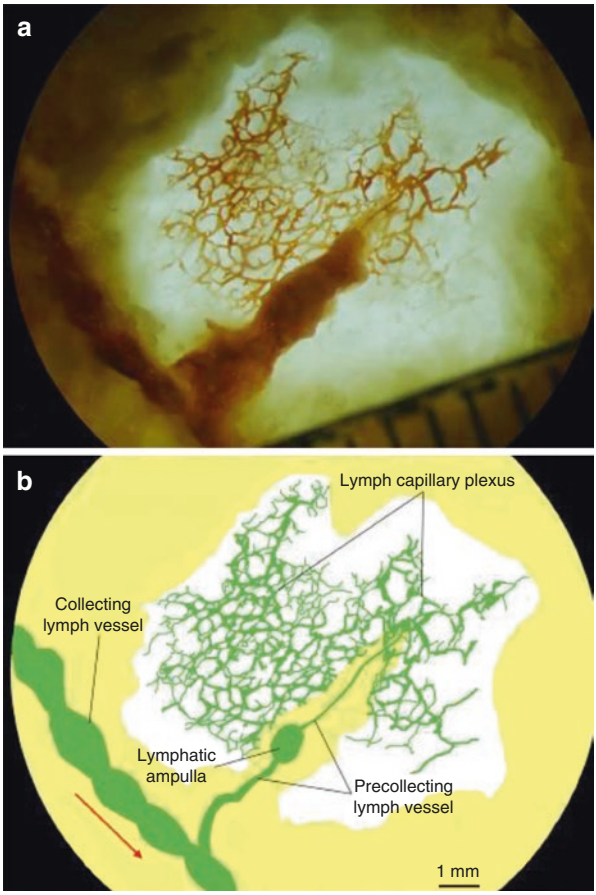

Fig. 2.51 (**a**) Transilluminated view of the injected lymphatics from the inner surface of the scalp. (**b**) The diagram is traced from the image above. The lymph capillary plexus links to the precollecting lymph vessels and then flows into the collecting lymph vessels. Swollen structure on the precollecting vessel is the "ampulla"

Clinical Implication

Erysipelas is a type of skin infection involving the lymph capillary plexus in dermis. It is most often caused by β-haemolytic streptococci and occurs most frequently on legs and the face. With a rapid onset, affected individuals typically develop symptoms including high fevers, chills, shaking, headaches, vomiting, malaise and general illness. The affected skin area is characterized clinically by shiny, swollen, warm, raised and tender scarlet lesions with distinct margins (Zhang 1984; Hall and Hall 2009).

3.2 *Lymph Capillary Plexus in the Galea (Epicranial Aponeurosis)*

Avalvular lymph capillary vessels were present in the galea layer. They formed a fine three-dimensional polygonal plexus. The calibre of vessels varied from as tiny as 0.014–0.2 mm. The network merged to link precollecting lymph vessels and drained to the collecting lymph vessel in the deep tissues (Figs. 2.3, 2.52, 2.53 and 2.54).

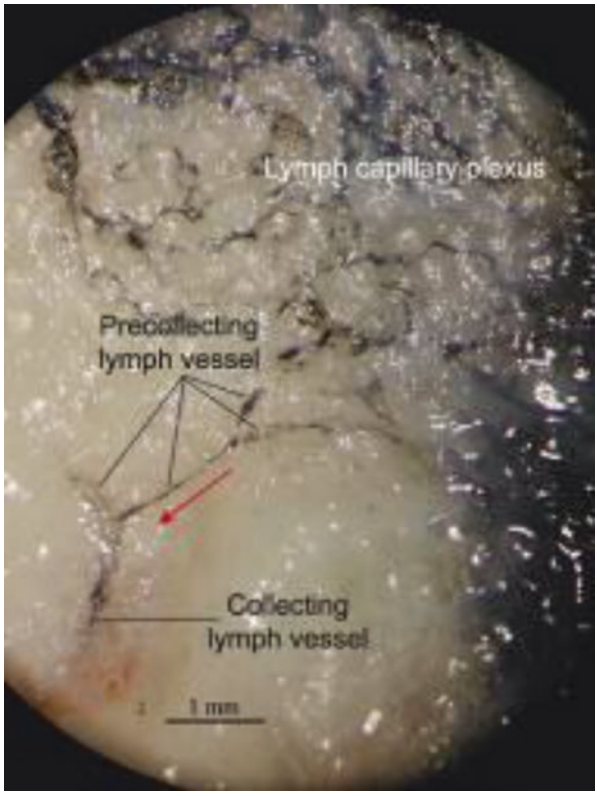

Fig. 2.52 Different sized vessels with irregular walls of the lymph capillary plexus filled with India ink and hydrogen peroxide mixture in the galea layer of the scalp. *Red arrow* indicates the direction of the lymph flow

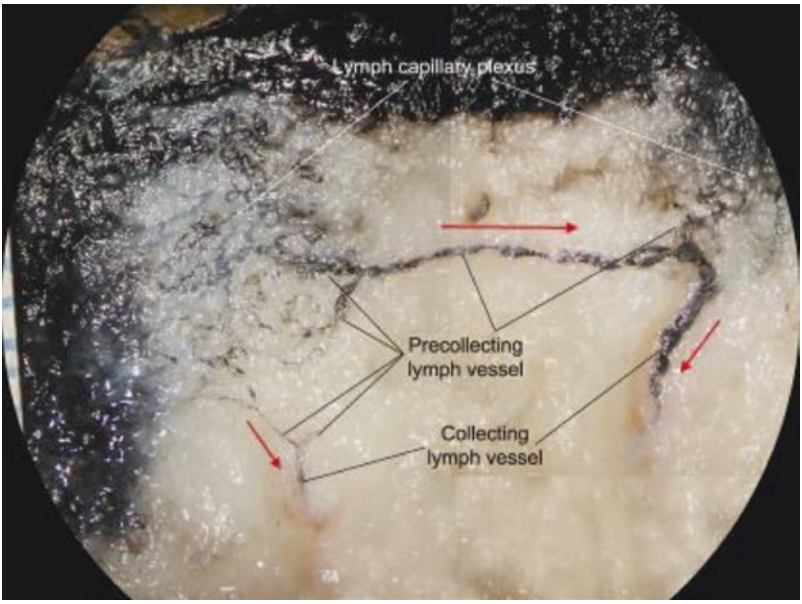

Fig. 2.53 The lymph capillary plexus filled with India ink and hydrogen peroxide mixture in the whitish galea layer of the scalp. The network merged to form different sized precollectors linking the lymph-collecting vessels lying in the yellowish subcutaneous tissue

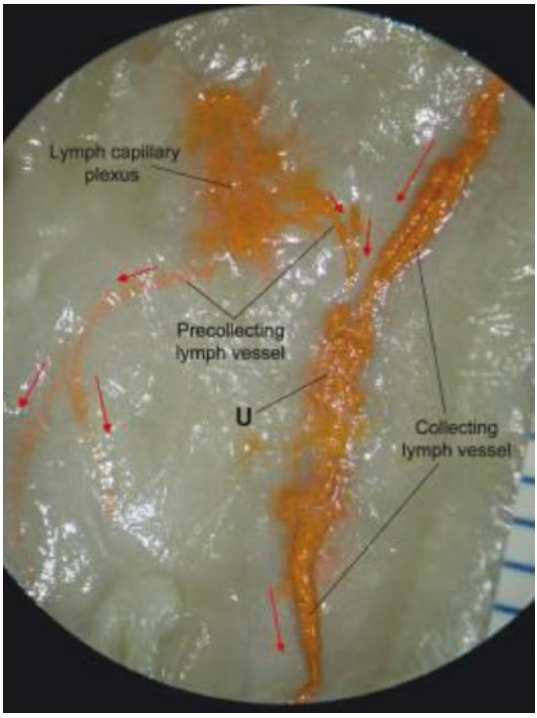

Fig. 2.54 The lymph capillary plexus filled with lead oxide mixture in the whitish galea layer of the occipital area. Capillary vessels merged and formed two precollecting lymph vessels linking the collecting lymph vessels. *Red arrows* indicate the direction of the lymph flow. *U* indicates an unknown "mop-like" lymphatic structure lying between three afferent vessels (one precollecting, two collecting) and an efferent lymph-collecting vessel

Clinical Implication
Lymphatic capillary vessels are widely distributed in the body and have an important role in the immune defence mechanism, which has been well described (Drinker and Yoffey 1941; Cowdry 1950). Those found in the galea layer (Pan et al. 2008a, b) may have a similar role to those in the skin, as the scalp is a common site of trauma.

3.3 *Lymph Capillary Plexus in the Auricle*

Avalvular lymph capillary vessels were seen in the skin (dermis) of the auricle. They formed a fine three-dimensional, polygonal structure. The calibre of vessels varied from as small as 0.014 to 0.2 mm (Figs. 2.55 and 2.56).

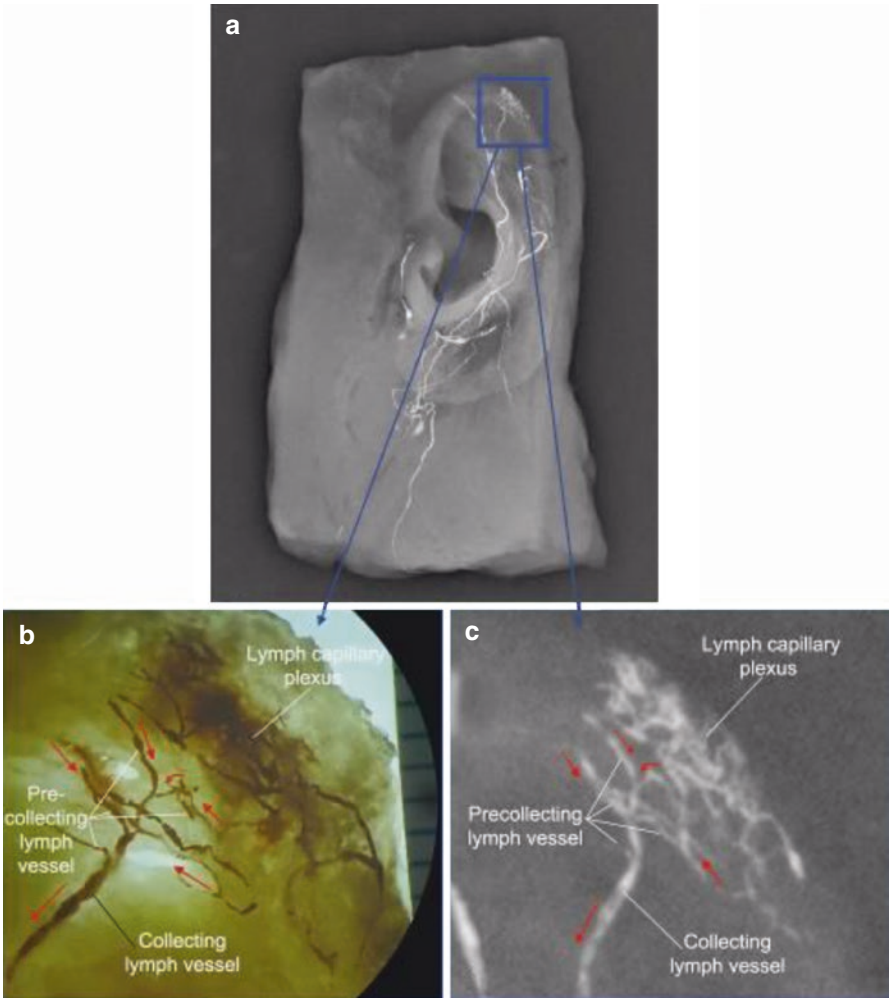

Fig. 2.55 (**a**) Lymphatic vessels of the left auricle were filled with lead oxide mixture. Transilluminated (**b**) and radiological (**c**) images are the magnified view of the *blue box* from (**a**). Lymph capillary vessels, in the helix of the left auricle, merged and formed several precollecting lymph vessels linking the collecting lymph vessels. *Red arrows* indicate the direction of the lymph flow

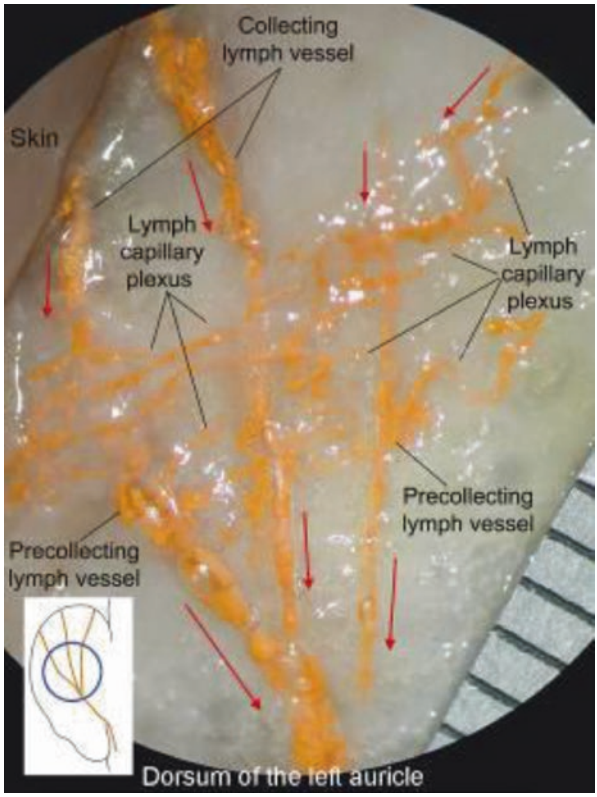

Fig. 2.56 The lymph capillary plexus in the dermis of the dorsum of the left auricle lying above the lymph-collecting vessels. *Red arrows* indicate the direction of the lymph flow

Note

Bionic tissue engineering and 3D printing technologies of the experimental auricle cartilage have been reported (Cao et al. 1997; Mannoor et al. 2013). The success of such technologies will allow researchers to open the way to manufacture tissues and organs of the human body for replacement in the clinic. Detailed vasculature (Houseman et al. 2000) including the lymphatic vessels (Pan et al. 2011a, b) of the auricle will provide a theoretical basis for completing an entire ear when these technologies will have been fully established in the future.

3.4 *Lymph Capillary Plexus in the Mucosa of the Nasal Cavity*

Avalvular lymph capillary vessels were seen as small "tree-like" branches in the mucosa of the nasal cavity. The calibre of vessels varied from 0.01 to 0.2 mm (Fig. 2.57).

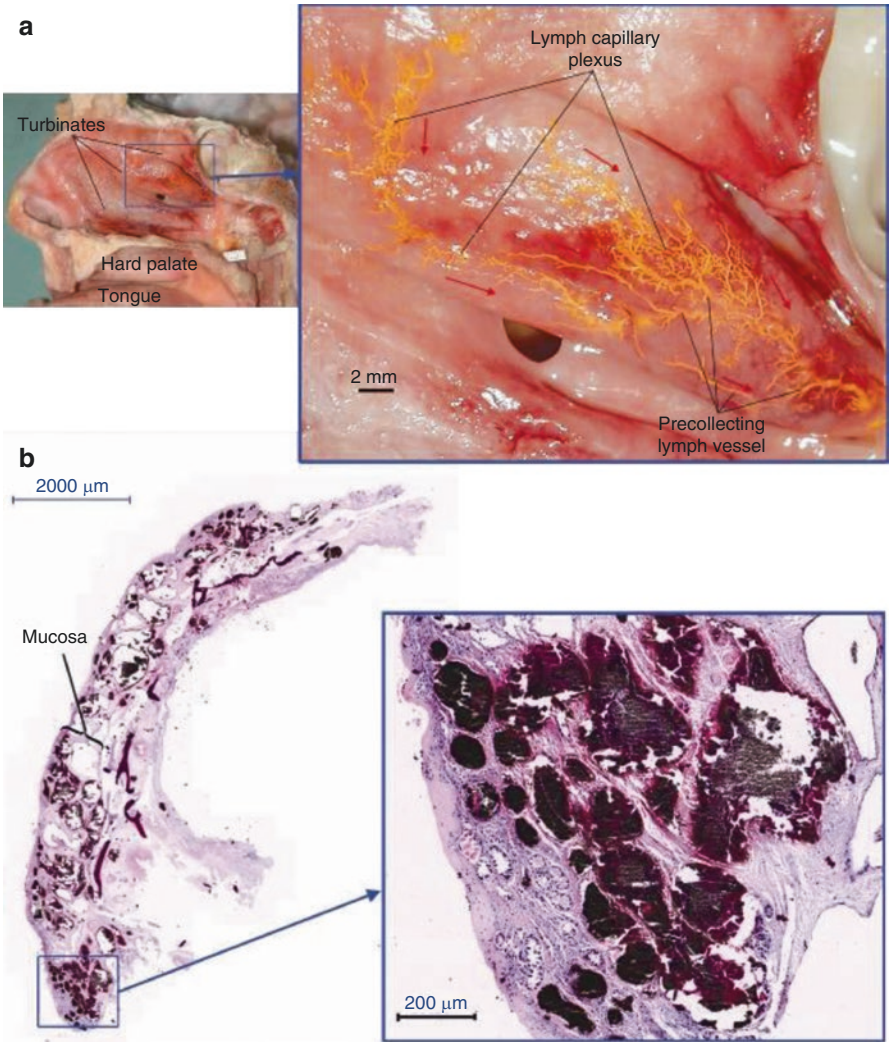

Fig. 2.57 (**a**) Lymph capillary plexus and precollecting lymph vessels filled with lead oxide mixture in the mucosa of turbinates of the nasal cavity. *Red arrows* indicate the direction of the lymph flow. A histological section (**b**), H&E stain, of the middle turbinate in the *blue box* of (**a**) showing the different sizes of the vessel at different depths. The *right images* are magnified views of the *blue boxes* from the *left images*

3.5 *Lymph Capillary Plexus in the Mucosa of the Nasal Pharyngeal Wall*

Avalvular lymph capillary vessels were presented as small loops and "tree-like" structures in the mucosa of the nasal pharyngeal wall. The calibre of vessels varied from 0.01 to 0.2 mm (Figs. 2.58 and 2.59).

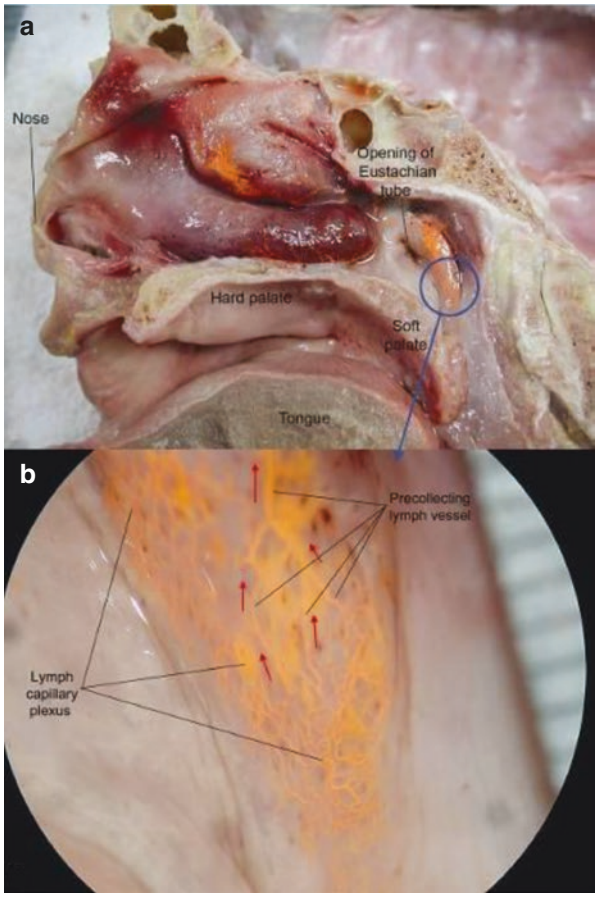

Fig. 2.58 (**a**) The lymph capillary plexus and precollecting lymph vessels filled with lead oxide mixture in the mucosa of the lateral nasopharyngeal wall. (**b**) A magnified view of *area circled* in (**a**). *Red arrows* indicate the direction of the lymph flow

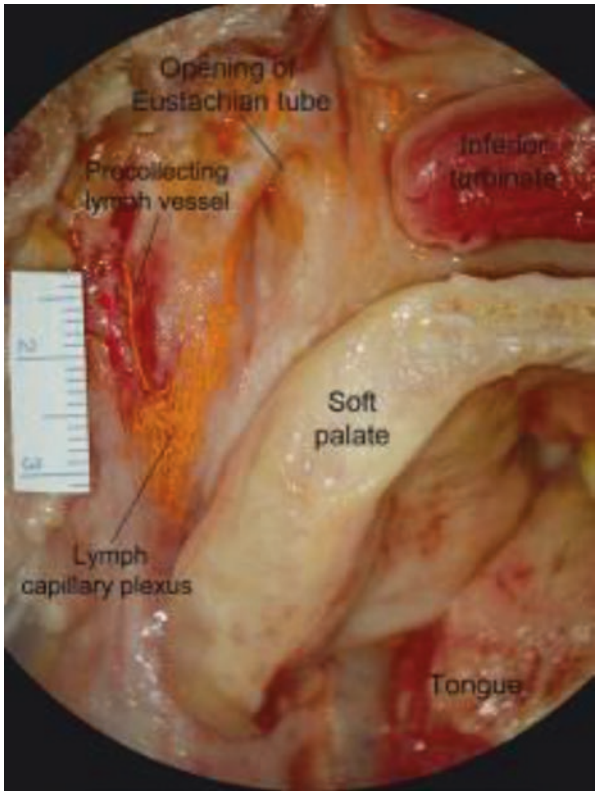

Fig. 2.59 The lymph capillary plexus in the mucosa of the lateral nasopharyngeal wall draining to the parapharyngeal space via a precollecting lymphatic vessel. *Red arrow* indicates the direction of lymph flow

3.6 *Lymph Capillary Plexus in the Mucosa of the Soft Palate*

Avalvular lymph capillary vessels were presented as small loops structure in the mucosa of the soft palate. The calibre of vessels varied from 0.01 to 0.1 mm (Fig. 2.60).

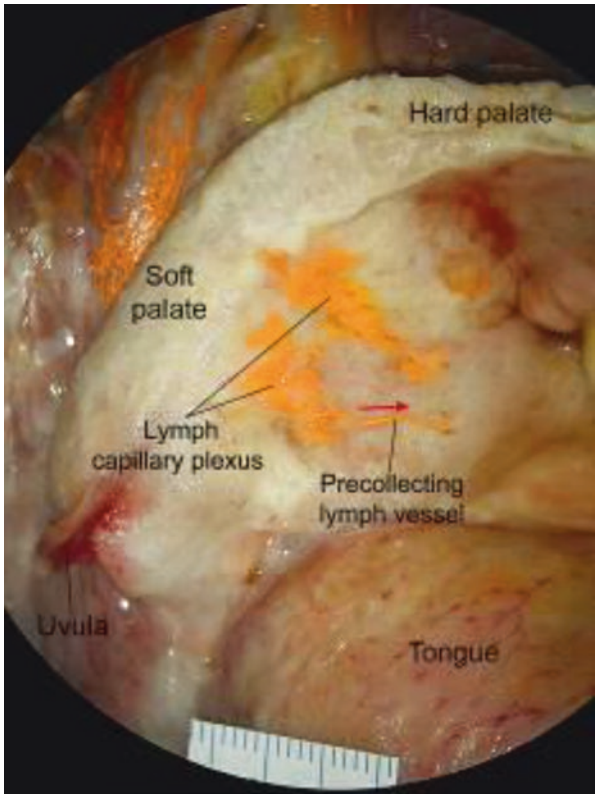

Fig. 2.60 The lymph capillary plexus linked to the precollecting lymphatic vessel in the mucosa of the soft palate. *Red arrow* indicates the direction of lymph flow

3.7 *Lymph Capillary Plexus in the Mucosa of the Oropharyngeal, Laryngeal and Oesophageal Walls*

The lymph capillary vessels were seen as a "coral-like" structure without valves in the mucosa of the oropharyngeal, laryngeal and oesophageal walls. The calibre of vessels varied from 0.01 to 0.2 mm (Figs. 2.61, 2.62, 2.63 and 2.64).

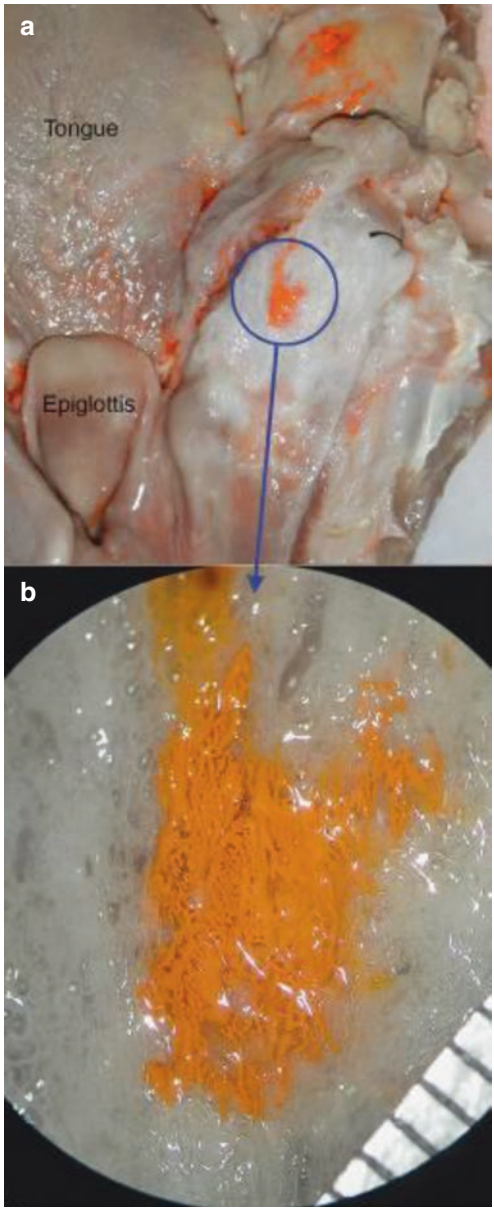

Fig. 2.61 (**a**) The "coral-like" lymph capillary plexus filled with lead oxide mixture *circled blue* in the mucosa of the oropharyngeal. (**b**) Magnified view of the structure

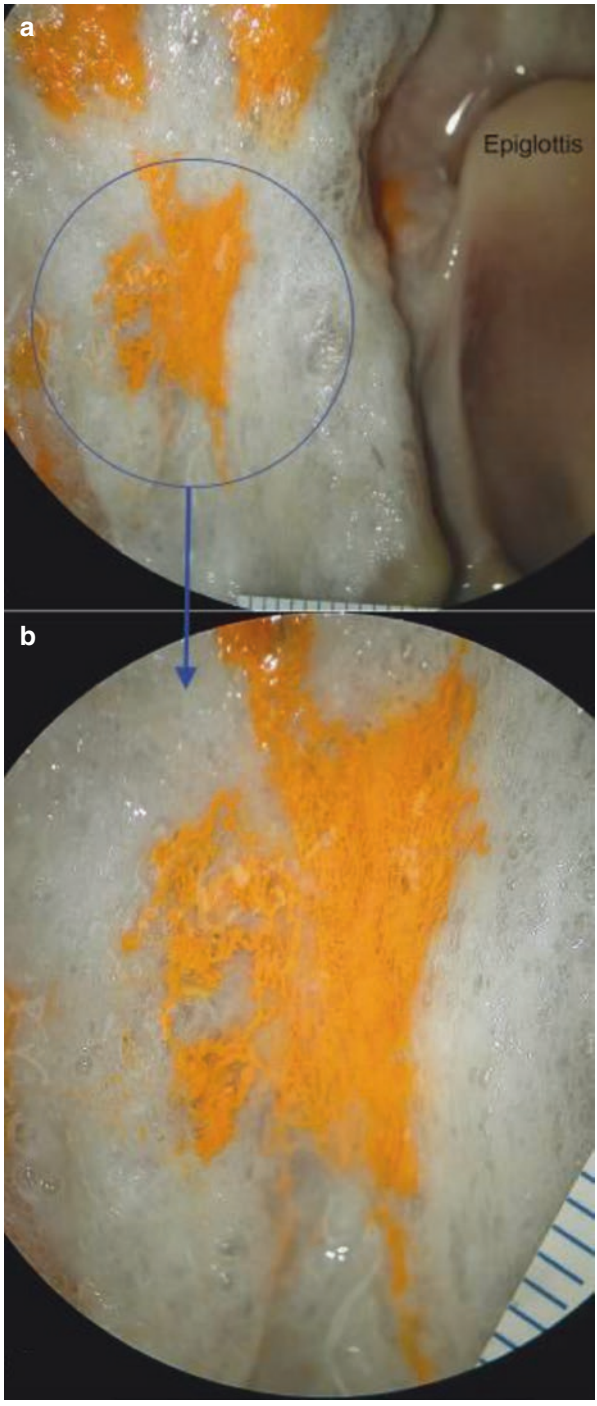

Fig. 2.62 (**a**) The "coral-like" lymph capillary plexus filled with lead oxide mixture *circled blue* in the mucosa of the pharyngeal. (**b**) Magnified view of the structure

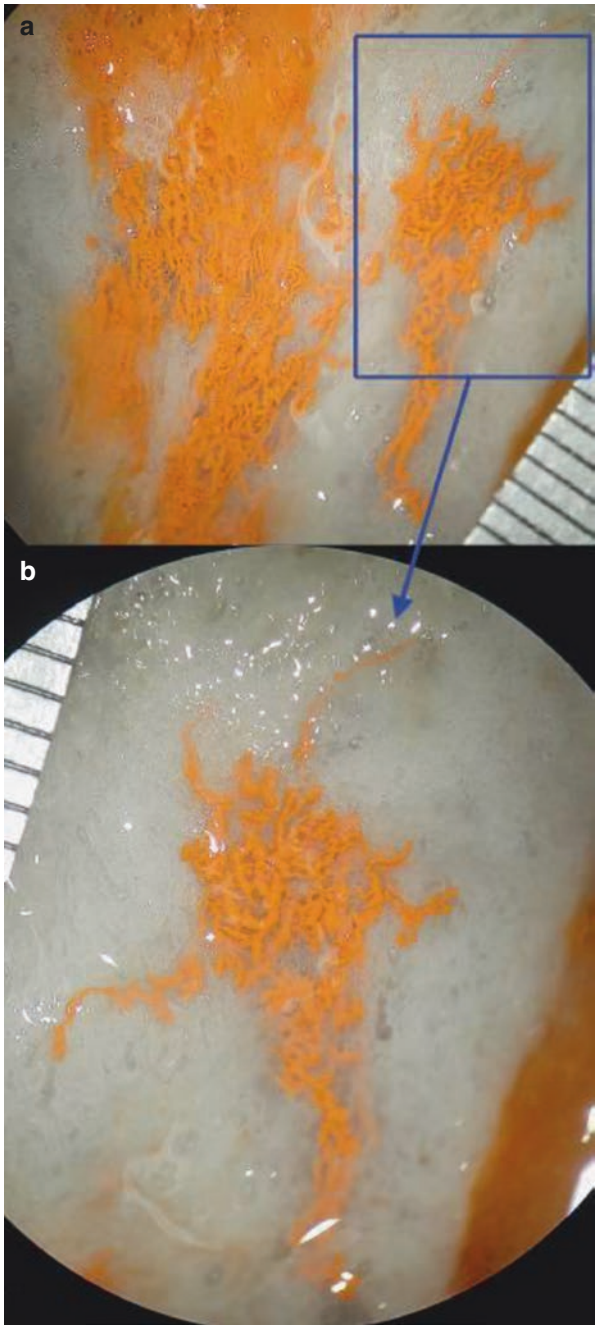

Fig. 2.63 (**a**) The "coral-like" lymph capillary plexus filled with lead oxide mixture in the mucosa of the oesophagus (superior portion). (**b**) A magnified view of the structure boxed in (**a**)

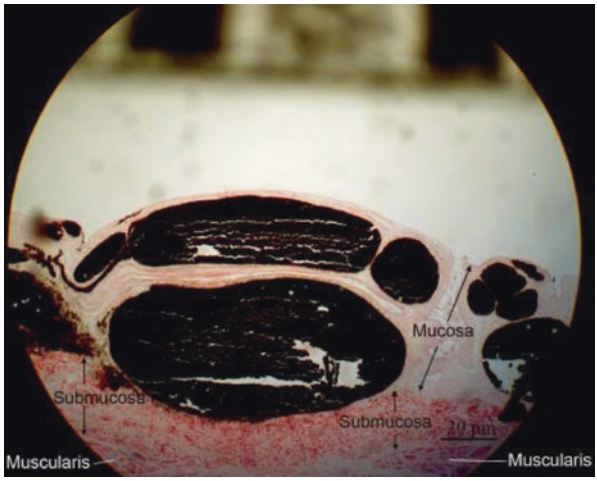

Fig. 2.64 The lymph capillary plexus filled with lead oxide mixture in the mucosa of the oesophagus. Histological section shows the different sizes of the vessels at different depths of the mucosa

Clinical Implication
Distribution of the lymph capillary vessels in the mucosa is extremely rich. They situate in the entire layer of the mucosa in different sizes and a 3D multi-level reticular formation. Similar to those found in the dermis, they have an important role in the immune defence mechanism which has been described (Roitt et al. 2003).

3.8 *Lymph Capillary Plexus in the Breast*

Lymph capillary vessels were found without valves in the subareola. They formed a three-dimensional polygonal plexus. The calibre of the vessels varied from as tiny as 0.014 to 0.2 mm. Vessels merged to become precollecting vessels and drained towards the axilla via the collecting lymph vessel (Fig. 2.65).

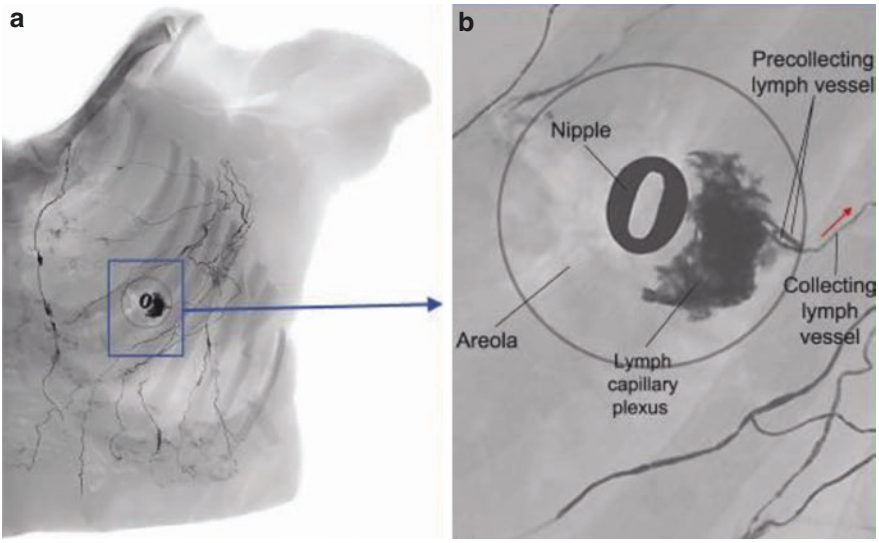

Fig. 2.65 (**a**) The lymph capillary plexus filled with lead oxide mixture in the subareola. (**b**) A magnified view of the *blue box* in (**a**). *Red arrow* indicates the direction of lymph flow

3.9 Abnormal Lymph Capillary Plexus (Figs. 2.66 and 2.67)

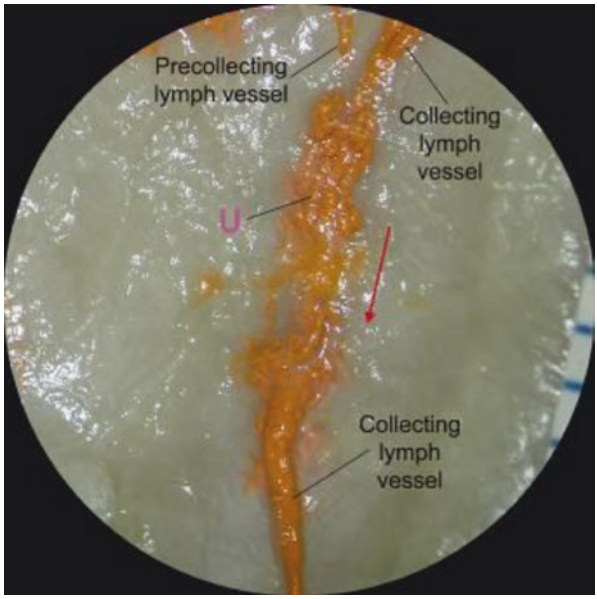

Fig. 2.66 The lymph capillary plexus (*U*) filled with lead oxide mixture in the parietooccipital galea layer. *Red arrow* indicates the direction of lymph flow

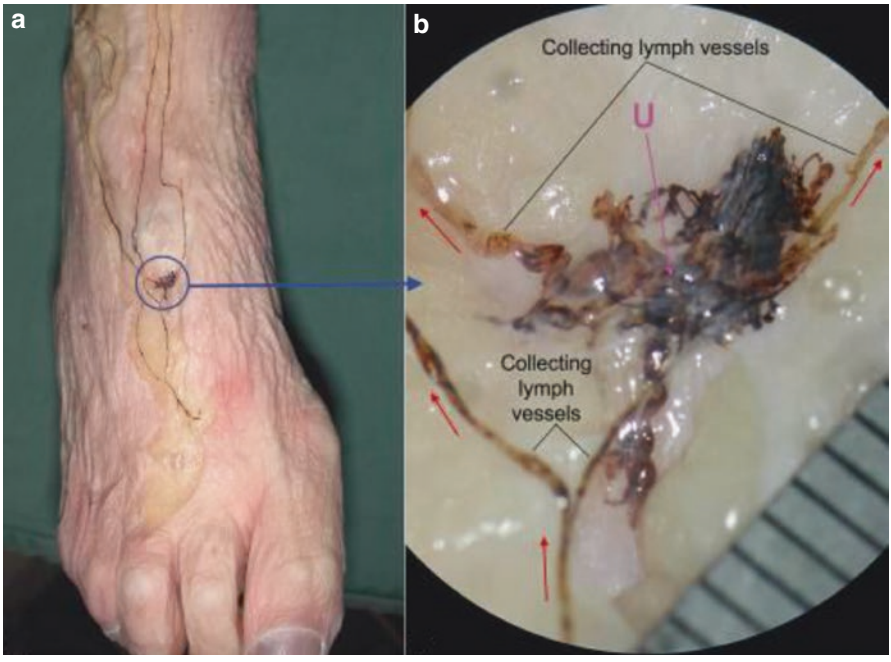

Fig. 2.67 (**a**) The lymph capillary plexus (*U*) filled with iodine mixture in the dorsum of the foot. (**b**) A magnified view of area circled in (**a**). *Red arrows* indicate the direction of lymph flow

Clinical Implication

Abnormal lymph capillary plexus was rare during the lymphatic dissection. Two of them were found during the entire study. They were small in sizes. One was 1 × 5 mm in the parietooccipital galea layer; the other one was 4 × 6 mm in the dorsum of the foot. Tiny vessels assembled irregularly connecting to either precollecting or collecting lymph vessels (Figs. 2.66 and 2.67). They may occur by two reasons: (1) congenital malformation of lymphatic capillary vessels (asymptomatic lymphangioma?) (Strigel 1996) and (2) acquired due to trauma (Zhang 1984).

4 Precollecting Lymph Vessels

Precollecting lymph vessels were seen to connect the lymph capillary plexus and collecting lymph vessels. They arose from the deep side of the dermis, mucosa, galea layer, etc. They travelled from the superficial to the deeper layer of the subcutaneous tissue in an ascending, descending, horizontal or looping manner and then drained into the collecting lymph vessels (Figs. 1.2, 1.3, 2.68, 2.69 and 2.70). The diameter of the precollecting lymph vessels varied from 0.1 to 0.3 mm in size when distended. The vessels contain lymphatic valves at 1 to 3 mm intervals giving the walls an irregular appearance similar to that of the bamboo trunk (Fig. 2.7).

In the scalp, two types of precollecting pathways were found. "Direct precollecting lymph vessel" arises from the lymph capillary plexus in the dermis or galea layer and directly links the collecting lymph vessels in the subcutaneous tissue (Figs. 1.2, 1.3 and 2.89). "Indirect precollecting lymph vessel (or bridge precollecting lymph vessel)" arises from the lymph capillary plexus in the dermis and crosses the subcutaneous tissue, bypasses collecting vessels to reach the galea layer where it merges with the other precollecting lymph vessels and then travels to the subcutaneous tissue again to link the collecting lymph vessels, which explains the lymphatic drainage between the dermis and the galea layer in the scalp (Figs. 1.2 and 2.89).

4.1 Direct Precollecting Lymph Vessels (Figs. 1.2, 1.3, 2.2, 2.3, 2.9 and 2.10, 2.50, 2.51, 2.52, 2.53, 2.54, 2.55, 2.56, 2.57, 2.58, 2.59, 2.60 and 2.65, 2.68, 2.69, 2.70, 2.71, 2.72, 2.73, 2.74, 2.75, 2.76, 2.77, 2.78, 2.79, 2.80, 2.81, 2.82, 2.83, 2.84, 2.85, 2.86, 2.87 and 2.88)

4.1.1 Head and Neck

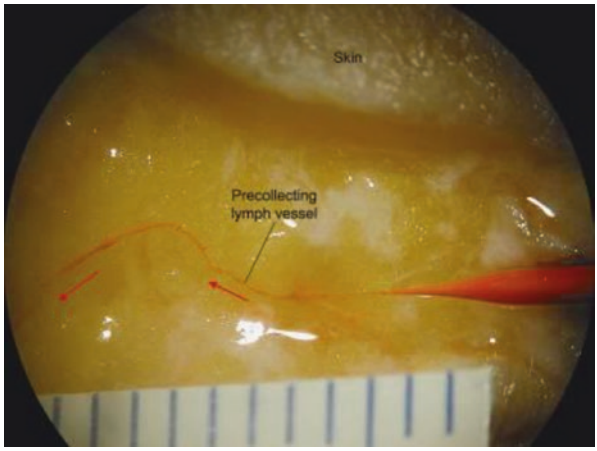

Fig. 2.68 A transverse precollecting lymph vessel injected by a fine glass needle filled with lead oxide mixture in the subdermis of the anterior neck. *Red arrows* indicate the direction of the lymph flow

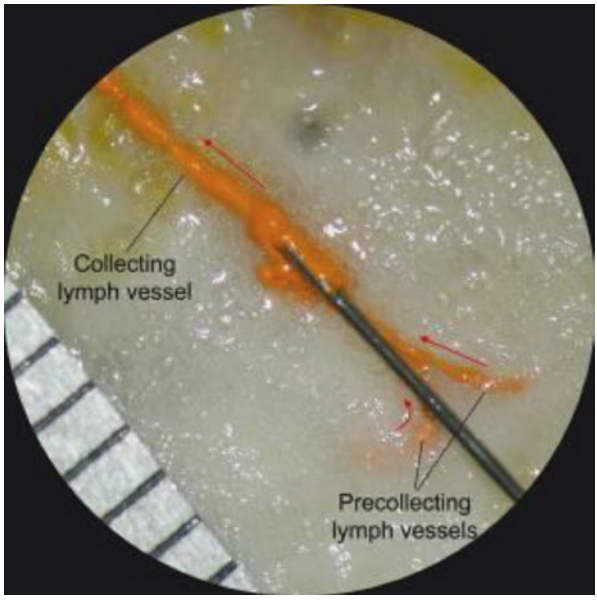

Fig. 2.69 A fine needle was inserted in a collecting lymph vessel in the yellowish subcutaneous of the scalp and filled with lead oxide mixture. Two precollecting lymph vessels were filled by retrograde perfusion in the whitish galea layer. *Red arrows* indicate the direction of the lymph flow

Fig. 2.70 A precollecting vessel in the dermis of the face next to the nose. *Red arrows* indicate the circuitous vessel pathway

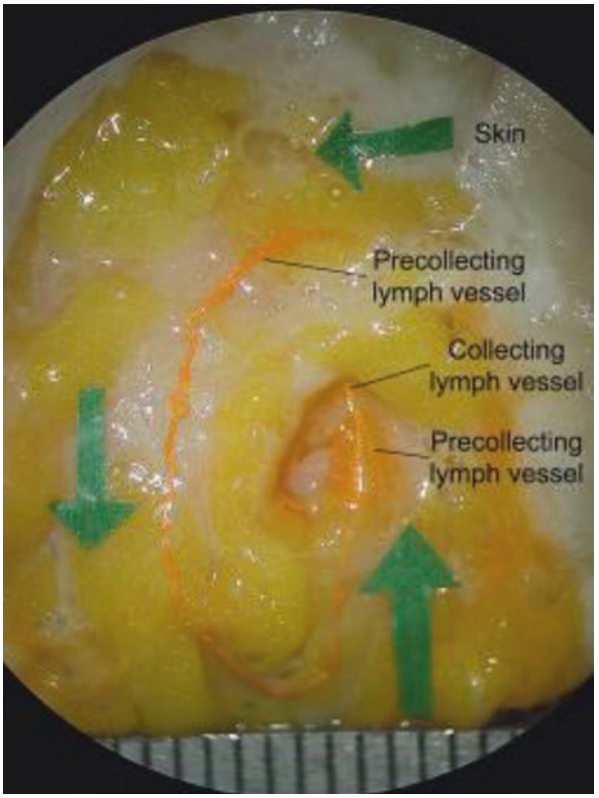

Fig. 2.71 A precollecting vessel in the dermis of the anterior neck. The looping vessel starts beneath the dermis and enters the deeper subcutaneous tissue to merge with another precollecting vessel before entering the collecting lymph vessel. *Green arrows* indicate the circuitous vessel pathway

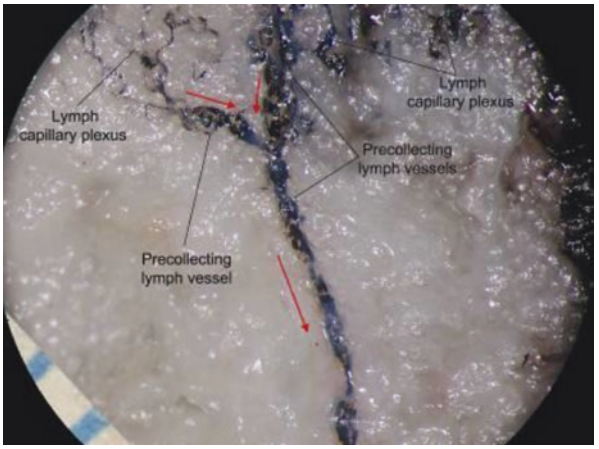

Fig. 2.72 Precollecting lymph vessels filled with Indian ink in the whitish galea layer of the parietal region of the head, viewed skin side down. *Red arrows* indicate the direction of the lymph flow

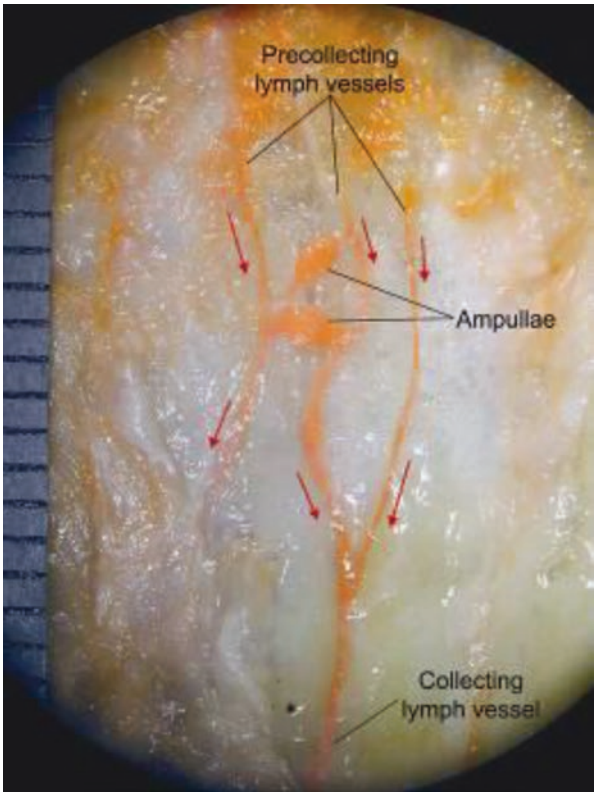

Fig. 2.73 Precollecting lymph vessels and ampullae in the whitish galea layer linked to a collecting lymph vessel in the yellowish subcutaneous tissue. Viewed from inner surface of the scalp

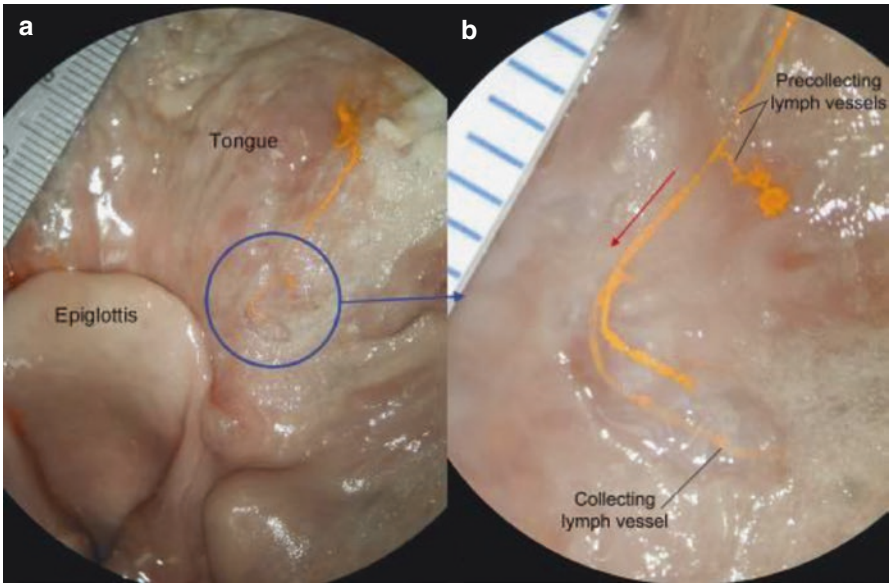

Fig. 2.74 (**a**) Precollecting lymph vessels in the mucosa on the root of the tongue. (**b**) A magnified view of the *area circled* in (**a**)

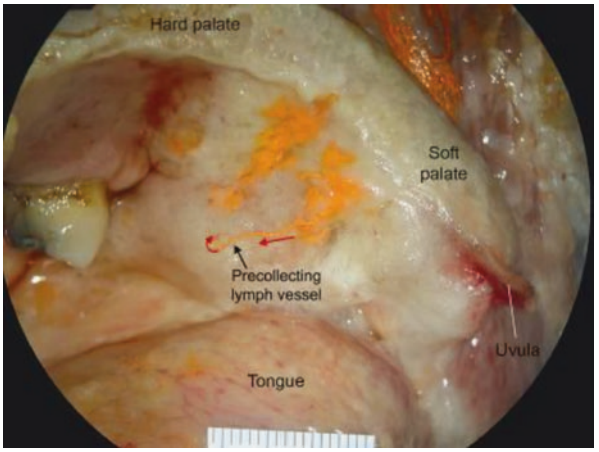

Fig. 2.75 Precollecting lymph vessels in the mucosa of the soft palate

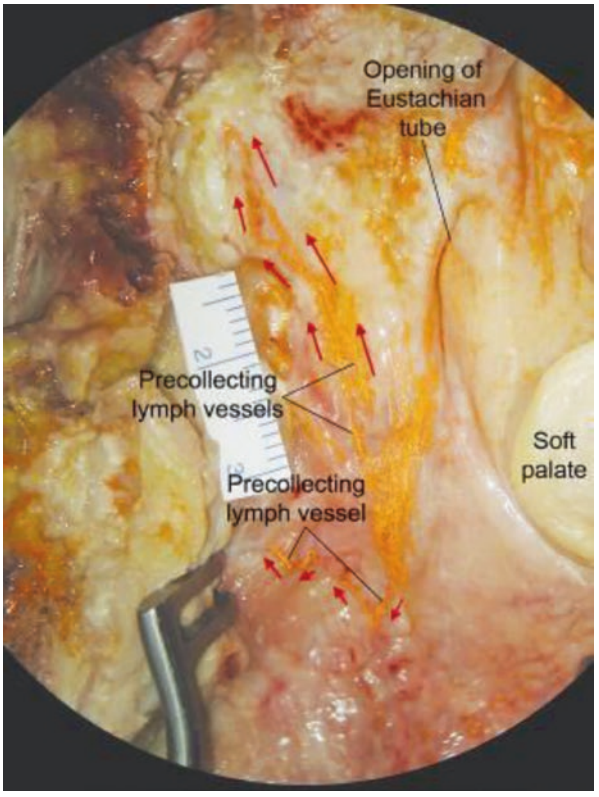

Fig. 2.76 Precollecting lymph vessels in the mucosa of the pharyngeal wall

4.1.2 Chest Wall

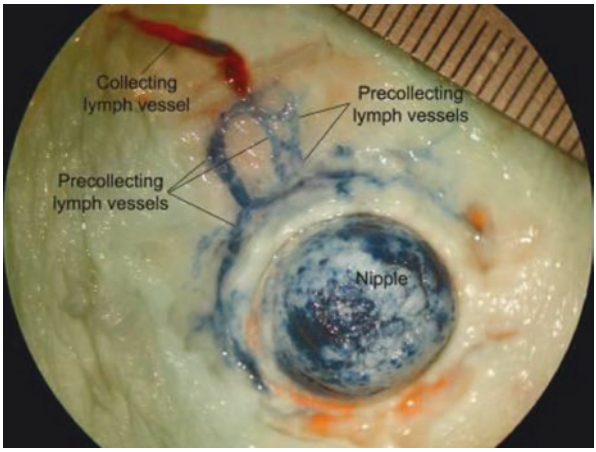

Fig. 2.77 Precollecting lymph vessels filled with ink mixture in the right subareola, linked to a collecting lymph vessel filled by lead oxide mixture in the subcutaneous of the right breast

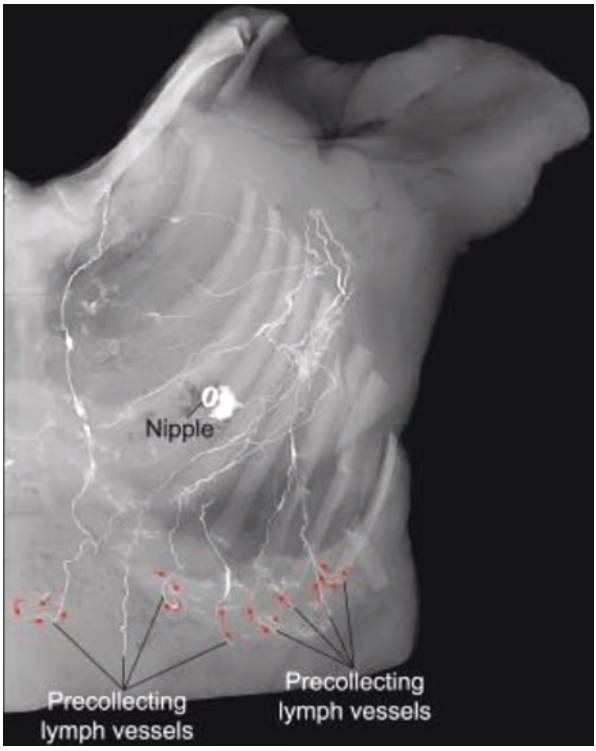

Fig. 2.78 Precollecting lymph vessels linked to collecting lymph vessels filled by lead oxide mixture in the left chest wall (radiological image). *Red arrows* indicate the direction of the lymph flows

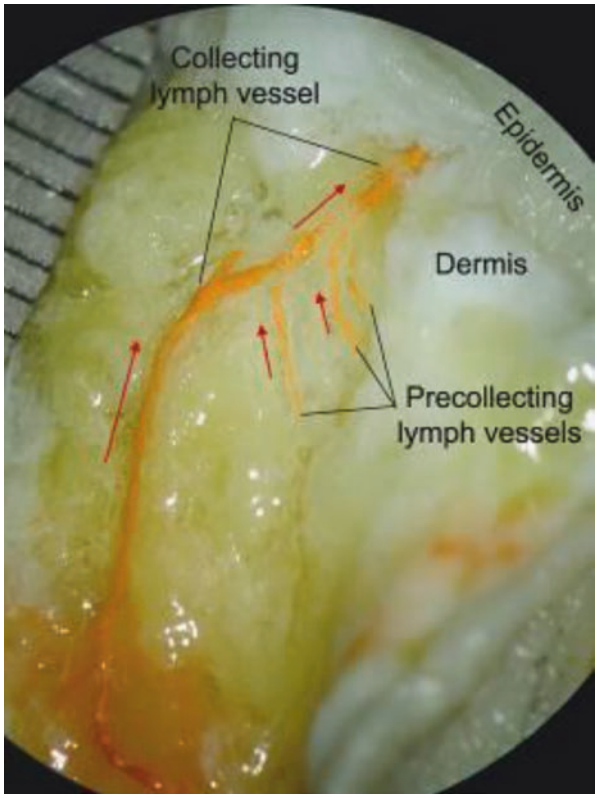

Fig. 2.79 Precollecting lymph vessels beneath the dermis linked to a collecting lymph vessel filled with lead oxide mixture in the left chest wall. *Red arrows* indicate the direction of the lymph flows

4.1.3 Upper Limb

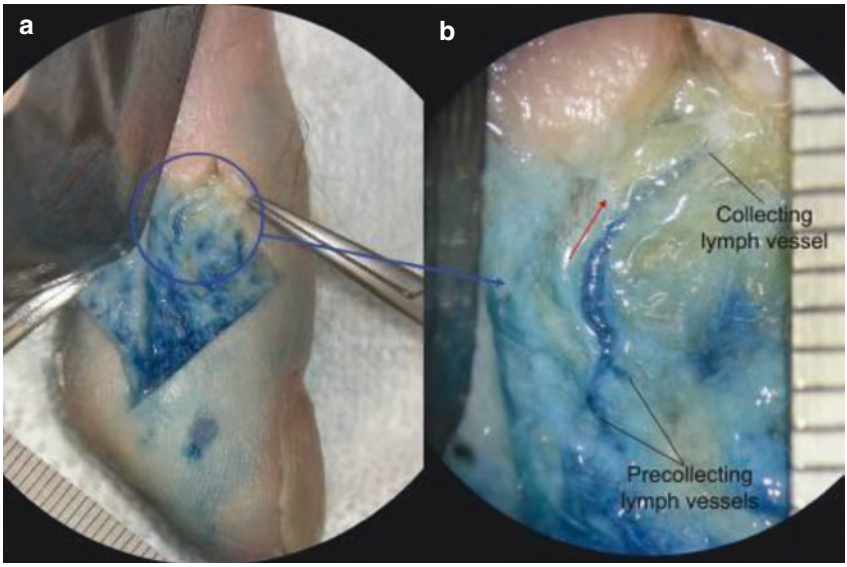

Fig. 2.80 (**a**) Precollecting lymph vessels filled with ink mixture in the dermis of the ulnar index finger. (**b**) A magnified view of the *area circled* in (**a**)

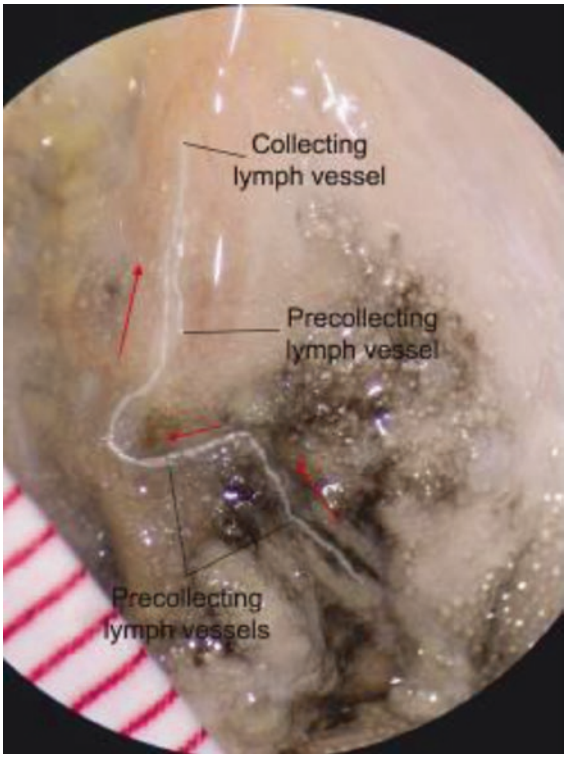

Fig. 2.81 Precollecting vessels filled by barium sulphate mixture beneath the dermis of the dorsum of the left hand. *Red arrows* indicate the direction of the lymph flow

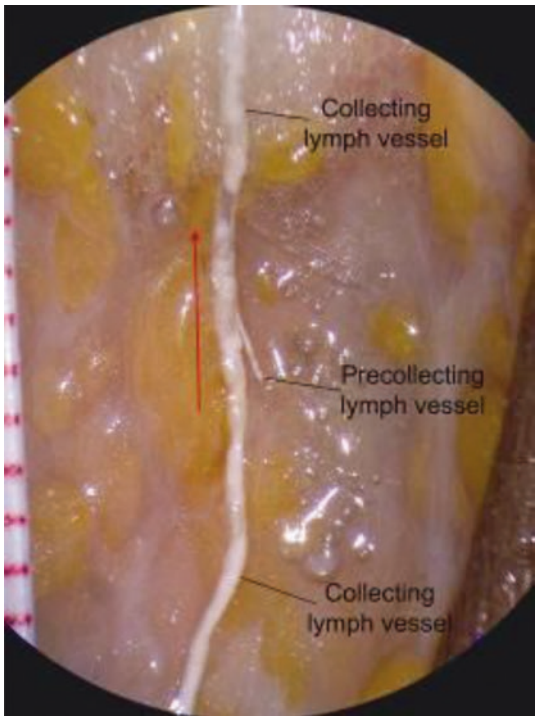

Fig. 2.82 A precollecting lymph vessel draining into a collecting vessel in the subcutaneous tissue of the left radial forearm. Vessels filled by barium sulphate mixture. *Red arrow* indicates the direction of the lymph flow

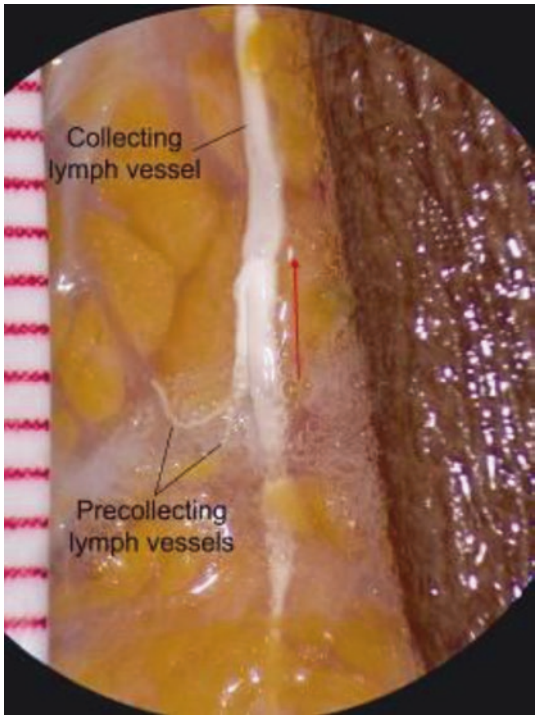

Fig. 2.83 Precollecting lymph vessels draining into a collecting vessel in the subcutaneous tissue of the left cubital fossa. *Red arrow* indicates the direction of the lymph flow

4.1.4 Lower Limb

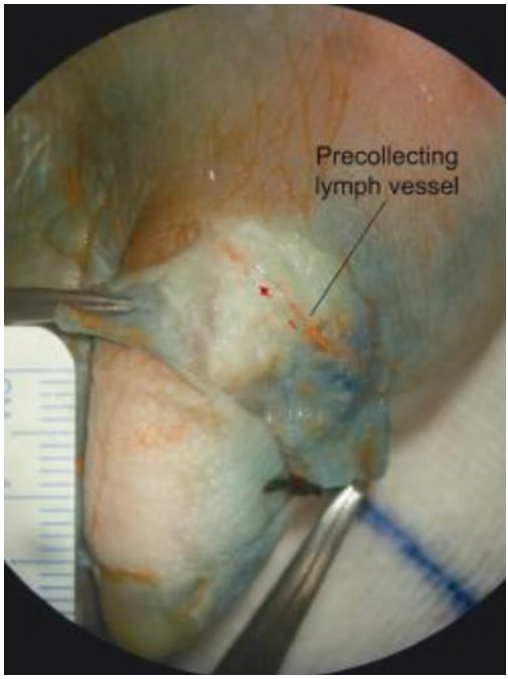

Fig. 2.84 A precollecting vessel filled by lead oxide mixture beneath the dermis in the dorsum of the left little toe. *Red arrows* indicate the direction of the lymph flow

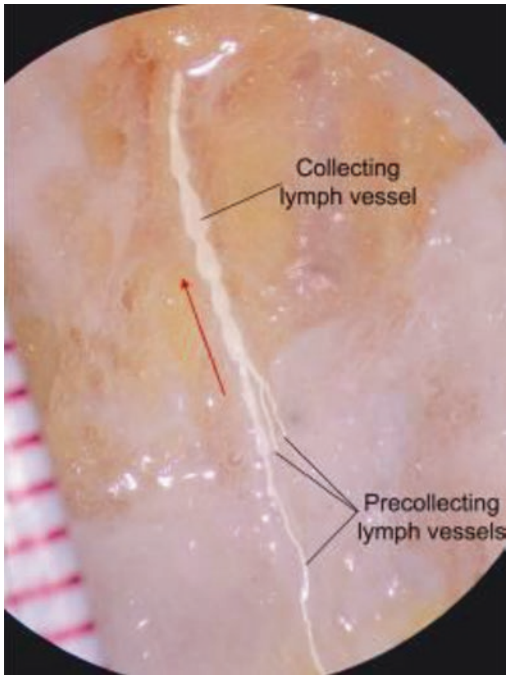

Fig. 2.85 Precollecting lymph vessels beneath the dermis draining to a collecting vessel in the subcutaneous tissue of the right lateral malleolus. Vessels filled with barium sulphate mixture. *Red arrow* indicates the direction of the lymph flow

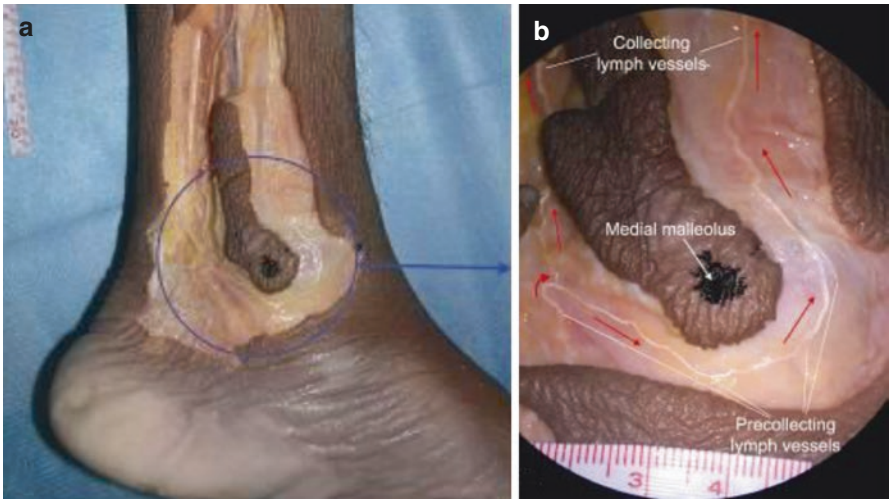

Fig. 2.86 (**a**) Precollecting lymph vessels beneath the dermis around the medial malleolus. (**b**) A magnified view of the *area circled* in (**a**). Vessels filled with barium sulphate mixture. *Red arrows* indicate the direction of the lymph flow

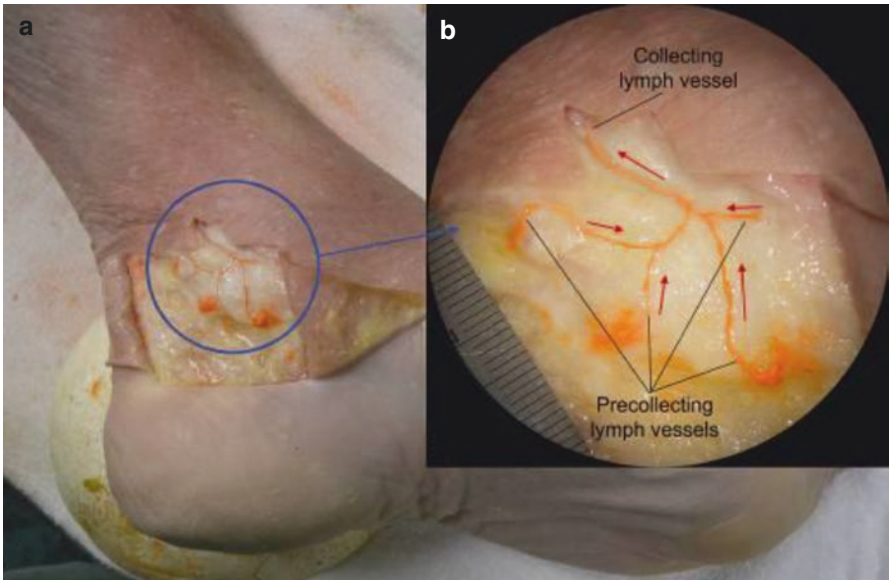

Fig. 2.87 (**a**) Precollecting lymph vessels beneath the dermis around the medial malleolus. (**b**) A magnified view of the *area circled* in (**a**). Vessels filled with lead oxide mixture. *Red arrows* indicate the direction of the lymph flow

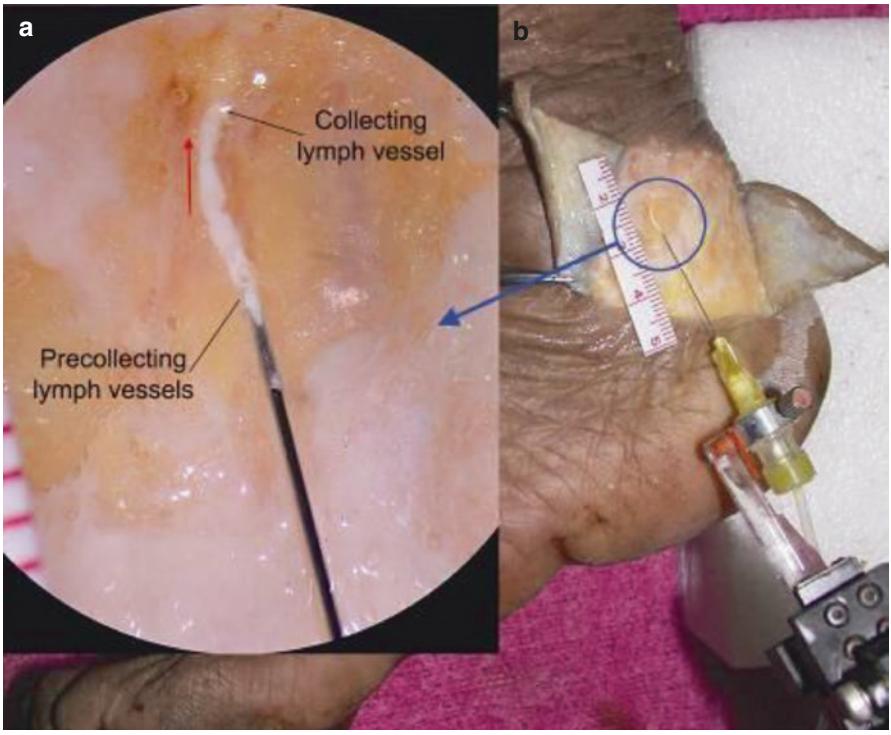

Fig. 2.88 A precollecting lymph vessel filled with barium sulphate mixture beneath the dermis behind the lateral malleolus. (**a**) A magnified view of the *area circled* in (**b**). *Red arrow* indicates the direction of the lymph flow

4.2 *Indirect (Bridge) Precollecting Lymph Vessels*

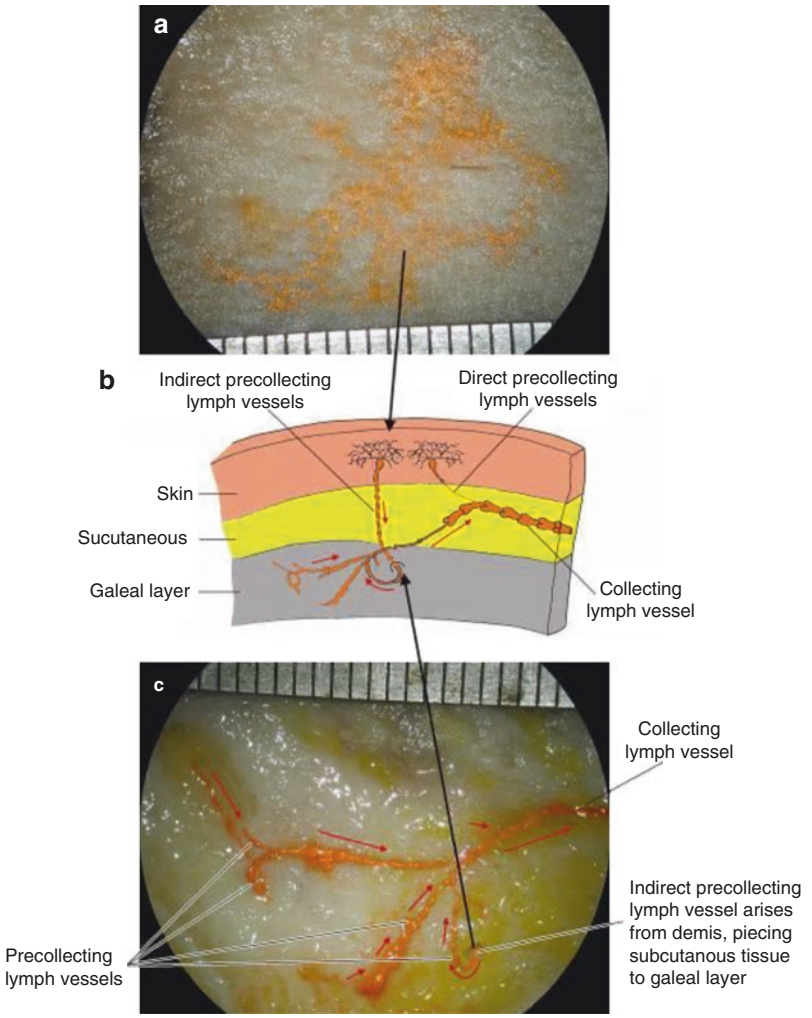

Fig. 2.89 (**a**) The lymph capillary plexus in the dermis of the scalp filled with lead oxide mixture, viewed from the skin. (**b**) The lymph capillary plexus of the dermis converges an indirect precollecting lymph vessel that crosses the subcutaneous and runs towards the galea, where it converges with the other precollectors that drain into the lymph-collecting vessel. (**c**) Lymphatic vessels are viewed from the galea layer. *Red arrows* indicate the direction of the lymph flow

Clinical Implication
During surgical treatment for patients with scalp cancer, the full thickness of the scalp should be resected, as the presence of indirect precollecting lymph vessels that connect lymphatics in the dermis and galea layer could result in cancer cells spreading to the deeper tissue.

5 Collecting Lymph Vessel

With numerous valves in the lumen, collecting lymph vessels were seen to connect precollecting lymph vessels and lymphatic trunks, running tortuously in the subcutaneous and submucosal tissues. During their centripetal courses, vessels branch or diverge, converge and sometimes undergo anastomosis with or cross over neighbouring vessels. Vessels are known as the afferent, the internodal (the vessel between the lymph nodes) and the efferent lymph vessels according to their relation with lymph nodes (Figs. 1.1, 1.4 and 1.5).

5.1 Afferent, Internodal and Efferent Collecting Lymph Vessels

The afferent collecting lymph vessels carry lymph into the lymph node.

The efferent collecting lymph vessels drain lymph away from the lymph node.

The internodal collecting lymph vessels can be the efferent vessel of the distal node or the afferent vessel of the proximal node (Figs. 2.90, 2.91, 2.92, 2.93, 2.94 and 2.95).

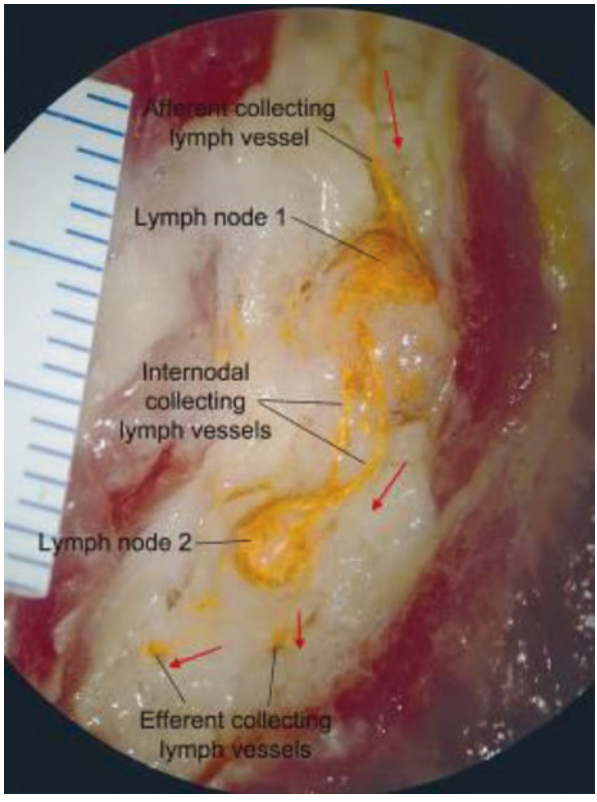

Fig. 2.90 The relationship of the afferent, intermodal and efferent collecting lymph vessels and lymph nodes in the left preauricular region. The internodal lymph vessels are efferent vessels to the lymph node 1 and afferent vessels to the lymph node 2. The lymph node 1 has a single afferent vessel that divides into several vessels before inserting into the node and multiple efferent vessels. The lymph node 2 has multiple afferent and efferent vessels

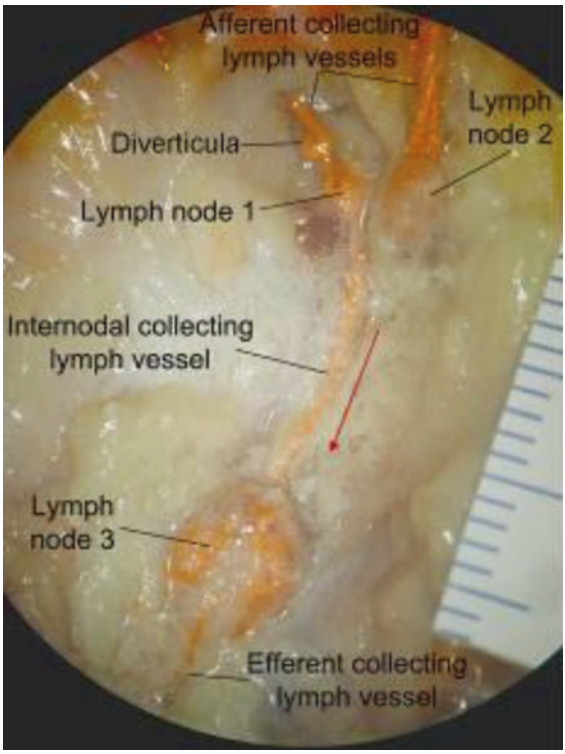

Fig. 2.91 The relationship of the afferent, intermodal and efferent collecting lymph vessels and lymph nodes in the right retroauricular region. The internodal lymph vessels are efferent vessels to lymph nodes 1 and 2 and the afferent vessel to the lymph node 3

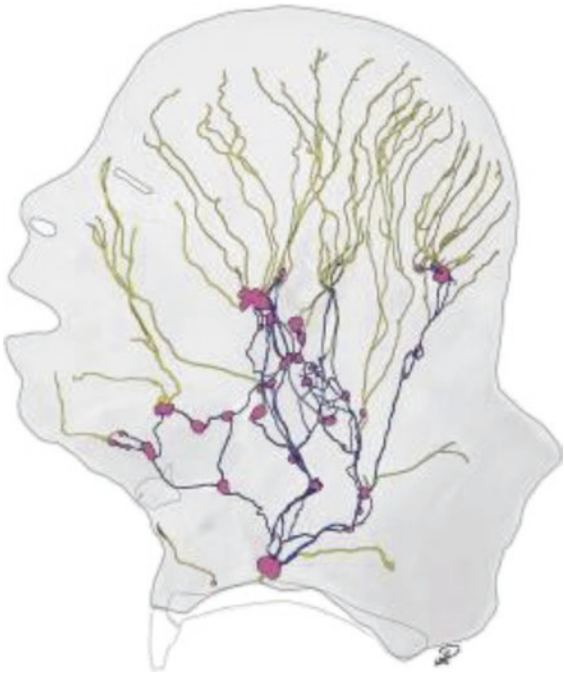

Fig. 2.92 Inversed lymphangiogram of the superficial tissue of the head and neck following lymphatic contrast injection. *Yellow* afferent lymph vessels, *blue* internodal lymph vessels, *green* efferent lymph vessels, *purple* lymph nodes

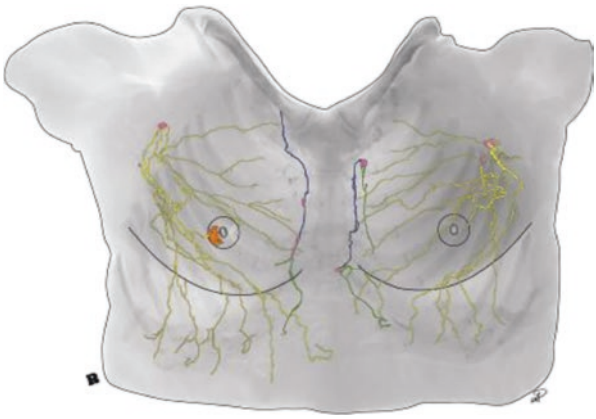

Fig. 2.93 Inversed lymphangiogram of the anterior upper torso following lymphatic contrast injection. *Orange* lymphatic plexus in the periareolar region, *yellow* afferent lymph vessels in the superficial tissue of the chest, *green* afferent lymph vessels of the internal thoracic, *blue* internodal lymph vessels of the internal thoracic, *purple* lymph nodes

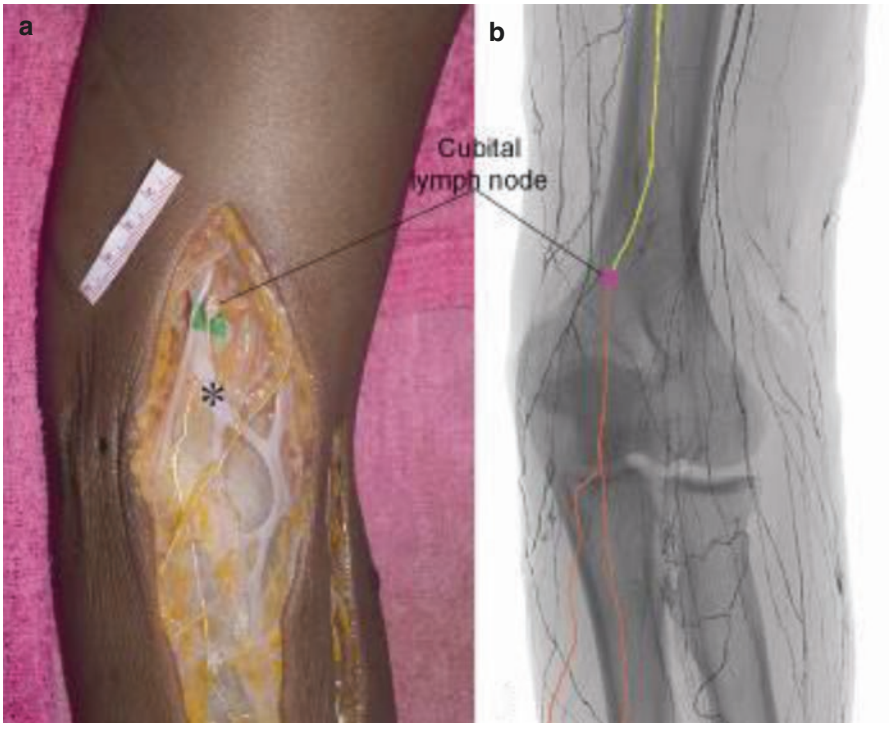

Fig. 2.94 The relationship of collecting lymph vessels, lymph node and veins in the superficial tissue of the left elbow after a lymphatic contrast injection of barium sulphate mixture. (**a**) Photograph shows the collecting lymph vessels (*white*), veins (*) and the cubital lymph node. (**b**) Inversed lymphangiogram shows an afferent vessel (*orange*) entering the cubital lymph node (*purple*) and an intermodal vessel (*yellow*) leaving the node and continuing its course to reach the axillary lymph node (unrevealed). The other vessels around the elbow bypass the cubital lymph node

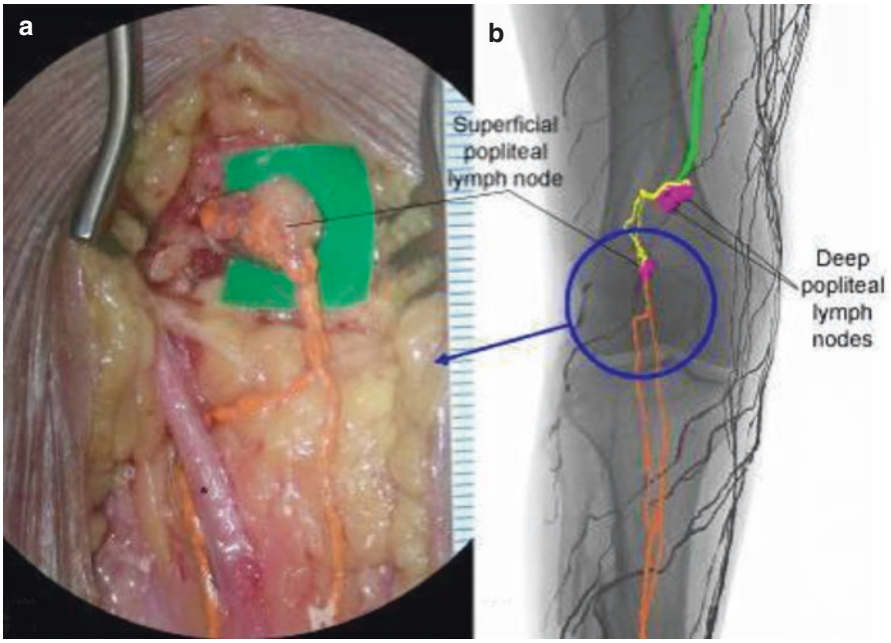

Fig. 2.95 (**a**) A magnified image from the *circled area* in the right radiograph. Lymphatic vessels after lead oxide mixture injection around the small saphenous vein (*) in the popliteal fossa entering the superficial popliteal lymph node. (**b**) A posteroanterior view of an inverted radiograph showing the lymphatic distribution in the knee region. Posterior lymph vessels (afferent) are represented in *orange*, internodal lymph vessels are represented in *yellow* and femoral lymph vessels are represented in *green*

Note
Internodal collecting lymph vessels can link lymph nodes either within the superficial group (Figs. 2.90, 2.91 and 2.92) or the deep group (Figs. 2.93 and 2.95), otherwise from the superficial to deep groups (Figs. 2.94 and 2.95).

5.2 *Morphology*

The diameter of collecting lymph vessels varied. The calibre was small distally and larger proximally; ranges were usually from 0.1 to 1.0 mm in afferent vessels, 0.1 to 1.5 mm in internodal vessels and 0.2 to 2 mm in efferent vessels. Different sized vessels were found in the same area (Figs. 2.96, 2.97, 2.98, 2.99, 2.100 and 2.101). The size of vessels changed along their courses. Usually afferent vessels were long, while internodal and efferent vessels were short. Collecting lymph vessels resembled bamboo trunks or a string of beads depending on the ratio of interval length of valves and the diameter of the vessel (Fig. 2.7).

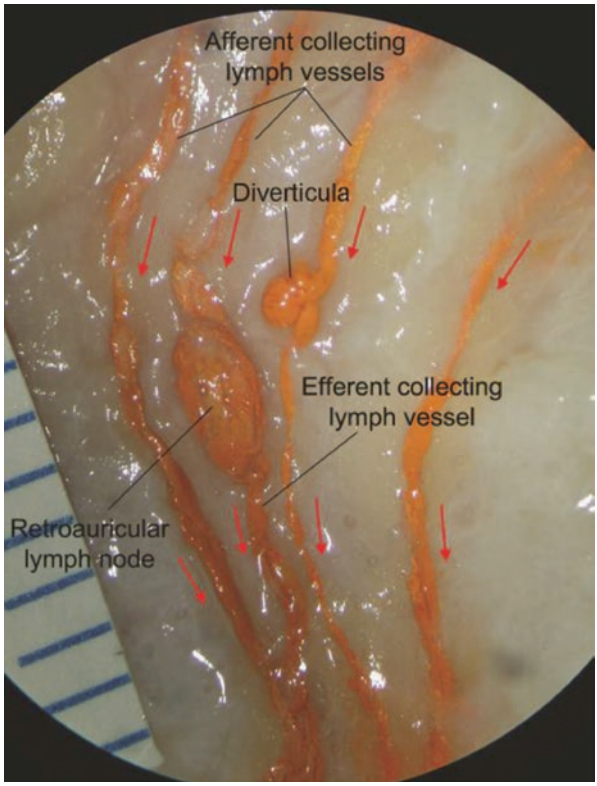

Fig. 2.96 Different calibre of collecting lymph vessels filled with lead oxide mixture in the left retroauricular area. One afferent vessel enters the retroauricular lymph node and an efferent vessel leaves it. The other three vessels bypass the node. *Red arrows* indicate the direction of the lymph flow

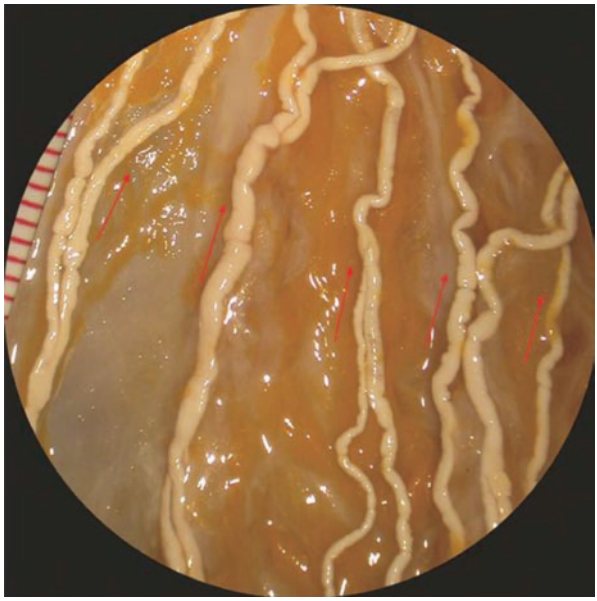

Fig. 2.97 Different calibre of collecting lymph vessels filled with barium sulphate mixture in the integument of the medial thigh. *Red arrows* indicate the direction of the lymph flow

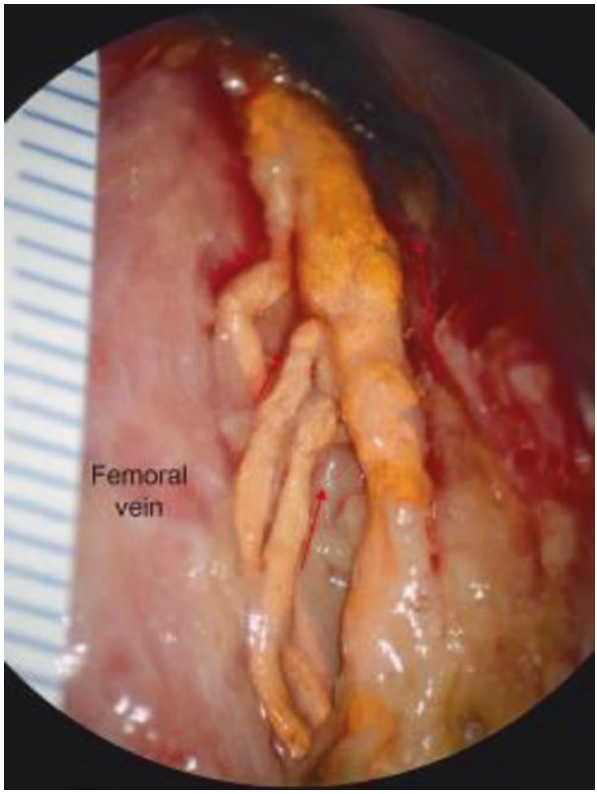

Fig. 2.98 Three small collecting lymph vessels entering a larger vessel next to the femoral vein in the left thigh. Lymphatic vessels were filled with lead oxide mixture. *Red arrows* indicate the flow of the lymph

Fig. 2.99 Different calibre of collecting lymph vessels filled with lead oxide mixture in the integument of the left posterior forearm. Four collecting lymph vessels formed an "X-shaped" connection. *Red arrows* indicate the direction of the lymph flow

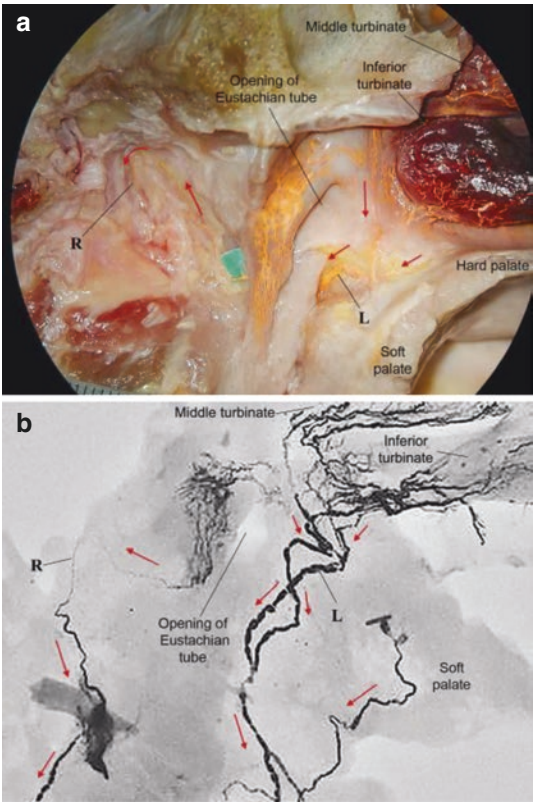

Fig. 2.100 Different calibre of lymph vessels filled with lead oxide mixture in the left nasopharyngeal area. One small collecting lymph vessel (*R*) travelling in the posterior space of the pharyngeal wall and one lager vessel (*L*) travelling in the lateral space of the pharyngeal wall. (**a**) A photograph under a microscope. (**b**) An inversed lymphangiogram. *Red arrows* indicate the direction of the lymph flow

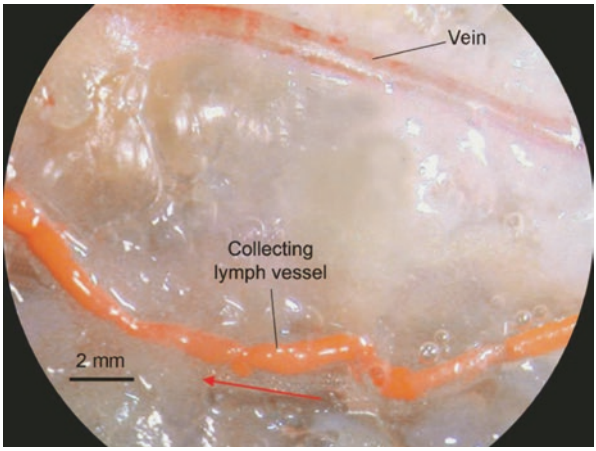

Fig. 2.101 Comparison of a collecting lymph vessel and a similar-sized vein in the dorsum of the right hand. The collecting lymph vessel filled with lead oxide mixture, showing multiple valves and resembling a bamboo-trunk fashion. The small vein inflated by hydrogen peroxide with a relatively straight wall and containing blood. Red arrow indicates the direction of the lymph flow

Clinical Implication

Lymphaticovenous anastomoses have been performed to treat secondary lymphoedema of extremities in microsurgery (Liu 2013). To understand the morphological characteristics of the collecting lymph vessels may help with recognizing the lymphatic vessel and the vein during surgery (Fig. 2.101).

5.3 Communicating Branches (Figs. 2.102, 2.103, 2.104, 2.105, 2.106, 2.107 and 2.108)

Fig. 2.102 Two collecting lymph vessels formed an "H-shaped" connection by a communicating branch in the left temporal of the head. *Red arrows* indicate the direction of the lymph flow

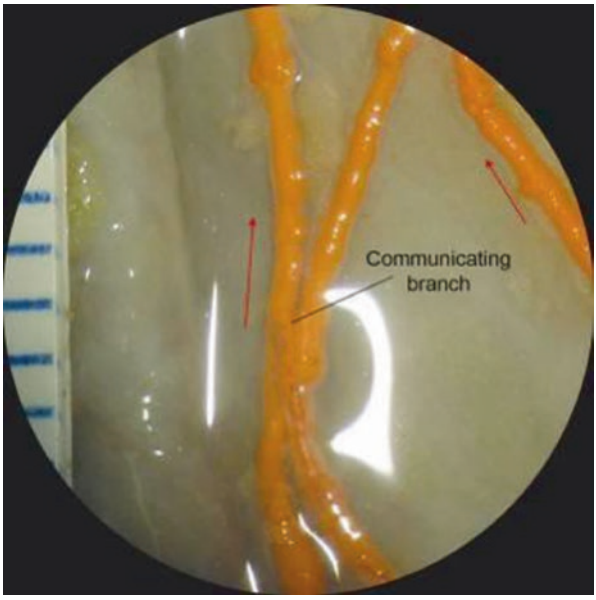

Fig. 2.103 Two collecting lymph vessels formed an "X-shaped" connection by a short communicating branch in the dorsum of the right hand. *Red arrows* indicate the direction of the lymph flow

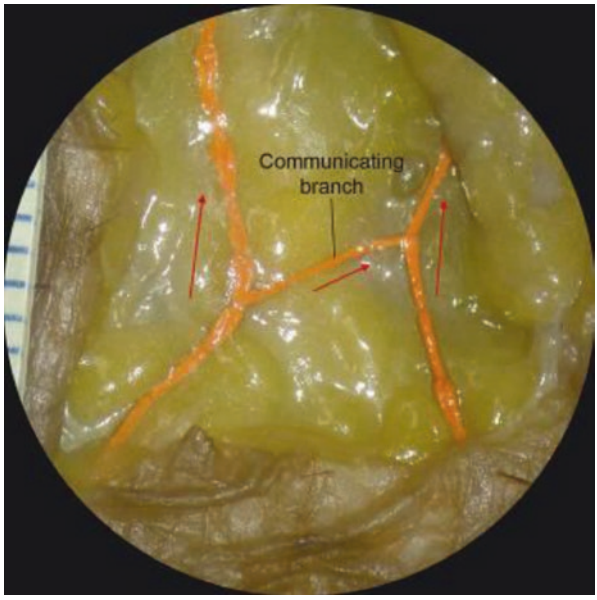

Fig. 2.104 Two collecting lymph vessels formed an "H-shaped" connection by a communicating branch in the left posterior forearm. *Red arrows* indicate the direction of the lymph flow

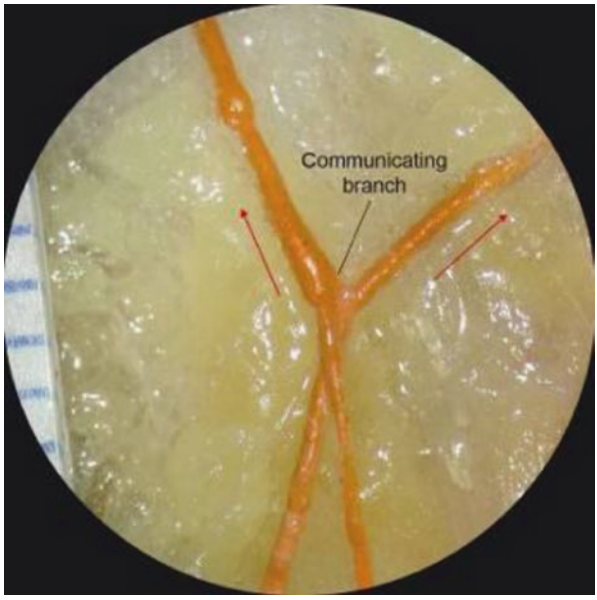

Fig. 2.105 Two collecting lymph vessels formed an "X-shaped" connection by a short communicating branch in the medial side of the right upper arm. *Red arrows* indicate the direction of the lymph flow

Fig. 2.106 Two collecting lymph vessels formed an "H-shaped" connection by a communicating branch in the medial side of the left leg. *Red arrows* indicate the direction of the lymph flow

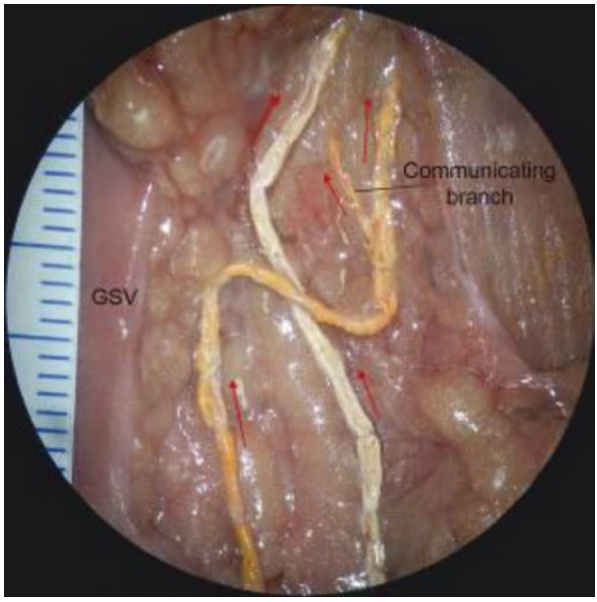

Fig. 2.107 Two collecting lymph vessels formed an "X-shaped" connection by a communicating branch next to the great saphenous vein (*GSV*) in the medial side of the left thigh. *Red arrows* indicate the direction of the lymph flow

Fig. 2.108 Two collecting lymph vessels formed an "H-shaped" connection by a short communicating branch in the medial side of the right upper arm. *Red arrows* indicate the direction of the lymph flow

Clinical Implication
The presence of the communicating branch, on the one hand, can direct the lymph draining into one vessel when the other one vessel is blocked; on the other hand, it may provide a metastasis pathway in cancer patients.

5.4 *Connection Types and Bypass Routes Between Collecting Lymph Vessels and Lymph Nodes*

5.4.1 Connection Types

It has been usually described that the lymph node connects multiple afferent and single efferent vessels in textbooks (Fig. 1.4). From recent study, four connection types have been noticed (Pan et al. 2010a, b, c). The number of vessels entering and exiting lymph nodes is different. Some nodes connect multiple afferent and single efferent vessels (Type A); some had multiple afferent and multiple efferent vessels (Type B); some had a single afferent and a single efferent vessels (Type C); and others had a single afferent and multiple efferent vessels (Type D) (Figs. 2.90, 2.91, 2.92, 2.93, 2.94, 2.95, 2.96, 2.109, 2.110, 2.111 and 2.112).

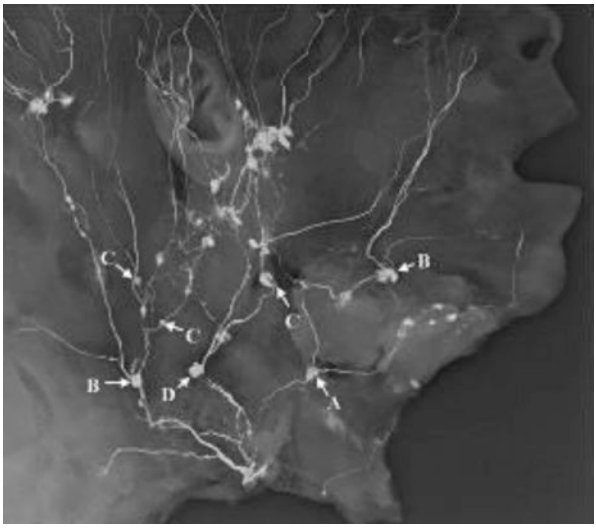

Fig. 2.109 A radiograph of the head and neck region after lead oxide mixture injected, showing the relationship of afferent, efferent lymph vessels and lymph nodes. *Type A* lymph node with multiple afferent and single efferent vessels. *Type B* lymph nodes with both multiple afferent and efferent vessels. *Type C* lymph nodes with both a single afferent and efferent vessels. *Type D* lymph node with a single afferent and multiple efferent vessels

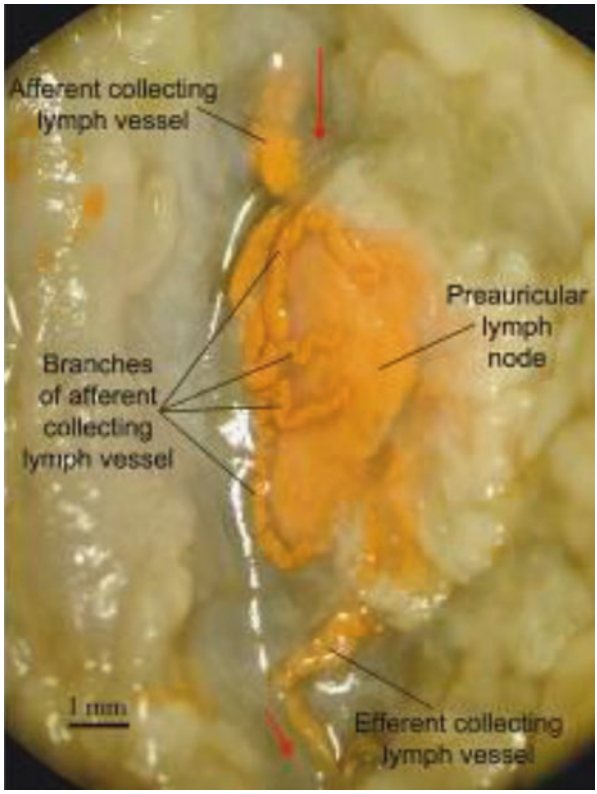

Fig. 2.110 The relationship of afferent, efferent lymph vessels and the preauricular lymph node after being filled with lead oxide mixture. Note that the afferent vessel is divided into several branches before entering the node. *Red arrows* indicate the direction of the lymph flow

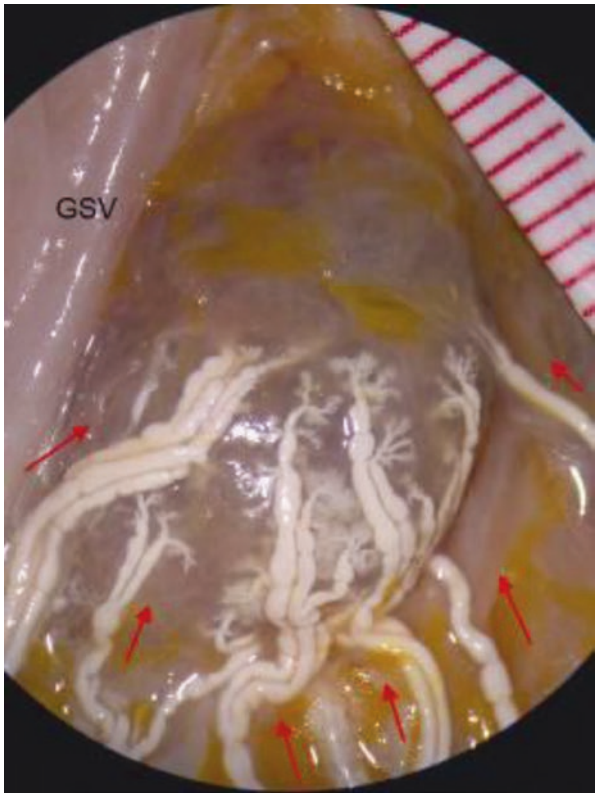

Fig. 2.111 The connections of afferent lymph vessels and the left superficial inguinal lymph node. Vessels have been filled with barium sulphate mixture. Note afferent lymph vessels divided into many branches before entering the node. *Red arrows* indicate the direction of the lymph flow. *GSV* great saphenous vein

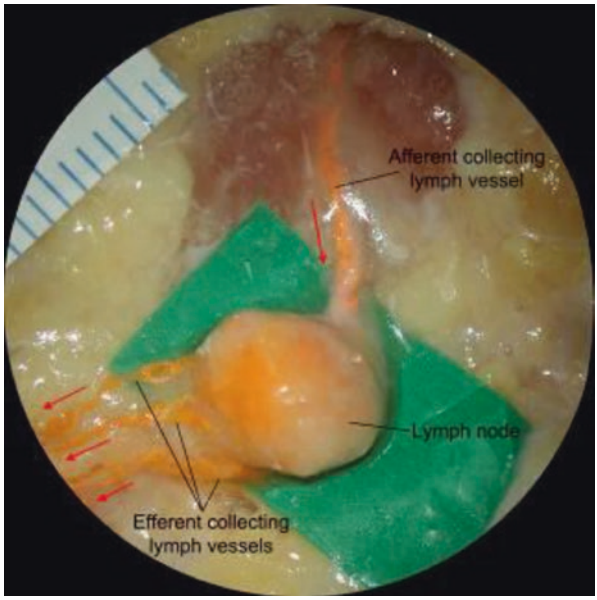

Fig. 2.112 Specimen of the right neck showing a lymph node with a single afferent and multiple efferent vessels after an injection of lead oxide mixture. *Red arrows* indicate the direction of the lymph flow

5.4.2 Bypass Routes

Collecting lymph vessels did not always enter the nearest lymph nodes but sometimes bypassed them (Figs. 2.96, 2.113 and 2.114).

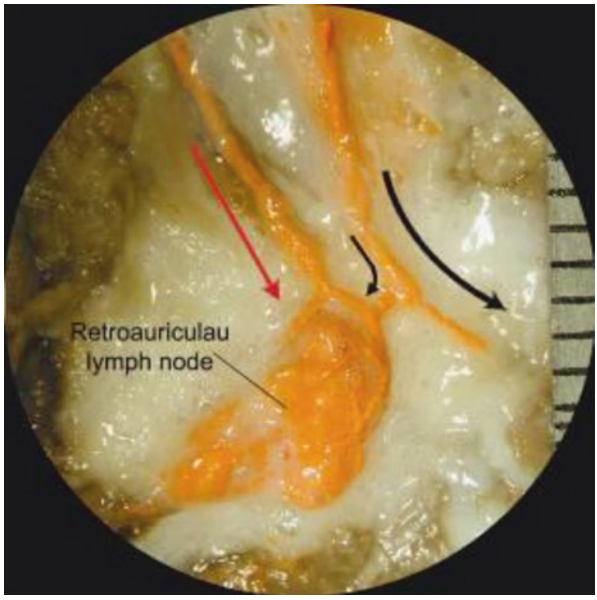

Fig. 2.113 Two lymphatic vessels approach the first-tier lymph node. One lymph vessel (*red arrow*) entering the node. The other one (*black arrow*) divides into two smaller braches. One enters the node and one bypasses it

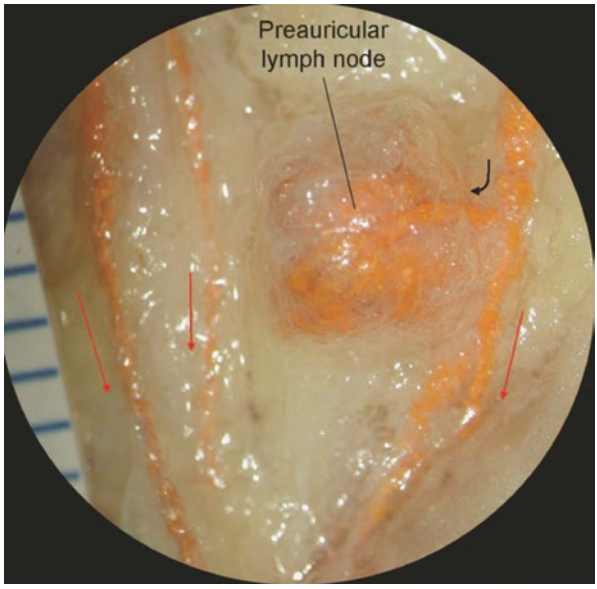

Fig. 2.114 Of multiple lymph vessels surrounding the preauricular lymph node, only one (*black arrow*) enters the lymph node; others (*red arrows*) bypass it

Clinical Implication
It may provide pathways of distant metastasis in cancer patients due to the presence of the lymphatic bypass routes. In these patients, cancer cells may not only enter the nearest lymph nodes but also the distant sites. Using lymphoscintigraphy and sentinel lymph node biopsy may reduce the risk of postoperative lymphatic metastasis and increase the clinical efficacy (Thompson et al. 2004).

5.5 *Relationship Between Collecting Lymphatic and Blood Vessels*

Lymphatic vessels run parallel to blood vessels, intertwine with them and cross over or under them anteriorly and posteriorly (Figs. 2.115, 2.116, 2.117, 2.118, 2.119, 2.120, 2.121, 2.122 and 2.123).

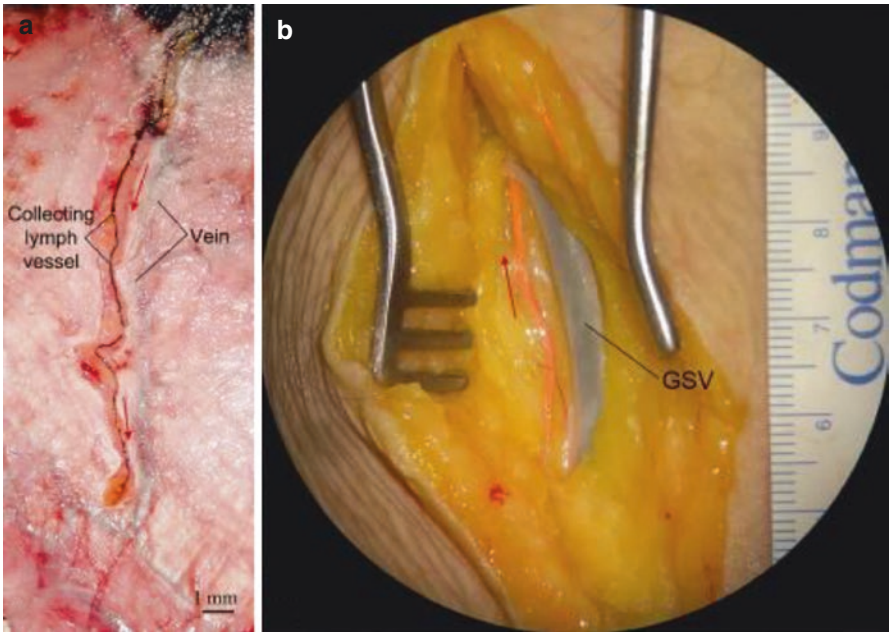

Fig. 2.115 (**a**) A collecting lymph vessel filled with Indian ink travelling parallel to a vein in the galea layer. (**b**) A collecting lymph vessel filled with lead oxide mixture travelling parallel to the great saphenous vein (*GSV*) in the left thigh

Fig. 2.116 Collecting lymph vessels filled with lead oxide mixture crossing over metacarpal veins (*V*) of the left hand

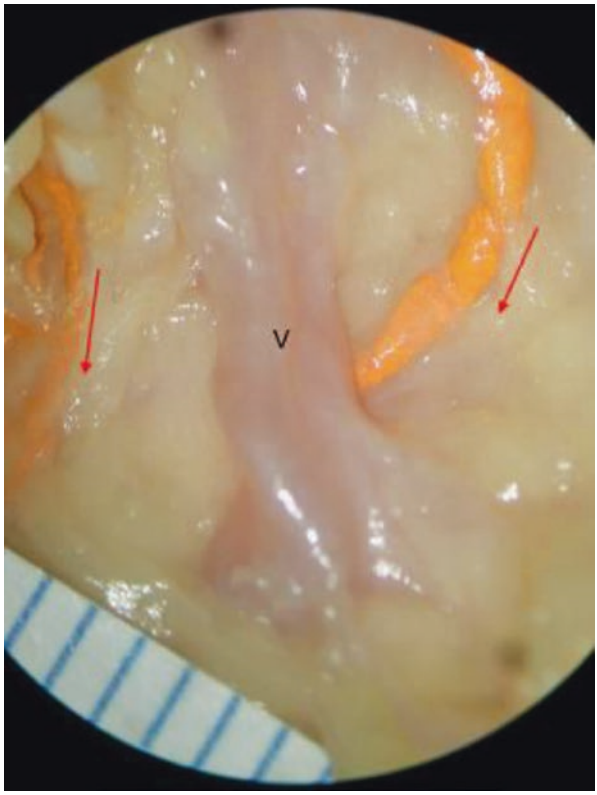

Fig. 2.117 A collecting lymph vessel filled with lead oxide mixture goes under a vein (*V*) in the scalp

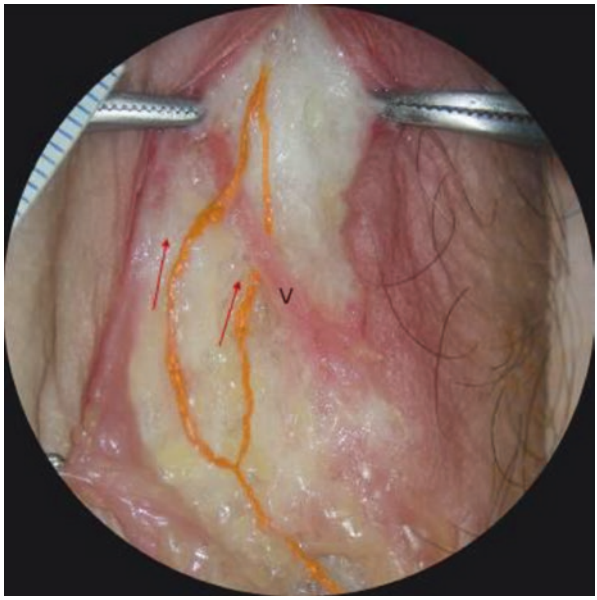

Fig. 2.118 Two lymphatic vessels divided by a collecting lymph vessel passing over and under a dorsal vein (*V*) of the right foot

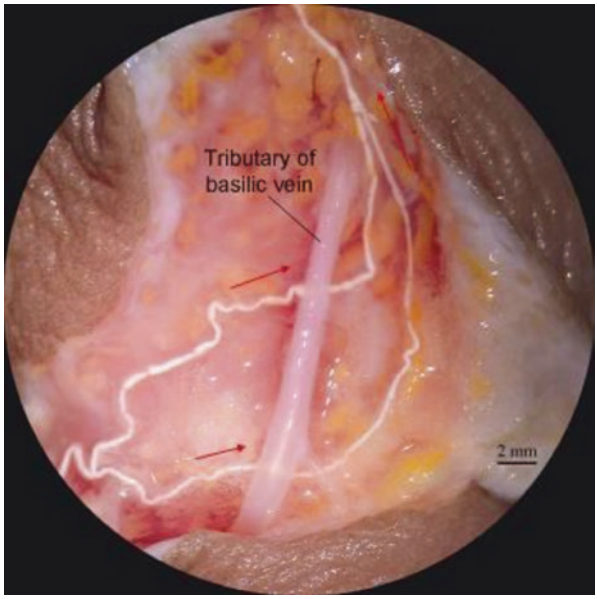

Fig. 2.119 Two lymphatic vessels divided by a collecting lymph vessel passing under a tributary of the basilic vein in the wrist. Lymphatic vessels were filled with barium sulphate mixture

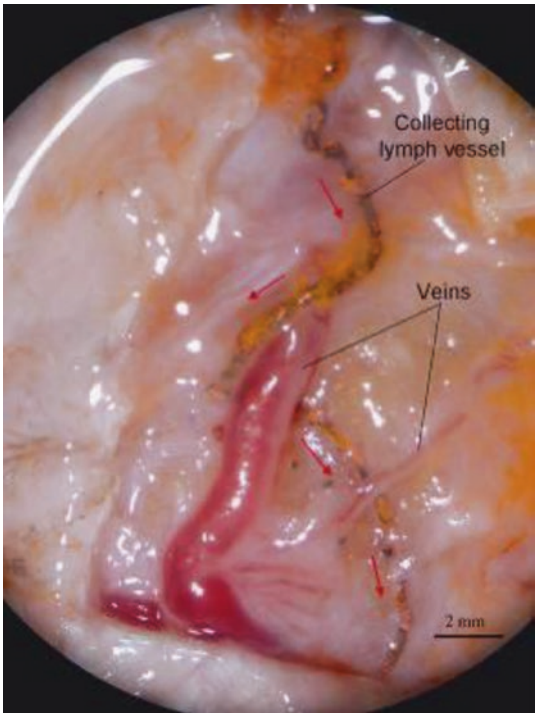

Fig. 2.120 A collecting lymph vessel filled with lead oxide mixture intertwining with veins in the scalp. *Red arrows* indicate the direction of the lymph flow

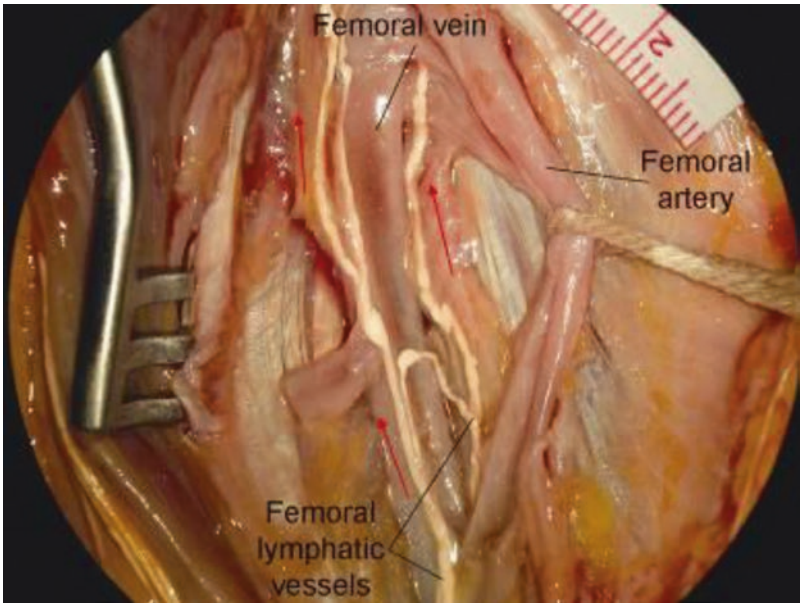

Fig. 2.121 Collecting lymph vessels filled with barium sulphate mixture travelling alongside the femoral artery and vein in the thigh. *Red arrows* indicate the direction of the lymph flow

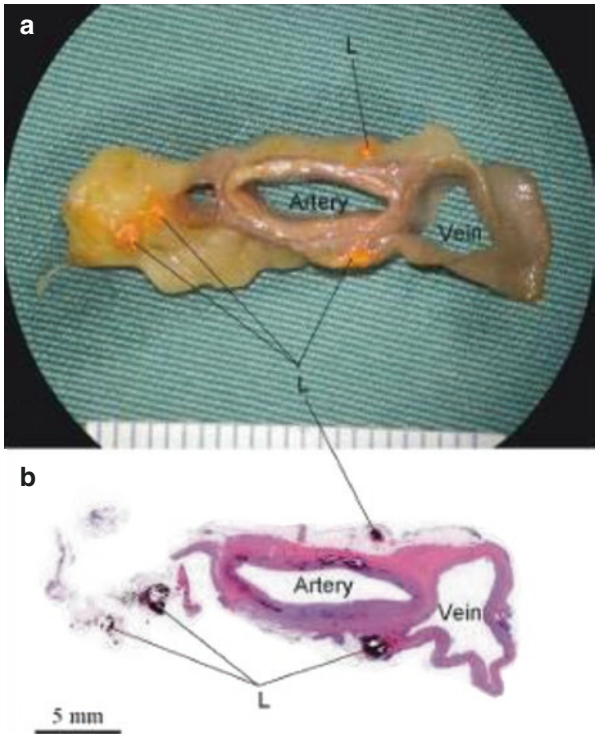

Fig. 2.122 (**a**) Cross-section of the femoral artery, vein and lymphatic (*L*) vessels. (**b**) Histology section and H&E staining. Lymph vessels filled with barium sulphate mixture travelling with the blood vessels

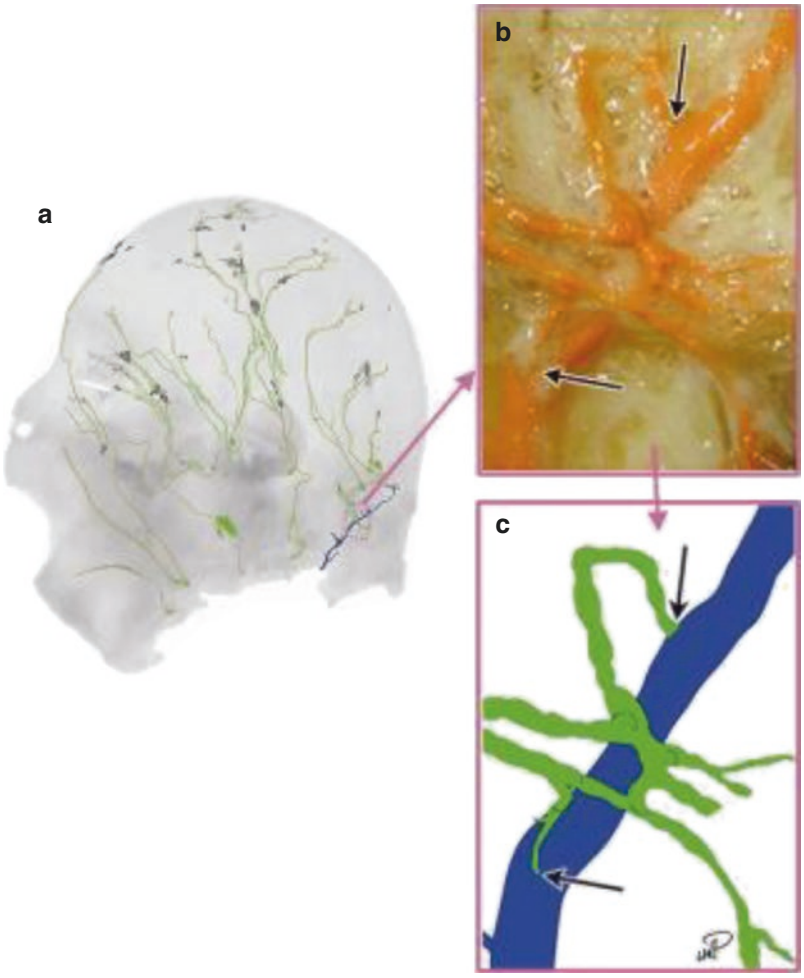

Fig. 2.123 (**a**) A radiograph of the superficial tissue of the left head and neck after lymphatic vessels was injected with lead oxide mixture, showing lymphaticovenous shunts in the occipital area. (**b**) A magnified view from the *purple boxed area* in (**a**), showing the lymphaticovenous anastomosis sites (*black arrows*). (**c**) A schematic drawing. *Green* lymphatic vessels, *Blue* vein

Note

An abnormal lymphaticovenous shunt was found in the superficial tissue of the left head and neck after lymphatic vessels were injected with lead oxide mixture. The efferent lymph vessels of the superficial occipital lymph nodes formed a lymphatic network from which two small lymphatic vessels emerged to drain to a superficial occipital vein in the subcutaneous layer (Fig. 2.123). This confirmed the clinical findings of Wallace et al. (1964). It should therefore be noted that the abnormal lymphaticovenous anastomosis may provide a systemic route for metastatic disease.

5.6 *Abnormal Collecting Lymph Vessel*

During the lymphatic injection and dissection, a few coarctation segments of collecting lymph vessel were found that blocked the injectant. The lumen of coarctation segment was narrowed by a thickening wall. The proximal vessel beyond the segment of coarctation was normal (Figs. 2.124, 2.125 and 2.126).

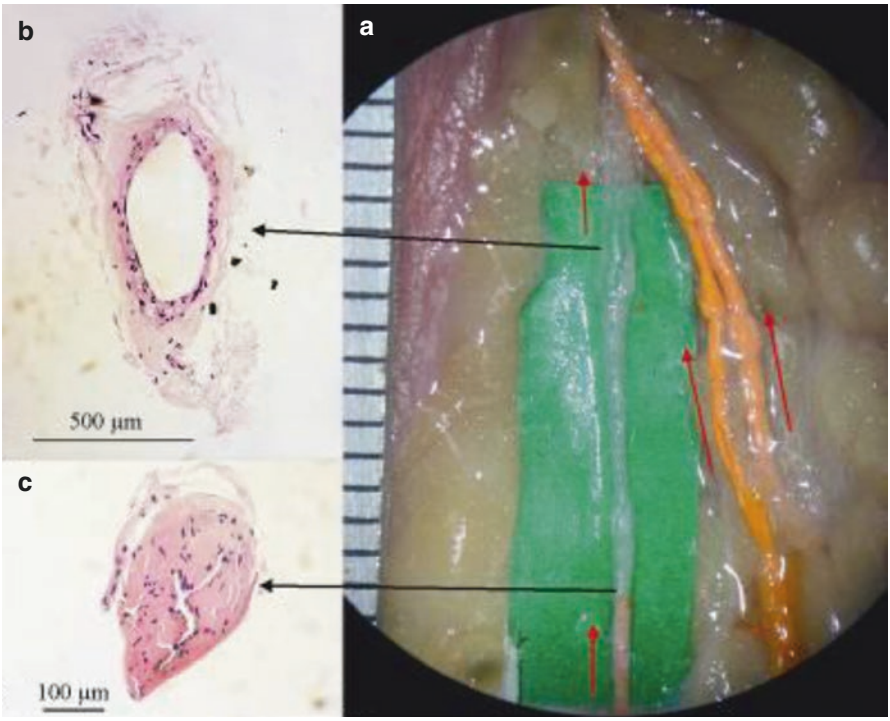

Fig. 2.124 (**a**) A coarctation segment of the collecting lymph vessel in the subcutaneous of the left ulnar forearm after vessels filled with lead oxide mixture. *Red arrows* indicate the direction of the lymph flow. (**b**) A histological section and H&E staining of the proximal vessel beyond the segment of coarctation showing its normal structure. (**c**) A histological section and H&E staining showing that the lumen of coarctation segment was narrowed by a thickening wall. Note that cells of the thickened wall were arranged in disorderly fashion

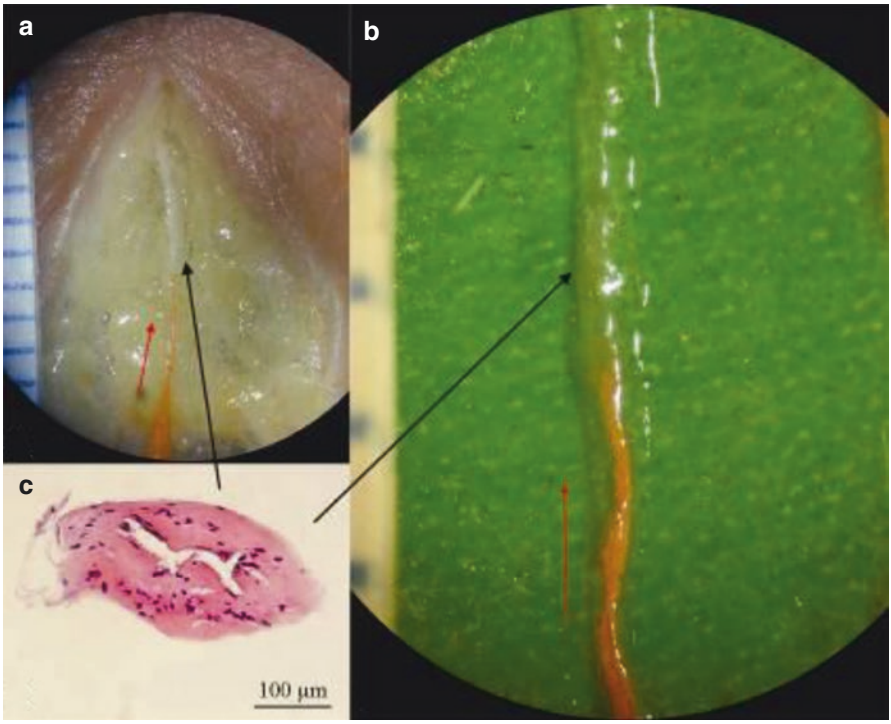

Fig. 2.125 (**a**) A coarctation segment of the collecting lymph vessel in the subcutaneous of the right ulnar forearm after vessels filled with lead oxide mixture. (**b**) A magnified view from (**a**). *Red arrows* indicate the direction of the lymph flow. (**c**) A histological section and H&E staining showing that the lumen of coarctation segment was narrowed by a thickening wall. Cells of the thickened wall were arranged in disorderly fashion

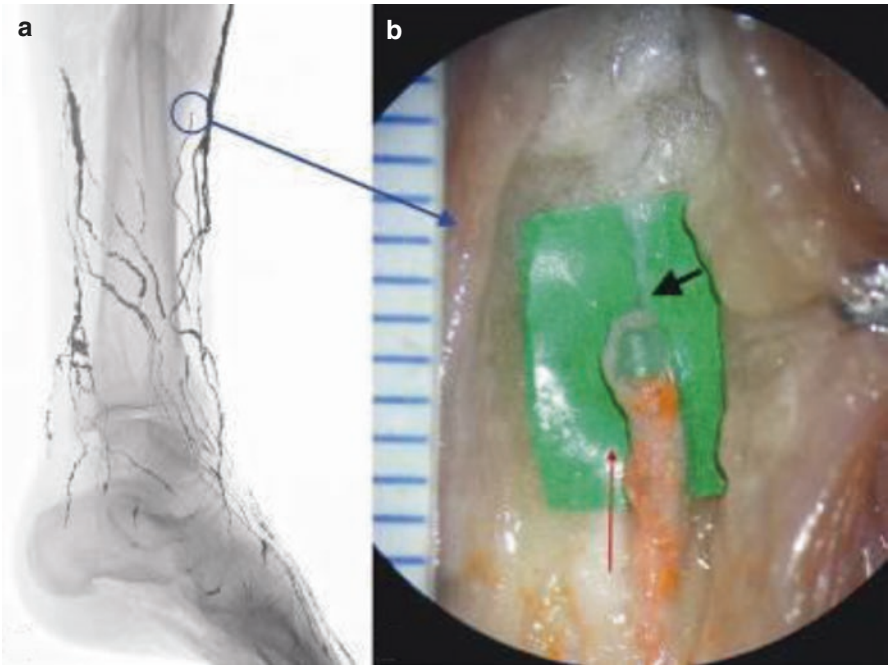

Fig. 2.126 (**a**) A coarctation segment of the collecting lymph vessel (*blue circled area*) in the subcutaneous of the left leg after vessels filled with lead oxide mixture. (**b**) A magnified view from the *blue circled area* in (**a**) showing a coarctation segment of the vessel (*black arrow*). *Red arrow* indicates the direction of the lymph flow

Clinical Implication
The occurrence of coarctation of collecting lymph vessels may be caused by trauma or inflammation. If a single lymphatic vessel is affected, it may not lead to lymphoedema as the lymph could pass through neighbouring vessels, communicating branch or bypass route (Figs. 2.102, 2.103, 2.104, 2.105, 2.106, 2.107, 2.108, 2.113 and 2.114).

6 Lymphatic Trunk and Duct (Figs. 2.127, 2.128, 2.129 and 2.130)

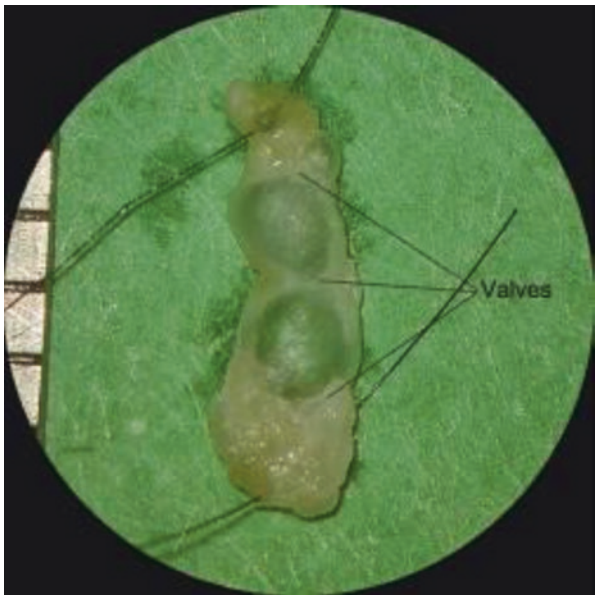

Fig. 2.127 A piece of the lymphatic trunk distended with hydrogen peroxide and harvested from the base of the neck. Note its transparent appearance

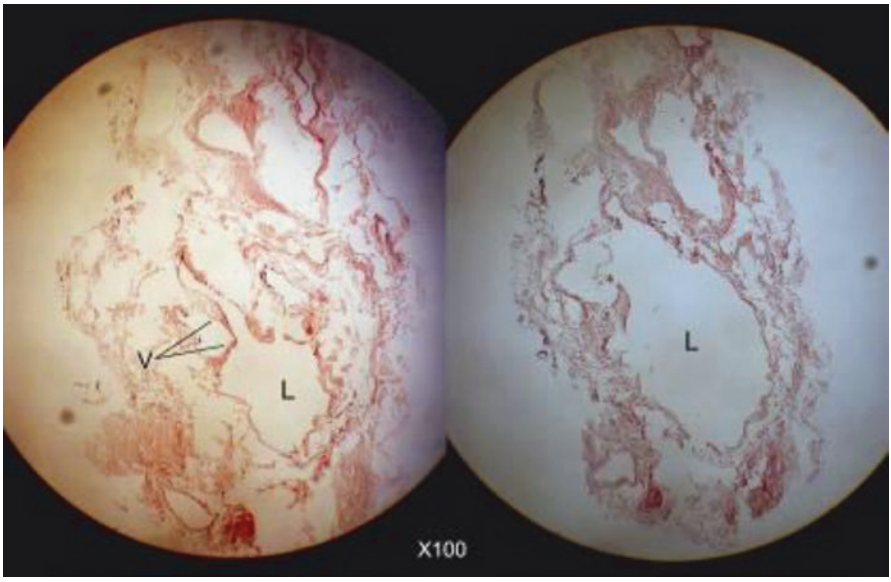

Fig. 2.128 Histological cross-sections of the lymphatic trunk showing the lumen (*L*) and valves (*V*)

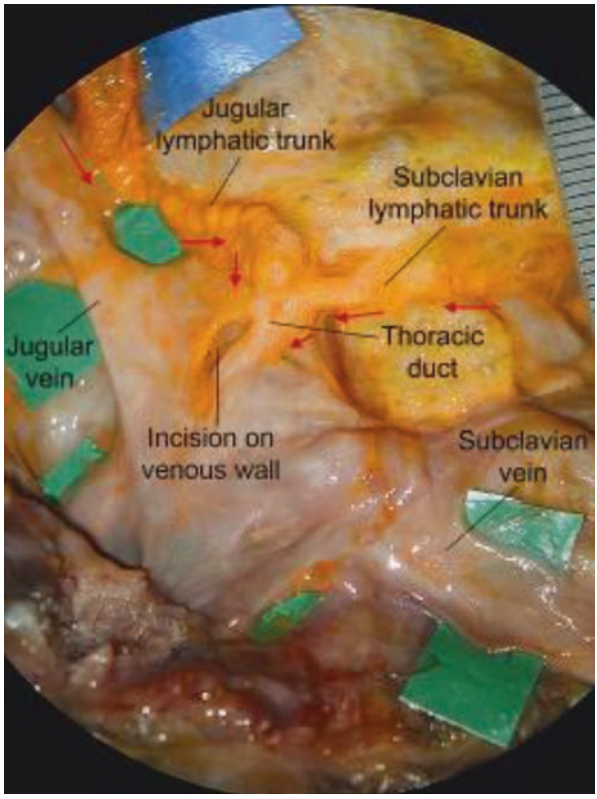

Fig. 2.129 The left jugular and subclavian trunks merged to the thoracic duct entering the angle of the internal jugular and subclavian veins at the root of the left neck. Incision made on the venous wall to show the thoracic duct entering the vein. See Fig. 2.130. Lymphatic vessels have been perfused by lead oxide mixture. *Red arrows* indicate the direction of the lymph flow

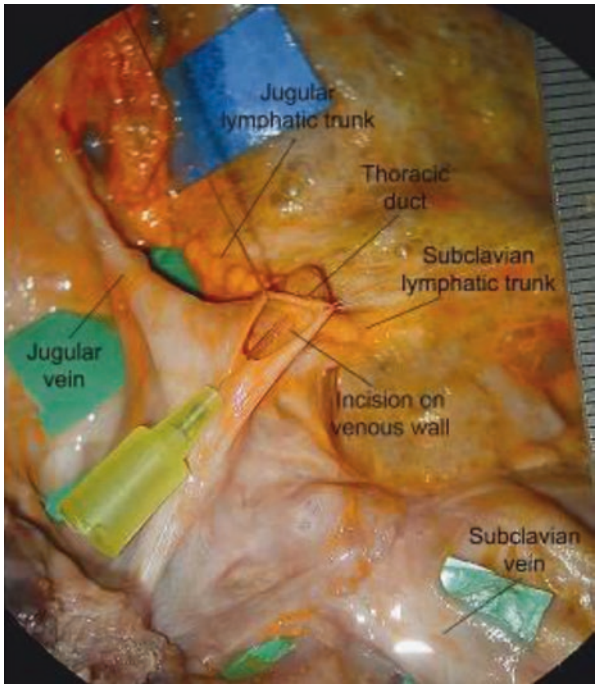

Fig. 2.130 The opening of the lymphatic duct (inserted by 24G needle) seen through the incision of the venous wall at the root of the neck

Clinical Implication

Cervical chylous leakage is an uncommon complication, with a reported incidence from 1% to 2% of radical neck dissections or trauma, which occurs mainly (75% to 92%) on the left side. It rarely occurs but may cause hypovolemia, electrolyte imbalance, decreased lymphocytes and hypoalbuminemia and could even lead to death if not treated properly (de Gier et al. 1996; Rollon et al. 1996; Ying 1997).

7 **Paralymphatics Arteriole Nutrient Vessels** (Figs. 2.131, 2.132, 2.133 and 2.134)

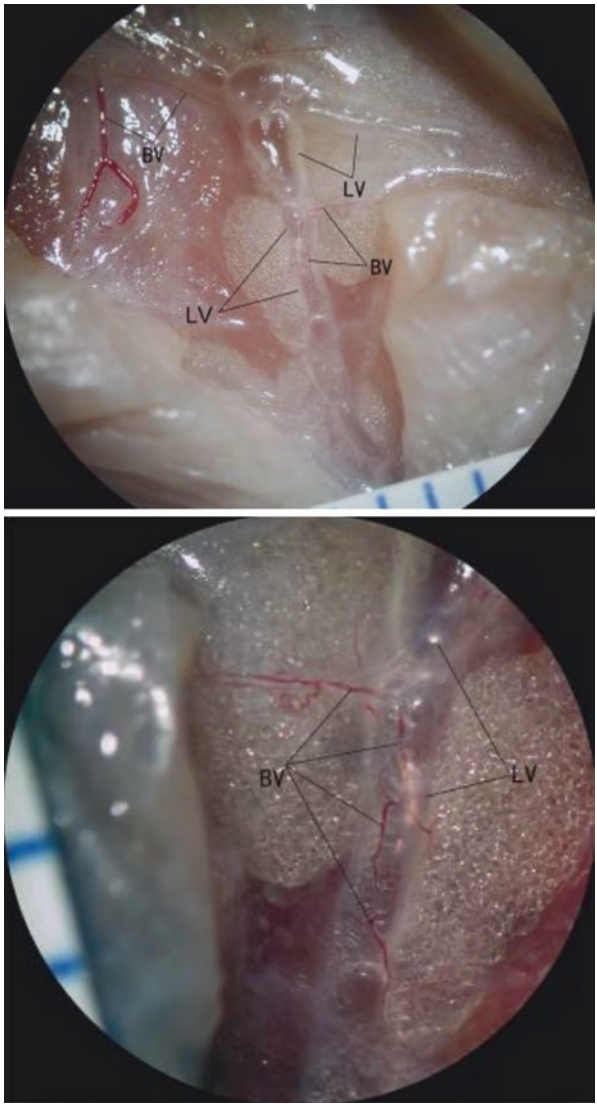

Fig. 2.131 The paralymphatics arteriole nutrient (PAN) vessels are supplying the inflated lymphatic vessels by applying hydrogen peroxide in the leg. *LV* lymphatic vessel, *BV* blood vessel

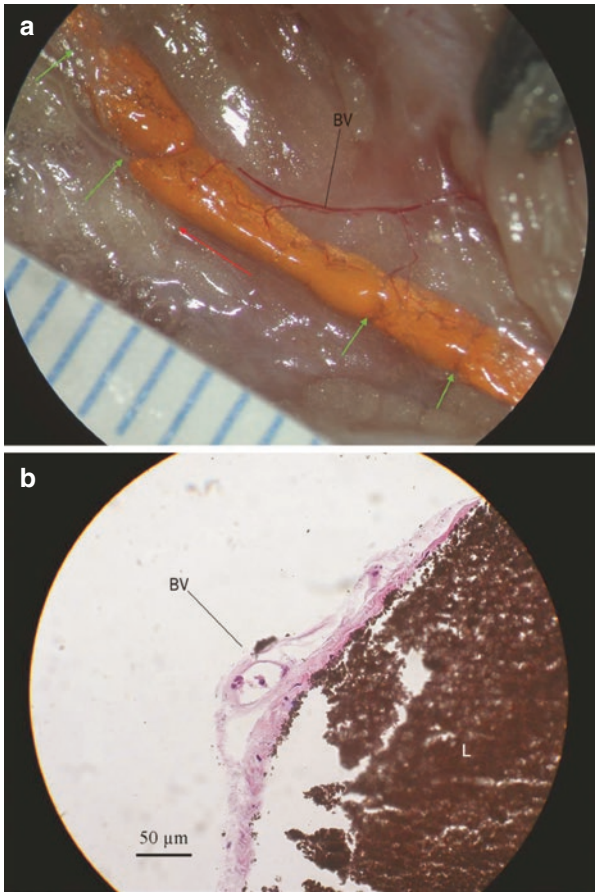

Fig. 2.132 (**a**) Microphotographs of the human lymphatics (injected with lead oxide) and blood vessels. The paralymphatics arteriole nutrient (PAN) vessels can be seen supplying the lymphatic vessels. *Green arrows* indicate lymphatic valves; *red arrows* indicate the direction of the lymph flow. (**b**) A lymphatic vessel with a blood vessel, H&E stained. Paralymphatics arteriole nutrient (PAN) vessel containing the blood cells situated beneath the tunica adventitia of the lymphatic wall. *L* lumen of the lymphatic vessels filled with lead oxide mixture, *BV* blood vessel

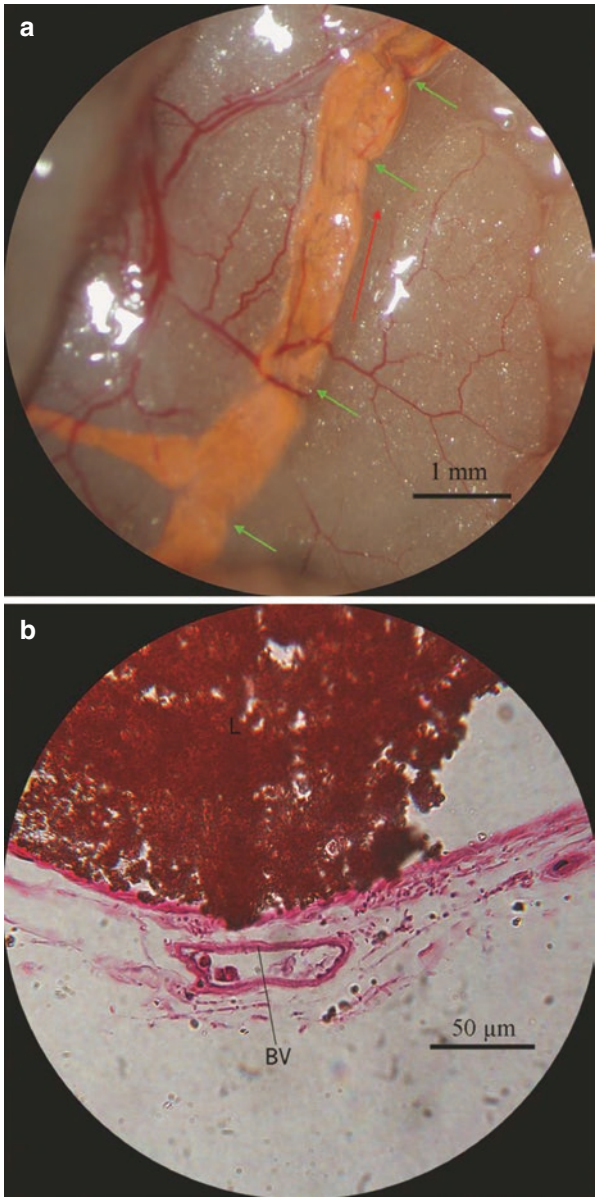

Fig. 2.133 (**a**) The paralymphatics arteriole nutrient (PAN) vessels can be seen supplying the lymphatic vessels (injected with lead oxide mixture). *Green arrows* indicate lymphatic valves; *red arrows* indicate the direction of the lymph flow. (**b**) A lymphatic vessel with a blood vessel, H&E stained. Paralymphatics arteriole nutrient (PAN) vessel containing the blood cells situated beneath the tunica adventitia of the lymphatic wall. *L* lumen of the lymphatic vessels filled with lead oxide mixture, *BV* blood vessel

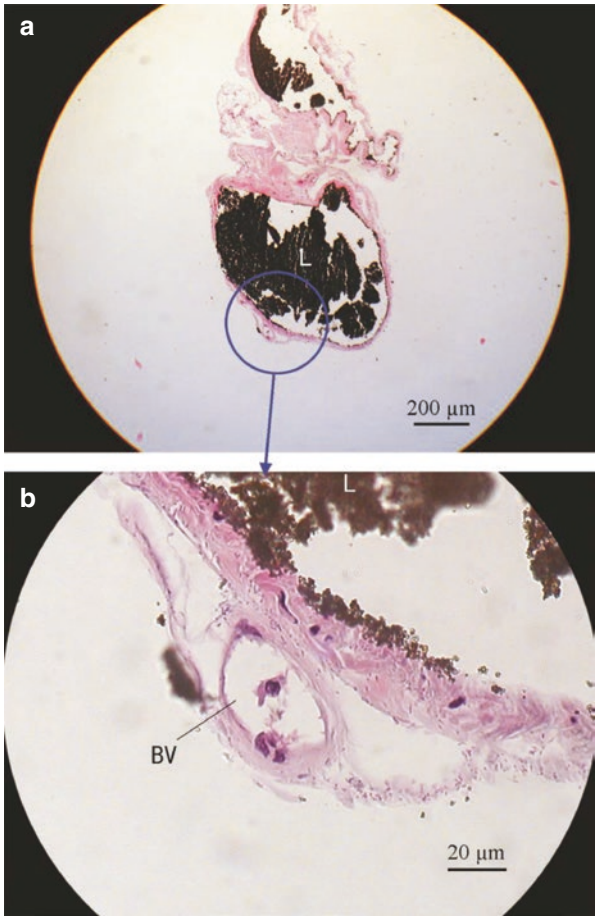

Fig. 2.134 (**a**) A lymphatic vessel with blood vessels, H&E stained. Paralymphatics arteriole nutrient (PAN) vessel situates close to the wall of the lymphatic vessel. (**b**) Magnified view of the *area circled* above, showing blood cells in the lumen of the blood vessel. *L* lumen of the lymphatic vessels filled with lead oxide mixture, *BV* blood vessel

Note

The existence of nutrient vessels in the lymphatic wall has been seldom reported in literature (Aglianò et al. 1997, Zezula-Szpyra et al. 1997), and the theoretical findings were based on histological studies. Over the last decade, lymphatic research has been carried out thoroughly that should attribute to the establishment of new technologies (Suami et al. 2005a, b; Shayan et al. 2006). On the basis of microinjections and dissections, the relationship between lymphatic vessels and their nutrient vessels, morphology and the pattern of nutrient vessels entering the lymphatic wall has been revealed by microphotographs and histological results. The results may provide fundamental knowledge for further studies in the human lymphatic system.

8 Lymph Nodes

The terminology of lymph nodes has been described in Chap. 1.

8.1 Appearance and Structure of Lymph Nodes

Lymph nodes had a minimum diameter of 1 mm and maximum diameter of 11 mm. Some of them looked like a kidney or garden beans, while some presented as a round, oval or irregular forms. Two different types of lymph nodes were found in all specimens, with either a solidified or transparent nature. Histological examinations have shown that different types of nodes had different tissue structures even if nodes were similar in appearance.

8.1.1 Solidified Lymph Node

These nodes had a three-dimensional bean shape and pinkish appearance in unembalmed specimens and a grey-whitish appearance in embalmed cadavers. They varied in size. Most solidified lymph nodes received multiple afferent lymphatics (Figs. 1.4, 1.6, 2.109 and 2.111), however, sometimes a single afferent vessel branched and wrapped around the node before entering it (Figs. 1.6, 2.110, 2.135, 2.136, 2.137, 2.138, 2.139 and 2.140). The lead oxide injectant did not pass through the solidified lymph nodes.

Nodes that were similar in appearance had different histological structures (Figs. 2.140 and 2.141). As can be seen from Fig. 2.141b, the cortex and medulla of lymphoid tissue degenerated, and the space was substituted by connective tissue presenting as a "foamlike" structure. The residual cortex remained near the subcapsular sinus, while the residual medulla remained in the centre part of the node.

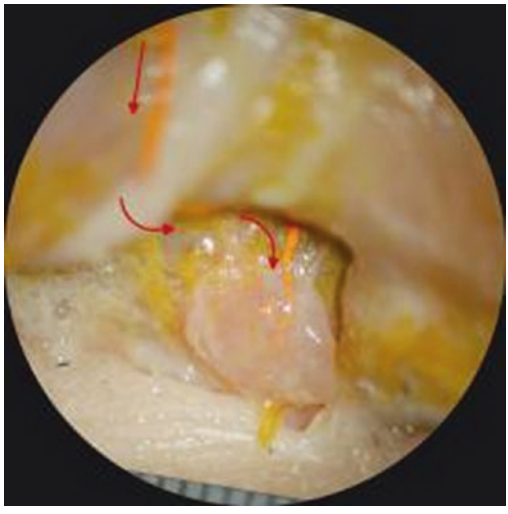

Fig. 2.135 A single collecting lymph vessel branched before entering the solidified submandibular lymph node. *Red arrows* indicate the direction of the lymph flow

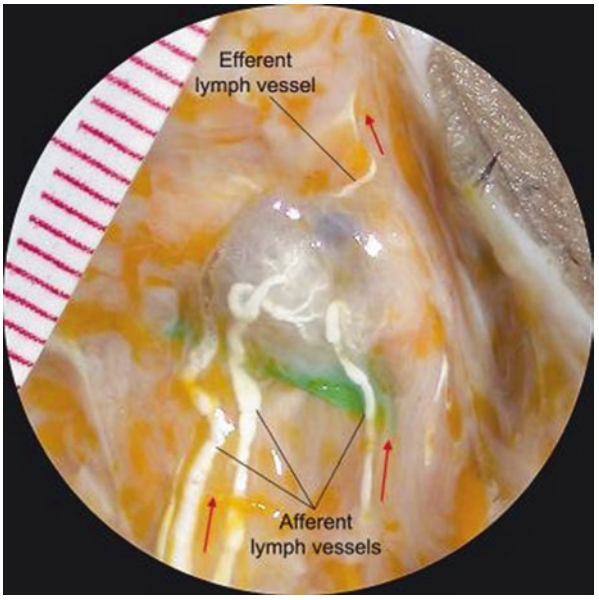

Fig. 2.136 Multiple collecting lymph vessels branched before entering the solidified axillary lymph node. *Red arrows* indicate the direction of the lymph flow

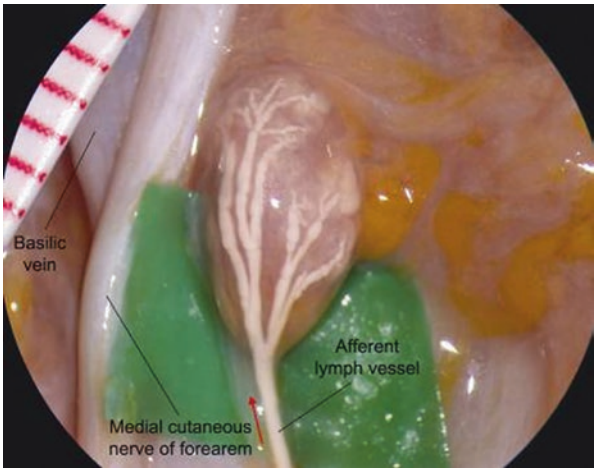

Fig. 2.137 A single lymph vessel branched before entering the solidified cubital lymph node. *Red arrow* indicates the direction of the lymph flow

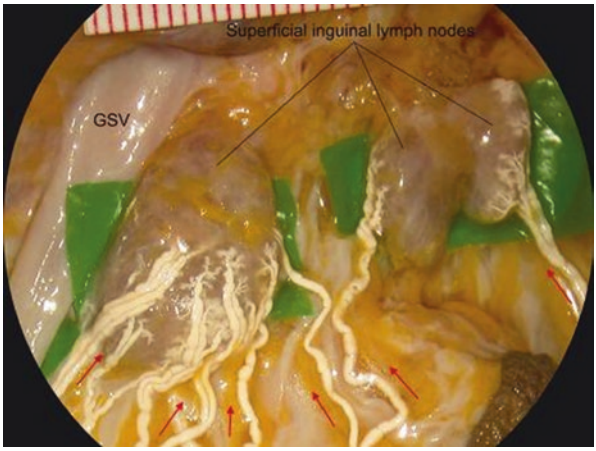

Fig. 2.138 Multiple collecting lymph vessels branched before entering the solidified lymph nodes. *Red arrows* indicate the direction of the lymph flow. *GSV* great saphenous vein

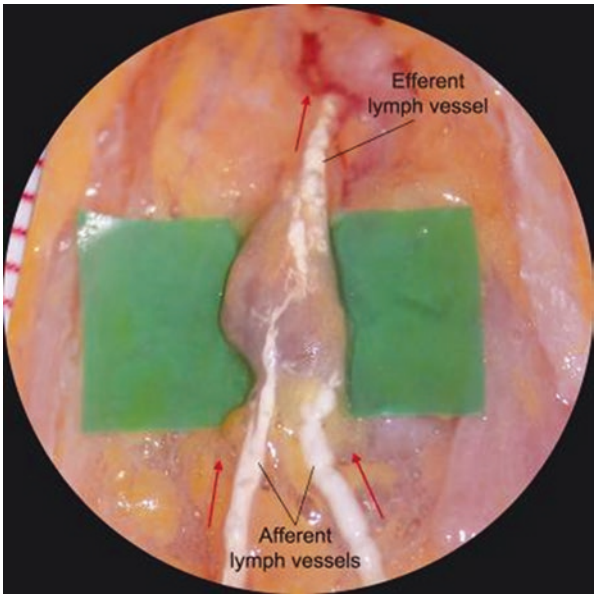

Fig. 2.139 Multiple collecting lymph vessels branched before entering the superficial popliteal lymph nodes (solidified). *Red arrows* indicate the direction of the lymph flow

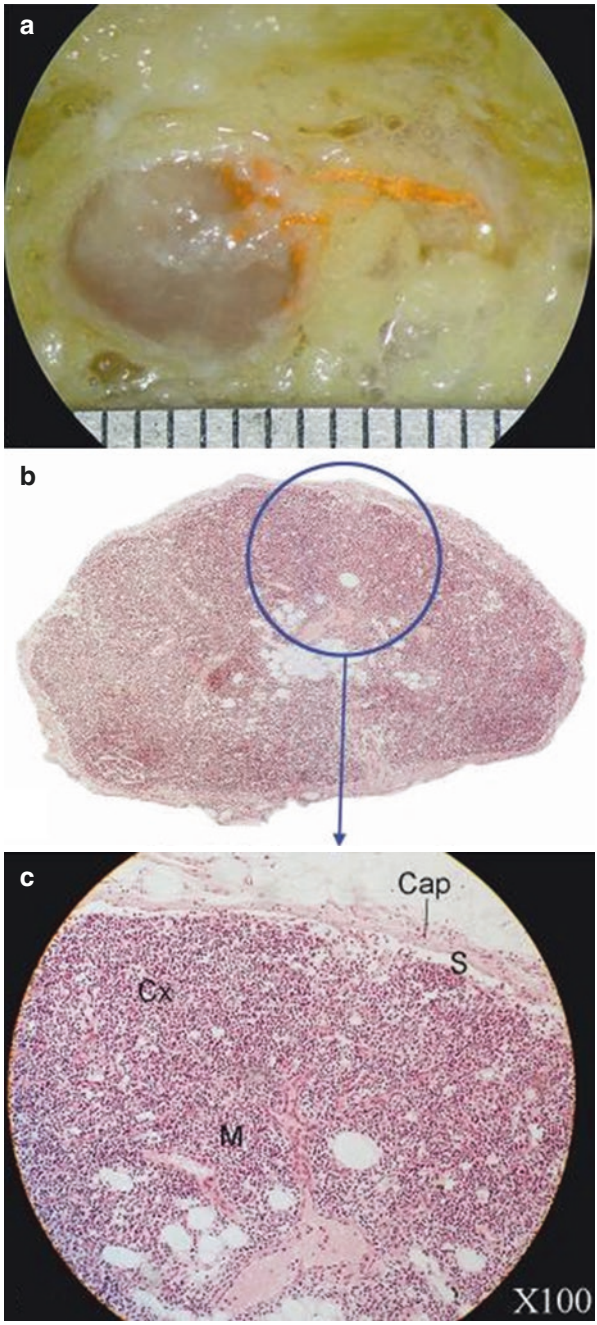

Fig. 2.140 (**a**) A single lymph vessel branched before entering the solidified submandibular lymph node. (**b**) Histological section and H&E staining. (**c**) A magnified view from the *circled area* in (**b**). *Cap* capsule, *S* subcapsular sinus, *Cx* cortex and cortical sinuses, *M* medulla and medullary sinuses

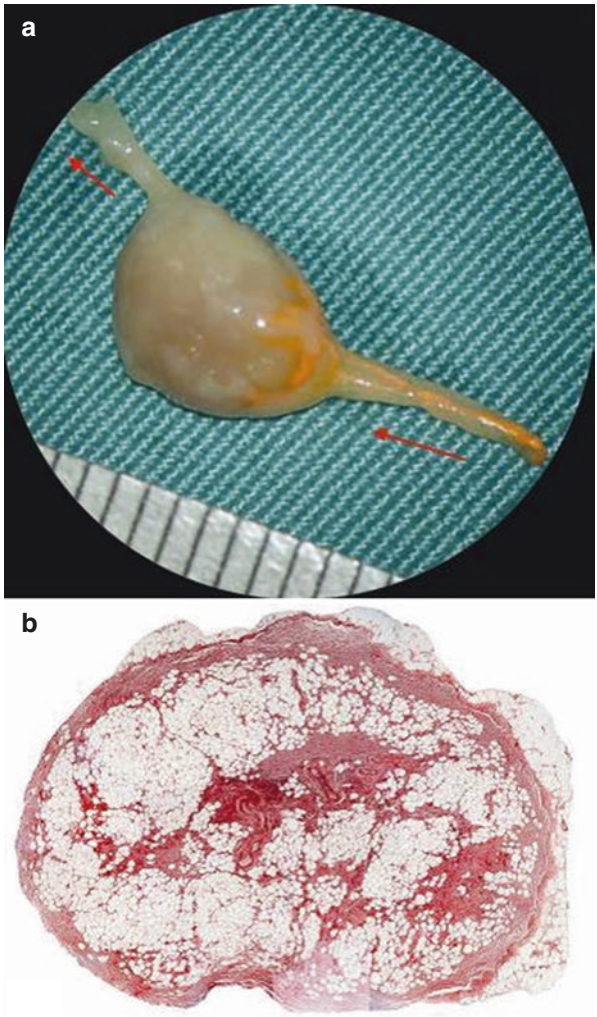

Fig. 2.141 (**a**) A single lymph vessel branched before entering the solidified submandibular lymph node. (**b**) Histological section and H&E staining. The cortex and medulla of lymphoid tissue degenerated and the space was substituted by connective tissue presenting as a "foamlike" structure. The residual cortex remained near the subcapsular sinus, while the residual medulla remained in the centre part of the node

8.1.2 Transparent Lymph Node

Transparent lymph nodes vary in size and shape, and the lead oxide/barium sulphate mixture is able to pass through these nodes. Most of the transparent nodes received only a single afferent and one efferent lymphatic vessel (Figs. 1.6, 2.142, 2.143, 2.145, 2.146 and 2.147). It is rare to observe multiple afferent and efferent vessels connect to the node (Figs. 2.144, 2.148 and 2.153). The lymphatic coils could be observed within the node (Figs. 2.148, 2.152, 2.153, 2.154, 2.155 and 2.156).

Three transparent nodes in different stages of degradation have been shown in Figs. 2.145, 2.146 and 2.147. Each of them had a single afferent and efferent vessel. As seen in the histological sections, a different quantity of residual lymphoid tissue remained in each node. The space was replaced by connective tissue. Of particular note are the dilated lymphatic coils that appear in these nodes.

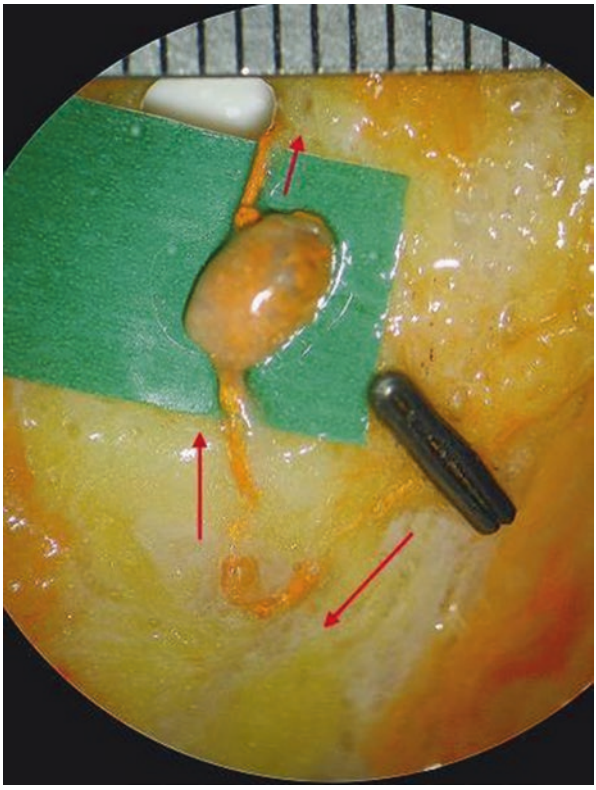

Fig. 2.142 The superficial anterior jugular lymph node filled with lead oxide mixture demonstrating its transparent nature and the internal lymphatic coils

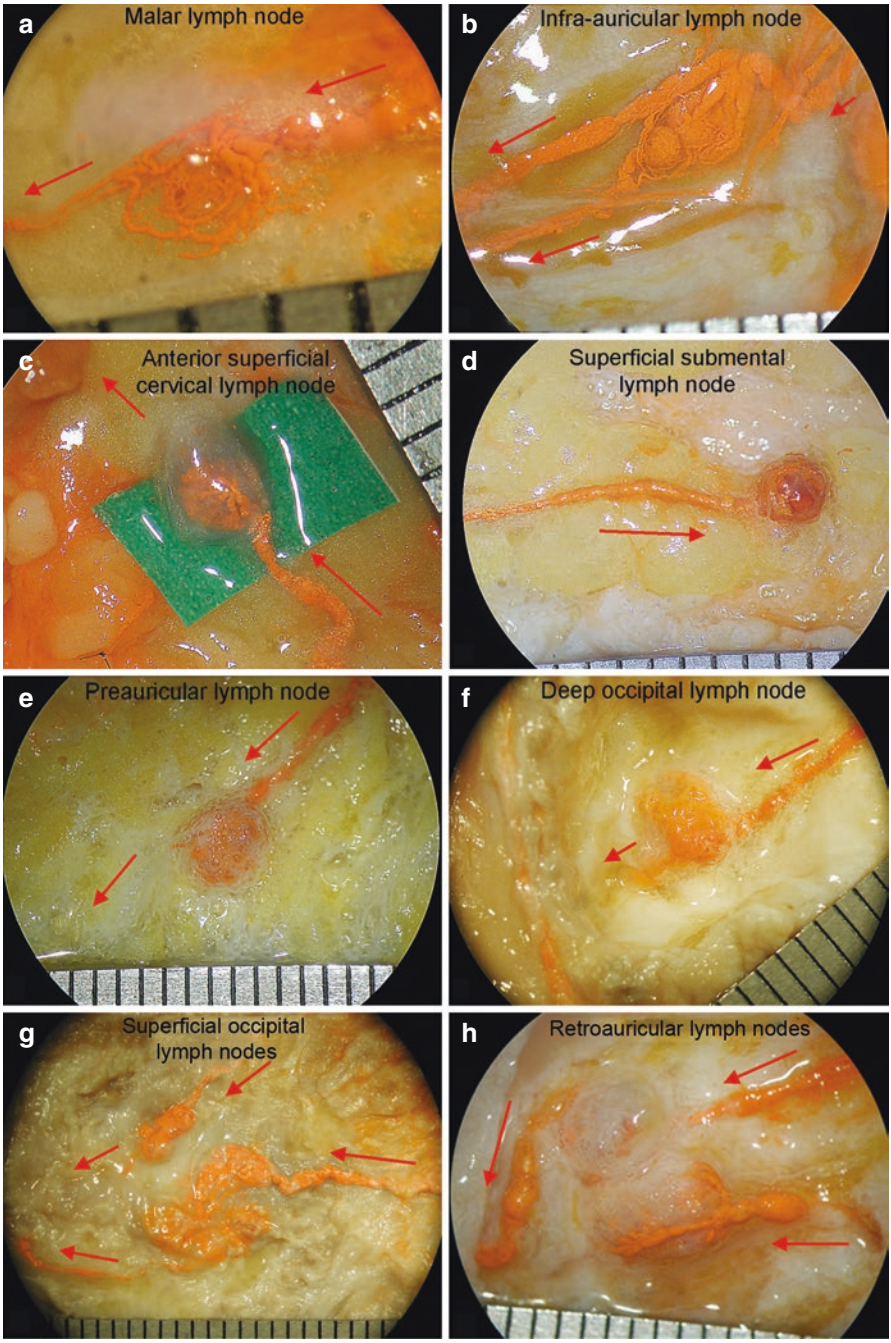

Fig. 2.143 Multiple transparent lymph nodes, filled with lead oxide mixture, showing different appearances, sizes and shapes. Note that the lymphatic coils are clearly visible in lymph nodes in (**a**–**c**). *Red arrows* indicate the direction of the lymph flow. (**a**) Malar lymph node; (**b**) Infra-auricular lymph node; (**c**) Anterior superficial cervical lymph node; (**d**) Superficial submental lymph node; (**e**) Preauricular lymph node; (**f**) Deep occipital lymph node; (**g**) Superficial occipital lymph node; (**h**) Retroauricular lymph node

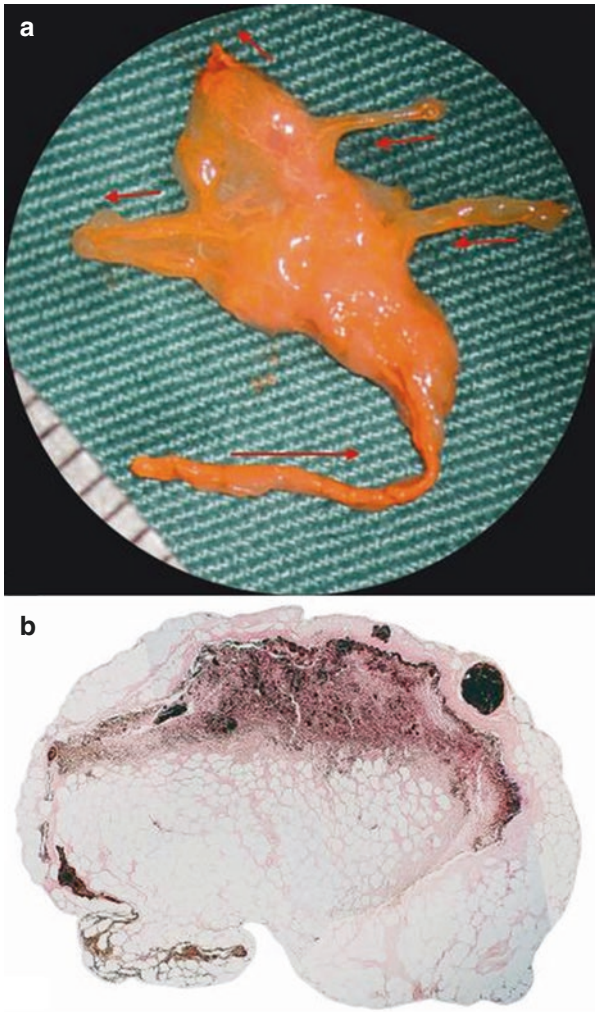

Fig. 2.144 (**a**) A transparent lymph node with several afferent lymphatic vessels and one efferent vessel. The lead oxide injectant can be seen passing through the node. (**b**) Histopathological cross-section demonstrated cortical and medullary degeneration on one side of the lymph node with the remaining space occupied by fat tissue that forms a "foamlike" structure pushing the remaining cortical and medullary lymphoid tissue towards the opposite side

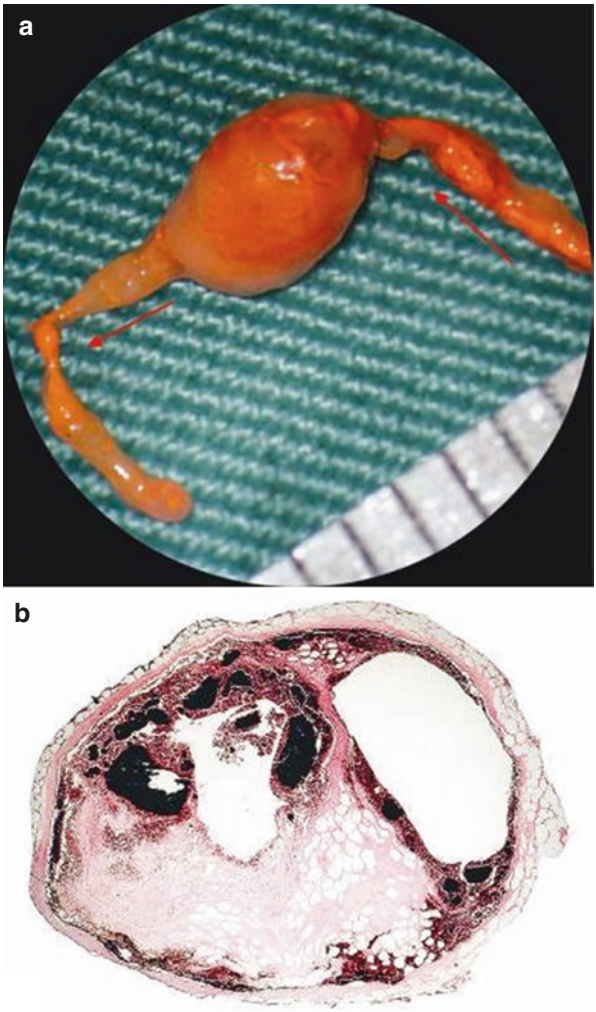

Fig. 2.145 (**a**) A transparent lymph node. (**b**) Histological section showing the internal structures. *Black* denotes lead oxide mixture in dilated lymphatic vessels

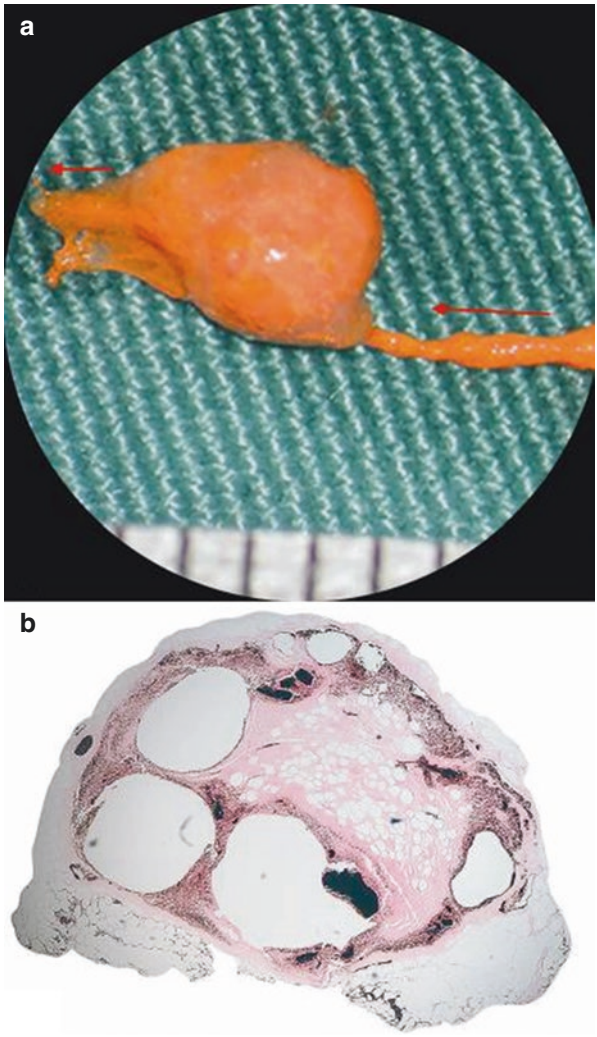

Fig. 2.146 (**a**) A transparent lymph node. (**b**) Histological section showing the internal structures. *Black* denotes lead oxide mixture in coiled lymphatic vessels

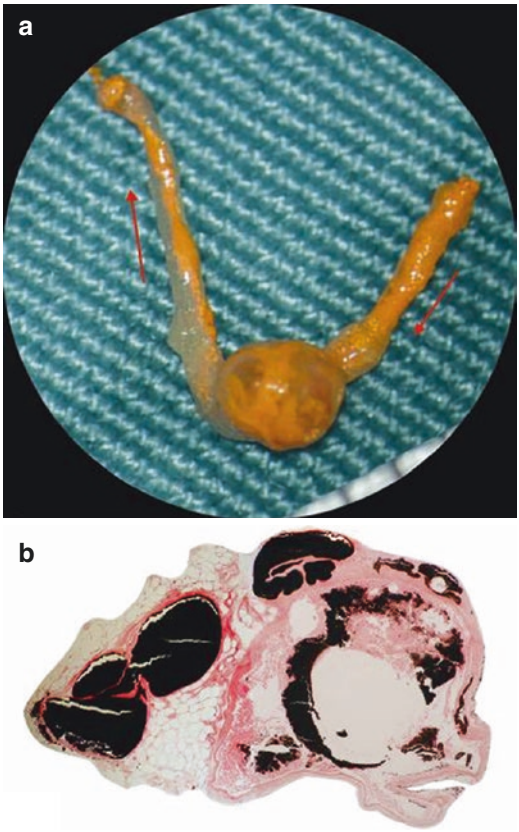

Fig. 2.147 (**a**) A transparent lymph node. (**b**) Histological section showing the internal structures. *Black* denotes lead oxide mixture in dilated lymphatic vessels

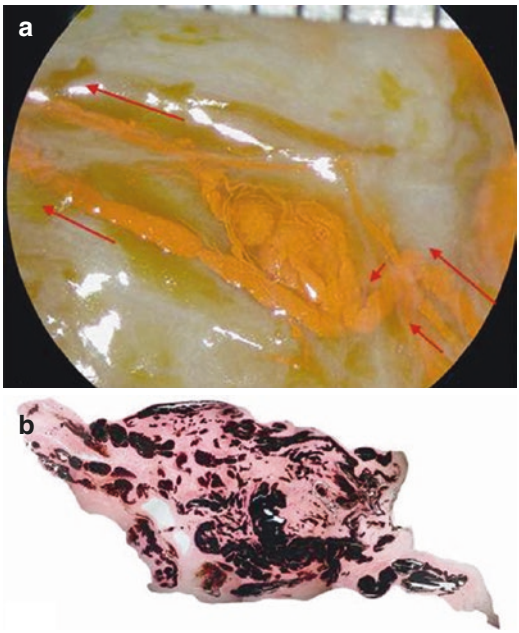

Fig. 2.148 (**a**) A transparent lymph node containing lymphatic coiled vessels. (**b**) Histological section showing the internal structures with no lymphoid tissue remaining. *Black* denotes lead oxide mixture in coiled lymphatic vessels

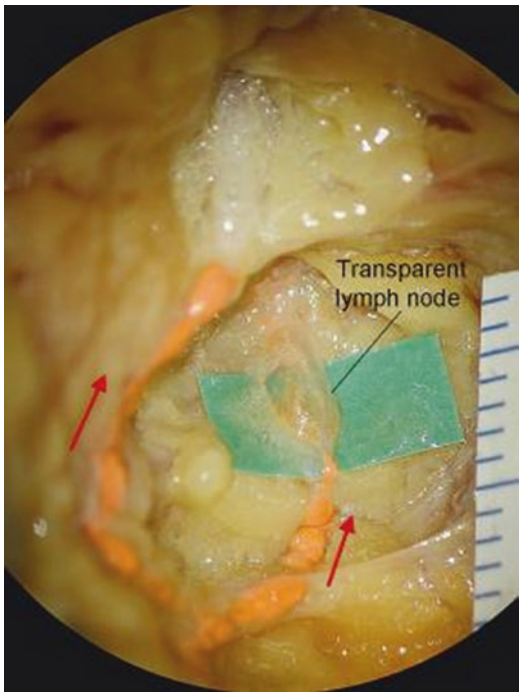

Fig. 2.149 A transparent lymph node in the right axilla

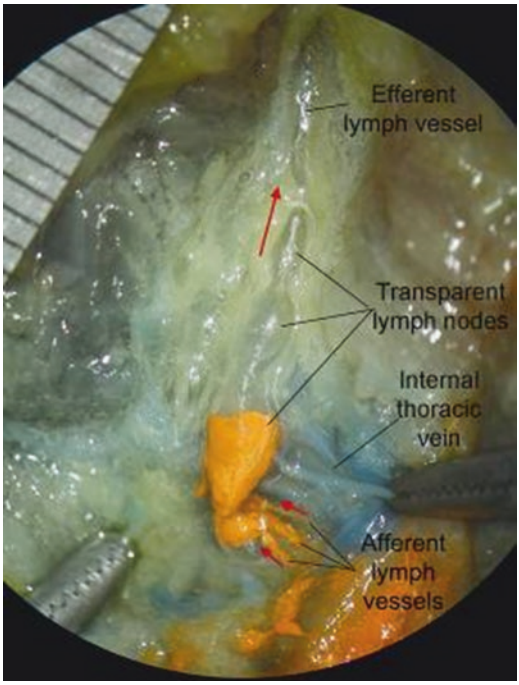

Fig. 2.150 A row of three transparent lymph nodes in the right internal thoracic vascular bundle with multiple afferent vessels and one efferent vessel

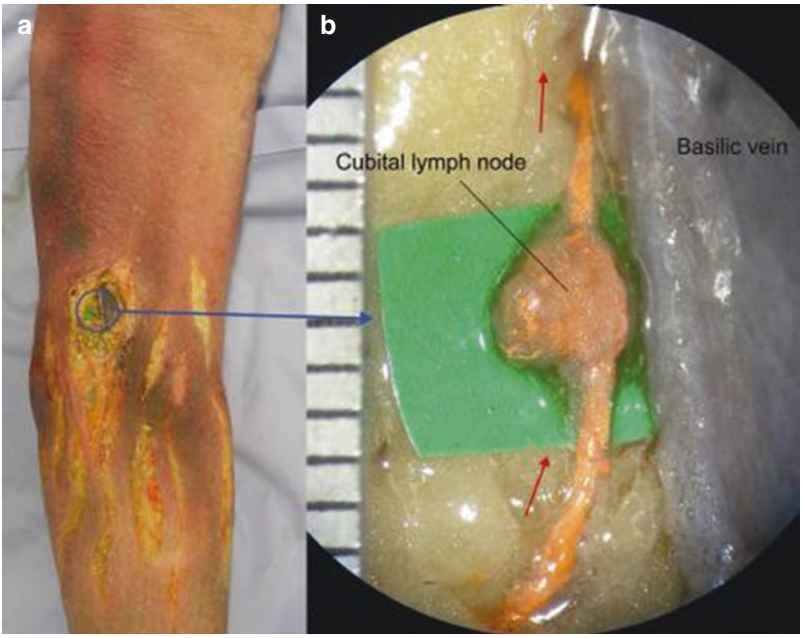

Fig. 2.151 (**a**) A transparent lymph node in the left elbow. (**b**) A transparent cubital lymph node located next to the basilica vein of the left elbow. *Red arrows* indicate the direction of the lymph flow

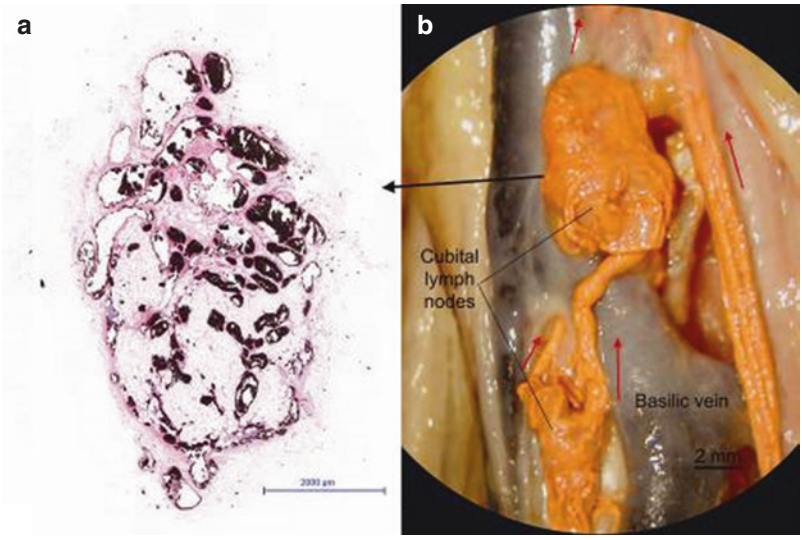

Fig. 2.152 (**a**) Histological section of a transparent lymph node in the left elbow showing the internal structures with coiled lymphatic vessels. *Black* denotes lead oxide mixture in vessels. (**b**) Two transparent cubital lymph nodes lying on the basilica vein in the left elbow. *Red arrows* indicate the direction of the lymph flow

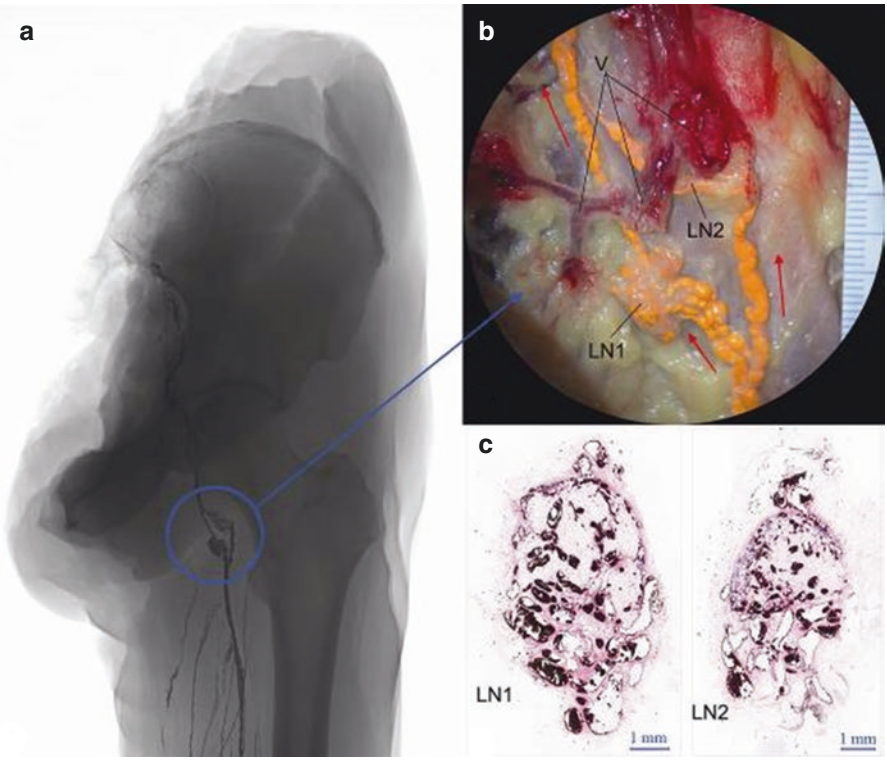

Fig. 2.153 (**a**) An inversed lymphangiogram of the left hip joint showing two transparent inguinal lymph nodes in the inguinal region. (**b**) A magnified view from the *blue circled area* in (**a**), showing transparent lymph nodes (*LN1, LN2*) around the great saphenous vein and its tributaries (*V*). *Red arrows* indicate the direction of the lymph flow. (**c**) Histological sections of two transparent lymph nodes (*LN1, LN2*) showing the internal structures with coiled lymphatic vessels. *Black* denotes lead oxide mixture in vessels

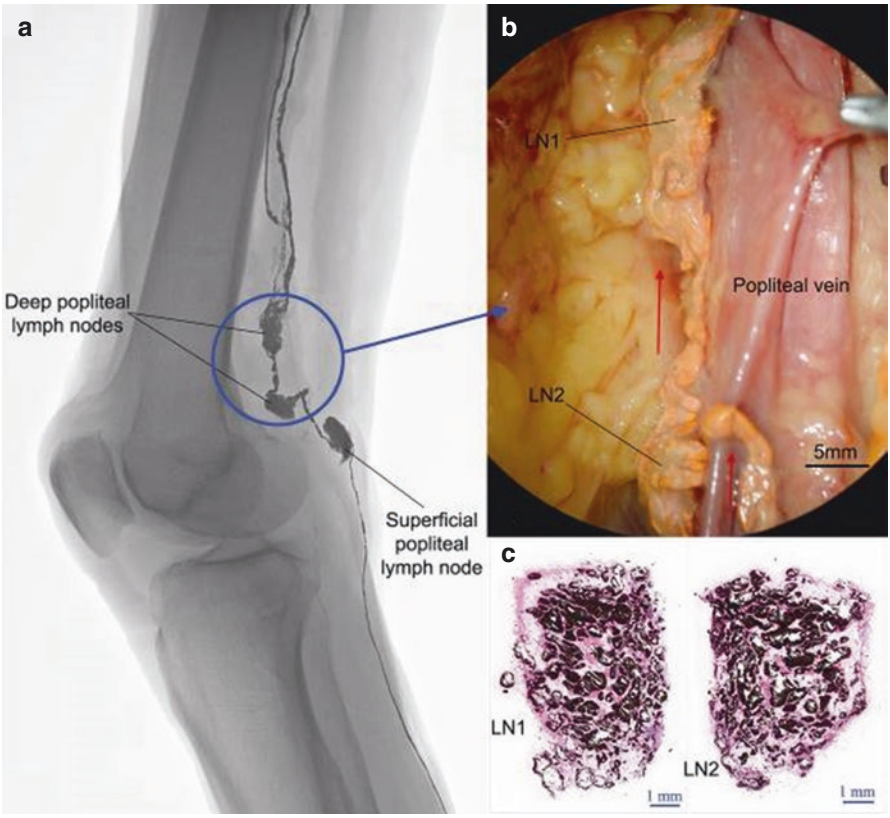

Fig. 2.154 (**a**) An inversed lymphangiogram of the right knee joint (lateral view) showing three transparent lymph nodes in the popliteal fossa. (**b**) A magnified view from the *blue circled area* in (**a**), showing the transparent nature of two deep popliteal lymph nodes (*LN1, LN2*) around the popliteal vein. *Red arrows* indicate the direction of the lymph flow. (**c**) Histological sections of two transparent lymph nodes (*LN1, LN2*) showing the internal structures with coiled lymphatic vessels. *Black* denotes lead oxide mixture in vessels

8.2 *Radiologic Manifestations of Lymph Nodes* (Figs. 2.155 and 2.156)

Fig. 2.155 An inversed lymphangiogram of the right inguinal area showing a transparent lymph node (*purple arrow*) and multiple solidified lymph nodes (*in purple circles*)

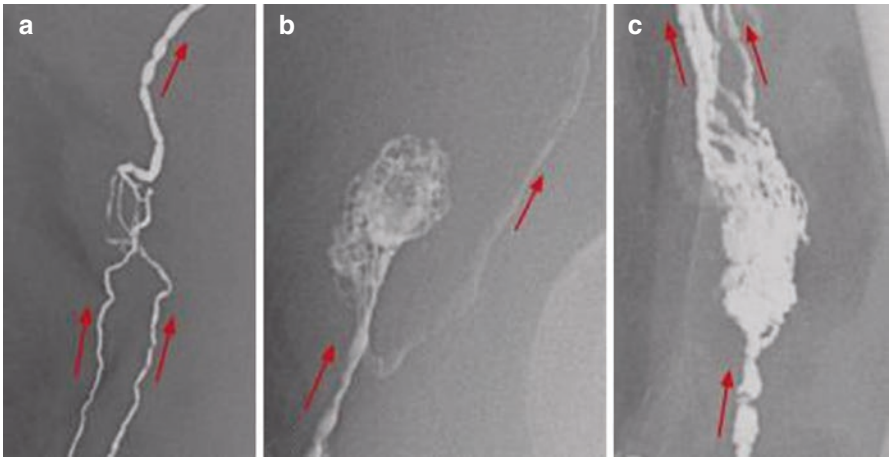

Fig. 2.156 Three lymphangiograms form individual popliteal areas showing three degenerating (transparent) lymph nodes of different sizes, shapes and densities. *Red arrows* indicate the direction of the lymph flow. (**a**) A degenerating lymph node contains sparse lymphatic tubules with two afferent and one efferent lymph vessels. (**b**) A degenerating lymph node contains dense lymphatic tubules with a afferent and a efferent lymph vessels. (**c**) A degenerating lymph node contains dense lymphatic tubules with a afferent and multiple efferent lymph vessels

8.3 Senile Changes in Human Lymph Nodes

Human lymph nodes have been studied and reported in many previous literatures. The details of their morphology, function, degeneration and regeneration have been described. However, most of these were based on studies of solidified lymph nodes (Delamère et al. 1913; Rouvière 1938; Denz 1947; Furuta 1947; Haagensen et al. 1972; Viamonte and Rüttimann 1980; van den Brekel et al. 1998; Uren et al. 1999; Young and Heath 2000; Földi et al. 2003; Junqueira and Carneiro 2003; Thompson et al. 2004; Rubin et al. 2005; Standring 2005; Guyton and Hall 2006; Male et al. 2006). In this section, the macroscopic and microscopic appearance, radiographic and photographic images and histological sections of various types of lymph nodes in the head, neck and limbs have been studied and shown in detail.

8.3.1 The Generating and Degenerating Cycle of Lymph Nodes

More than a century ago, Gulland (1894) reported that the lymph nodes were fully developed in the neck, axilla, groin and the root of the mesentery in fetal life. Then, in 1905, Sabin reported a detailed process outlining the development of lymph nodes in pig embryos. It was found that the development of lymph nodes is related to the appearance of the lymphatic heart (sac). In 1909, Lewis found and reported that lymph glands (nodes) appeared in early human embryos (30–45 mm in size), while Denz (1947), after studying over 300 human lymph nodes, concluded that lymph nodes reached their maximum development in childhood and decreased in size after puberty. He found that the cortical tissue decreased steadily and formed an island surrounding the medullary tissue in the nodes of the elderly. In some cases lymph nodes gradually decreased to return to the fetal type in extremely old age. Moore and Persaud (1998) reported that the lymph sacs were transformed into groups of lymph nodes during the early fetal period in their embryological study. However, all these studies focused on solidified lymph nodes. After studying 362 lymph nodes harvested from 22 specimens of the head and neck in elderly cadavers, Pan et al. (2008a, b) presented a new concept – transparent (inactive) lymph nodes. Figures 2.157 and 2.158 represent the concept of the generation and degeneration of lymph nodes combining previous studies with more recent findings.

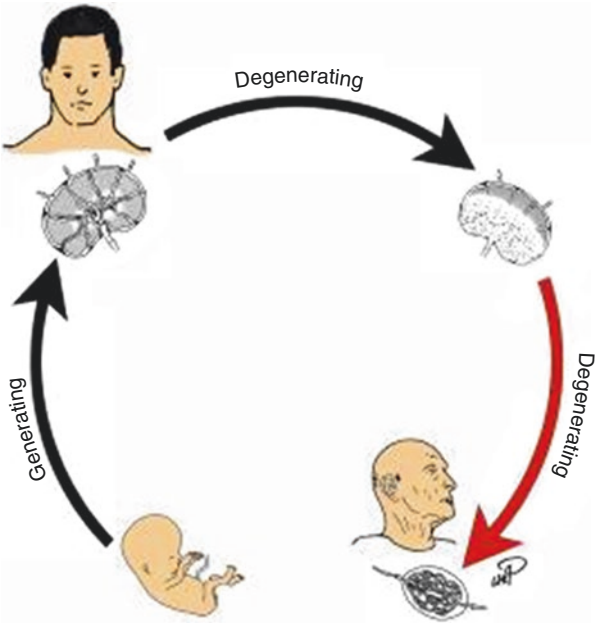

Fig. 2.157 A drawing of the generation and degeneration cycle of human lymph nodes. The *red arrow* indicates the degenerating period of lymph nodes presented in this section

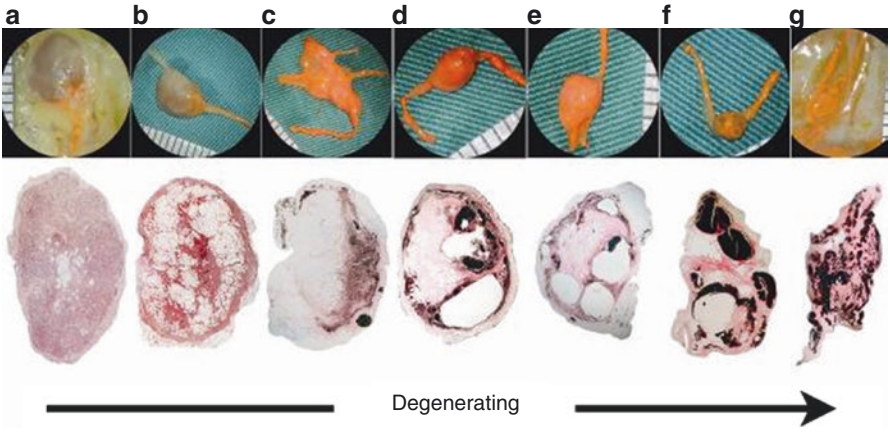

Fig. 2.158 The degenerative process of the lymph node. The *top row* shows the appearances of lymph nodes. In the *bottom row*, histological sections show that the quantity of lymphoid tissue gradually decreases in nodes from the left to the right. Lymphoid tissue has totally disappeared in the lymph node **g**

8.3.2 Types of Lymph Nodes

Haagensen et al. (1972) modified Ludwig's diagrams (1962) to classify lymph nodes into five types according to the relationship between the nodes and the lymphatic vessels. Using lymphoscintigraphy (Uren et al. 1999, 2000a, b; Thompson et al. 1995, 2004; Thompson and Uren 2005; Martini et al. 1994; Krag 1998; Cascinelli et al. 1998; Gould et al. 1960 and Morton et al. 1992), clinicians described nodes as sentinel nodes, interval nodes (in transit) or regional lymph nodes. In this section of the book, lymph nodes were classified into solidified or transparent nodes according to their appearance, active or inactive (degenerated) lymph nodes based on their histological features and generating or degenerating lymph nodes according to their stage in the cycle of generation and degeneration (Figs. 1.6, 2.32, 2.33, 2.90, 2.91, 2.92, 2.93, 2.94, 2.95, 2.96, 2.110, 2.111, 2.112, 2.113, 2.114, 2.135, 2.136, 2.137, 2.138, 2.139, 2.140, 2.141, 2.142, 2.143, 2.144, 2.145, 2.146, 2.147, 2.148, 2.149, 2.150, 2.151, 2.152, 2.153, 2.154, 2.155, 2.156, 2.157 and 2.158).

8.3.3 Changes in the Structure and the Functions of Lymph Nodes with Age

In the early studies, it has been reported that senile involution predominately affected the medulla, while the cortex remained unaffected. Our results showed that the degenerating process was progressive from solidified to transparent nodes. Senile involution affected all elements of the lymph node including the cortex and medulla. The medulla was affected during the early degenerative stage. The lymph node was gradually becoming transparent as the lymphoid tissue was reducing (Figs. 2.135, 2.136, 2.137, 2.138, 2.139, 2.140, 2.141, 2.142, 2.143, 2.144, 2.145, 2.146, 2.147, 2.148, 2.149, 2.150, 2.151, 2.152, 2.153, 2.154, 2.155, 2.156, 2.157 and 2.158). The degeneration continued until the transparent lymph node turned to an inactive lymph node without any lymphoid tissue. The cortex and medulla gradually decreased as seen in Fig. 2.158, while the lymphoid tissue of the node was totally absent, as shown in Fig. 2.158g. This node contained only coils of lymphatic vessels and fibrous connective tissue. The histological section showed that the node contained neither cortex nor medulla. The result differed from previous reports that senile involution affected only the medulla predominately and that the cortex remained unaffected. It seems that the later stage of the degenerating process in the nodes was not observed in the earlier studies.

Denz (1947) stated that the size of the lumen of the lymph sinuses in the node was 40–70 μm in the subcapsular and cortical sinuses and 70–100 μm in medullary sinuses. Fujita et al. (1972) showed the detailed structures of the lumen of a sinus in a mesenteric lymph node of the dog using the scanning electron microscope. Forkert et al. (1977) and Krstić (1991) also provided detailed microstructure of the sinuses in the human lymph node and showed that the vacant sinus spaces within the lymph node were filled with reticular cells that form a micro-network and act as a micro-

filter. These studies were based on solidified lymph nodes. In this section, the inactive (transparent) lymph node only contained lymph coils and connective fibres without any lymphoid tissue and sinus. The result suggested that these nodes in the elderly had lost their ability to filter out bacteria or cancer cells and might therefore make this group more susceptible to the spread of cancer or infection.

Clinical Implication

Lymph nodes are an important part of the immune system in the human body. They are distributed widely throughout the body such as in the axilla, supraclavicular, inguinal and popliteal fossae of the superficial tissue or around the deep tissues and organs in the body. Lymph nodes are major sites of T and B cells. Approximately 75% are T cells and 25% are B cells. Sensitized T cells and antibodies, produced by T and B cells in the immune response, are brought together in the medullary sinuses and leave the node with the lymph through the efferent vessels. They then enter the blood circulation to take part in the immune activity. The lymph nodes have a filtering effect; if small amounts of antigens, such as microorganisms, cancer cells and other harmful substances, enter the lymph nodes, they may be eliminated by macrophages and antibodies in the node. When the quantity of the antigen exceeds the defence capabilities of the node, they may continue to spread and enter the bloodstream through the lymphatic pathways and cause systemic disease (Male et al. 2006). It can be seen from this section. As the aging of the human body, lymph nodes gradually degenerated. The lymphoid tissue and lymph sinuses gradually reduced in size until they have disappeared, and the space is replaced by fibrous connective tissue or lymphatic coiled vessels, resulting in the diminished ability of the immune system and lymphatic filtration. Whether this phenomenon is related to the elderly immunocompromised, resulting in elderly cancer patients being more susceptible to systemic metastasis, further studies are required to clarify these uncertainties.

Lymph nodes are small, bean-shaped glands throughout the body. They may be found singularly or in groups, as small as the head of a pin or as large as an olive. Most lymph nodes in the body cannot be felt, but a few of them may be palpable in the neck, groin and axilla. They are generally tender and not painful. Lymph nodes often swell in one location when a problem such as an injury, infection or tumour develops, in or near the lymph node. Lymph node enlargement is very common; it can occur in any age group. Each group of them corresponds to a particular region of the body and reflects abnormalities in that region. Three general kinds of lymphadenopathy are recognized:

1. Benign lymphadenopathy is caused by various infections, connective tissue diseases or allergic reaction. Full recovery can be achieved with the removal of the cause, within a certain period of time.

2. The texture of malignant lymphadenopathy, including primary malignancies such as lymphoma, lymphocytic leukaemia, malignant histiocytosis and the lymph node metastasis of various malignant tumours, is very hard. They enlarge persistently and progressively, adhere to the surrounding tissue and are immovable.
3. Lymphadenopathy is between benign and malignant such as immune cells of the primitive vascular disease and angiofollicular lymph node hyperplasia. They are rare and often start off benign and develop to become vicious and deadly.

Therefore the key is to determine the cause and nature of lymphadenopathy. If there is significant pain with a smooth surface and no adhesions to surrounding tissue, it often suggests benign lesion. While, progressive painless swelling with hardness, immovableness and adhesions often prompts to malignant disease. The diagnosis should be made in conjunction with medical history, symptoms, clinical examination and laboratory examinations such as ultrasound, radiography, lymph node biopsy, etc.

Chapter 3
Distribution of Lymphatics

1 Superficial Lymphatics of the Head and Neck

Lymphatic vessels arose in the dermis, the galea aponeurotica and the subcutaneous tissues around the canthi of the eyelids, the side of the nose, the corner of the mouth and the neck. Vessels tracked radially towards their first-tier lymph nodes, branching, diverging and converging along their course. Sometimes, vessels were seen crossing or anastomosing with neighbouring vessels (Figs. 3.1 and 3.2).

The lymphatic drainage patterns were different from person to person and even asymmetrical on each side of the same body (Fig. 3.1). The majority of the vessels converged to form large collectors, and some of them diverged before entering their first-tier lymph nodes (Figs. 2.20, 2.21 and 2.22).

Importantly, it was found that collecting lymph vessels in the head and neck did not always enter their first-tier lymph nodes but sometimes bypassed them (Figs. 2.24, 2.25, 3.1, 3.2 and 3.3).

Figures 3.4 and 3.5 show the quantity, origin and course of lymph vessels and relationship between vessels; they also show how lymph vessels travel to the nodes in the superficial tissue of the head and neck.

Three lymphatic territories were represented in the superficial tissues of the head and neck – the scalp, the face and the cervical regions.

W.-R. Pan, *Atlas of Lymphatic Anatomy in the Head, Neck, Chest and Limbs*,
DOI 10.1007/978-981-10-3749-8_3

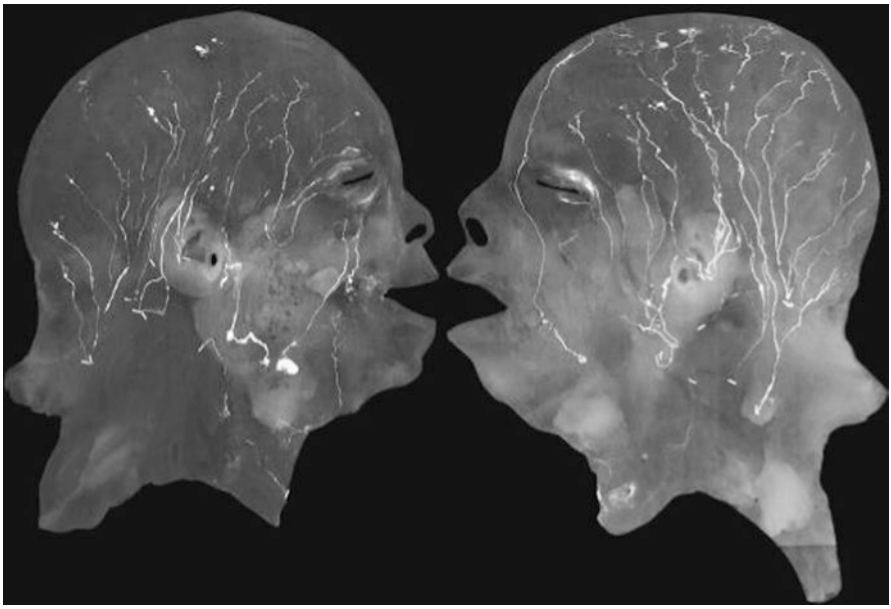

Fig. 3.1 A radiograph of the superficial tissue on both sides of the head and neck region of the same cadaver after lead oxide injection showing the distribution of the lymph vessels and lymph nodes. Note the asymmetrical lymphatic pathway patterns

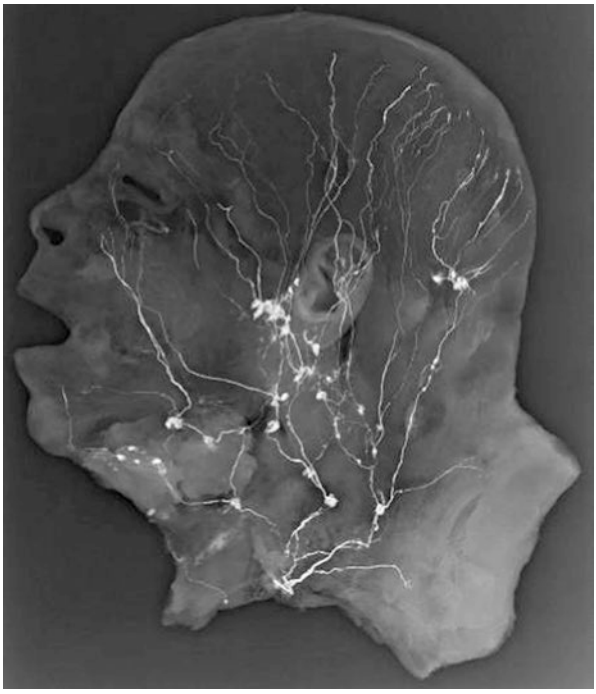

Fig. 3.2 Distribution of the lymphatics in the superficial tissue of the left head and neck (including the platysma)

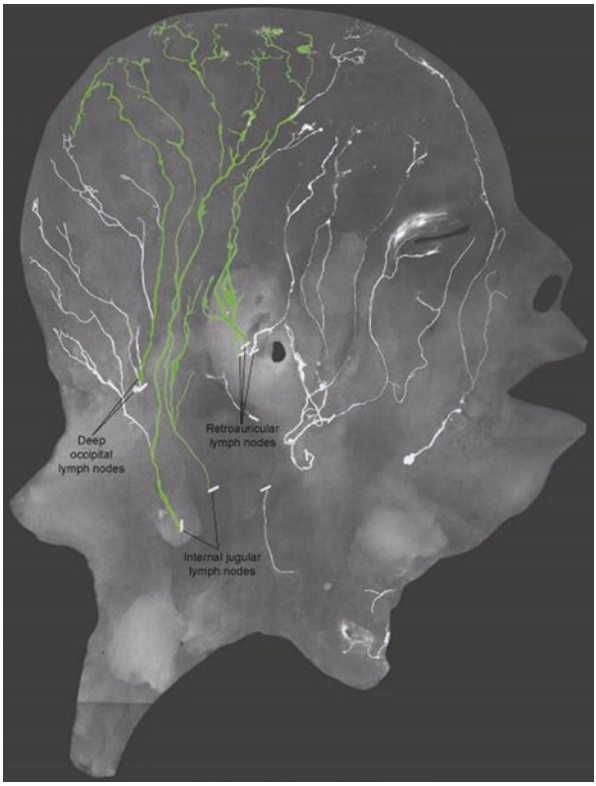

Fig. 3.3 Distribution of the lymphatics in the superficial tissue of the right head and neck. Some of the parietal lymphatic vessels (*highlighted in green*) bypass the retroauricular lymph nodes and enter the deep occipital and internal jugular lymph nodes

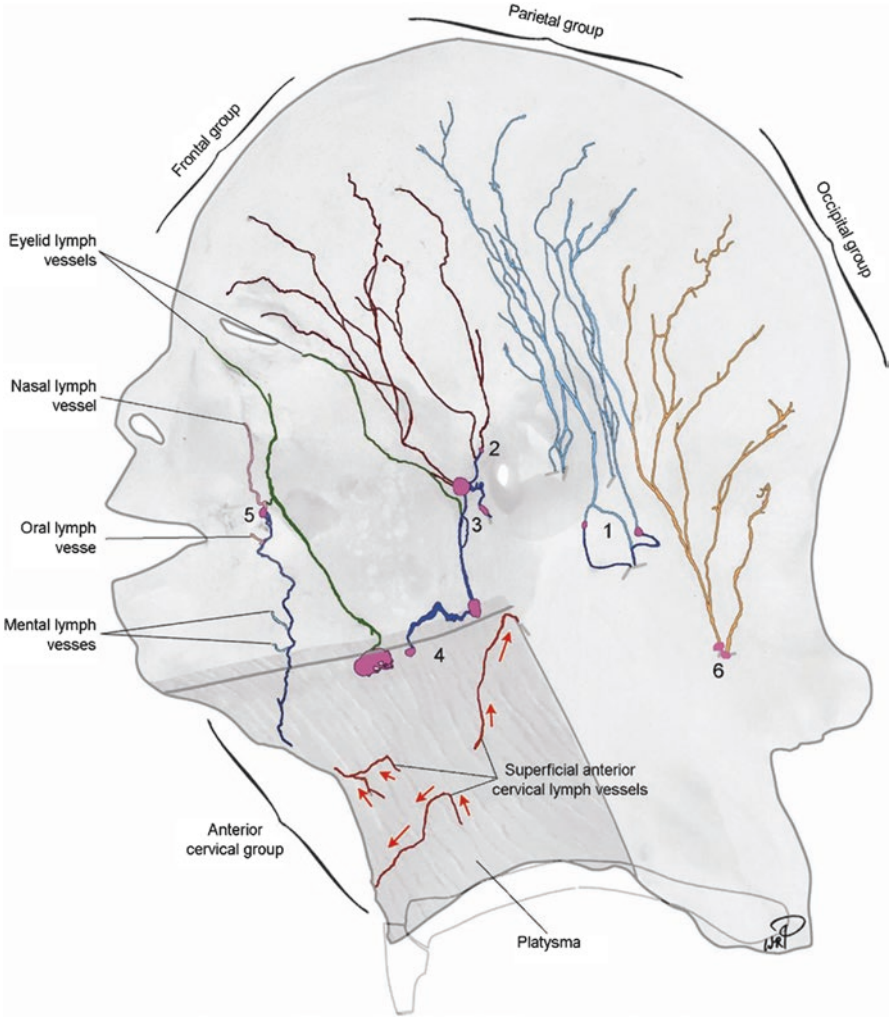

Fig. 3.4 Distribution of the lymphatics in the superficial tissue of the left head and neck above the platysma. Vessels are colour coded, highlighting the different vessel groups and lymph nodes. (*1*) Retroauricular lymph node. (*2*) Preauricular lymph nodes. (*3*) Parotid lymph nodes. (*4*) Submandibular lymph nodes. (*5*) Buccinator lymph node. (*6*) Deep occipital lymph nodes

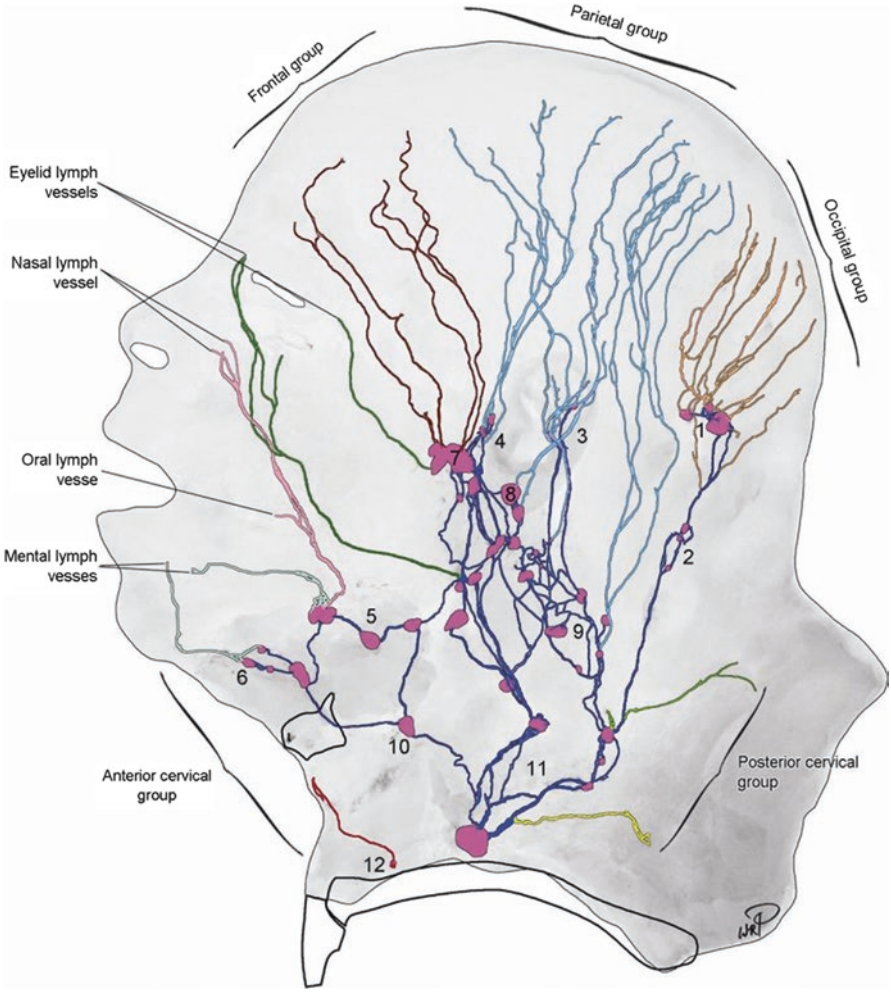

Fig. 3.5 Distribution of the lymphatics in the superficial tissue of the left head and neck deep to the platysma. Vessels are colour coded, highlighting the different vessel groups and lymph nodes. (*1*) Superficial occipital lymph nodes. (*2*) Deep occipital lymph nodes. (*3*) Retroauricular lymph node. (*4*) Preauricular lymph nodes. (*5*) Submandibular lymph nodes. (*6*) Submental lymph nodes. (*7*) Parotid lymph nodes. (*8*) Infra-auricular lymph nodes. (*9*) Internal jugular lymph nodes. (*10*) Anterior jugular lymph node. (*11*) Supraclavicular lymph nodes. (*12*) Anterior jugular lymph node

1.1 Scalp Region

The lymph-collecting vessels were dense in the scalp region and arose from precollectors about 2 cm from the midline, which ran downwards and backwards and travelled in a "wavelike" or "snakelike" fashion to reach their first-tier (sentinel) lymph nodes in the subcutaneous tissue (Figs. 3.4 and 3.5). The lymphatic vessels diverged and converged along their course. Sometimes they crossed over or anastomosed with neighbouring vessels. The scalp lymphatic vessels include the frontal, the parietal and the occipital groups.

1.1.1 Frontal Group

An average of four collecting lymph vessels (ranging from three to six) were identified in the frontal section. Between the superior edge of the eyebrow and the coronal suture, vessels coursed radially in the deep aspect of the subcutaneous tissue towards their first-tier lymph nodes. They then branched, diverged and converged along their course; vessels drained to the preauricular and/or parotid lymph nodes (Figs. 3.4 and 3.5), and the preauricular and retroauricular lymph nodes (Fig. 3.6); the nasolabial, preauricular and retroauricular lymph nodes (Fig. 3.7); and the buccinator, preauricular, retroauricular and deep parotid lymph nodes (Fig. 3.8).

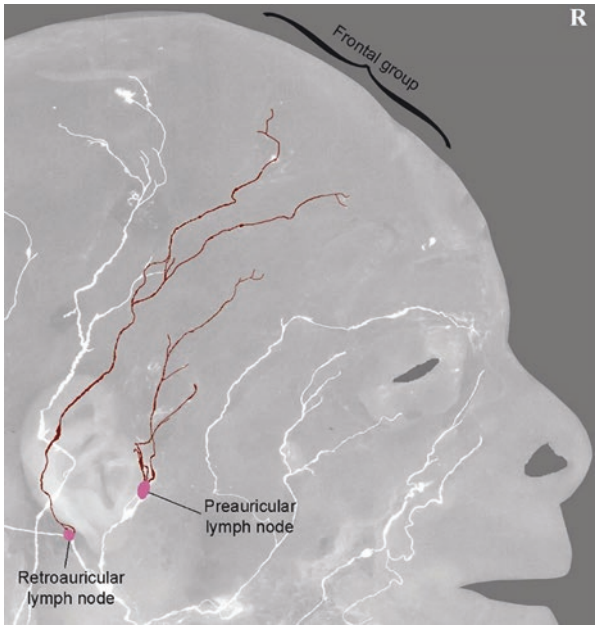

Fig. 3.6 Lymphangiogram of the integument of the head and neck after a lymphatic contrast injection. The frontal group of lymph vessels (*brown*) enters the preauricular and retroauricular lymph nodes (*purple*)

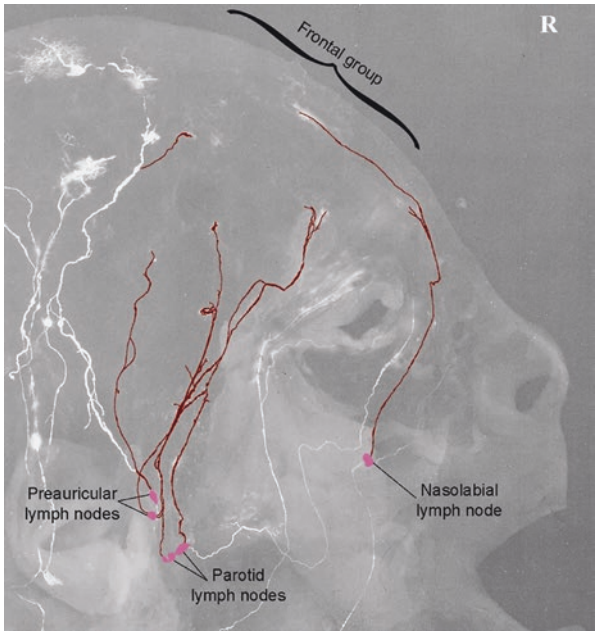

Fig. 3.7 Lymphangiogram of the integument of the head and neck after a lymphatic contrast injection. The highlighted region shows the frontal group of lymph vessels (*brown*) and related lymph nodes (*purple*)

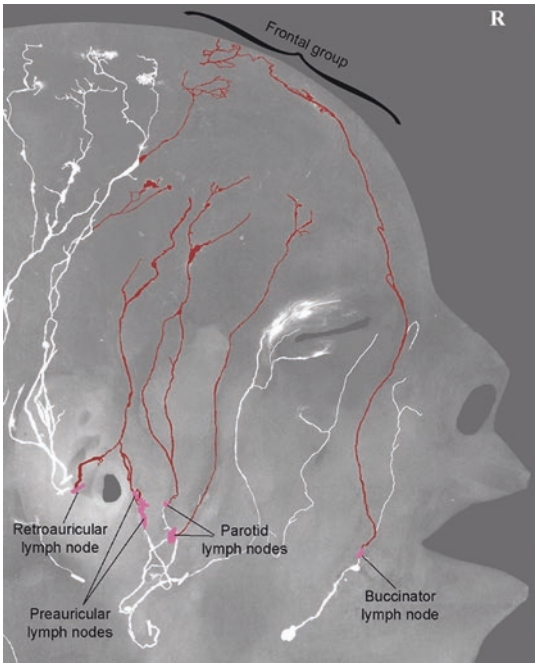

Fig. 3.8 Lymphangiogram of the integument of the head and neck after a lymphatic contrast injection. The frontal group of lymph vessels (*highlighted brown*) and related lymph nodes (*purple*)

1.1.2 Parietal Group

An average of 6 collecting lymph vessels (ranging from 4 to 12) were identified in the parietal section. Vessels travelled radially in the deep aspect of the subcutaneous tissue between the coronal and the lambdoid sutures towards their first-tier lymph nodes. They drained to one or multiple groups of the preauricular, retroauricular, deep occipital or internal jugular lymph nodes (Figs. 3.4, 3.5, 3.9, 3.10 and 3.11).

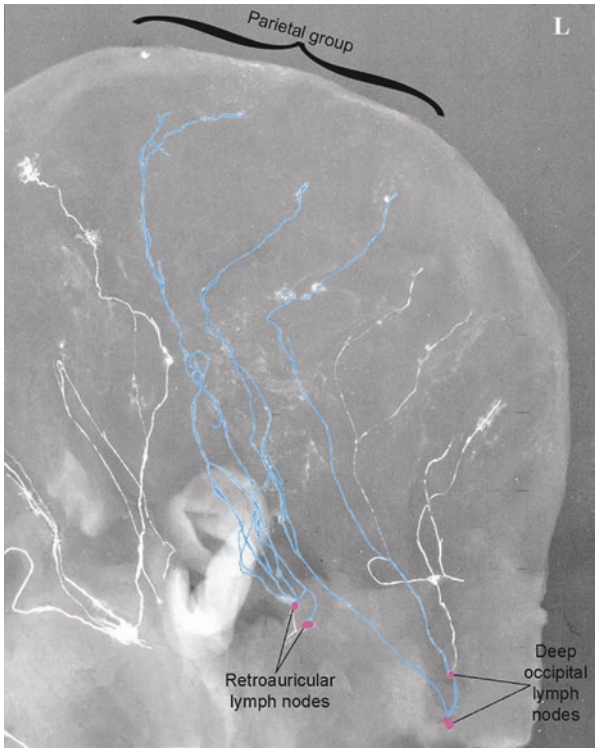

Fig. 3.9 Lymphangiogram of the integument of the head and neck after a lymphatic contrast injection. The parietal group of lymph vessels (*highlighted light blue*) and related lymph nodes (*purple*)

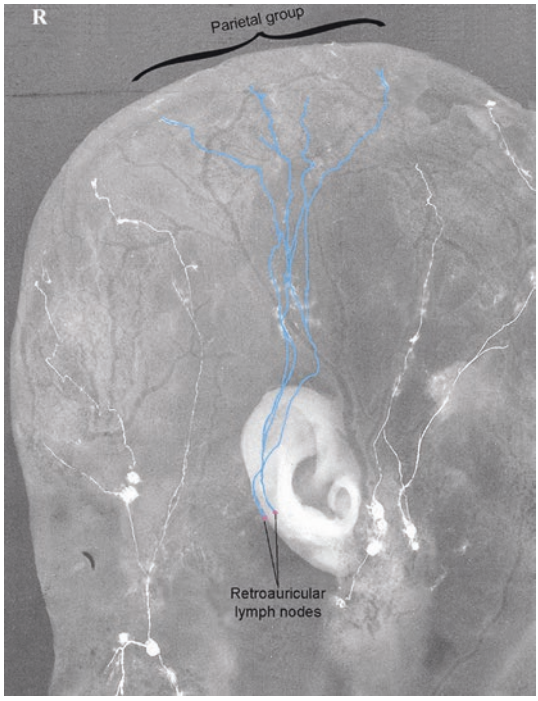

Fig. 3.10 Lymphangiogram of the integument of the head and neck after a lymphatic contrast injection. The parietal region of lymph vessels (*highlighted light blue*) enters retroauricular lymph nodes (*purple*)

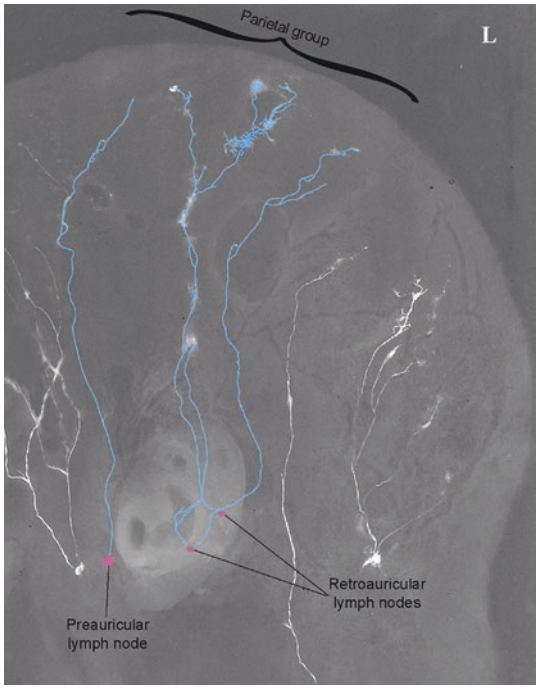

Fig. 3.11 Lymphangiogram of the integument of the head and neck after a lymphatic contrast injection. The parietal group of lymph vessels (*highlighted light blue*) enters preauricular and retroauricular lymph nodes (*purple*)

1.1.3 Occipital Group

An average of six collecting lymph vessels (ranging from four to nine) were identified in the occipital section. Vessels travelled radially in the deep aspect of the subcutaneous tissue between the lambdoid suture and the posterior hairline towards their first-tier lymph nodes. They drained to one or multiple groups of the superficial, deep occipital and internal jugular lymph nodes (Figs. 3.4, 3.5, 3.14, 3.15 and 3.16).

Clinical Implication
The incidence of skin cancer, especially melanoma, is very high in Western countries (particularly in Australia) (Uren et al. 1999; Thompson et al. 2004). Reports have shown that, after statistical analysis by using lymphoscintigraphy for scalp cancer patients, lymphatic drainage (or metastasis) of up to 43% of patients was not to the closest or regional lymph nodes, but to unpredictable or distant lymph nodes. It can be seen, from Figs. 3.1, 3.2, 3.3, 3.4, 3.5, 3.6, 3.7, 3.8, 3.9, 3.10, 3.11, 3.12, 3.13, 3.14, 3.15 and 3.16, there were individual differences in lymphatic pathways within the scalp.

1.2 Facial Region

Lymphatic vessels were sparse in the facial region. An average of four lymph vessels (ranging from three to five) were found. Vessels travelled radially from medial to lateral towards their first-tier lymph nodes in the subcutaneous tissue between the eyebrow and the inferior border of the mandible. Four groups of vessels were identified in the origin.

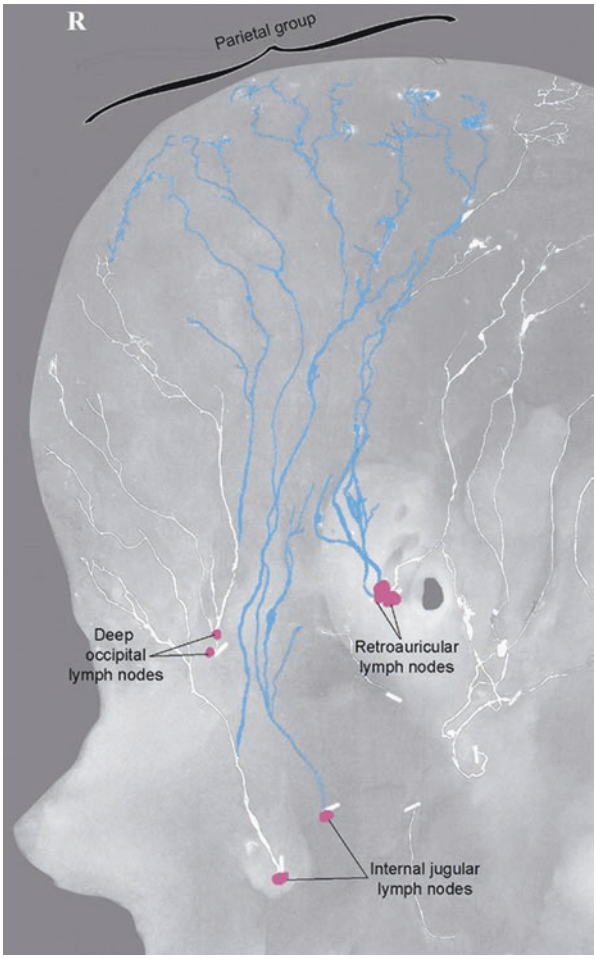

Fig. 3.12 Lymphangiogram of the integument of the head and neck after a lymphatic contrast injection. The parietal group of lymph vessels (*highlighted light blue*) and related lymph nodes (*purple*). Note some of them merge with neighbouring vessels before entering the lymph nodes

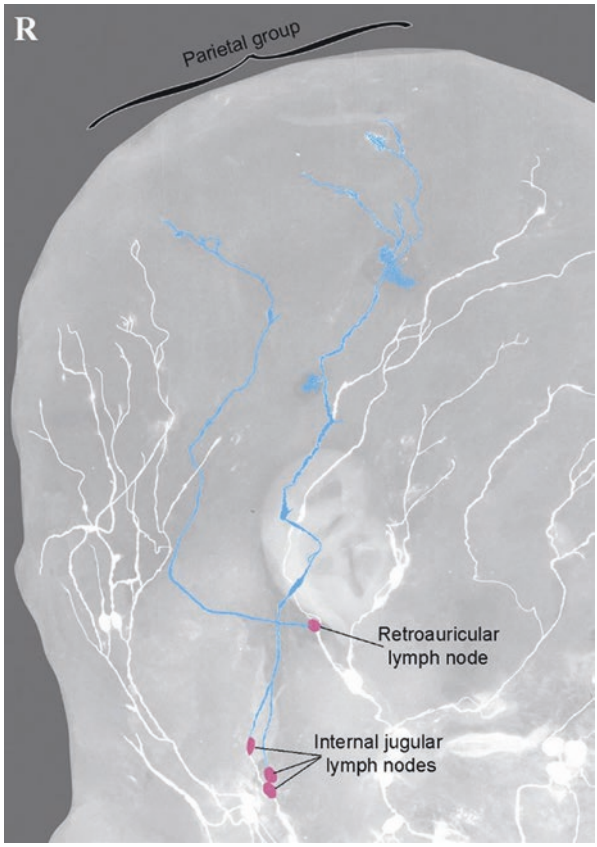

Fig. 3.13 Lymphangiogram of the integument of the head and neck after a lymphatic contrast injection. The parietal group of lymph vessels (*highlighted light blue*) enters the retroauricular and internal jugular lymph nodes (*purple*)

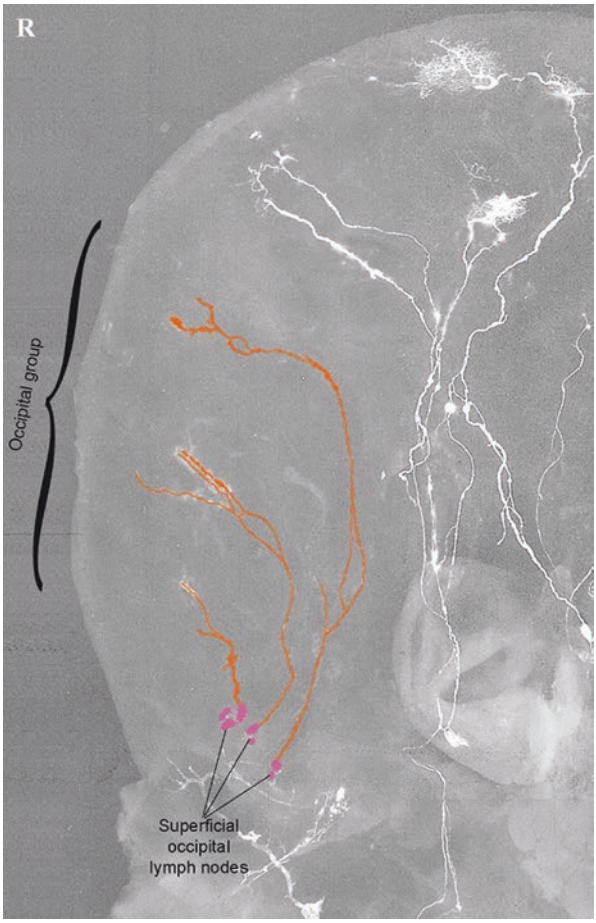

Fig. 3.14 Lymphangiogram of the integument of the head and neck after a lymphatic contrast injection. The occipital group of lymph vessels (*orange*) enters superficial occipital lymph nodes (*purple*)

Fig. 3.15 Lymphangiogram of the integument of the head and neck after a lymphatic contrast injection. The occipital group of lymph vessels (*orange*) enters deep occipital lymph nodes (*purple*)

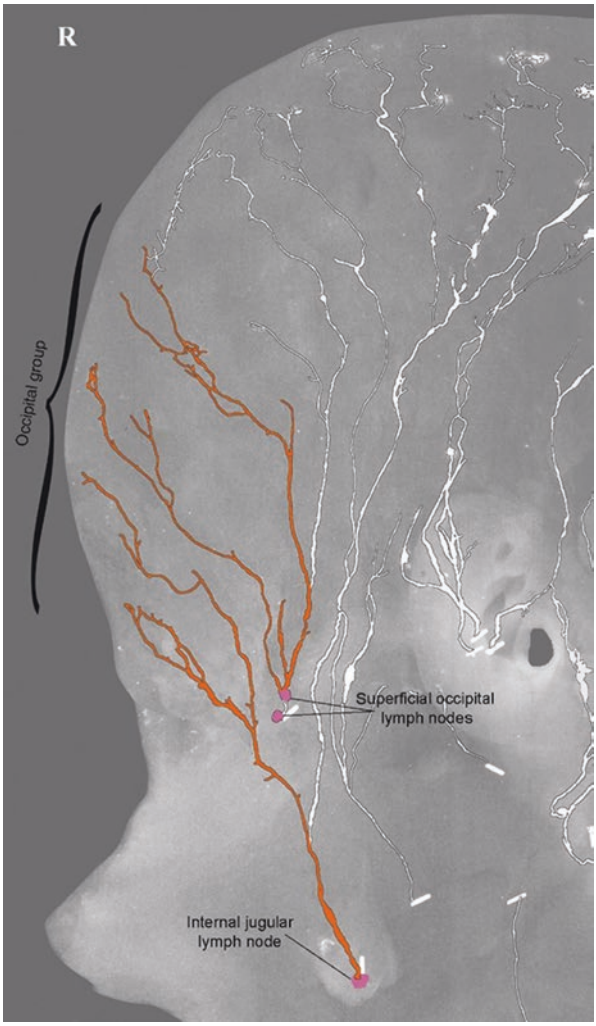

Fig. 3.16 Lymphangiogram of the integument of the head and neck after a lymphatic contrast injection. The occipital group of lymph vessels (*orange*) enters superficial occipital and internal jugular lymph nodes (*purple*)

1.2.1 Eyelid Lymph Vessels

The lymph capillary plexus arose in the dermis of the upper and lower eyelids. They formed an outer canthus lymph vessel at the outer canthus, an inner canthus lymph vessel at the inner canthus and an inferior eyelid lymph vessel at the middle-inferior section of the lower eyelid (Fig. 3.17).

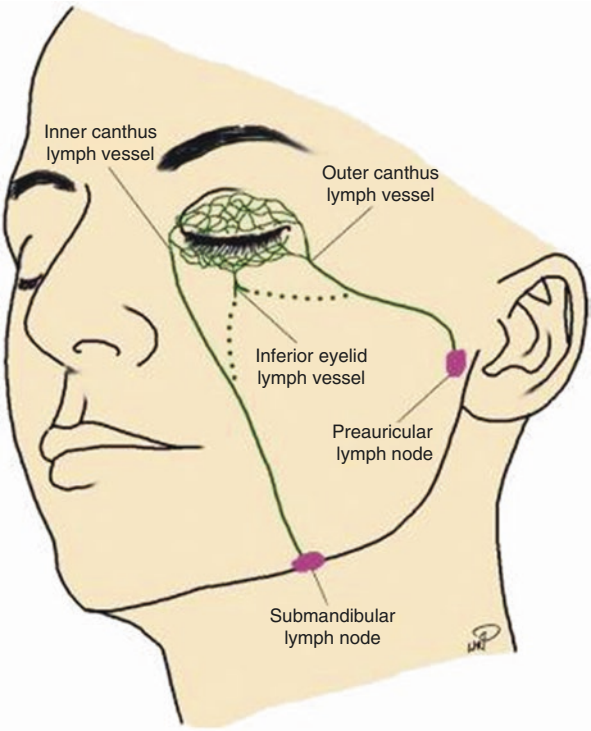

Fig. 3.17 A schematic diagram of eyelid lymph vessels. Note that the inferior eyelid lymph vessel (*dotted line*) can merge with either the outer or inner canthus lymph vessels

Outer Canthus Lymph Vessel

An average of two vessels (ranging from one to three) formed a main collecting lymph vessel in the subcutaneous tissue at the outer canthus. They travelled obliquely and then drained to the preauricular, parotid or submandibular lymph nodes (Figs. 3.4, 3.5, 3.17, 3.18, 3.19 and 3.20).

Inner Canthus Lymph Vessel

Formed by the lymph capillary plexus, a collecting lymph vessel arose in the inner canthus, travelled obliquely in the subcutaneous tissue and drained to the submandibular, parotid or buccinator lymph nodes (Figs. 3.4, 3.5, 3.17, 3.18, 3.19 and 3.20). Occasionally, one upper-inner canthus vessel was found running horizontally and laterally above the superior edge of the eyebrow. It then travelled obliquely backwards and downwards on the lateral side of the eyebrow, passed over the zygomatic process, descended to converge with the outer canthus vessel and drained to the submandibular lymph node (Fig. 3.20).

Inferior Eyelid Lymph Vessel

A collecting lymph vessel was formed by the lymph capillary plexus in the middle-inferior spot of the lower eyelid; it travelled obliquely in the subcutaneous tissue and converged either with the outer or inner canthus lymph vessels and then drained into related lymph nodes (Figs. 3.4, 3.5, 3.17, 3.18, 3.19 and 3.20).

Clinical Implication
As eyelid lymph vessels are situated superficially in the orbital area, they are easily damaged by injury or due to iatrogenic reasons, thus causing eyelid lymphoedema (Klapper and Patrinely 2007; Chalasani and McNab 2010; Aveta et al. 2011). The avalvular lymph capillary vessels connect the outer, inner canthus and inferior eyelid lymph vessels in the upper and lower eyelids (Fig. 3.17). Lymph flows to either the outer or inner canthus vessels in the upper eyelid and the outer, inner canthus or inferior eyelid lymph vessels in the lower eyelid. Due to this, lymphoedema of the eyelid will occur if multiple vessels are damaged (for details, see pages 198–199).

The lymphatic drainage patterns of the eyelid are differed from person to person. It is suggested to locate the sentinel lymph node by using lymphoscintigraphy for biopsy in the treatment of eyelid cancer patients, which may help to reduce the recurrent rate.

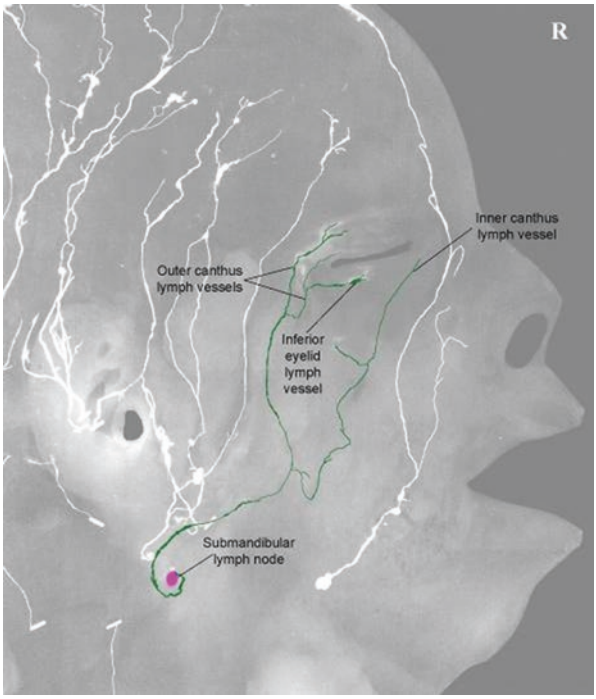

Fig. 3.18 Lymphangiogram of the face after lymphatic contrast injection. The inferior eyelid vessel merges to a tributary of the outer canthus lymph vessels (*dark green*) and forms a main vessel in the zygomaticus, which converges with the inner canthus lymph vessel in the cheek and then drains to the submandibular lymph node (*purple*)

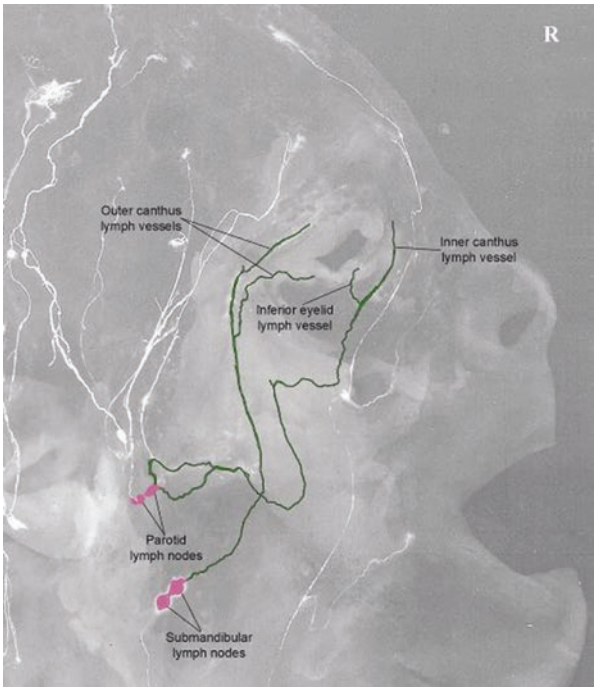

Fig. 3.19 Lymphangiogram of the face after lymphatic contrast injection. The outer canthus lymph vessels (*dark green*) drain to the submandibular lymph nodes (*purple*). The inner canthus lymph vessel converges with the inferior eyelid vessel (*dark green*), crosses over the outer canthus lymph vessel in the cheek and then flows into the parotid lymph node (*purple*)

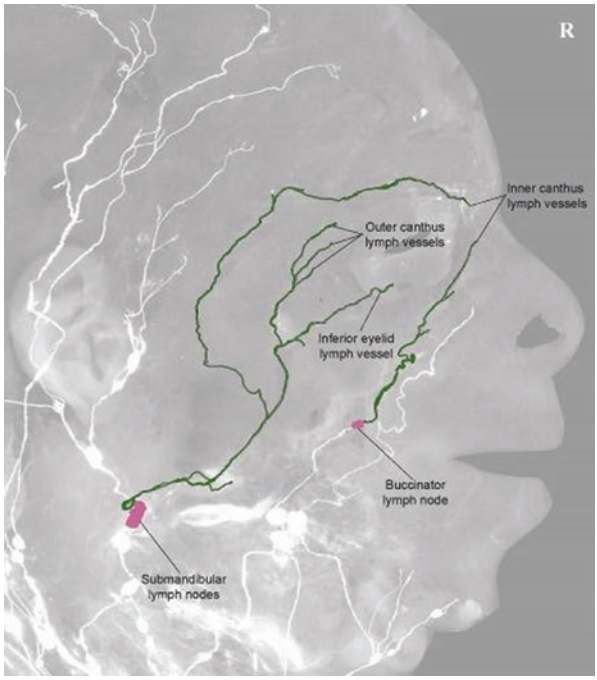

Fig. 3.20 Lymphangiogram of the face after lymphatic contrast injection. The outer canthus lymph vessels (*dark green*) converge with the inferior eyelid lymph vessel in the zygomaticus and the upper tributary of the inner canthus vessel in the cheek draining to the submandibular lymph nodes (*purple*). The inner canthus lymph vessel flows into the buccinator lymph node (*purple*)

1.2.2 Nasal Lymph Vessels

Arising from the lateral side of the external nose, nasal lymph vessels travelled obliquely downwards from median to lateral sides in the subcutaneous tissue of the cheek. They drained to the nasolabial, buccinator or submandibular lymph nodes or merged with neighbouring vessels before entering the related nodes (Figs. 3.4, 3.5, 3.21, 3.22, 3.23, 3.24 and 3.25).

1.2.3 Oral Lymph Vessels

Arising from the corner of the mouth in each side, one or two collecting lymph vessels travelled in the subcutaneous and drained directly to the buccinator, submandibular or submental lymph nodes or merged with neighbouring lymph vessels before entering the related nodes (Figs. 3.4, 3.5, 3.21 and 3.22).

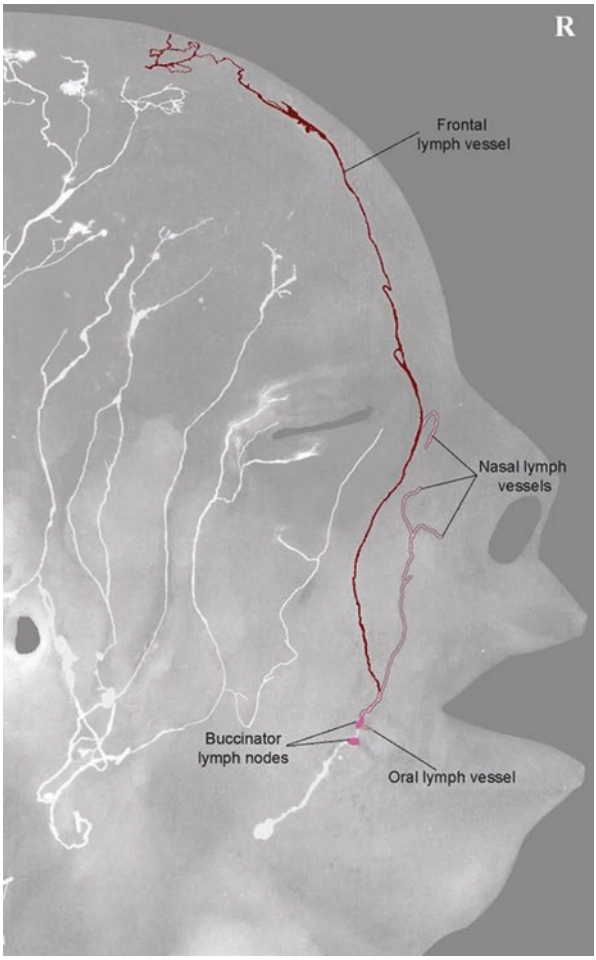

Fig. 3.21 Lymphangiogram of the face after lymphatic contrast injection. Nasal lymph vessels (*pink*) and a short oral lymph vessel (*light orange*) enter one of the buccinator lymph nodes (*purple*). Note that a tributary of nasal lymph vessels converges with the frontal lymph vessel (*brown*) before entering the node

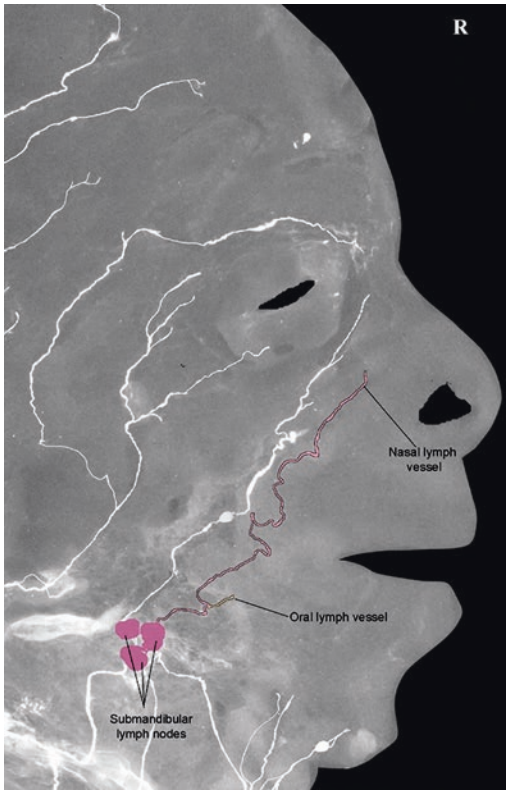

Fig. 3.22 Lymphangiogram of the facial region after lymphatic contrast injection. A nasal lymph vessel (*pink*) converging with an oral lymph vessel (*light orange*) drains to one of the submandibular lymph nodes (*purple*)

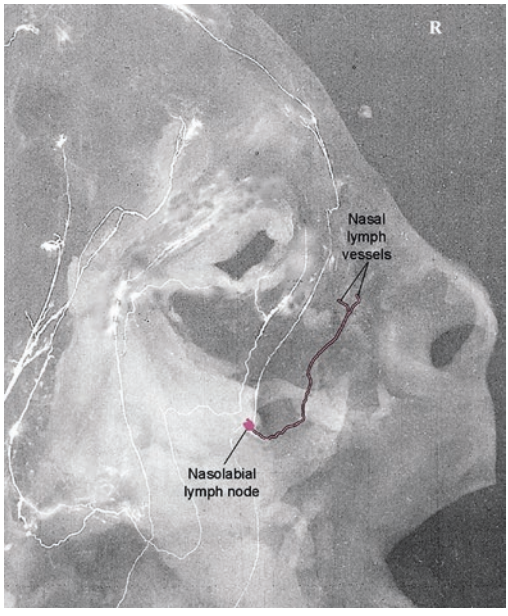

Fig. 3.23 Lymphangiogram of the face after lymphatic contrast injection. Nasal lymph vessels (*pink*) drain to the nasolabial lymph node (*purple*)

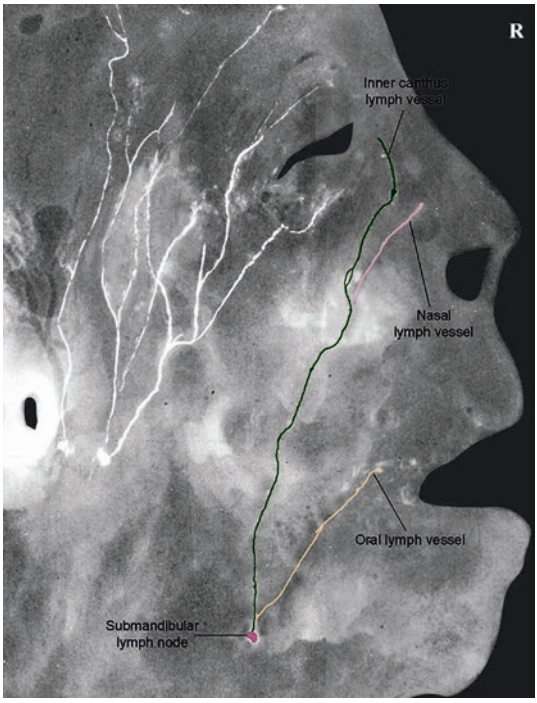

Fig. 3.24 Lymphangiogram of the face after lymphatic contrast injection. Nasal (*pink*) and oral (*light orange*) lymph vessels merge to the inner canthus lymph vessel (*green*) and drain to the submandibular lymph node (*purple*)

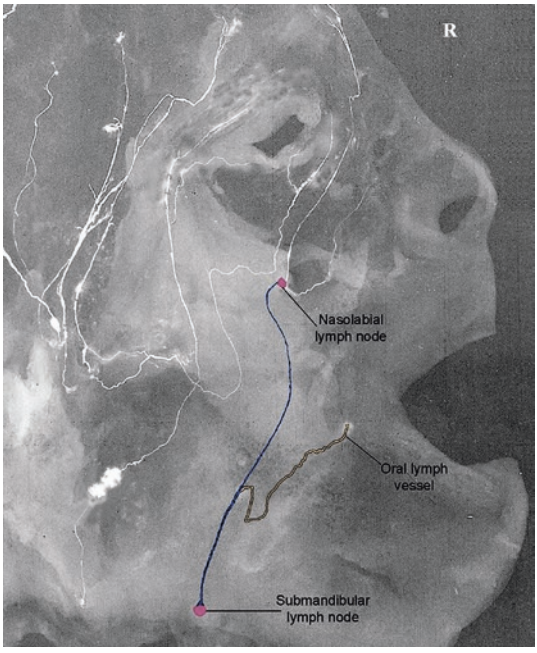

Fig. 3.25 Lymphangiogram of the face after lymphatic contrast injection. An oral lymph vessel (*light orange*) merges to the internodal lymph vessel (*blue*) and then drains to the submandibular lymph node (*purple*)

1.2.4 Mental Lymph Vessels

An average of three collecting lymph vessels (ranging from two to four) were found in the chin. They travelled in the deep aspect of the subcutaneous tissue of the chin and drained to the submental and/or submandibular lymph nodes (Figs. 3.4, 3.5 and 3.26).

1.3 Cervical Region

Three groups of collecting lymph vessels were identified in the cervical region.

1.3.1 Anterior Cervical Group

Two layers of lymphatic vessels were identified in the anterior superficial neck.

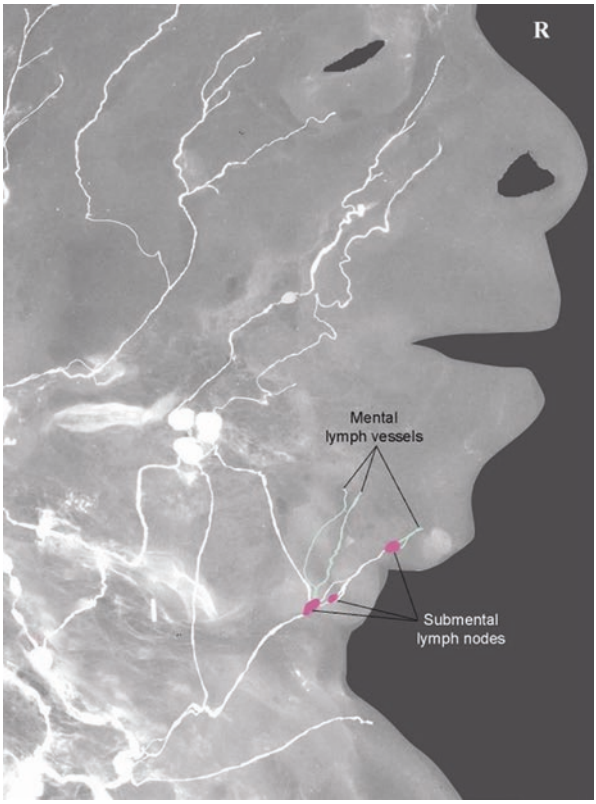

Fig. 3.26 Lymphangiogram of the face after lymphatic contrast injection. Mental lymph vessels (*aqua blue*) drain to submental lymph nodes (*purple*)

Superficial Anterior Cervical Lymph Vessels

Above the platysma, each lymphatic vessel travelled in a different direction, running upwards, horizontally or obliquely. Medially, between the inferior border of the mandible and the laryngeal prominence vessels, they pierced the platysma near the midline and drained to the submental lymph node; between the laryngeal prominence and jugular notch, they pierced the platysma and drained to the supraclavicular lymph node. Laterally, vessels turned over the lateral edge of the platysma and then drained to the submandibular lymph node (Figs. 3.4, 3.5, 3.27, 3.28 and 3.29).

Occasionally, medial vessels between the laryngeal prominence and jugular notch drained into the anterior superficial jugular lymph nodes (Fig. 3.28).

Anterior Cervical Lymph Vessels

Below the platysma, vessels travelled above the deep fascia and drained to the anterior jugular lymph node (Fig. 3.5) or supraclavicular lymph node (Fig. 3.29).

1.3.2 Lateral Cervical Group

In the lateral side of the neck, lymph vessels were abundant and complex. They are situated between the inferior border of the earlobe and the root of the neck and travel in different directions and multiple layers – the subcutaneous (superficial), the inter- and/or intramuscular (middle) and the perivascular (deep) layers. Most of them were sited between lymph nodes and named the internodal collecting lymph vessels (Figs. 3.5 and 3.29).

1.3.3 Posterior Cervical Group

Collecting lymph vessels were sparse in the posterior area of the neck. Two sets of the vessels were found. The diameter of the collecting lymph vessel was about 1 mm after lymphatic injection.

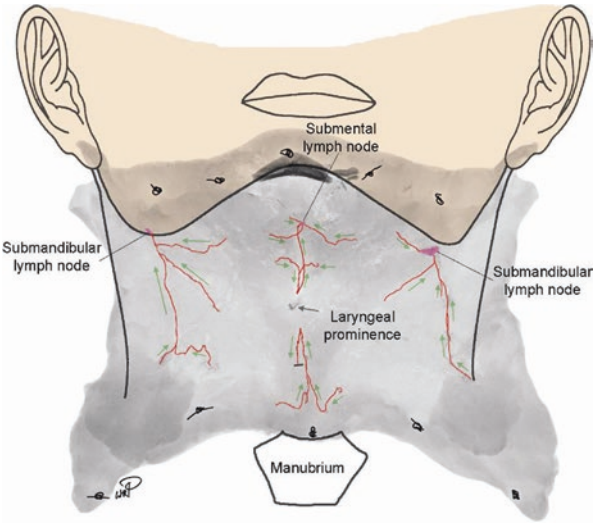

Fig. 3.27 Composite drawing and X-ray of the jaw and the skin of the anterior neck. Above the platysma, the superficial anterior cervical lymph vessels (*red*) travel in different ways and drain into the related lymph nodes (*purple*). *Green arrows* indicate the direction of the lymph flow

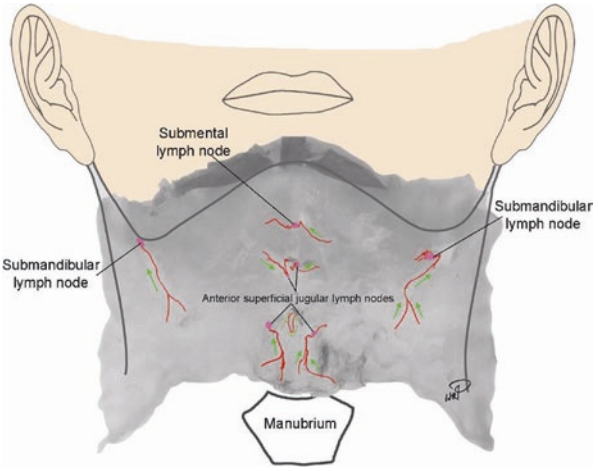

Fig. 3.28 Composite drawing and X-ray of the jaw and the skin of the anterior neck. Above the platysma, the superficial anterior cervical lymph vessels (*red*) travel in different ways and drain into the related lymph nodes (*purple*). *Green arrows* indicate the direction of the lymph flow

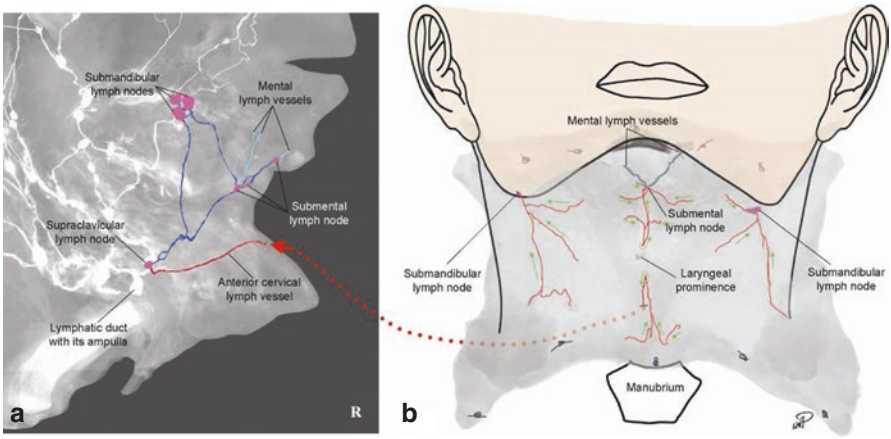

Fig. 3.29 (**a**) Lymphangiogram of the right face and neck after lymphatic contrast injection shows the distribution of the anterior cervical lymph vessels below the platysma. *Aqua* highlights the mental lymph vessels; *blue* indicates the intermodal lymph vessels. The red-coloured vessel is a continuing lymph vessel arising above the platysma; its position is indicated by a *doted red line* and *arrow*. They drain into the related lymph nodes (*purple*). (**b**) The distribution of the superficial anterior cervical lymph vessels (*red*) above the platysma and their related lymph nodes (*purple*). *Green arrows* indicate the direction of the lymph flow

Supratrapezoid Lymph Vessels

The vessel travelled anteromedially in the deep aspect of the subcutaneous in the root of the neck draining to the supraclavicular lymph nodes (Figs. 3.5 and 3.30).

Supraclavicular Lymph Vessels

Vessels travelled anteromedially in the deep aspect of the subcutaneous in the root of the neck draining to lateral internal jugular and/or supraclavicular lymph nodes (Figs. 3.5 and 3.30).

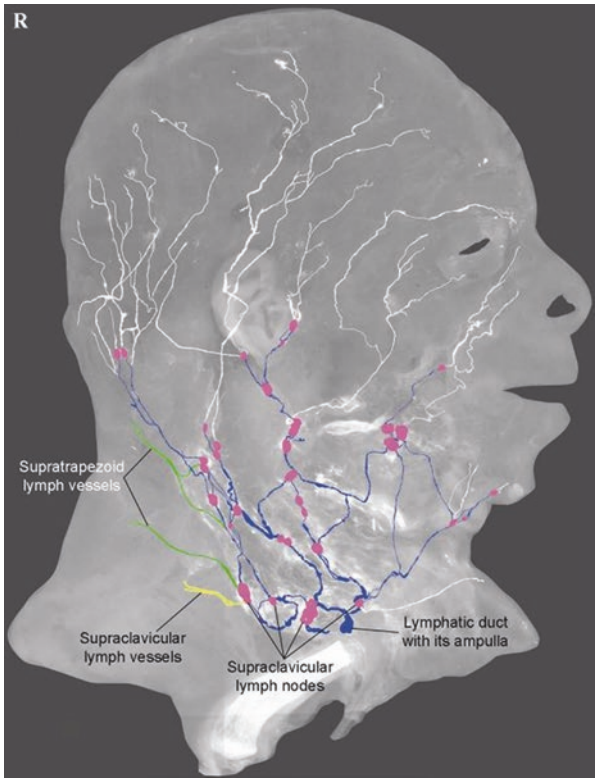

Fig. 3.30 Lymphangiogram of the head and neck after lymphatic contrast injection, showing the internodal lymph vessels (*blue*), supratrapezoid vessels (*light green*), supraclavicular vessels (*yellow*) and related lymph nodes (*purple*)

1.4 Auricular Region

Four groups of lymph vessels were identified in the auricle (Figs. 3.31, 3.32, 3.33, 3.34 and 3.35).

1.4.1 Preauricular Lymph Vessels

The lymph capillary plexus was distributed over most of the anterior aspects of the auricle. Medially, they converged to form a collecting lymph vessel running in the subcutaneous of the crus of helix. The vessel drained directly or indirectly (merged with a frontal lymph vessel) to the preauricular lymph nodes (Figs. 3.31, 3.32, 3.33 and 3.34 green vessels).

1.4.2 Supraauricular Lymph Vessels

An average of three collecting lymph vessels (ranged from two to four), arising in the superior aspect of the helix, travelled in the subcutaneous of the back of the auricle and converged together and then ran in the subcutaneous of the upper lateral neck to reach the infra-auricular and/or substernocleidomastoid lymph nodes. Occasionally, they were divided into two branches to reach the related lymph nodes (Figs. 3.31, 3.32, 3.33 and 3.34 orange vessels).

1.4.3 Midauricular Lymph Vessels

Arising from the scaphoid fossa near the auricular tubercle, collecting lymph vessels ran downwards, passed over the cartilage at the middle of the rim and then travelled obliquely in the subcutaneous of the back of the auricle, continuing their course in the subcutaneous of the upper lateral neck vessels until the infra-auricular lymph node is reached (Figs. 3.31, 3.32, 3.33, 3.34 yellow and 3.35 orange vessels). Occasionally, the vessel was divided into two branches. One entered the infra-auricular lymph node (Fig. 3.32 yellow vessels), while the other bypassed the node continuing its course (Fig. 3.32, indicated by a large white arrow).

1.4.4 Infra-auricular (Lobule) Lymph Vessels

Arising in the lobule of the auricle, collecting lymph vessels converged and travelled obliquely down to reach the infra-auricular node directly (Figs. 3.31, 3.32 and 3.33 blue vessels) or converged with neighbouring vessels before entering the node (Fig. 3.34 blue vessels). Occasionally, the vessel bifurcated into two branches before

reaching the infra-auricular lymph node. One of them entered the node, while the other one bypassed the node and continued its course (Fig. 3.33, indicated by a large white arrow).

Clinical Implication

Primary malignant melanoma of the auricle is rare, but the prognosis is poor. Lymphoscintigraphy for mapping sentinel lymph nodes of the auricle has shown varied patterns (Wey et al. 1998; Cole et al. 2003; Thompson et al. 2004). The early anatomical knowledge of the lymphatic drainage in the auricle made it hard to explain the complete lymph drainage patterns. This section has shown that lymph vessels arising from different zones in the auricle could drain to the same or different groups of lymph nodes. Sometimes vessels could bypass the nearest lymph node to reach the node in the distal site. This information may help clinical management of malignancies in this region.

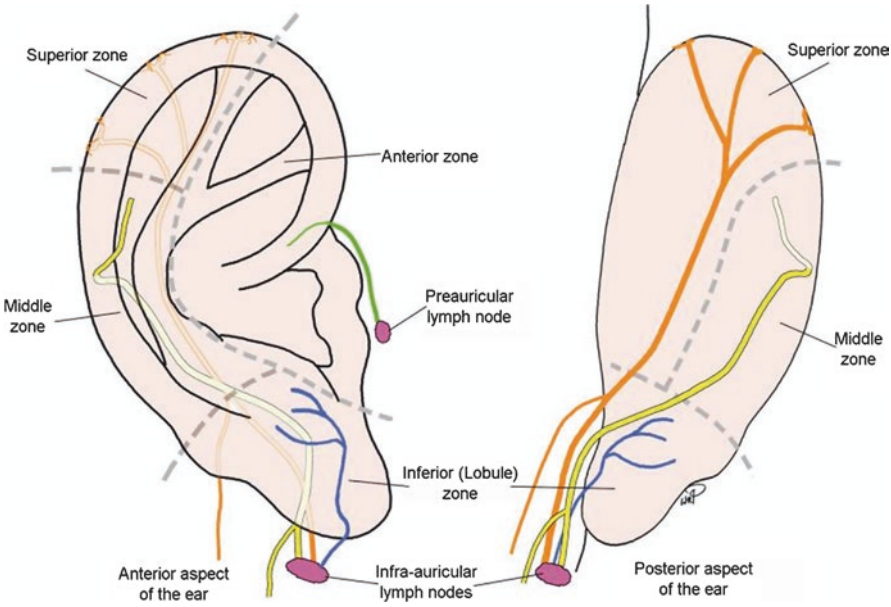

Fig. 3.31 A diagram of the lymphatic drainage zones in the anterior and posterior aspects of the auricle. Dashed grey lines divide the auricle into four zones draining, respectively, by the anterior (*green*), superior (*orange*), meddle (*yellow*) and inferior (*blue*) groups of auricular lymph vessels

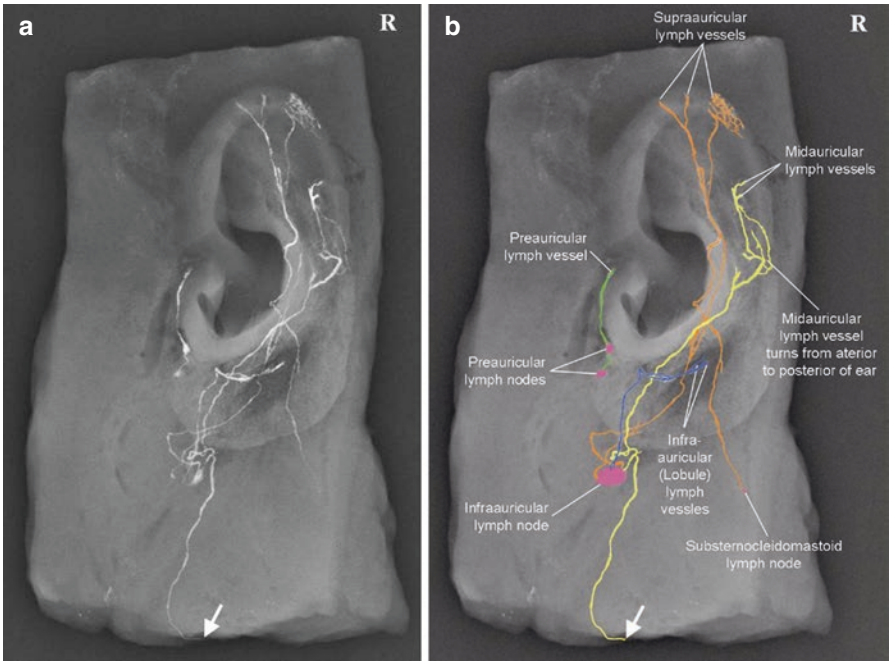

Fig. 3.32 (**a**) Lymphangiogram of the auricle after lymphatic contrast injection. (**b**) Lymphatic pathways from different origins are highlighted in different colours

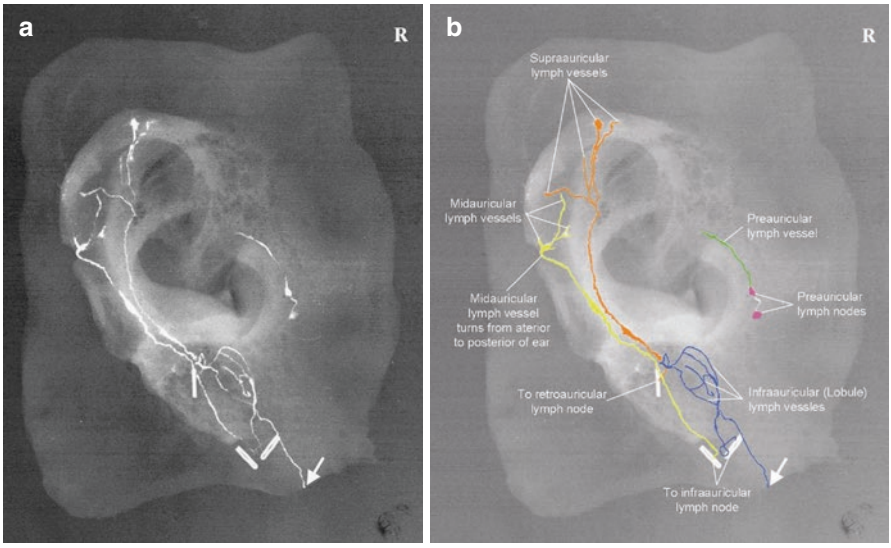

Fig. 3.33 (**a**) Lymphangiogram of the auricle after lymphatic contrast injection. (**b**) Lymphatic pathways from different origins are highlighted in different colours

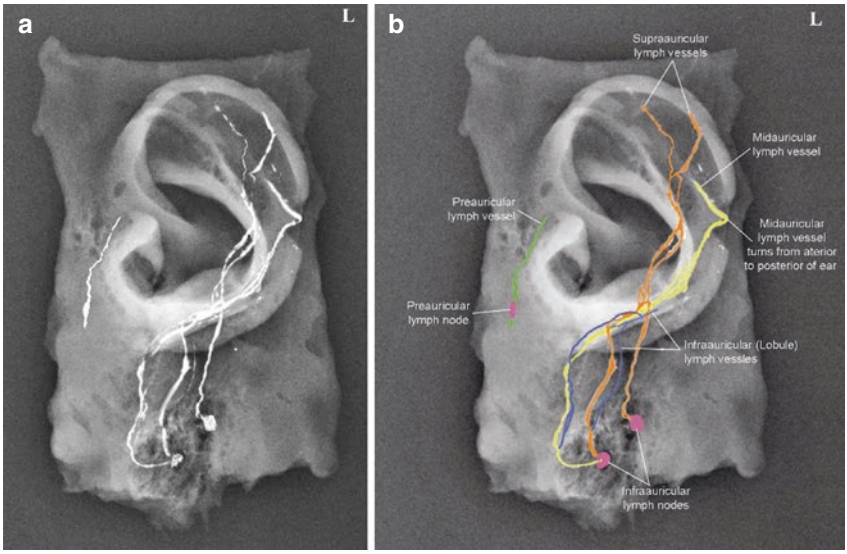

Fig. 3.34 (**a**) Lymphangiogram of the auricle after lymphatic contrast injection. (**b**) Lymphatic pathways from different origins are highlighted in different colours

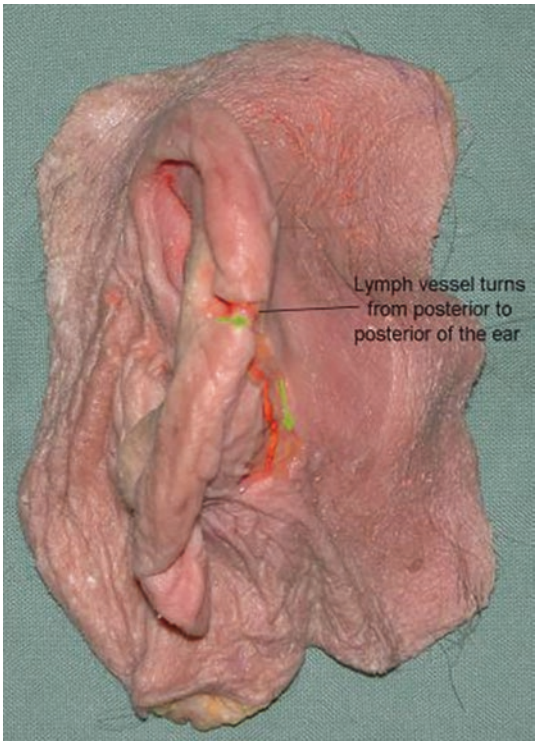

Fig. 3.35 The midauricular lymph vessel filled with lead oxide mixture is shown turning over the cartilage of the rim travelling from the anterior to the posterior aspects of the auricle

2 Deep Lymphatics of the Head and Neck

2.1 Nasal Cavity and Nasopharynx

The lymph capillary plexus originated from the mucosa of the atrium, three turbinates and the floor of the nasal cavity. They formed a network of precollecting lymph vessels in the submucosa of the lateral wall of the choana (Fig. 3.36). Then, vessels travelled intricately to form two groups of the collecting lymph vessels running in the lateral and retropharyngeal spaces (Figs. 3.36, 3.37, 3.38, 3.39, 3.40 and 3.41).

2.1.1 Lateral Pharyngeal Group

The lateral part of the precollecting lymph vessels in the submucosa of the lateral wall of the choana descended and passed through the lateral wall of the nasopharynx and formed two collecting lymph vessels that descended laterally into the lateral pharyngeal space (Figs. 3.36, 3.37, 3.38, 3.39, 3.40 and 3.41).

Anterolateral Lymph Vessels

The collecting lymph vessels descended anteriorly and then turned posteriorly. It travelled obliquely on the medial side of the external carotid artery to reach its first-tier lymph node – the lateral pharyngeal node. It entered the posterior portion of the node that is situated on the lateral side of the external carotid artery, which is at the level of the origin of the facial artery (Figs. 3.37, 3.38, 3.39, 3.40 and 3.41).

Posterolateral Lymph Vessels

The collecting vessel descended on the medial aspect of the external carotid artery, and one vessel branched off above the origin of the facial artery and then divided into two vessels above the lateral pharyngeal node. One of them entered the lateral pharyngeal lymph node anteriorly. One bypassed the node and crossed the lateral side of the internal carotid artery entering the third-tier lymph node of the retropharyngeal lymph node chain in the retropharyngeal space. The vessel, branching above the origin of the facial artery, travelled medially along the external carotid artery and then divided into two vessels again. One entered the middle portion of the lateral pharyngeal lymph node. The other one bypassed the node and descended to divide again into two vessels on the lateral side just above the bifurcation of the internal and external carotid arteries. One ran anteriorly to enter the subdigastric lymph node, while the other one ran posteriorly to enter the fifth-tier lymph node of the retropharyngeal lymph node chain in the retropharyngeal space (Figs. 3.37, 3.38, 3.39, 3.40 and 3.41).

2.1.2 Retropharyngeal Group

The posterior part of the precollecting lymph vessels in the submucosa of the lateral wall of the choana descended and connected to the lymph capillary plexus in the mucosa around the eustachian tube orifice. On the proximal side of the lymph capillary plexus, one or two precollecting lymph vessels were formed (Figs. 2.76 and 3.36). They travelled horizontally and penetrated the pharyngobasilar fascia near the lateral pterygoid plate of the sphenoid bone and passed through the posterior wall of the pharynx. The vessels then converged to a lymph collector descending in the retropharyngeal space. It entered the first-tier lymph node of the retropharyngeal chain at the level of the styloid process and then the second to seventh tiers lymph nodes of the retropharyngeal chain that lined up in two columns in the lower part of the retropharyngeal space. Three of them were situated more medially and the other three more laterally. The size of lymph nodes varied from 2 mm to 9 mm (Figs. 3.38, 3.39, 3.40 and 3.41).

Note
The group of the retropharyngeal lymph node was found by Rouvière (1938) and was named as Rouvière nodes (Watanabe et al. 1985). According to the description in early studies, retropharyngeal lymph nodes could be subdivided into the lateral and medial groups. The lymph from the mucosa of the nasal cavity drained to the lateral group of node and subdigastric node, while the lymph from the mucosa of the nasopharynx drained to the medial group, the lateral pharyngeal and/or internal jugular lymph nodes. While it can be seen there are two groups of lymphatic pathways in Figs. 3.36, 3.37, 3.38, 3.39, 3.40 and 3.41, the lateral and retropharyngeal lymph vessels, they link the lymph capillary plexus of the nasal cavity and nasopharynx and drain to multiple first-tier lymph nodes. Two groups of lymph vessels connect to each other by precollecting lymph vessels in the choana and collecting lymph vessels around the bifurcation of the carotid arteries, although they travel, respectively, in the lateral and retropharyngeal spaces. This anatomical feature may direct clinical management of cancer treatment.

Clinical Implication
Primary malignant melanoma in the mucosa of the nasal cavity is rare, but the prognosis is poor despite the advances in radical neck surgery, postoperative radiotherapy and chemotherapy (Bhattacharyya 2002; Martin et al. 2004). The recurrence may have an anatomical base. Firstly, the abundant lymph capillary plexus that is distributed on the wall of the nasal cavity and the nasopharynx and the avalvular capillary vessels allow the lymph to drain in various directions. Secondly, two separate pathways travelling in the

parapharyngeal spaces have rich connections between them. Thirdly, those vessels can reach multiple first-tier lymph nodes.

Therefore it is suggested that treatment should include both groups of lymph nodes for patients with cancer in the nasal cavity or nasopharynx.

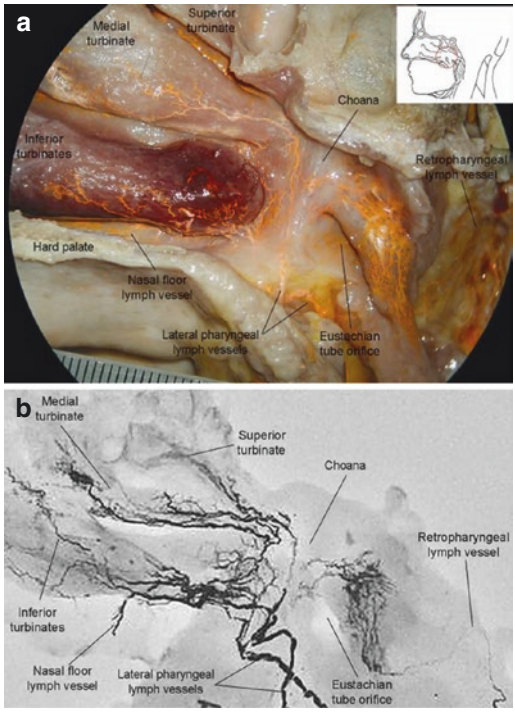

Fig. 3.36 Photograph (**a**) and radiograph (**b**) showing the lymphatic vessels in the nasal fossae and nasopharynx area filled with lead oxide mixture

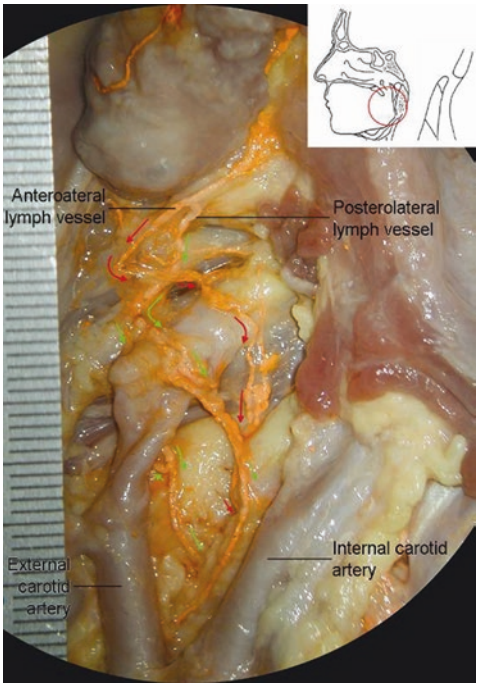

Fig. 3.37 Photograph (internal view) showing the lymphatic vessels in the lateral pharyngeal space filled with lead oxide mixture. *Red* and *green arrows* indicate the flow direction of the anterolateral and posterolateral lymph vessels

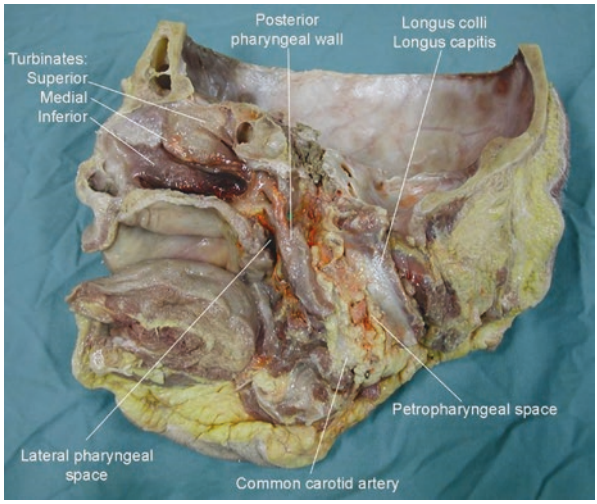

Fig. 3.38 Photograph of the interior view of the right half of the head and neck showing the lymph capillary plexus originating in the mucosa of the atrium, three turbinates, the floor of the nasal cavity, the nasopharynx and their pathways. They drain to the related lymph nodes in the parapharyngeal space

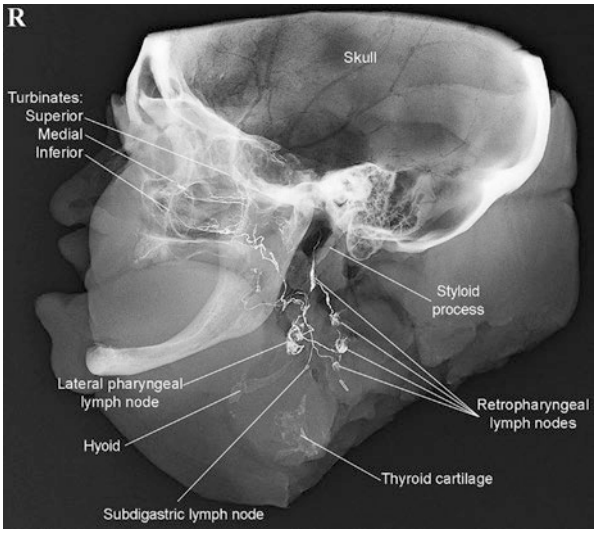

Fig. 3.39 Inverted radiograph (medial view) of the right half of the head and neck showing lymphatic pathways in the nasal fossae and nasopharynx

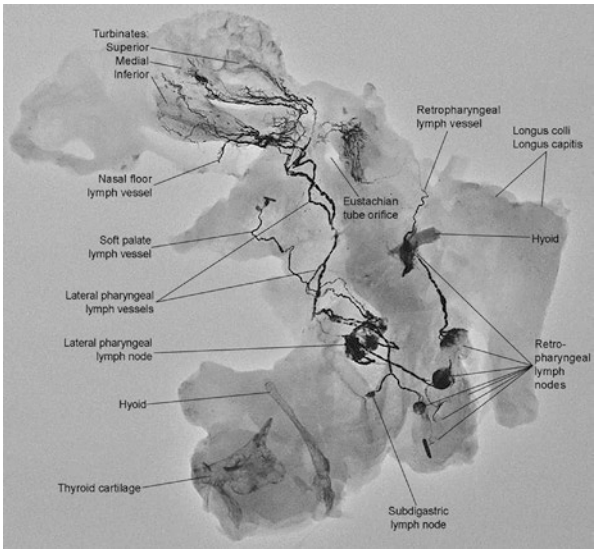

Fig. 3.40 Inverted radiograph of the nasal fossae and pharyngeal and laryngeal tissue, showing the distribution of the lymph vessels and lymph nodes

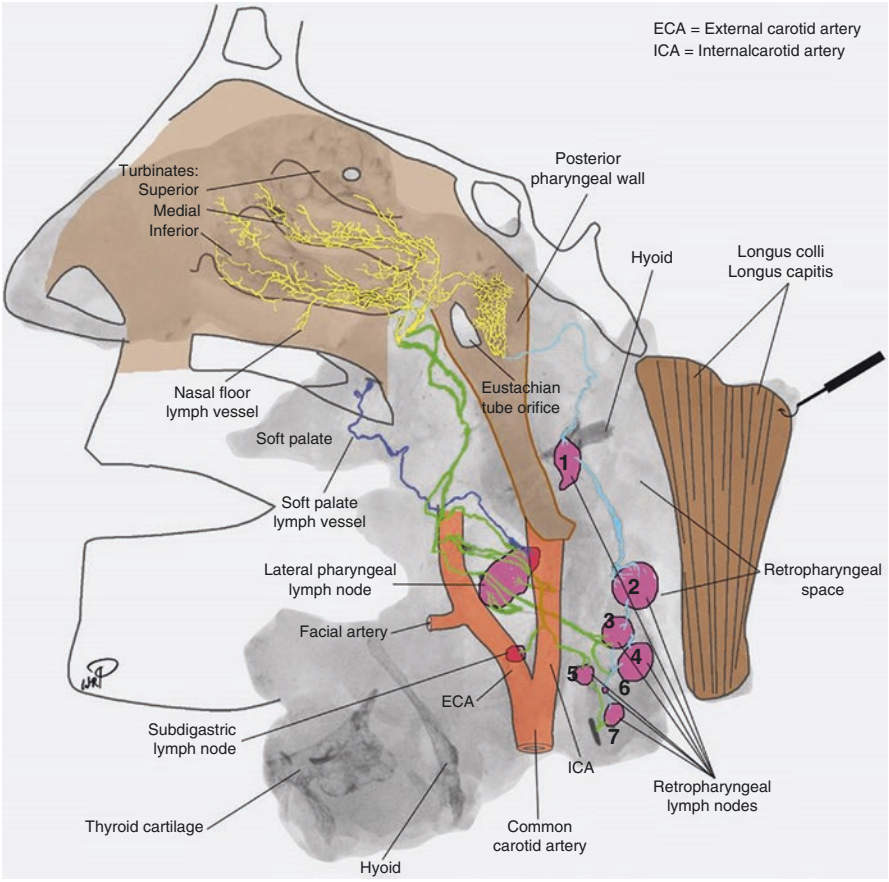

Fig. 3.41 A composite image of the lymphatic distribution of the nasal cavity, nasopharynx and parapharyngeal area. *Yellow*, lymph vessels in mucosae of the nasal cavity and nasopharynx. *Green*, lateral pharyngeal lymph vessels. *Light blue*, retropharyngeal lymph vessels. *Blue*, lymphatic vessels from soft palate. *Purple*, lymph nodes (retropharyngeal nodes are numbered). *Red*, carotid artery. *Dark brown*, longus muscles. *Light brown*, remaining wall of the nasal cavity and pharynx

2.2 *Soft Palate and Oropharynx*

On each side, one or two precollecting lymph vessels arose from the lymph capillary plexus in the mucosa of the inferior aspect of the soft palate (Fig. 2.75). They travelled horizontally towards the lateral oropharyngeal wall and penetrated the wall to form one or two collecting lymph vessels. Then vessels descended to reach the lateral pharyngeal lymph node and/or the subdigastric lymph node (Figs. 3.40, 3.41, 3.42, 3.43, 3.44 and 3.45).

The lymph capillary plexus originating in the mucosa of the oropharynx formed one to three precollecting lymph vessels (Fig. 3.46) in the submucosal layer. They penetrated the para-oropharyngeal wall and merged with collecting lymph vessels in the parapharyngeal spaces to reach the retropharyngeal and/or lateral pharyngeal lymph nodes (Figs. 3.37, 3.38, 3.39, 3.40 and 3.41).

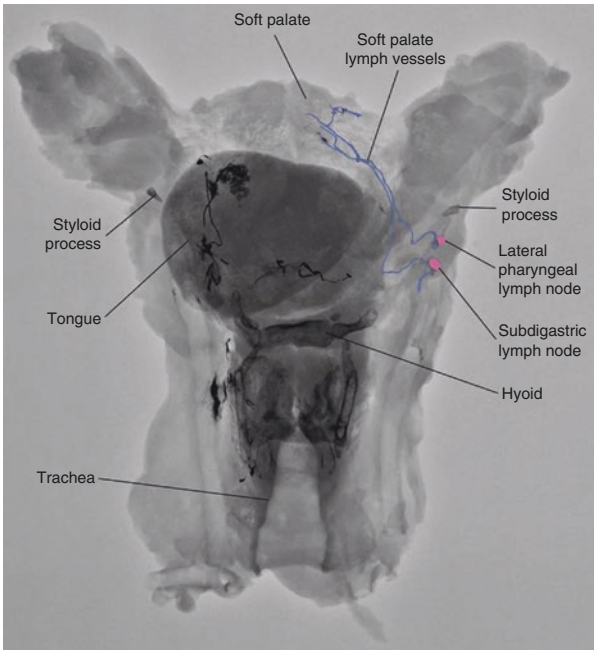

Fig. 3.42 Inverted radiograph of the tongue, soft palate, trachea and oesophagus shows the lymphatic pathway of the soft palate (*blue*) draining to both the subdigastric and lateral pharyngeal lymph nodes

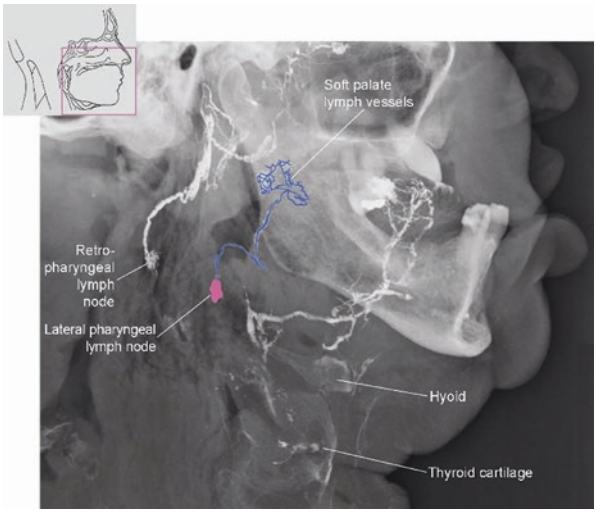

Fig. 3.43 Radiograph (medial view) of the left half of the head and neck after lead oxide injection shows the lymphatic pathway of the soft palate (*blue*) draining to the lateral pharyngeal lymph node (*purple*)

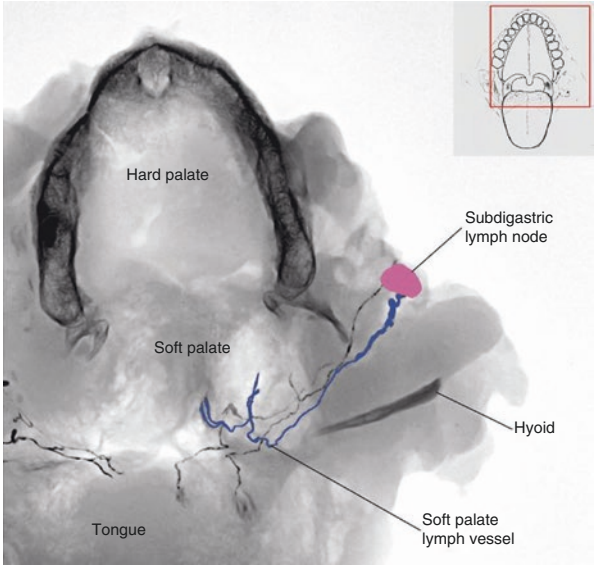

Fig. 3.44 Inverted radiograph of the tongue, soft palate, hard palate and surrounding soft tissue shows the lymphatic pathway of the soft palate (*blue*) draining to the subdigastric lymph node (*purple*)

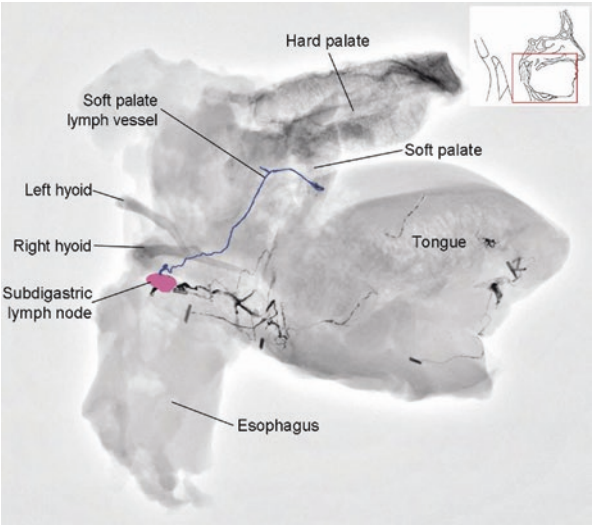

Fig. 3.45 Inverted radiograph of the tongue, soft palate, hard palate and surrounding soft tissue (lateral view) shows the lymphatic pathway of the soft palate (*blue*) draining to the subdigastric lymph node (*purple*)

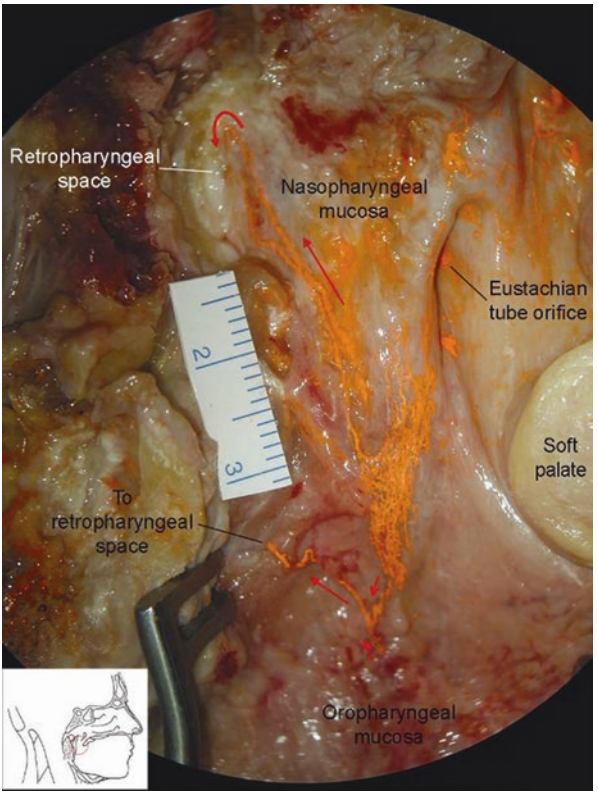

Fig. 3.46 Photograph of the pharyngeal wall after lead oxide mixture injection. The lymph capillary plexus originates in the mucosa of the pharyngeal wall and forms three precollecting lymph vessels draining towards the retropharyngeal space. *Red arrows* indicate the direction of the lymph flow

2.3 Tongue and Oropharynx

An average of four collecting lymph vessels (ranging from three to five vessels) were found in each side of the tongue. They were described as the apical, anterolateral, posterolateral and posterior lingual lymph vessels (Figs. 3.47, 3.48, 3.49, 3.50, 3.51 and 3.52). The average diameter of the vessels was 0.2 mm (ranging from 0.1 to 0.3 mm).

2.3.1 Apical Lingual Lymph Vessels

The lymph vessel arising from the inferior side on the apical of the tongue travelled backwards 2 mm away from and parallel to the lingual frenulum in the submucosal layer. Above the floor of the mouth, it crossed the midline and ran posterolaterally on the superior side of the contralateral digastric muscle (anterior belly) and then drained into the submandibular node and/or submental node (Figs. 3.47, 3.48, 3.49 and 3.50).

2.3.2 Lateral Lingual Lymph Vessels

They include the anterolateral and the posterolateral lingual lymph vessels.

Anterolateral Lingual Lymph Vessels

On the inferior aspect, the vessel arose from the anterolateral side on the body of the tongue and ran slightly posteroinferiorly in the submucosal layer. When the vessel reached the floor of the mouth, it turned laterally draining to the submandibular lymph node (Fig. 3.51).

Posterolateral Lingual Lymph Vessels

The vessel arose from the posterolateral border on the body of the tongue and ran posteroinferiorly in the submucosal layer. The vessel drained into the submandibular lymph node (Figs. 3.47 and 3.51).

2.3.3 Pharyngeal Lingual Lymph Vessels

Lymph vessels arose from the posterior part (root) of the tongue and ran posteroinferiorly and laterally in the submucosal layer. They passed through the lateral side of the oropharyngeal wall and drained into the subdigastric lymph node (Figs. 3.47, 3.48 and 3.52).

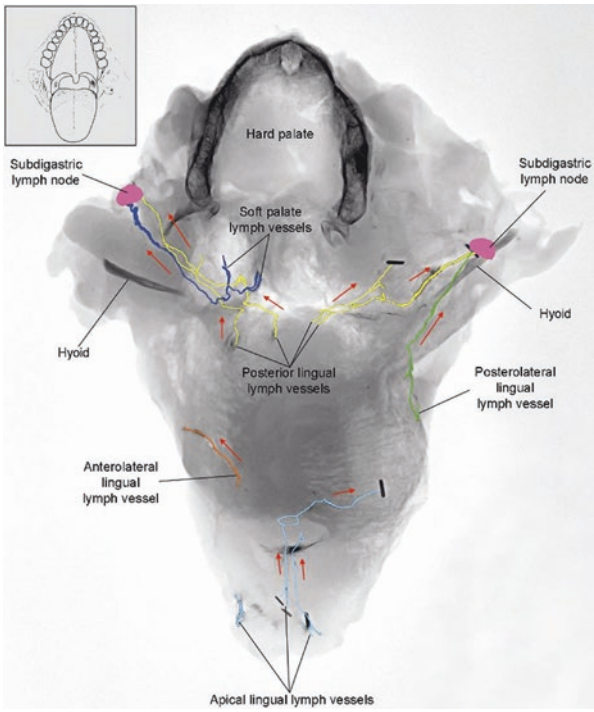

Fig. 3.47 Inverted radiograph of the tongue, hard and soft palates after lead oxide injection showing the lymphatic distribution. *Red arrows* indicate the direction of the lymph flow

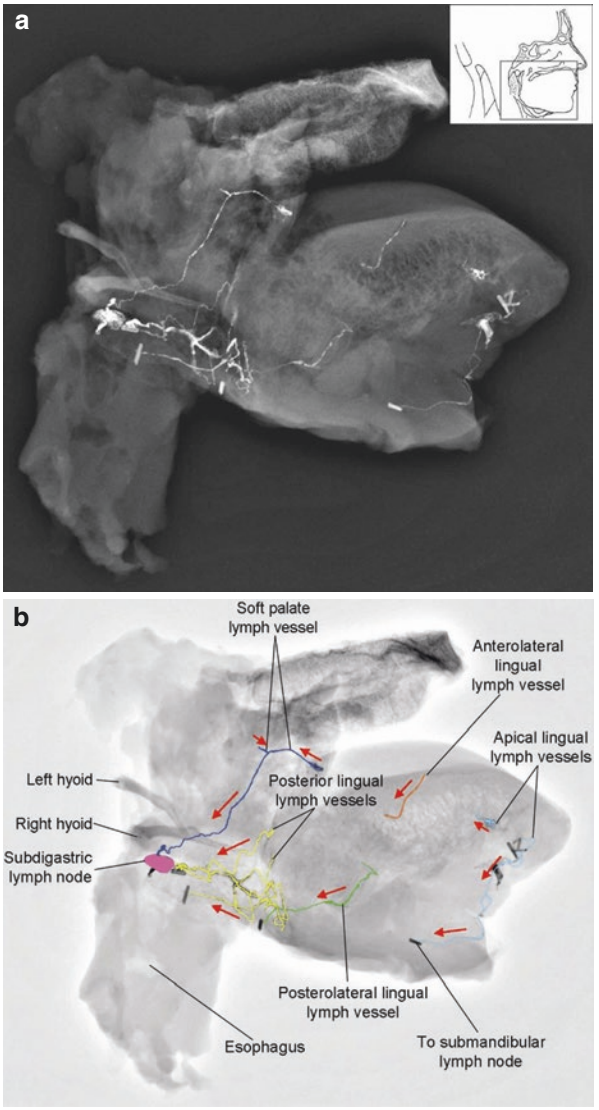

Fig. 3.48 Lateral view of radiograph (**a**) and inverted radiograph (**b**) of the tongue, oesophagus, hard and soft palates after lead oxide injection showing the lymphatic distribution. *Red arrows* indicate the direction of the lymph flow

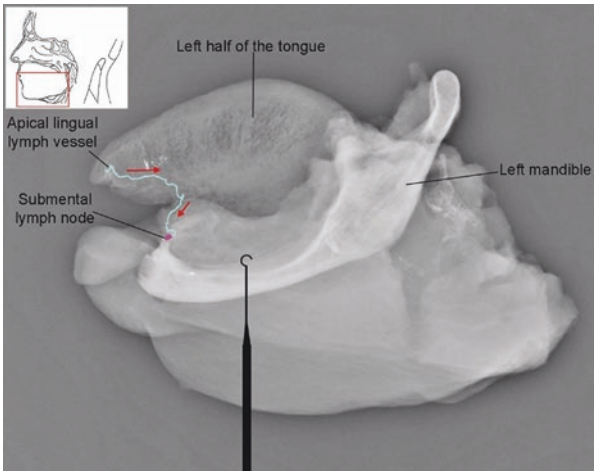

Fig. 3.49 Radiograph of the tongue, left half of the mandible and the floor of the mouth (lateral view) after lead oxide injection. The lymphatic vessel arises from the tip of the tongue and crosses the midline continuing on the contralateral side and then drains into the submental lymph node

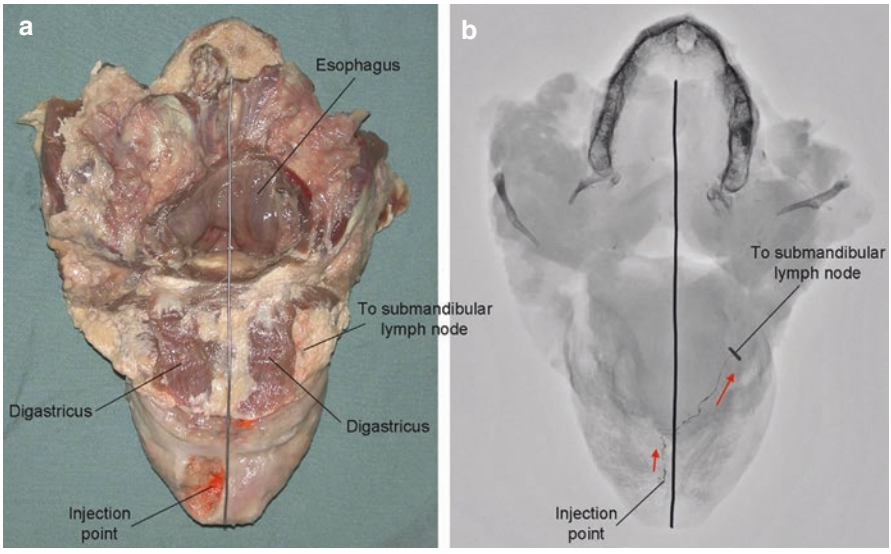

Fig. 3.50 Photograph of the inferior view of the tongue and superior view of the palate, after lead oxide injection (**a**) and an inverted radiograph (**b**) showing that the apical lingual lymph vessel arises from the tip of the tongue, crosses the midline and continues its course on the contralateral side

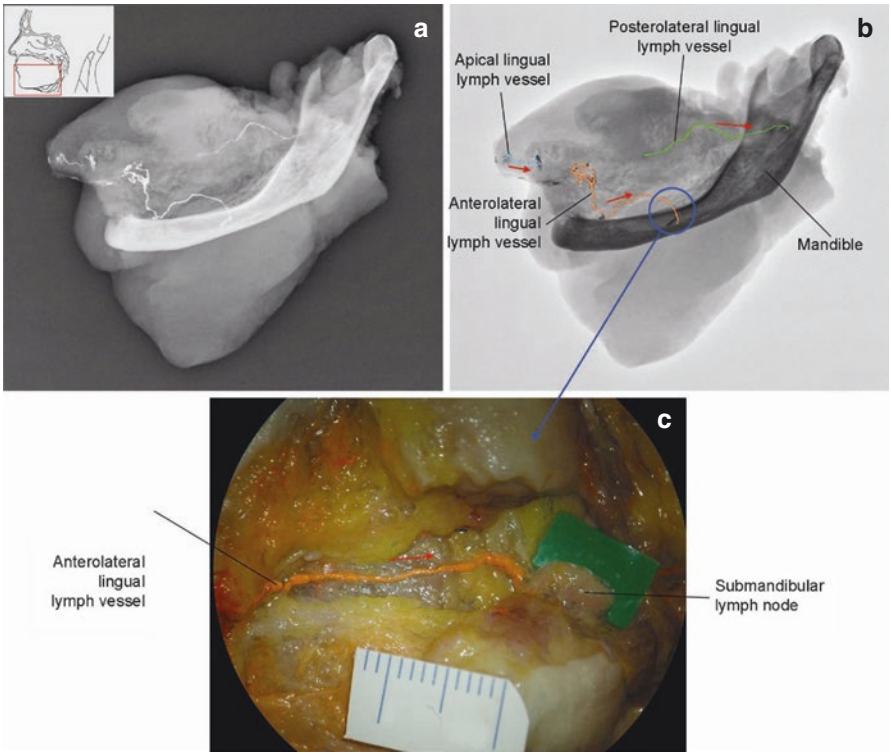

Fig. 3.51 Radiograph (**a**) and inverted radiograph (**b**) of the right half of the tongue after lead oxide injection showing the drainage direction (*red arrows*) of lymphatic vessels. The magnified image (**c**) from the *blue circled area* of the above radiograph (**b**) showing the anterolateral lingual lymph vessel draining to a submandibular lymph node

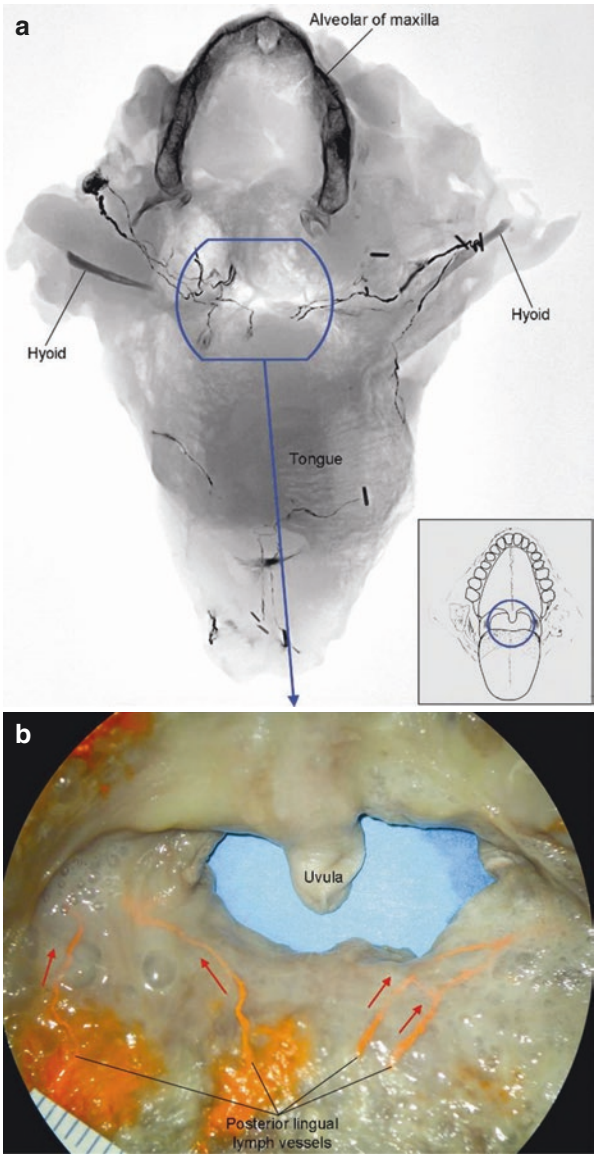

Fig. 3.52 (**a**) Inverted radiograph of the tongue, hard and soft palates after lead oxide injection. (**b**) Magnified image from the *blue circle area* of the above image, showing posterior lingual lymph vessels on the posterior part of the tongue which arise from the submucosal layer and drain to the subdigastric lymph node

2.4 *Laryngopharynx and Oesophagus*

The lymph capillary plexus arising from the mucosa of the laryngopharyngeal region (Fig. 2.63) formed the precollecting vessels beneath the mucous membrane. They penetrated the laryngopharyngeal wall and drained into the internal jugular lymph node (Fig. 3.53).

The lymph capillary plexus arising from the mucosa of the oesophagus (Figs. 2.64 and 2.65) formed the precollecting vessels beneath the mucous membrane. They penetrated the oesophageal wall and drained into the internal jugular lymph node (Fig. 3.54).

Clinical Implication
The tongue is the most common site of primary squamous cell carcinoma (SCC) in the oral cavity. Successful treatment of SCC relies largely on a thorough knowledge of the lymphatic anatomy. Surgeons have utilized clinical information to map the lymphatics of the tongue, which helps neck dissection with glossectomy. Neck dissection classification is the key for the procedure but only locates levels (areas) of the cervical lymph nodes (Robbins et al. 2002). Recently, lymphoscintigraphy has been used for locating the sentinel lymph nodes and mapping the lymphatic vessel pathways (De Cicco et al. 2006; Wang et al. 2007), minimizing the extent of the operation and reducing iatrogenic morbidity through the selection of neck nodes potentially at risk of harbouring cancer. In this section, the information may help clinicians with cancer management.

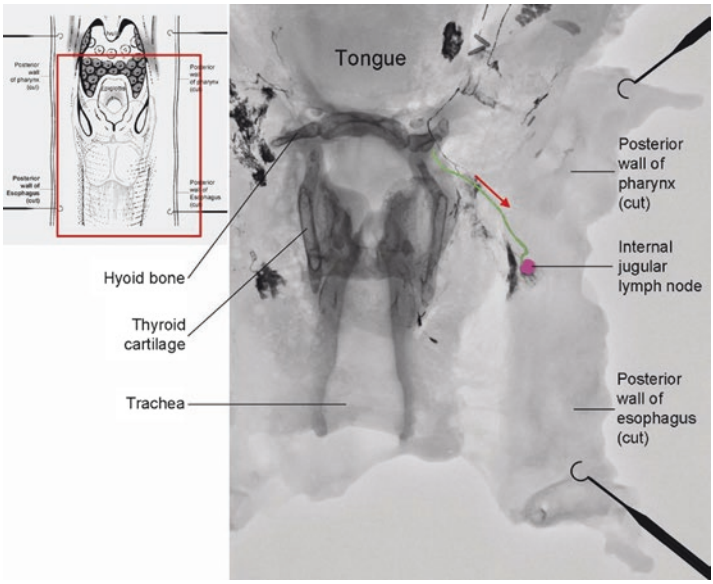

Fig. 3.53 Converted radiograph of the posterior view of the laryngopharyngeal region after lead oxide mixture injection showing the lymph vessel (*green*) from the mucosa of the laryngopharyngeal wall drains to the internal jugular lymph node (*purple*)

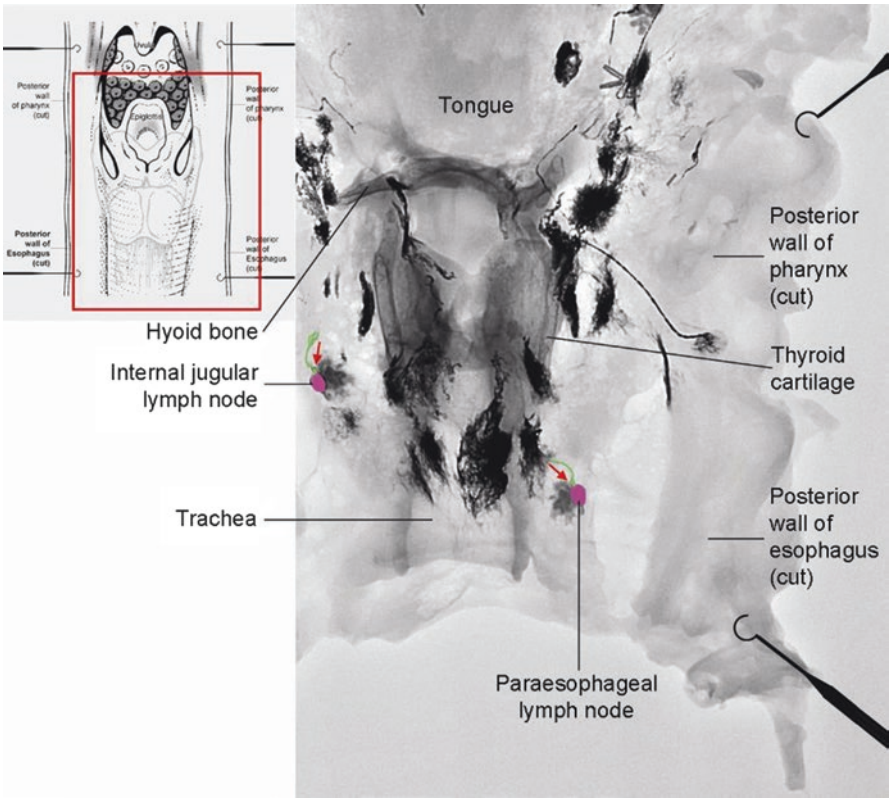

Fig. 3.54 Converted radiograph of the posterior view of the pharyngoesophageal region after lead oxide mixture injection showing lymph vessels (*green*) from the mucosa of the oesophageal wall drains to the internal jugular and paraoesophageal lymph nodes (*purple*)

3 Distribution of Lymph Nodes in the Head and Neck

The micromorphology of lymph nodes has been presented in Chap. 2. Two different types of lymph nodes were found in all specimens (Figs. 2.134, 2.135, 2.136, 2.137, 2.138, 2.139, 2.140, 2.41, 2.42, 2.43, 2.44, 2.45, 2.46, 2.47, 2.48, 2.49, 2.50, 2.51, 2.52, 2.53, 2.54, 2.55, 2.56 and 2.57). Within the 338 lymph nodes harvested from the head and neck section of 7 elderly human cadavers, 128 of them were solidified lymph nodes (37.87%) and 210 of them were transparent nodes (62.13%). The type, number and distribution of them are listed in Figs. 3.55, 3.56 and 3.57 and Table 3.1.

Within the 227 transparent nodes, 7 of them were located between the dermis and the platysma of the superficial anterior neck in 3 specimens. These unidentified nodes were named the *superficial submental* and the *superficial anterior jugular lymph nodes* (Fig. 3.57).

Notes

Previous studies have shown that some lymph nodes of the head and neck in the elderly gradually degenerated (Pan et al. 2008a and b). The lymphatic tissue especially in superficial lymph nodes of the head and neck was gradually reduced until it disappeared, and the sinus cavity vanished and the space was replaced by adipose and fibrous connective tissues or lymphatic tubules so that the immune and filtration function of lymph nodes were decreased and eventually lost. Thus, it raises some questions for us, such as does the degeneration process of lymph nodes occur in any other parts of the body? Is this phenomenon related to the weak immunity of the elderly? Is it one of the reasons that elderly patients with cancer are more likely to suffer from systemic metastasis? These are all questions that require further studies to confirm.

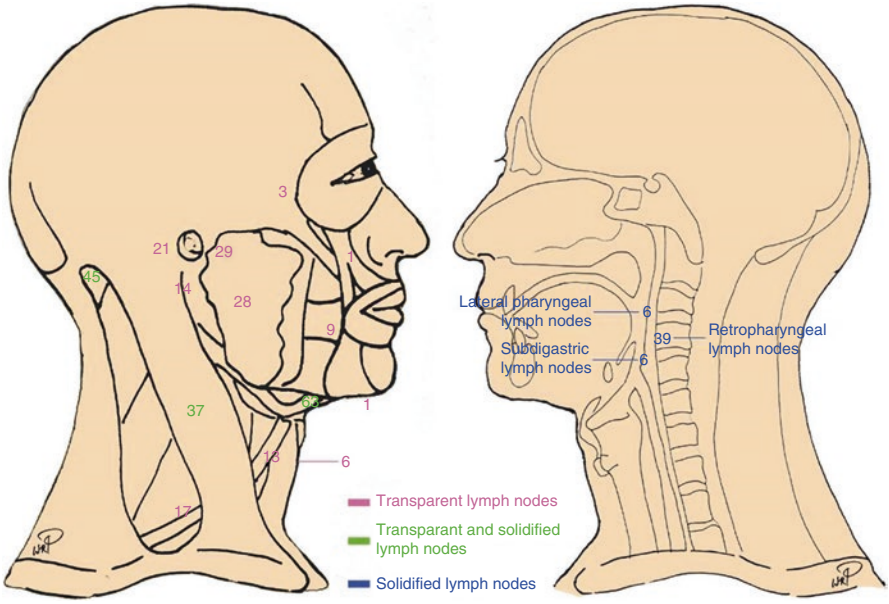

Fig. 3.55 The type and number of lymph nodes distributed in each region of the head and neck

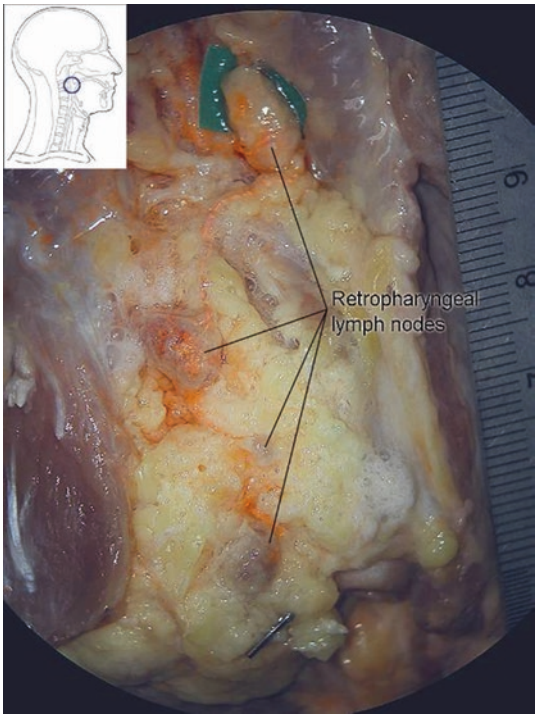

Fig. 3.56 Solidified lymph nodes in the retropharyngeal space

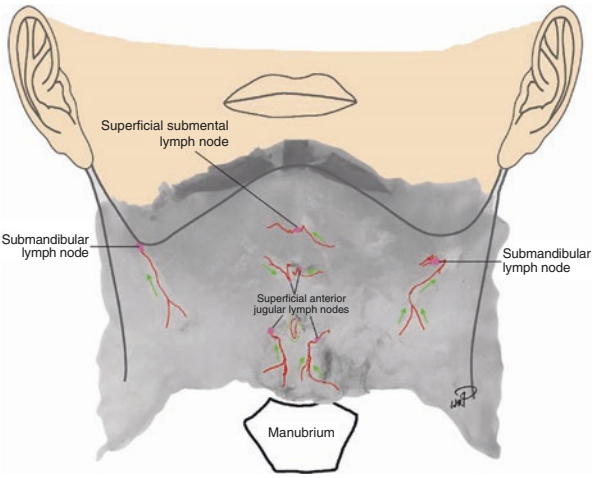

Fig. 3.57 Composite drawing and X-ray of the jaw and the neck. The radiograph shows the pathways of anterior cervical lymph vessels (*red*) situated between the dermis and platysma in the anterior neck and related lymph nodes (*purple*). *Green arrows* indicate the direction of the lymph flow

Table 3.1 The type, number and name of lymph nodes in the head neck region of the elderly

Name of the lymph node	Solidified lymph nodes (active LNs)	Transparent lymph nodes (inactive or degenerated LNs)
Malar LN	0	3
Buccinator LN	0	9
Parotid LN	0	31
Preauricular LN	0	28
Postauricular LN	0	33
Occipital LN	12	35
Infra-auricular	0	14
Superficial submental LN	0	1
Submandibular LN	47	34
Superficial anterior jugular	0	6
LN	7	6
Anterior jugular LN	7	10
Supraclavicular LN	39	0
Retropharyngeal LN	8	0
Lateral pharyngeal LN	8	0
Subdigastric LN	128	210
Total		

4 Anterior Chest and Female Breasts

Lymph capillary plexus and precollecting lymph vessels in the anterior chest have been presented in previous sections (Figs. 2.65, 2.77 and 2.78).

Multiple collecting lymph vessels were found in the anterior chest. Based on the drainage territories of the first-tier lymph nodes, distributing patterns of lymphatics were different in individuals and even asymmetrical between sides of the same body (Figs. 3.58 and 3.59). Two layers (the superficial and deep) and three groups of lymph vessels were identified. In the superficial layer, they included (1) the superficial anterior group and (2) the paraareolar group. In the deep layer, there was the parasternal group (Figs. 3.58, 3.59, 3.60 and 3.61).

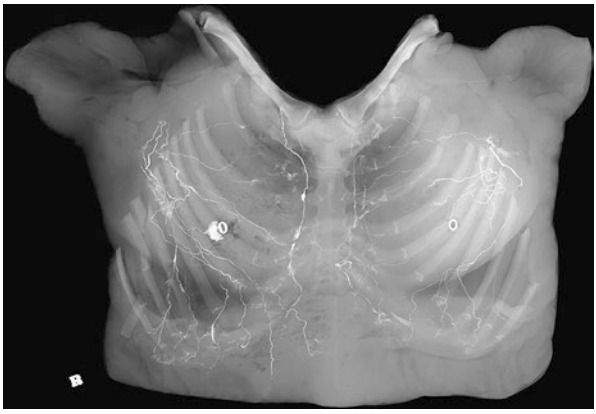

Fig. 3.58 Radiograph of the lymphatic distribution of the chest after lead oxide mixture injection

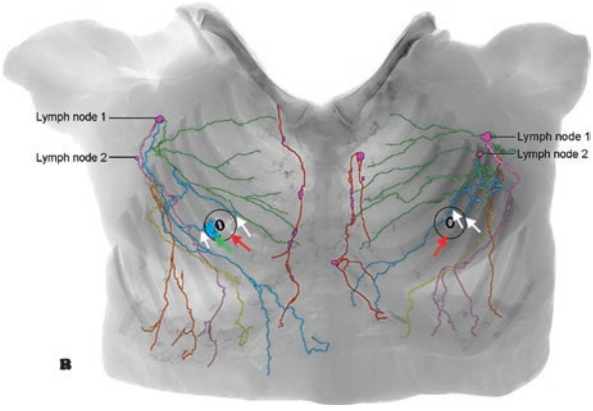

Fig. 3.59 Converted radiograph of the lymphatic distribution of the chest after lead oxide mixture injection. An asymmetrical drainage pattern of lymphatics is highlighted by different colours. *Red arrows* indicate areolas. *Green arrow* points out the lymph capillary plexus in the areola. *White arrows* point out lymph vessels arising from the areolas

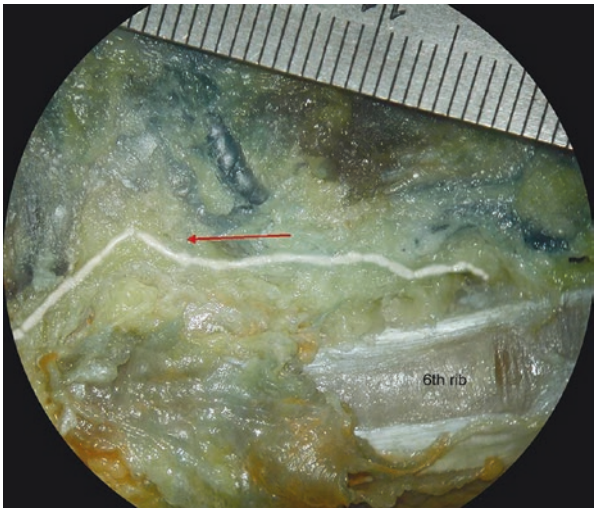

Fig. 3.60 A collecting lymph vessel perfused by barium sulphate mixture travels in the intercostal space. *Red arrow* indicates the direction of the lymph flow

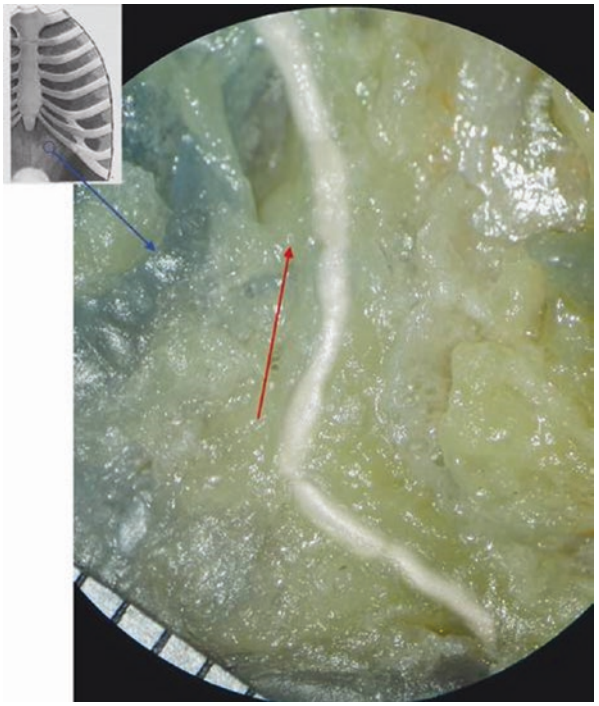

Fig. 3.61 The collecting lymph vessel in the inner surface of infrasternal angle area. *Red arrow* indicates the direction of the lymph flow

4.1 Superficial Anterior Group

The group of collecting lymph vessels originating in the subcutaneous tissues around the costal margin and the lateral border of the sternum coursed radially towards the first-tier lymph nodes (axillary lymph nodes). Most vessels converged to form larger lymph-collecting vessels, and some of them diverged before entering the lymph nodes. The size and number of vessels varied (Figs. 3.62 and 3.63).

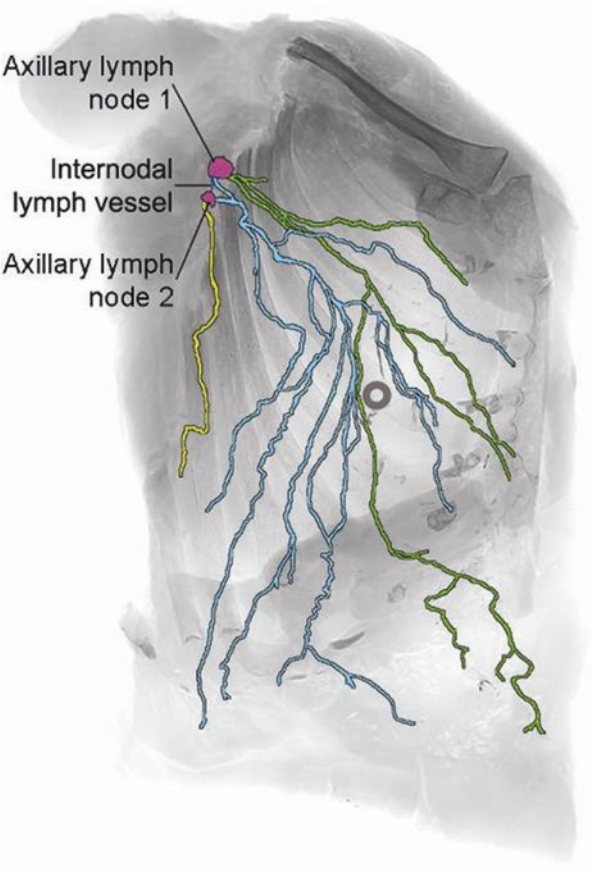

Fig. 3.62 Converted radiograph of the superficial lymphatic distribution of the right chest in a male after lead oxide mixture injection. Vessels coloured in *green* drain into lymph node (*1*) Vessels coloured in *yellow* drain into lymph node (*2*) Vessels coloured in *aqua blue* drain into both lymph nodes 1 and 2

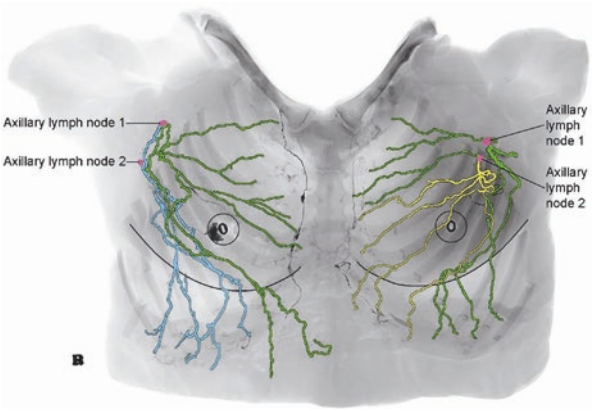

Fig. 3.63 Converted radiograph of the superficial lymphatic distribution of the chest in a female after lead oxide mixture injection. Vessels coloured in green drain into lymph node (*1*) Vessels coloured in *yellow* drain into lymph node (*2*) Vessels coloured in *aqua blue* drain into both lymph nodes 1 and 2

4.2 *Paraareolar Lymph Group*

Precollecting lymph vessels arose in the dermis of the areola (Figs. 2.65 and 2.77). They formed, on average, two collecting vessels in the subcutaneous around the areola. After travelling a short distance, vessels converged with the superficial anterior group and entered the first-tier lymph node (axillary lymph node) (Figs. 3.64 and 3.65).

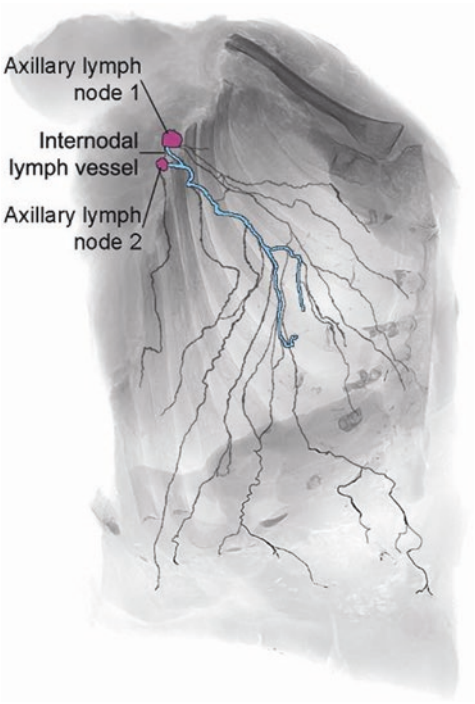

Fig. 3.64 Converted radiograph of the anterior chest following lymphatic contrast injection. Lymphatic vessels (*aqua blue*) arising from the areola region drain to both axillary lymph nodes

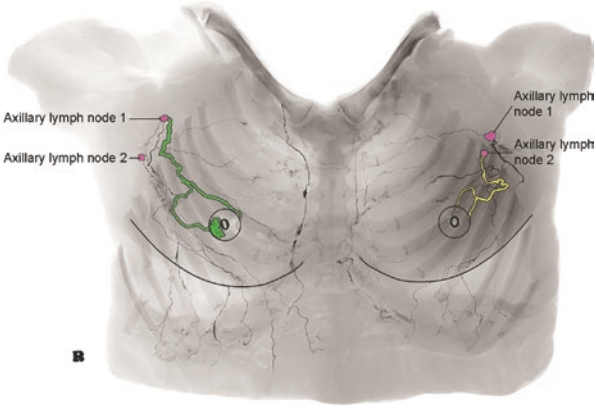

Fig. 3.65 Converted radiograph of the anterior chest following lymphatic contrast injection. Lymphatic vessels (*green*) arising from the areola region drain to lymph node 1 in the right, vessels (*yellow*) drain to node 2 in the left

4.3 *Parasternal and Intercostal Group*

On each side of the chest, one or two parasternal lymph vessels arose beneath the partial pleura of the infrasternal angle area (Fig. 2.149). Vessels ascended along the internal thoracic vascular bundle and merged to vessels in the supraclavicular region. During their course, vessels traversed a row of parasternal lymph nodes (Fig. 3.66).

Arising from the intercostal spaces, intercostal lymph vessels converged with the parasternal vessels at different levels and entered the relevant parasternal lymph nodes (Figs. 3.60 and 3.66).

Once again, the size, type and number of lymph nodes were markedly different between the left and right sides (Figs. 2.149, 3.59 and 3.66).

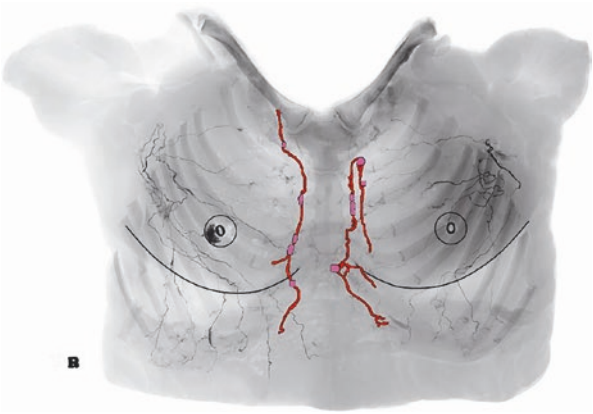

Fig. 3.66 The distribution of parasternal and intercostal lymph vessels (*red*) and related lymph nodes (*purple*)

4.4 Cross-Sectional Views

In the female chest, the majority of the collecting lymph vessels coursed in the subcutaneous tissue, with only a minority of them running through the breast parenchyma (indicated by white arrows in slice 7 of Fig. 3.67b and slice 5 of Fig. 3.68a).

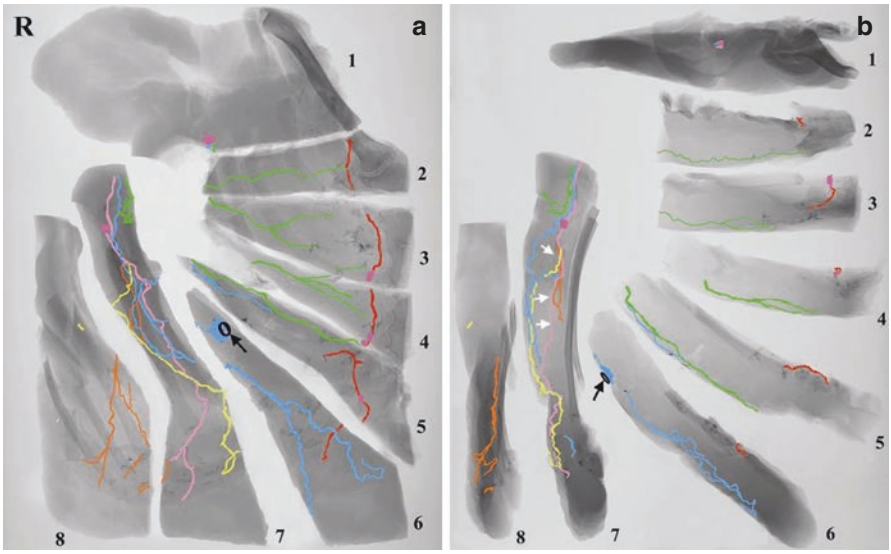

Fig. 3.67 Converted radiographs of the right chest following lead oxide mixture injection. (**a**) Anteroposterior view of the sections. (**b**) Cross-sectional views of each section (rotated 90°). Lymph vessels are highlighted to show their frequent course in the subcutaneous, but a few of them travel through the breast parenchyma indicated by *white arrows* in slice 7. *Black arrows* indicate the position of the nipple

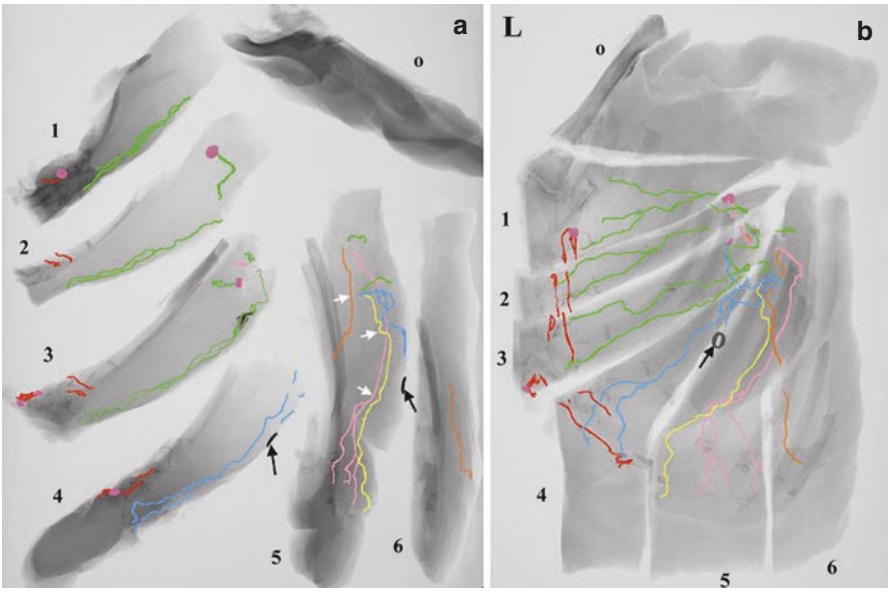

Fig. 3.68 Converted radiographs of the left chest following lead oxide mixture injection. (**a**) Cross-sectional views of each section (rotated 90°). (**b**) Anteroposterior view of the sections. Lymph vessels are highlighted to show their frequent course in the subcutaneous, but a few of them travel through the breast parenchyma indicated by *white arrows* in slice 5. *Black arrows* indicate the position of the nipple

4.5 *Relationship Between Lymph Vessels and Nodes in the Chest, Axilla and Upper Limb*

Once again, based on the drainage territories of the first-tier lymph nodes, drainage patterns of lymphatics were different in individuals and even asymmetrical between sides of the same body (Figs. 3.58, 3.59 and 3.69).

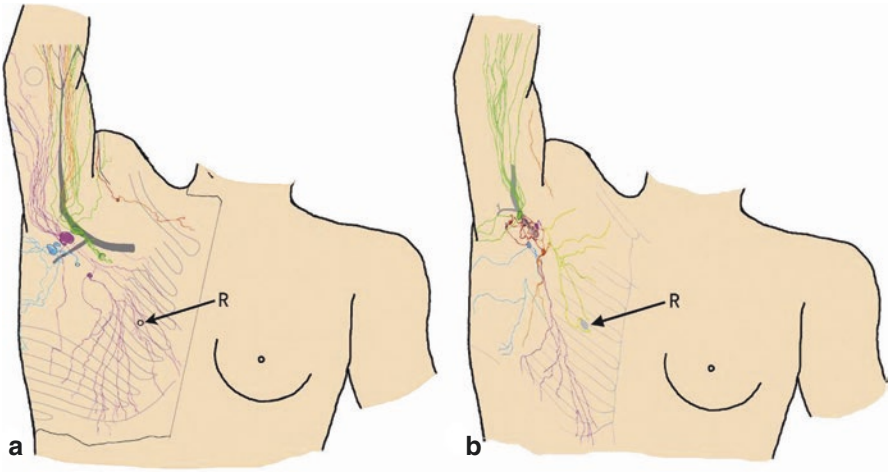

Fig. 3.69 (**a**) One large axillary lymph node drains almost the entire anterior chest and breast as well as most of the medial surface of the upper limb. (**b**) More than one node is represented

4.6 Computed Tomographic Lymphangiography

The three-dimensional (3D) anatomy of the lymphatics of the breast could be demonstrated by a computed tomographic lymphangiography (CTL). Reconstructions of volume-rendered technique (VRT) (Figs. 3.70, 3.71, 3.72 and 3.73) were utilized to digitally remove the required volume for analysing the deep anatomy, such as the removal of the skin (Figs. 3.70 and 3.71) and breast parenchyma (Fig. 3.72), or for the generation of oblique sections of the tissue of any thickness (Fig. 3.73).

CTL images were able to highlight the information obtained from plain film imaging (Fig. 3.71), in being able to reveal the lymphatics and their course. Selective cropping of the skin on 3D CTL images (Fig. 3.70) presented the preferential superficial pathway of lymphatics throughout the breast, showing lymphatics coursing immediately underneath the skin. Deeper selective cropping of the anterior part of the breast (Fig. 3.72) was able to present the absence of lymphatics in the deeper tissue of the breast parenchyma. Axial sections of the entire specimen in multiple planes (Fig. 3.73) were able to reveal occasional lymphatics traversing the breast parenchyma. Asymmetry between sides was again evident.

Clinical Implication

The surgical treatment of breast cancer has been one of the most rapidly changing fields in the clinic. For example, lymphoscintigraphy and sentinel lymph node biopsies are now widely applied for the treatment of patients with breast cancer, especially in the early stages (Uren et al. 1999; Thompson et al. 2004). The information provided from this section updated the knowledge of the lymphatic anatomy in the region. The findings (Figs. 3.60, 3.61, 3.62, 3.63, 3.64, 3.65, 3.66, 3.67, 3.68, 3.69, 3.70, 3.71, 3.72 and 3.73) emphasize several important points regarding the utilization of sentinel lymph node mapping and biopsy. Varying patterns of lymphatic drainage between sides indicate a requirement for an individualized approach to each breast. Intraparenchymal lymph vessels course superficially and thus are amenable to surgical approaches; lymph vessels do coalesce at the nipple; however many lymph vessels bypass the nipple, and thus a periareolar injection (rather than peritumoural injection) of nuclear tracer or dye may not map the appropriate lymph nodes.

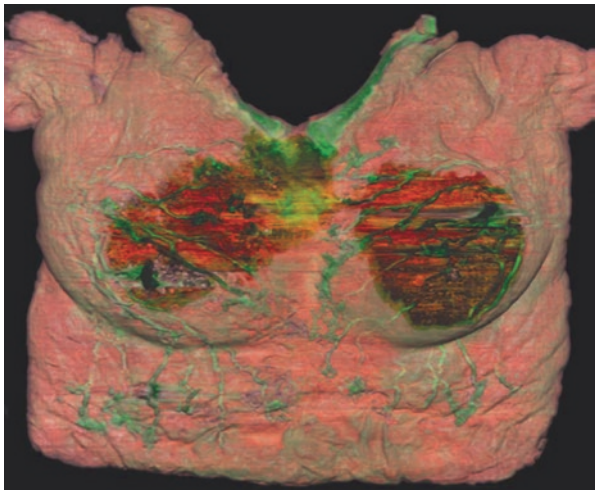

Fig. 3.70 The skin of the anterior chest has been removed by using volume-cropping computer software to reveal the superficial lymph vessels immediately beneath the skin. *Green*, contrast-filled lymph vessels; *pink*, *skin*; *red*, breast parenchyma

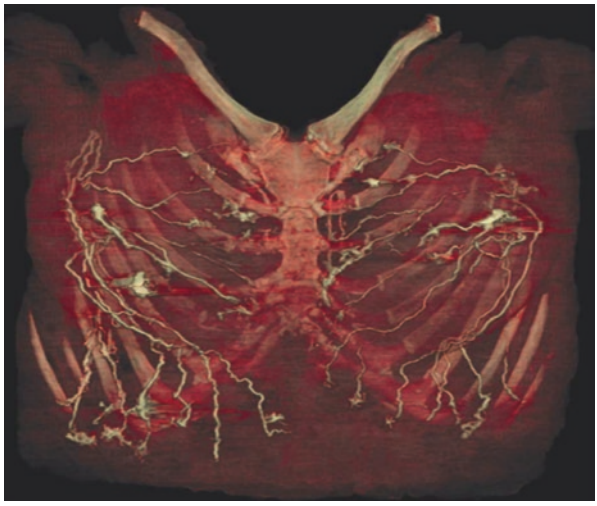

Fig. 3.71 The contrast resolution has been adjusted to reveal the relationship between lymph vessels of the breast and the underlying intercostal spaces. *White*, contrast-filled lymphatics; *red*, skin and breast parenchyma

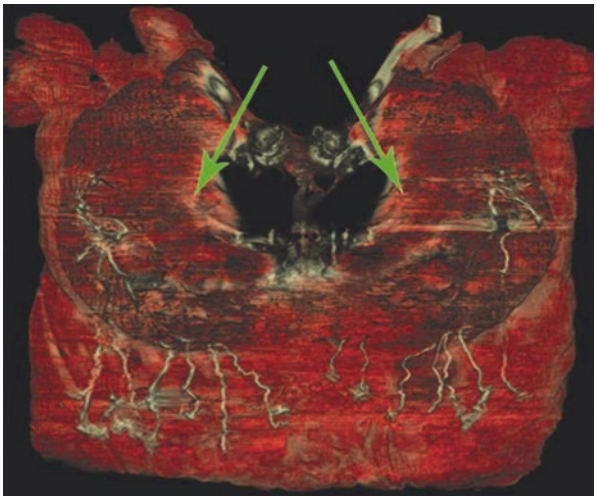

Fig. 3.72 The anterior two-thirds of the breast parenchyma has been removed by using volume-cropping computer software to reveal the paucity of lymph vessels within the depths of the breast parenchyma (indicated by *green arrows*). *White*, contrast-filled lymphatics; *light red*, skin; *dark red*, breast parenchyma

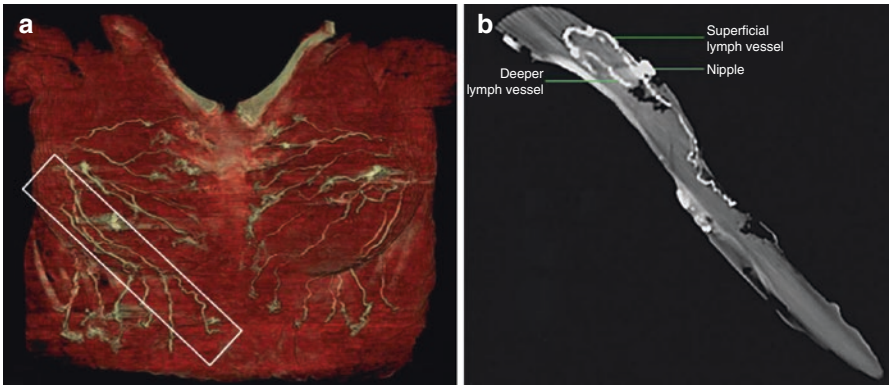

Fig. 3.73 (**a**) A portion of the breast tissue containing lymph vessels from the anterior chest is highlighted. (**b**) Cross-sectional view of the same portion, revealing the superficial and deeper lymph vessels within the breast

5 Upper Extremity

Superficial collecting lymph vessels were identified in the subcutaneous of the upper extremity (Figs. 3.74, 3.75, 3.76, 3.77 and 3.78). They originated beneath the dermis on each side of the fingers, the wrist crease and the lateral side of the upper arm. The size of the vessels varied from 0.2 mm to 1.2 mm. Vessels meandered their way and ascended in different depths of the subcutaneous towards lymph nodes in the axilla, a few of them traversed the cubital node in the medial elbow. During their course some vessels branched, diverged or converged, sometimes anastomosed with or crossed over neighbouring vessels. Most vessels converged to form larger collecting vessels while some diverged before entering lymph nodes.

Fig. 3.74 Radiographs of the superficial lymphatic distribution in the upper left extremity after a lead oxide mixture injection. (**a**) Anteroposterior view. (**b**) Lateral view. (**c**) Lymphatic distribution of the integument. *a*. Styloid process of the radius, *b*. Styloid process of the ulna, *c*. Lateral epicondyle of the humerus, *d*. Olecranon, *e*. Medial epicondyle of the humerus, *f*. Acromion of the scapula

Fig. 3.75 Inverted radiograph of the lymphatic distribution in the integument of the left upper extremity. Each group of lymph vessels is colour coded. Vessels coloured in *green* were divided by the incision. *a*. Styloid process of the radius, *b*. Styloid process of the ulna, *c*. Lateral epicondyle of the humerus, *d*. Olecranon, *e*. Medial epicondyle of the humerus, *f*. Acromion of the scapula

Fig. 3.76 Radiographs of the lymphatic distribution in fingers and the dorsal hand after a barium sulphate mixture injection. (**a**) Posteroanterior view. (**b**) Lateral view

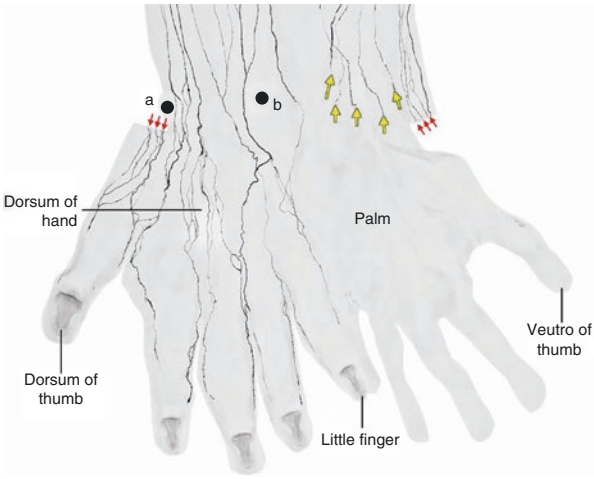

Fig. 3.77 Inverted radiograph showing the lymphatic distribution in the integument of the fingers of the left hand. *Red arrows* indicate cut points of lymph vessels by the incision. *Yellow arrows* indicate the origin of lymph vessels at the skin creases of the anterior wrist. *a*. Styloid process of the radius, *b*. Styloid process of the ulna

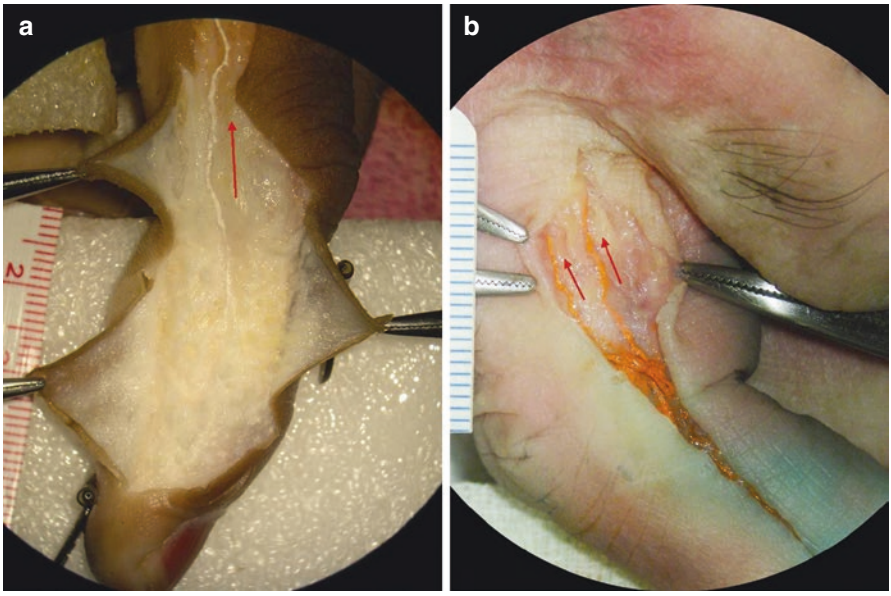

Fig. 3.78 (**a**) A digital lymph vessel ascends in the medial side of the left index finger (after a barium sulphate mixture injection). (**b**) Two digital lymph vessels travel in the lateral side of the left middle finger (filled by a lead oxide mixture). *Red arrows* indicate the direction of the flow

5.1 Digits

Originating beneath the dermis, one or two collecting lymph vessels on each side of the digit ascended tortuously in the subcutaneous along the mid-axial lines (Figs. 3.74, 3.75, 3.76, 3.77, 3.78, 3.79 and 3.80). The mean vessel diameter was 0.4 mm (ranging from 0.2 to 0.5 mm). Generally, vessels of neighbouring digits merged into the web spaces of the dorsal hand with the exception being those on the lateral side of the thumb and the medial side of the little finger that travelled radially to merge with lymph vessels in the dorsal hand (Figs. 3.74, 3.75, 3.76 and 3.77). Digital lymph vessels paralleled with digital arteries, veins and nerves (Figs. 3.79 and 3.80).

Clinical Implication
Replantation is one of the most common surgical treatments after a finger amputation injury. A variety of factors can influence the survival rate after surgery. The patency of the digital artery and vein is an important factor for the preservation of the replantated finger. Generally clinical indicators, such as the skin tone and temperature, tension of the replanted finger, capillary refill test and so on, are able to judge the vascular patency (Yang et al. 2003). It has been proposed (Cheng et al. 1997) that the skin of the replantated finger occasionally turned to wax-whitish colour with constant tension in the post-operative period, while the outflow of the fresh red blood was observed from a small dermic incision cutting on the side of the replanted finger, which indicated that the vascular patency and the blood supply were satisfactory. It was believed that the appearance of the phenomenon was mainly due to ischaemia of the severed finger; some of the cells had begun to denature so that capillary permeability increased. Once the blood flow re-perfused, cell (tissue) oedema occurred, peripheral circulatory obstructed and finally the replanted finger oedema took place. However, we believe that this phenomenon should be regarded as lymphedema. The reason is that the digital lymph vessels were not anastomosed in the surgery. The lymph (cellular waste) was unable to be removed and isolated in the tissue.

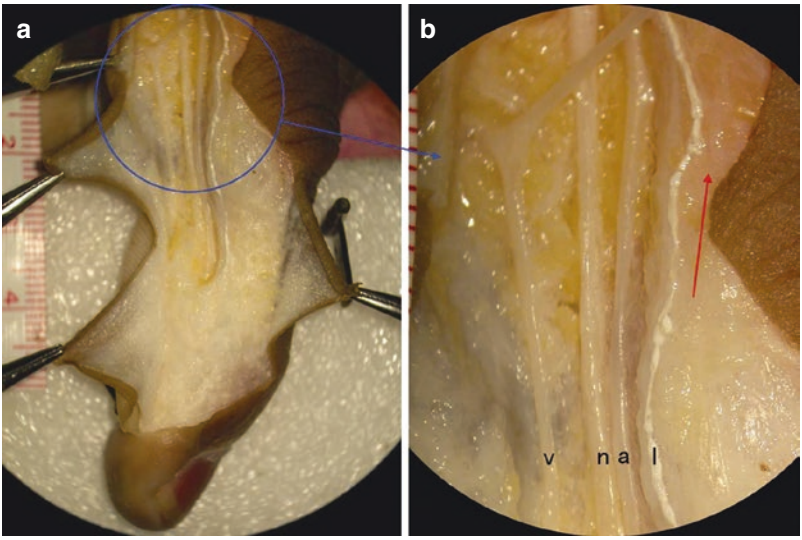

Fig. 3.79 A digital lymph vessel (*l*) (filled by a barium sulphate mixture) parallels to the digital artery (*a*), vein (*v*) and nerve (*n*) in the medial side of the left index finger. *Red arrow* indicates the direction of the flow

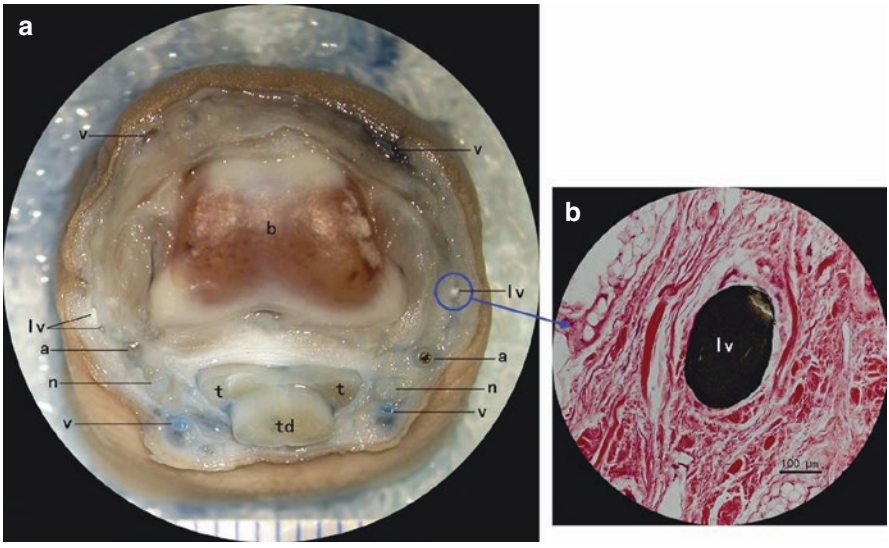

Fig. 3.80 (**a**) Photograph of the transversal section in the proximal joint of the right middle finger. *lv*. Digital lymphatic vessels (filled by a barium sulphate mixture), *a*. Digital arteries (inserted metal wires), *v*. Digital veins, *n*. Digital nerves, *b*. Head of proximal phalanx of the middle finger, *t*. Flexor digitorum superficialis tendon, *td*. Flexor digitorum profundus tendon. (**b**) Histological section with H&E staining of the digital lymphatic vessel. *lv*. Barium sulphate mixture in the lumen of the lymph vessel

5.2 *Hand*

Arising from digits, an average of 6 (ranging from 14 to 18) collecting lymph vessels were distributed in the subcutaneous tissue of the dorsum of the hand (Figs. 3.74, 3.75, 3.76 and 3.77). The mean vessel diameter was 0.4 mm (ranging from 0.2 to 0.6 mm). Vessels diverged and converged to each other and crossed over or below the superficial veins when meeting them (Figs. 3.81, 3.82 and 3.83). They formed two groups.

5.2.1 Dorsoradial Group

Lymph vessels arose from the radial three digits (the thumb, index and middle fingers) and distributed on the dorsoradial side of the hand (Fig. 3.75 green vessels).

5.2.2 Dorsoulnar Group

Lymph vessels arose from the ulnar two digits (the ring and little fingers) and distributed on the dorsoulnar side of the hand (Fig. 3.75 blue vessels).

Fig. 3.81 Lymphatic distribution of the dorsum of the left hand (after a barium sulphate mixture injection)

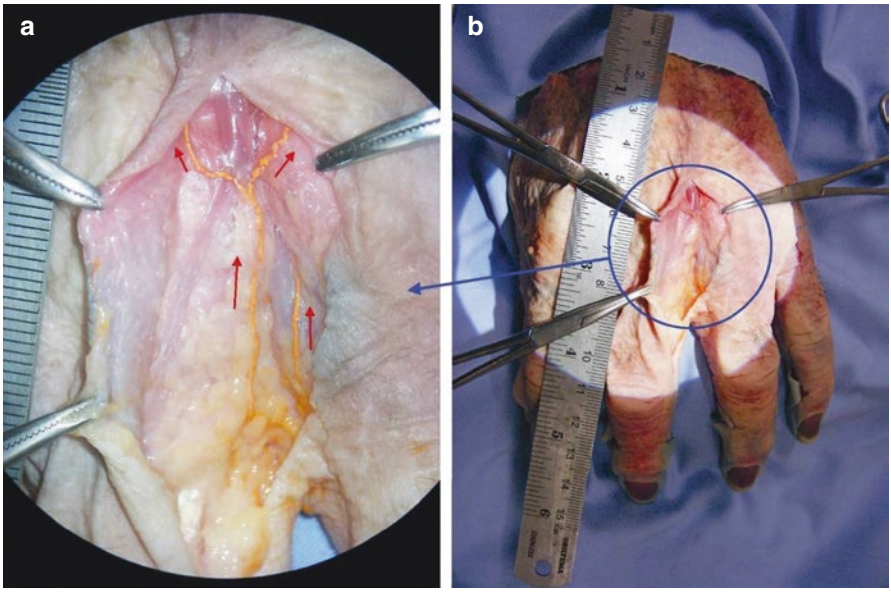

Fig. 3.82 The relationship of lymph vessels and veins on the dorsum of the left hand (after a lead oxide mixture injection). Lymph vessels cross over veins. A magnified image (**a**) captured from the circled area in image (**b**)

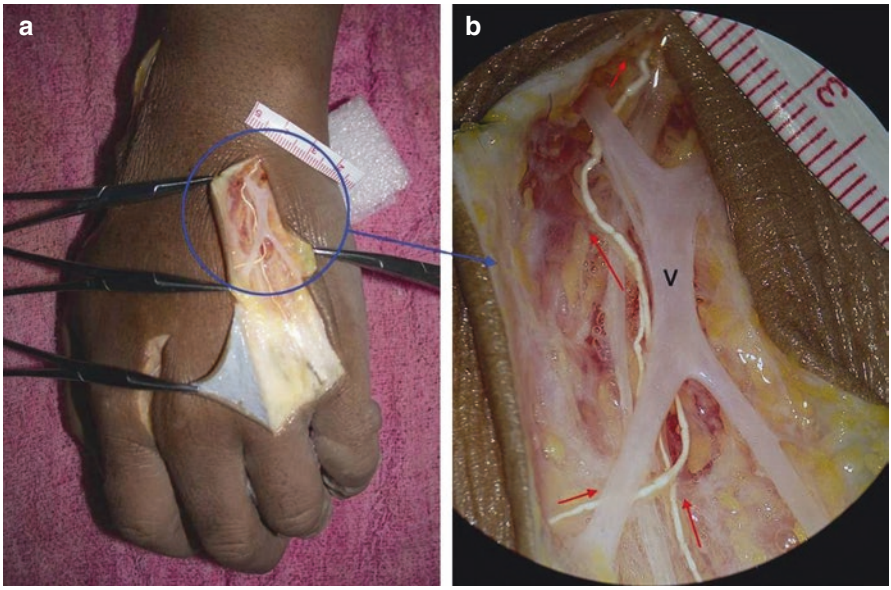

Fig. 3.83 The relationship of lymph vessels and veins on the dorsum of the left hand (after a barium sulphate mixture injection). Lymph vessels traverse under veins. *v*. Dorsal venous network of the hand. A magnified image (**b**) captured from the circled area in image (**a**)

5.3 *Wrist*

There is an average of 16 (ranging from 14 to 18) collecting lymph vessels distributed in the subcutaneous tissue around the wrist region (Figs. 3.74, 3.75, 3.76 and 3.77). The mean vessel diameter was 0.5 mm (ranging from 0.3 to 0.7 mm). On the anterior aspect, vessels arose beneath the dermis at the skin creases of the wrist. On the posterior aspect, they were continuous lymph vessels arising from the digits and the dorsum of the hand. They traversed over and/or under veins when meeting them (Figs. 3.84, 3.85, 3.86, 3.87, 3.88 and 3.89).

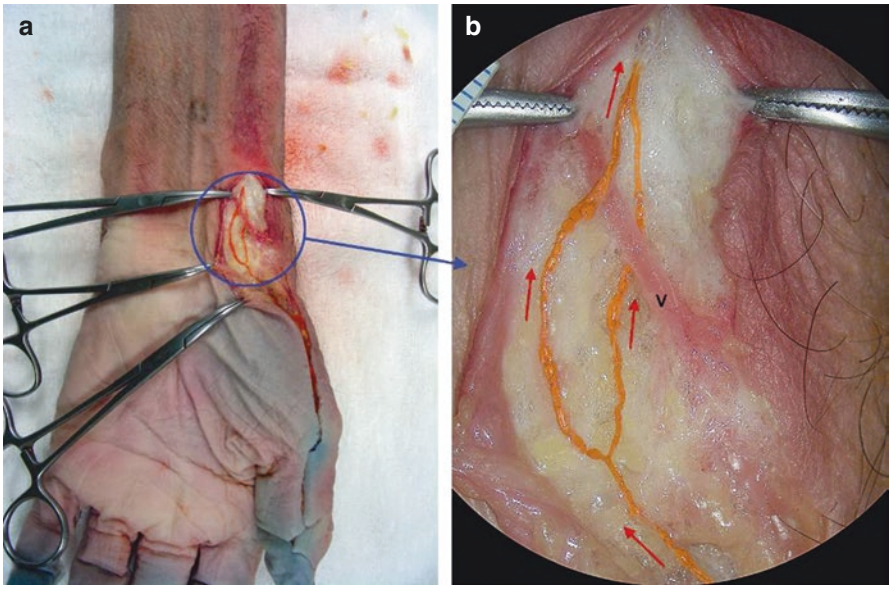

Fig. 3.84 The relationship of lymph vessels and the vein on the anteroradial side of the left wrist (after a lead oxide mixture injection). Lymph vessels cross over and traverse under the vein. *v*. Tributary of the cephalic vein. A magnified image (**b**) captured from the circled area in image (**a**)

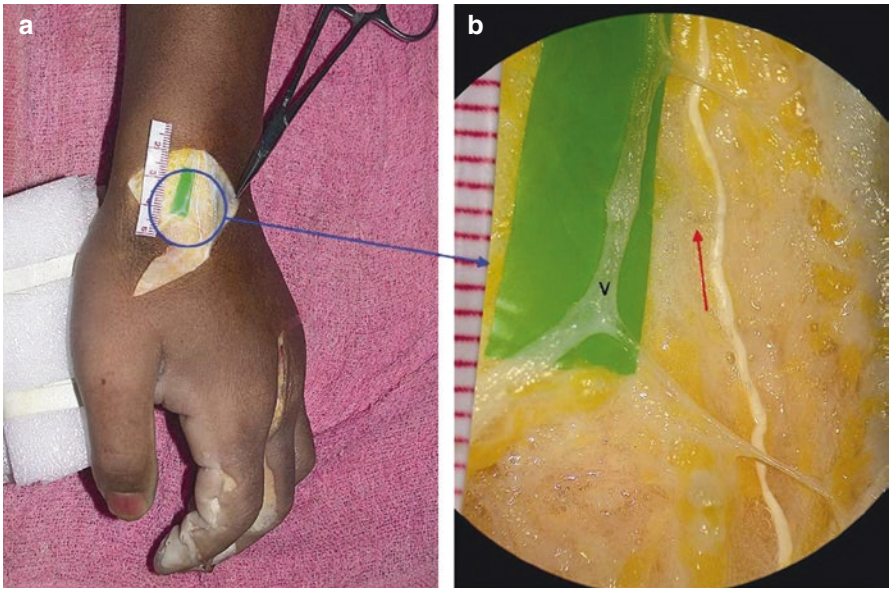

Fig. 3.85 The relationship of the lymph vessel and veins on the dorsoradial aspect of the left wrist (after a barium sulphate mixture injection). A lymph vessel traverses under veins. *v*. Tributaries of the cephalic vein. A magnified image (**b**) captured from the circled area in image (**a**)

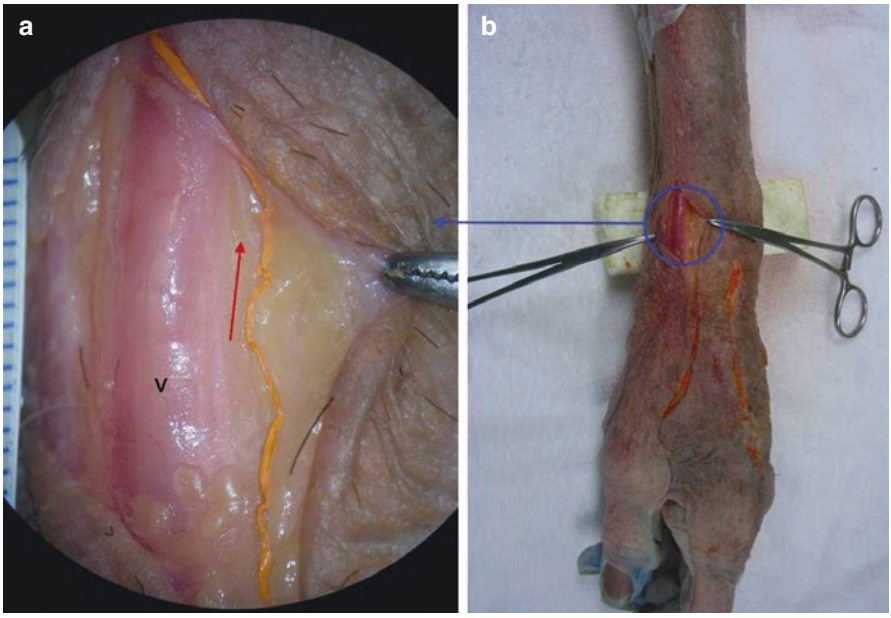

Fig. 3.86 The relationship of lymph vessels and the vein on the radial side of the left wrist (after a lead oxide mixture injection). A lymph vessel parallels the cephalic vein (*v*). A magnified image (**a**) captured from the circled area in image (**b**)

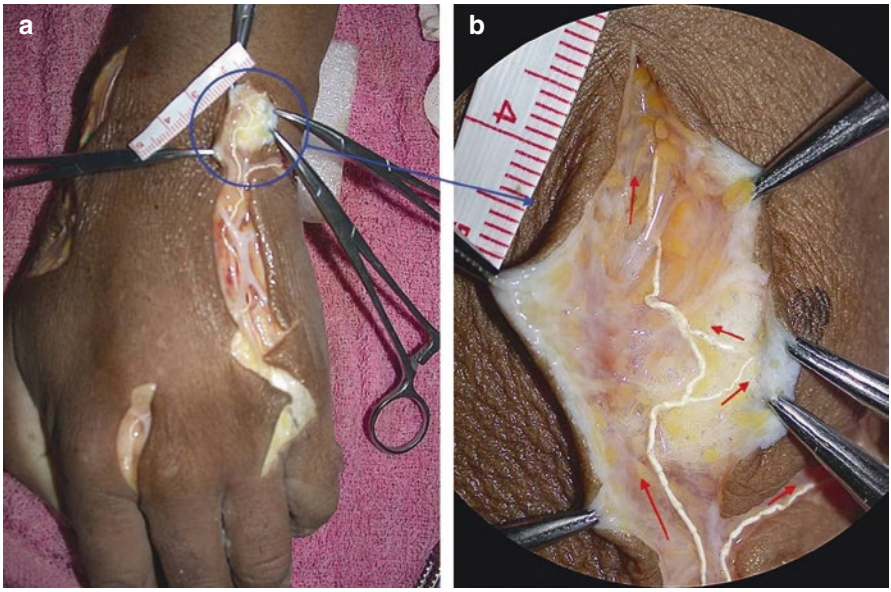

Fig. 3.87 The relationship of lymph vessels and veins on the dorsum of the left wrist (after a barium sulphate mixture injection). Lymph vessels traverse under veins. A magnified image (**b**) captured from the circled area in image (**a**)

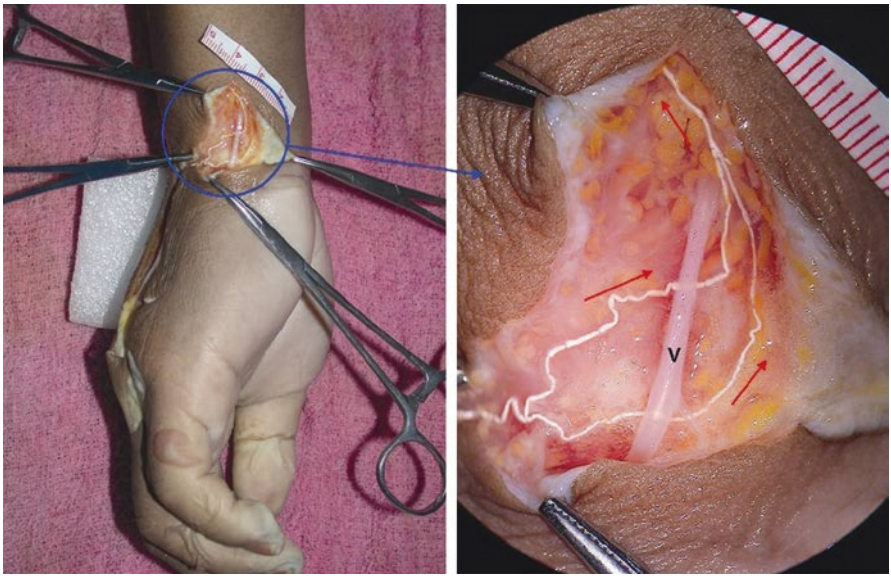

Fig. 3.88 The relationship of lymph vessels and the vein on the ulnar side of the left wrist (after a barium sulphate mixture injection). Two lymph vessels traverse under veins. *v*. Tributary of the basilic vein. A magnified image (**b**) captured from the circled area in image (**a**)

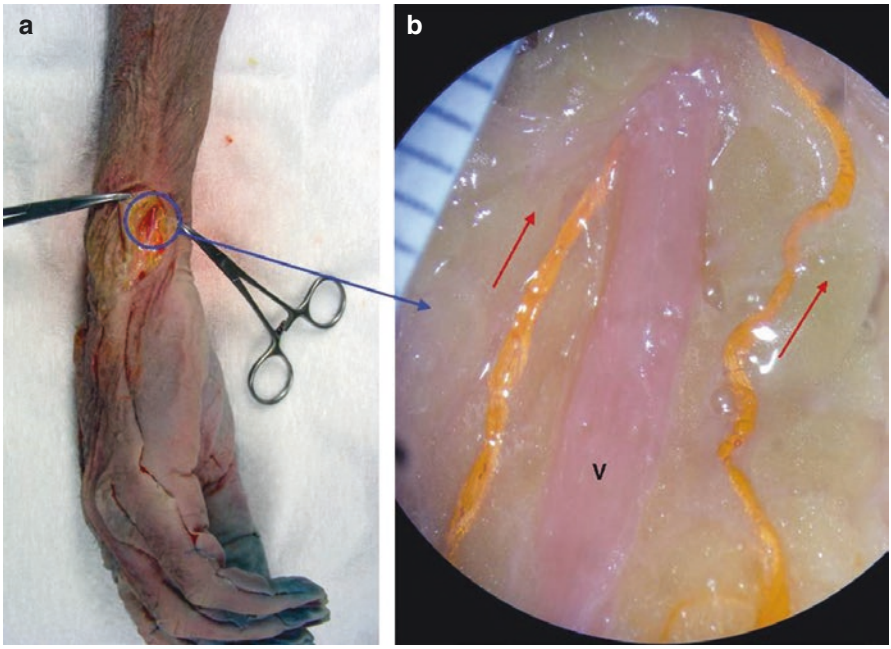

Fig. 3.89 The relationship of lymph vessels and the vein on the ulnar side of the left wrist (after a lead oxide mixture injection). A lymph vessel traverses under the vein. *v*. Tributary of the basilic vein. A magnified image (**b**) captured from the circled area in image (**a**)

5.4 Forearm

There is an average of 26 (ranging from 22 to 34) collecting lymph vessels distributed around the forearm region (Figs. 3.74, 3.75 and 3.90). The mean vessel diameter was 0.5 mm (ranging from 0.3 to 0.6 mm). They were a continuation of vessels arising from fingers, the dorsum of the hand and the skin crease of the wrist. They were dense and parallel with the cephalic and basilic vein systems meandering in the subcutaneous tissue and traversing over and/or under the veins when meeting them (Figs. 3.91, 3.92 and 3.93). Three groups of collecting lymph vessels were presented.

5.4.1 Radial Group

Arising from the dorsoradial group of the hand, lymph vessels ascended in the dorsoventral direction and crossed the radial forearm margin from the dorsoradial side of the wrist to the lateral part of the cubital fossa (Fig. 3.90 green vessels).

5.4.2 Ulnar Group

Arising from the dorsoulnar group of the hand, lymph vessels ascended in the dorsoventral direction and crossed the ulnar forearm margin from the dorsoulnar side of the wrist to the medial part of the cubital fossa and the elbow (Fig. 3.90 blue vessels).

5.4.3 Volar Group

Arising near to the wrist crease, lymph vessels ascended in the subcutaneous tissue of the volar of the forearm towards the cubital fossa (Fig. 3.90 yellow vessels).

Clinical Implication
It has been reported that intra-lymphatic administration of anticancer agents was performed for treating advanced metastatic tumours (Pizza et al. 1988; Zhang et al. 1998). The foot or leg was selected for lymphatic infusion sites; anticancer agents were perfused and expected to have an effect on the metastatic lesions of the groin, pelvis, abdomen and supraclavicular fossa, while the dorsal hand, wrist and forearm contain rich collecting lymph vessels that

may provide additional lymphatic infusion sites for the treatment of metastatic lesion in the supraclavicular fossa.

Besides the dorsal hand, wrist and forearm, with abundant collecting lymph vessels in the subcutaneous tissue, may provide some potential sites for lymphaticovenous anastomosis and vascularized groin lymph node flap transfer in the treatment of the secondary lymphoedema (O'Brien et al. 1990; Demirtas et al. 2009; Lin et al. 2009; Narushima et al. 2010).

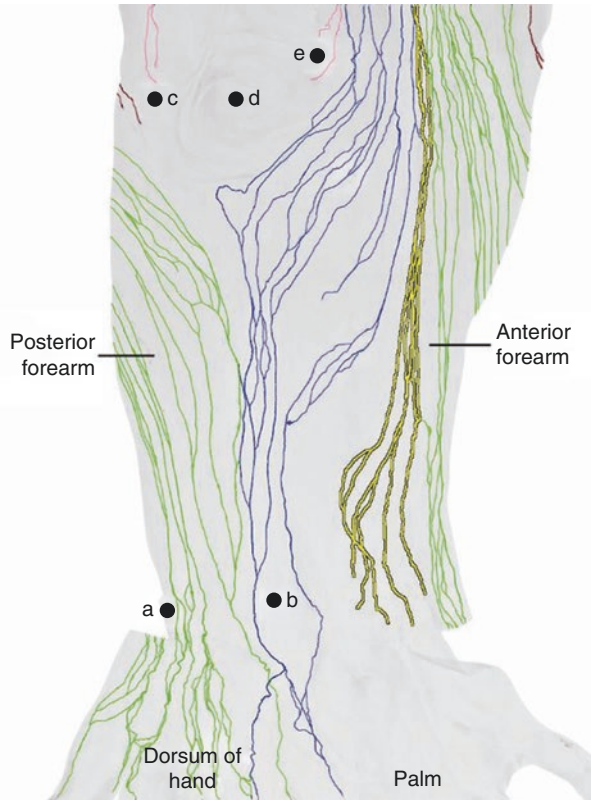

Fig. 3.90 Inverted radiograph of the lymphatic distribution in the integument of the forearm. Groups of lymph vessels are highlighted by different colours. Vessels coloured in *green* were divided by the incision. *a*. Styloid process of the radius, *b*. styloid process of the ulna, *c*. lateral epicondyle of the humerus, *d*. olecranon, *e*. medial epicondyle of the humerus

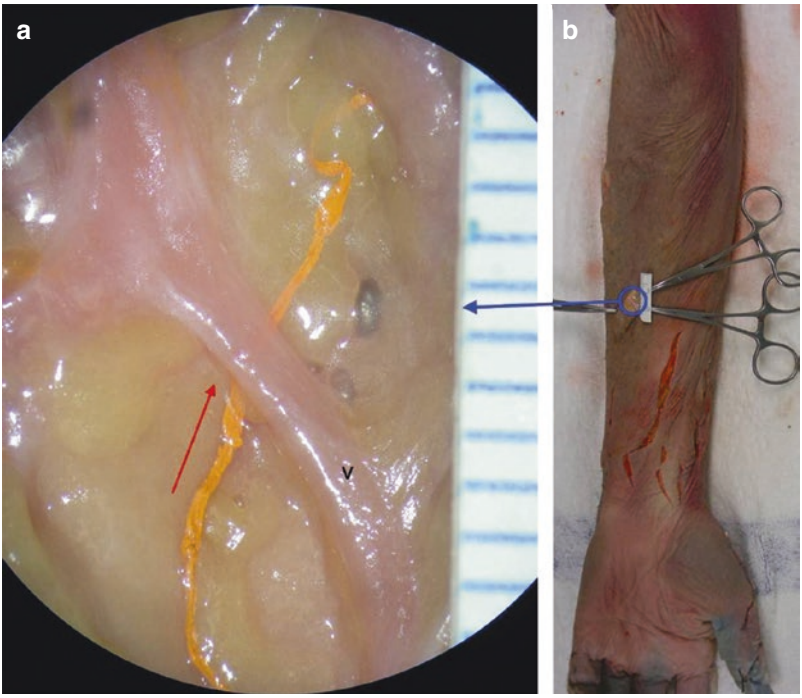

Fig. 3.91 The relationship of the lymph vessel and the basilic vein (*v*) in the left anterior forearm (after a lead oxide mixture injection). A lymph vessel traverses under the vein. A magnified image (**a**) captured from the circled area in image (**b**)

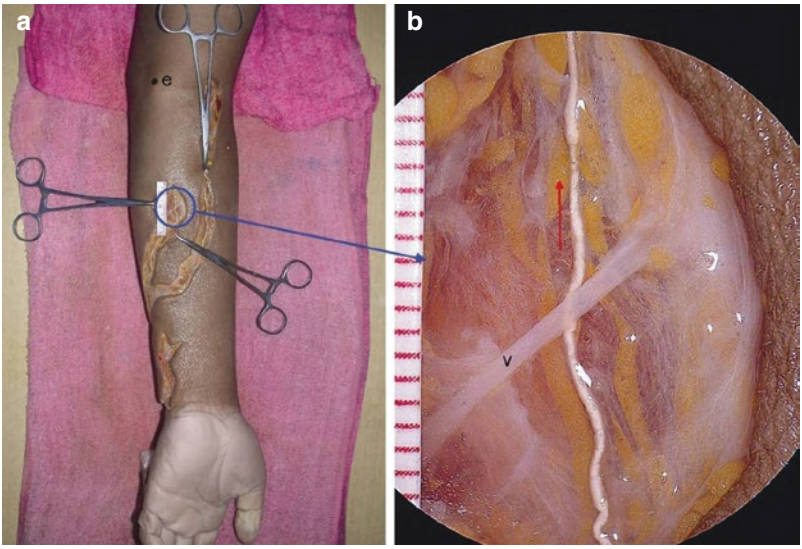

Fig. 3.92 The relationship of the lymph vessel and vein on the ulnar side of the left anterior forearm (after a barium sulphate mixture injection). A lymph vessel traverses under the vein. *v*. Tributary of the basilic vein. A magnified image (**b**) captured from the circled area in image (**a**)

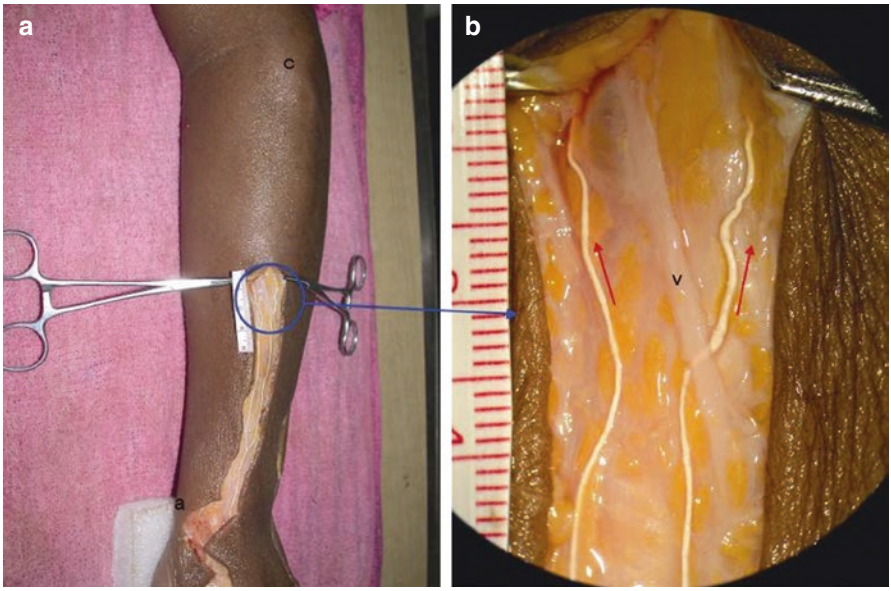

Fig. 3.93 The relationship of the lymph vessel and vein on the ulnar side of the left anterior forearm (after a barium sulphate mixture injection). A lymph vessel traverses under the vein. *v*. Tributary of the basilic vein. A magnified image (**b**) captured from the circled area in image (**a**)

5.5 *Elbow*

There is an average of 22 (ranging from 20 to 24) collecting lymph vessels distributed in the subcutaneous tissue around the elbow region (Figs. 3.74 and 3.75). The mean vessel diameter was 0.5 mm (ranging from 0.3 to 0.8 mm). They were a continuation of vessels arising from the fingers, the dorsal aspect of the hand and the forearm. Most vessels were clustered in the ulnar side of the elbow, while only a few of them were distributed in the posteroradial side. They meandered in the subcutaneous tissue and traversed over and/or under the veins when meeting them (Figs. 3.74, 3.75, 3.90, 3.94, 3.95 and 3.96).

Clustering in the anteromedial aspect of the elbow, three groups of lymph vessels arising from the forearm paralleled basilic veins and crossed over and below the median and basilic veins when meeting them. In some cases, a cubital lymph node presented next to the basilica vein in the cubital fossa connected by a single afferent and efferent lymph vessels, while the other vessels bypassed it (Figs. 3.95 and 3.97).

Fig. 3.94 The relationship of lymph vessels and the cephalic vein (*v*) in the left elbow (after a lead oxide mixture injection). A lymph vessel crosses over the vein. A magnified image (**b**) captured from the circled area in image (**a**)

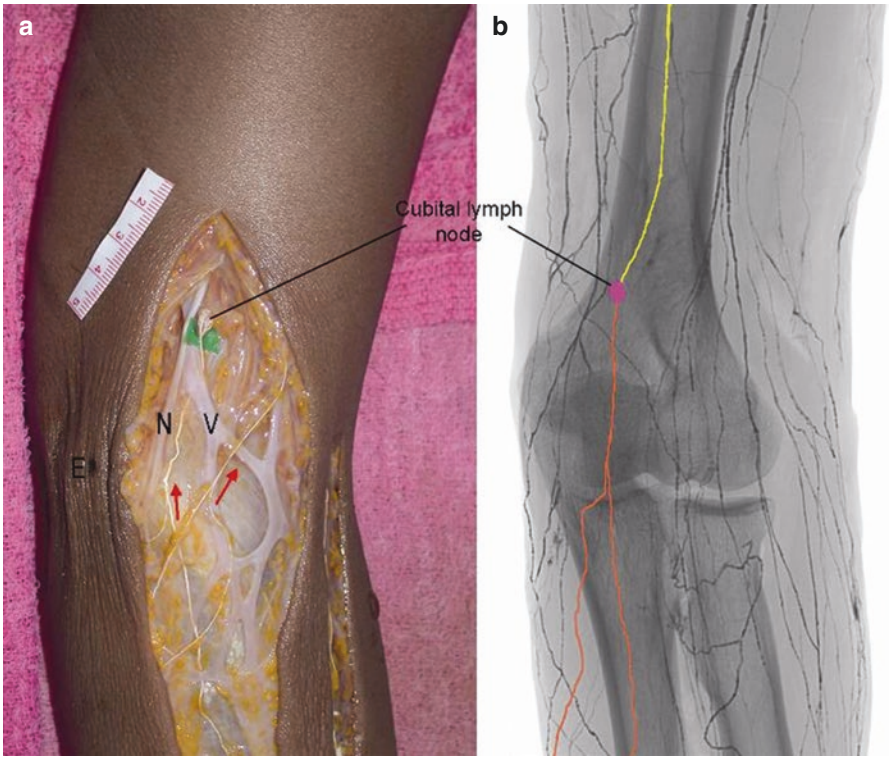

Fig. 3.95 The relationship of the lymph vessel (after a barium sulphate mixture injection), cubital lymph node, basilic vein (*V*) and medial cutaneous nerve of the forearm (*N*) in the left elbow. Afferent and efferent lymph vessels link to the cubital lymph node. (**a**) Photograph. (**b**) Inverted radiograph of the left elbow

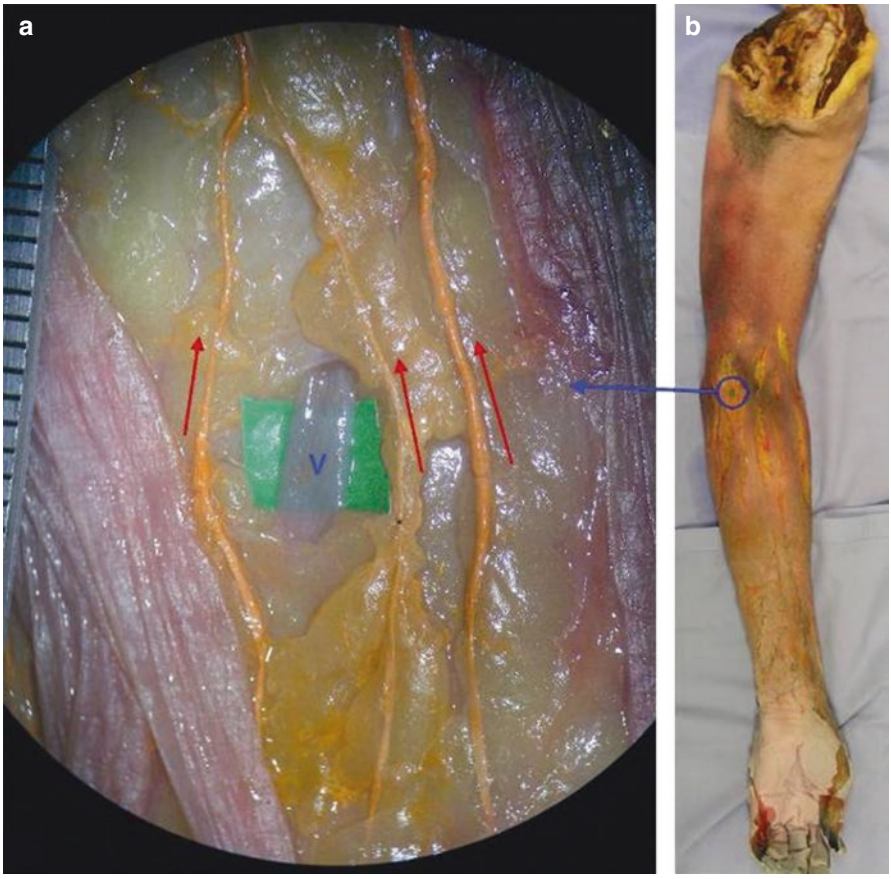

Fig. 3.96 The relationship of the lymph vessel and the basilica vein (*v*) of the left elbow (after a lead oxide mixture injection). Lymph vessels are parallel to the vein and one of them crosses over it. A magnified image (**a**) captured from the circled area in image (**b**)

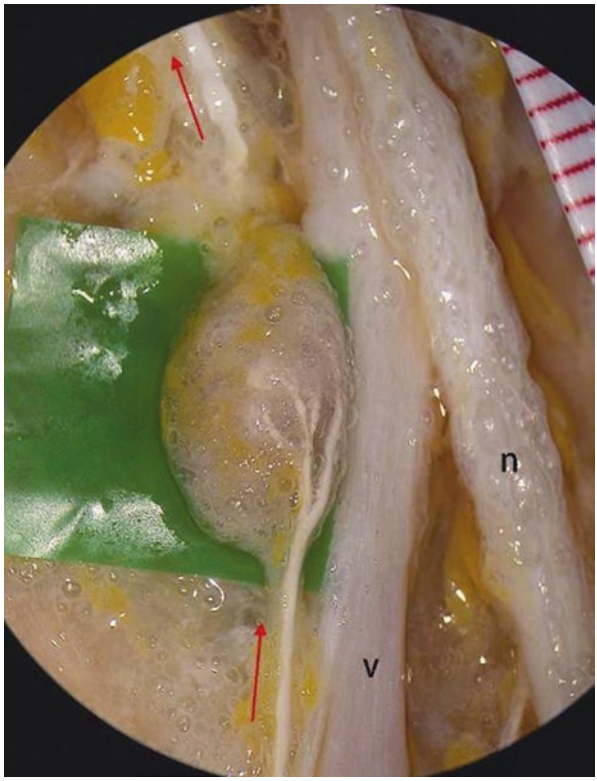

Fig. 3.97 The relationship of the lymph vessel (after a barium sulphate mixture injection) and the cubital lymph node in the right elbow. Afferent and efferent lymph vessels linked to the cubital lymph node. *v*. Basilic vein, *n*. Medial cutaneous nerve of the forearm

5.6 *Upper Arm*

There is an average of 19 (ranging from 17 to 21) collecting lymph vessels, counted in the midsection of the upper arm and distributed in the subcutaneous tissue of the upper arm (Figs. 3.74, 3.75 and 3.98). The mean vessel diameter was 0.6 mm (ranging from 0.3 to 1.2 mm). Lymph vessels were larger and denser on the medial side and thinner and more sparse on the lateral side. They converged centrally to form larger vessels before entering the lymph nodes in the axilla. There was a definite tendency for postaxial clustering and increased diameter of the vessel in the region. Three groups of lymph vessels were presented.

5.6.1 Anterolateral Group

Originating from the lateral side of the upper arm, the anterolateral group of lymph vessels travelled obliquely or horizontally via the anterior aspect of the upper arm to merge with the medial group of vessels in different levels to reach the axillary lymph node (Figs. 3.75 and 3.98 brown vessels).

5.6.2 Medial Group

Clustering just above the elbow joint in the medial side of the upper arm, the medial group of lymph vessels in the upper arm was formed by three groups of lymph vessels prolonged from the forearm. They converged to form larger diameter vessels before entering the lymph nodes in the axilla (Figs. 3.75 and 3.98). Lymph vessels, of those accompanying with the basilic vein and medial cutaneous nerve, pierced the deep fascia above the elbow and travelled beneath the deep fascia before entering the lymph nodes in the axilla (Figs. 3.75 and 3.98 blue, yellow and green vessels).

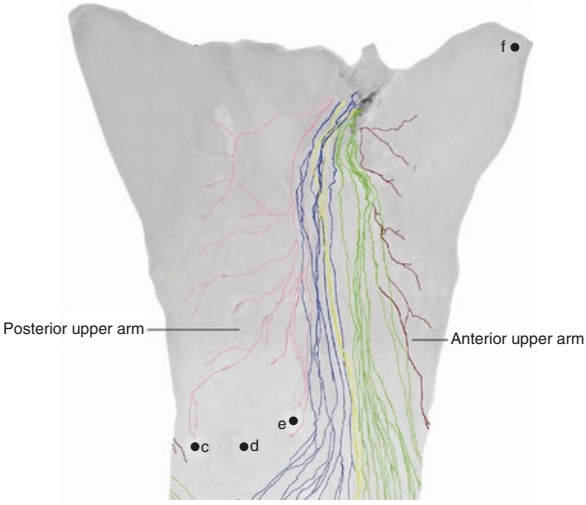

Fig. 3.98 Inverted radiograph of the lymphatic distribution in the integument of the upper arm. Groups of lymph vessels are indicated by different colours: the medial group (*green*, *blue* and *yellow*), the anterolateral group (*brown*) and the posterolateral group (*pink*). *c*. Lateral epicondyle of the humerus, *d*. Olecranon, *e*. Medial epicondyle of the humerus, *f*. Acromion of the scapula

5.6.3 Posterolateral Group

Originating from the lateral side of the upper arm, the posterolateral group of lymph vessels travelled obliquely or horizontally via the dorsal aspect to merge with the medial group of vessels before entering the axillary lymph node (Figs. 3.75 and 3.76 pink vessels, 3.99, 3.100 and 3.101).

Clinical Implication

Lymphangitis can be caused by any injury or infection in the upper extremity, especially in the hand and fingers. Besides systemic symptoms such as chills, fever, malaise, headache, loss of appetite and throbbing pain along the affected area, local signs appear in the affected extremity; thin red lines may be observed running along the course of the lymph vessels, especially in the anteromedial aspect of the upper extremity associated with lymphadenitis (Zhang 1984).

Lymphovenous anastomosis is one of the existing options for treating secondary lymphoedema in surgery (O'Brien et al. 1990). Detailed lymphatic awareness of the upper extremity may help with locating the collecting lymph vessels for the proposed procedure. In order to obtain the best result, it has been suggested to perform as many anastomoses as possible in each case (Huang et al. 1985). Information in this section provides a roadmap for surgeons when searching for potential lymphaticovenous anastomotic sites in the upper extremity where lymph vessels are situated close to the major veins in the subcutaneous tissue.

Fig. 3.99 Distribution of the lymph vessels (after a barium sulphate mixture injection), cubital lymph node, basilic vein (*v*) and medial cutaneous nerve (*n*) in the left medial upper arm

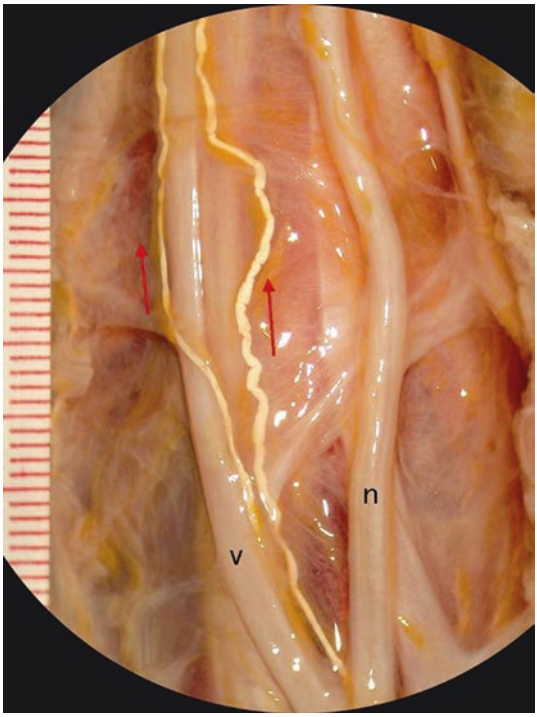

Fig. 3.100 The relationship of lymph vessels (after a barium sulphate mixture injection), basilic vein (*v*) and medial cutaneous nerve (*n*) in the left medial upper arm. Two winding lymph vessels accompany the vein and nerve

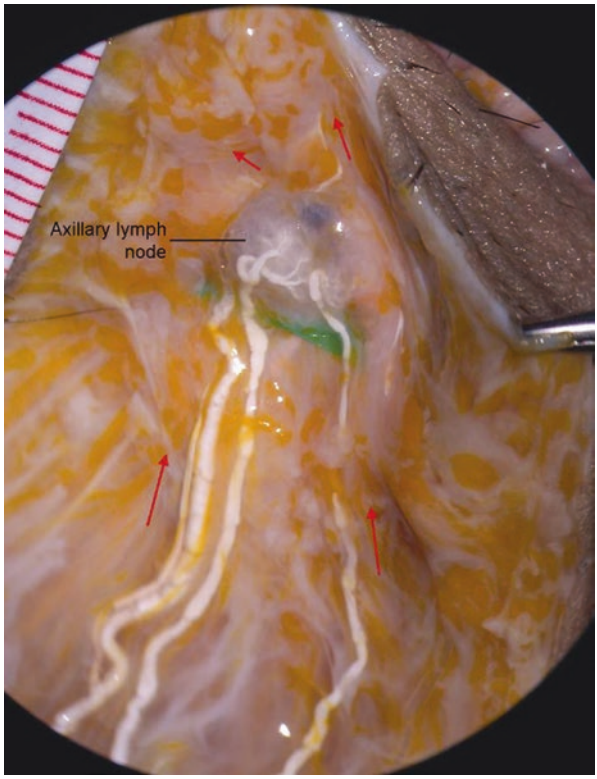

Fig. 3.101 Multiple afferent lymph vessels enter the axillary lymph node (after a barium sulphate mixture injection). *Red arrows* indicate the direction of the lymph flow

6 Lower Extremity

Superficial collecting lymph vessels of the lower extremity originated beneath the dermis on each side of the toes, the foot and the lateral thigh (Figs. 2.84, 2.85, 2.86, 2.87 and 2.88, 3.102, 3.103, 3.104 and 3.105). The diameter of the vessels varied from 0.2 to 2.2 mm. They travelled in a tortuous fashion to different depths of the subcutaneous tissue towards the lymph nodes in the popliteal fossa, those adjacent to the superficial femoral vessels and in the inguinal region. Again vessels branched, diverged or converged; sometimes they anastomosed with or crossed over neighbouring vessels during their course. As they approached the lymph nodes, they converged to form larger vessels and then split into small branches before entering the lymph nodes (Fig. 2.137). The size, number and pathways of the vessel's drainage patterns were different with each individual and even between each side of the same body.

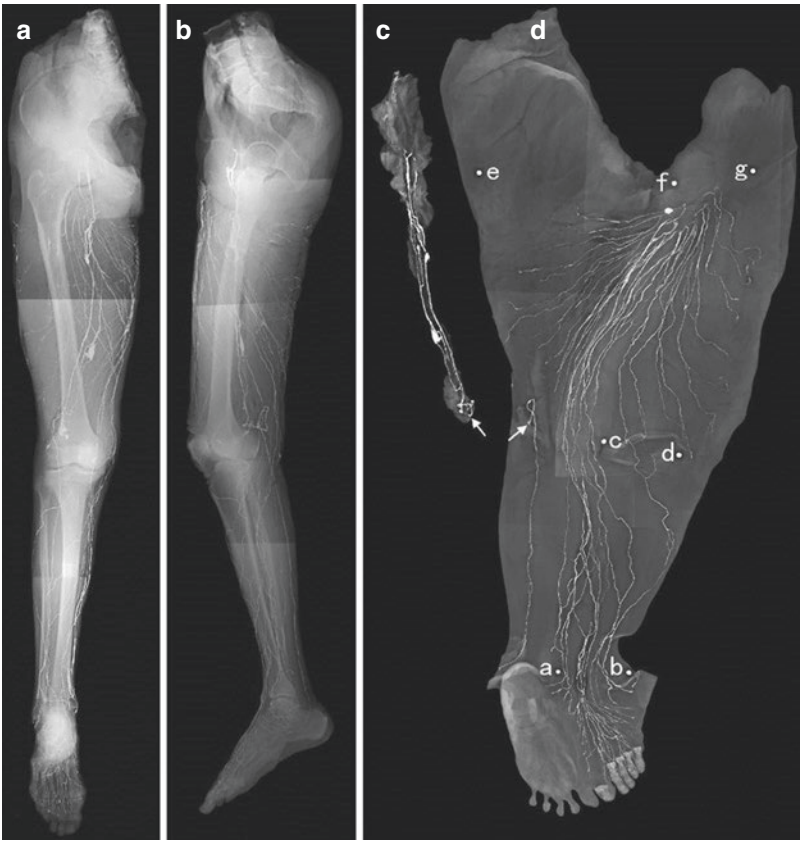

Fig. 3.102 Radiographs of the lymphatic distribution in the lower left extremity after a lead oxide mixture injection. (**a**) Anteroposterior view. (**b**) Lateral view. (**c**) Lymphatics in the femoral neurovascular bundle. (**d**) Lymphatic distribution of the integument. *a*. Medial malleolus, *b*. Lateral malleolus, *c*. Medial epicondyle, *d*. Lateral epicondyle, *e*. Ischial tuberosity, *f*. Pubic tubercle, *g*. Anterosuperior iliac spine, *p*. *White arrows* indicate the cut points of the vessels

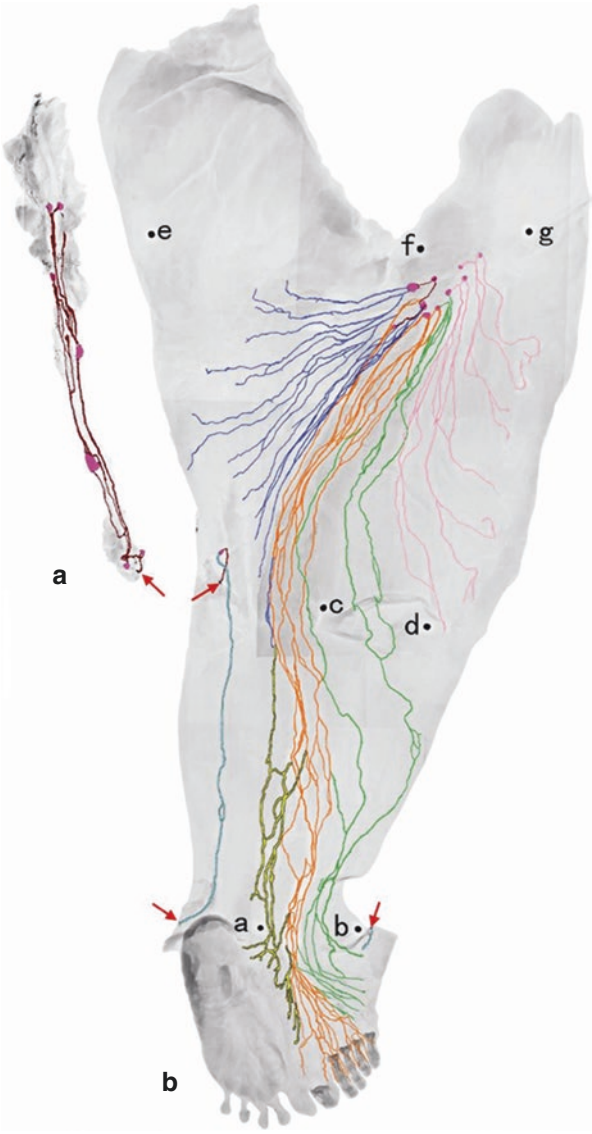

Fig. 3.103 Inverted radiographs of the lymphatic distribution in the lower extremity. (**a**) Lymphatics in the femoral neurovascular bundle. (**b**) The lymphatic distribution in the integument of the lower extremity. Groups of lymph vessels are highlighted by different colours. *a*. Medial malleolus, *b*. Lateral malleolus, *c*. Medial epicondyle, *d*. Lateral epicondyle, *e*. Ischial tuberosity, *f*. Pubic tubercle, *g*. Anterosuperior iliac spine. *Red arrows* indicate cut points of lymph vessels

6.1 Toes

Collecting lymph vessels originated beneath the dermis one on each side of the toes, alongside the base of the distal phalanges, and generally travelled tortuously along the mid-axial lines in the subcutaneous tissue. The mean vessel diameter was 0.5 mm (ranging from 0.2 to 0.8 mm). Vessels of neighbouring toes converged in the web spaces of the foot, with the exception of those on the lateral border of the great toe and the medial border of the little toe. These then travelled radially to merge with lymphatic vessels in the dorsum of the foot (Figs. 3.102, 3.103, 3.104 and 3.105).

Clinical Implication
The toe-to-thumb transplantation is a procedure of choice for thumb defect reconstruction. Although, the technique has been well established (Lutz and Wei 2002), a variety of factors can influence the survival rate after surgery. The patency of the digital artery and vein is an important factor for the preservation of the replanted digits (Cheng et al. 1997). As a donor site, awareness of the detailed lymphatic anatomy of toes may help for managing postoperative oedema and increasing the survival rate.

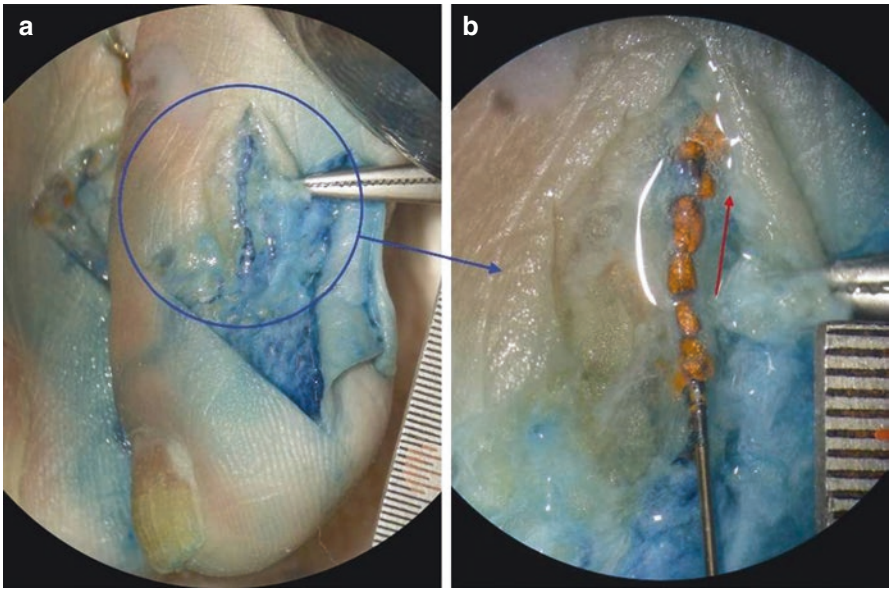

Fig. 3.104 (**a**) A lymphatic vessel distended by a mixture of 6% hydrogen peroxide and ink on the lateral side of the left second toe. (**b**) The vessel filled with a lead oxide mixture

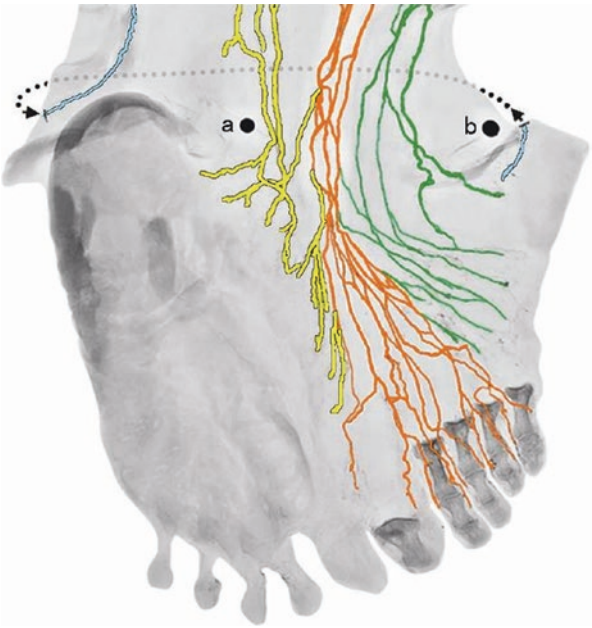

Fig. 3.105 Inverted radiograph of the integument of the left foot. Each group of lymphatic vessel originates from the toes (*orange*) and the medial (*yellow*) and lateral borders (*green* and *aqua blue*) of the foot forming the lymphatic network on the dorsal foot. *Black arrows* and the dotted line link the divided vessels. *a*. Medial malleolus, *b*. lateral malleolus

6.2 Foot

In the subcutaneous of the dorsal foot, an average of 14 (ranging from 9 to 19) collecting lymph vessels were found. The mean vessel diameter was 0.6 mm (ranging from 0.2 to 1.2 mm). They converged with or crossed over neighbouring vessels, forming a large lymphatic network in three groups (Figs. 3.102, 3.103, 3.104, 3.104, 3.105, 3.106 and 3.107).

6.2.1 Anterior Group

Collecting lymph vessels arose from the toes forming the front and centre parts of the lymphatic network on the dorsal foot (Fig. 3.105 orange vessels).

6.2.2 Medial Group

Collecting lymph vessels arose from the medial border of the foot to form the medial part of the lymphatic network on the dorsal foot (Fig. 3.105 yellow vessels).

6.2.3 Lateral Group

Collecting lymph vessels arose from the lateral border of the foot forming the lateral part of the lymphatic network on the dorsal foot (Fig. 3.105 green vessels).

Clinical Implication
The procedure of the lymphatic skin flap transplantation, with valves oriented favourably, may provide a potential solution for treating secondary lymphedema. The skin of the dorsal foot contains not only rich blood vessels but also abundant collecting lymph vessels that may be the potential donor site for the procedure (Taylor and Pan 2014).

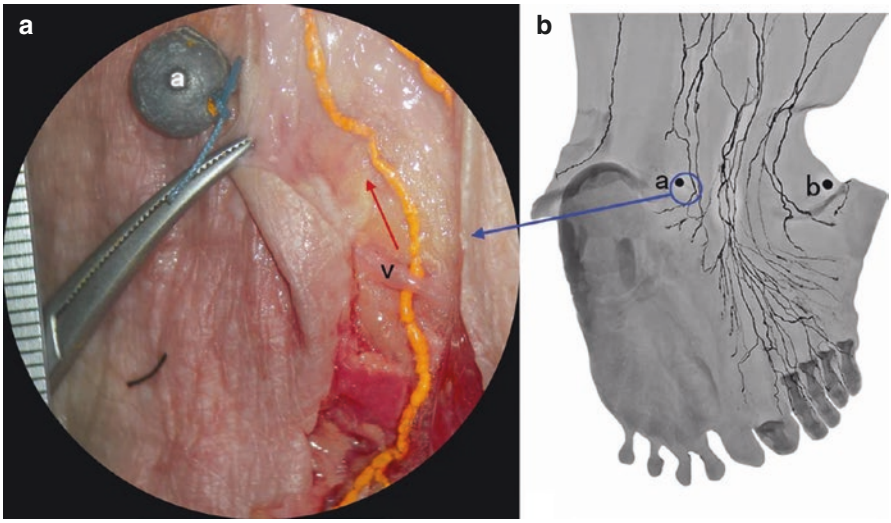

Fig. 3.106 A collecting lymph vessel filled with a lead oxide mixture traverses under a small vein next to the medial malleolus of the right foot. *a*. Medial malleolus, *b*. Lateral malleolus, *v*. Tributary of the GSV. A magnified photograph (**a**) took from the circled area on a radiograph of the superficial tissue of the right foot (**b**)

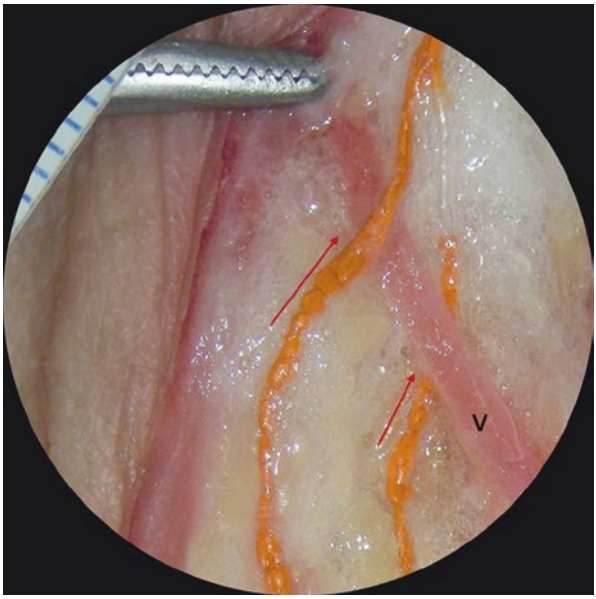

Fig. 3.107 Collecting lymph vessels filled by a lead oxide mixture cross over and traverse under a small vein of the right dorsal foot. *v*. Tributary of the GSV

6.3 *Ankle*

Arising from the foot, an average of 12 (ranging from 9 to 17) collecting lymph vessels were found in the subcutaneous tissue around the ankle. The mean vessel diameter was 1.0 mm (ranging from 0.2 to 2.0 mm) (Figs. 3.102, 3.103, 3.105 and 3.106). Vessels were dense on the anterior aspect and sparse in the posterior aspect (Figs. 3.102, 3.103, 3.105 and 3.106).

6.3.1 Anterior Group

An average of 10 collecting lymph vessels (ranging from 8 to 13) were presented in the anterior aspect of the ankle between the lateral and medial malleoli. They were continuous with the vessels from the dorsal foot.

6.3.2 Posterior Group

An average of two collecting lymph vessels (ranging from one to four) were presented in the posterior aspect of the ankle, arising from the area next to the Achilles tendon (tendo-calcaneus) bilaterally in the subcutaneous tissue just above the heel. Generally they could be further classified into the posterolateral and posteromedial lymph vessels. The former travelled in the area between the Achilles tendon and the lateral malleolus and the latter between the Achilles tendon and the medial malleolus (Figs. 3.108, 3.109 and 3.110).

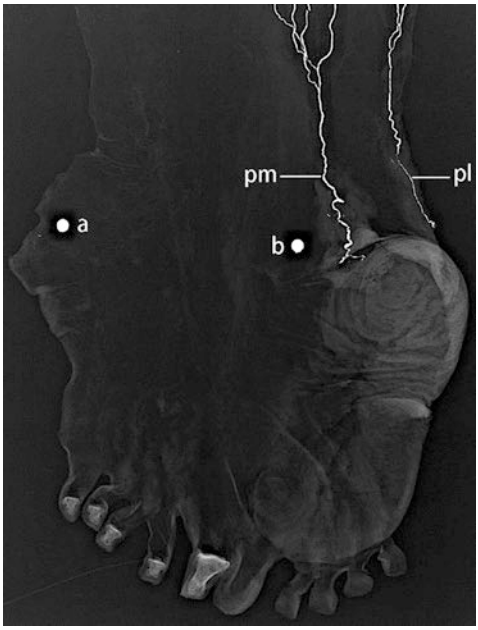

Fig. 3.108 Radiograph of the integument of the right foot and ankle shows the posterolateral (*pl*) and posteromedial (*pm*) lymph vessels (filled by a lead oxide mixture) in the posterior ankle. *a*. Medial malleolus, *b*. lateral malleolus

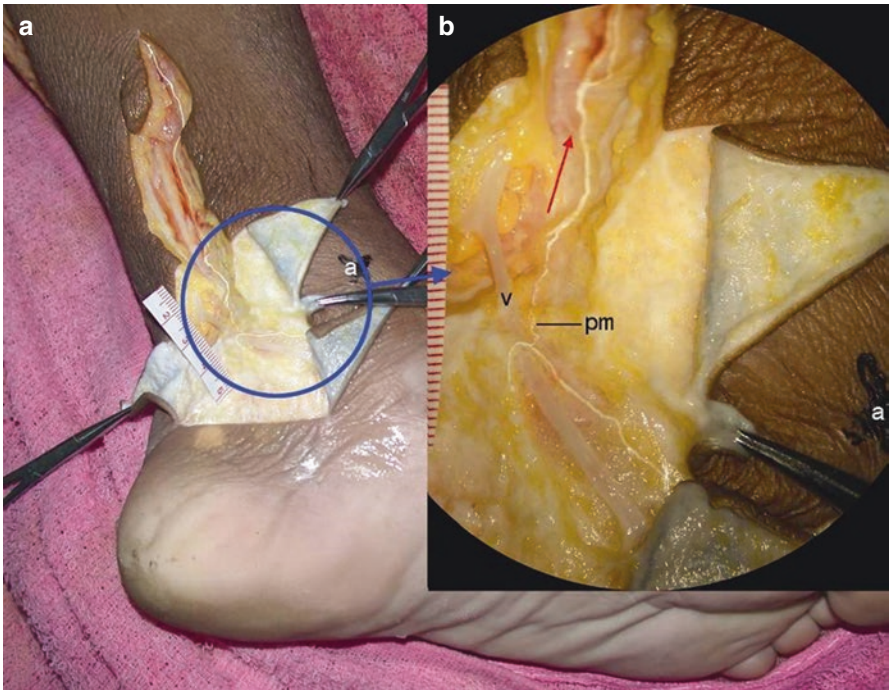

Fig. 3.109 The posteromedial (*pm*) lymph vessel (filled by a barium sulphate mixture) travels next to GSV (*v*). *a*. Medial malleolus. A magnified image (**b**) captured from the circled area in image (**a**)

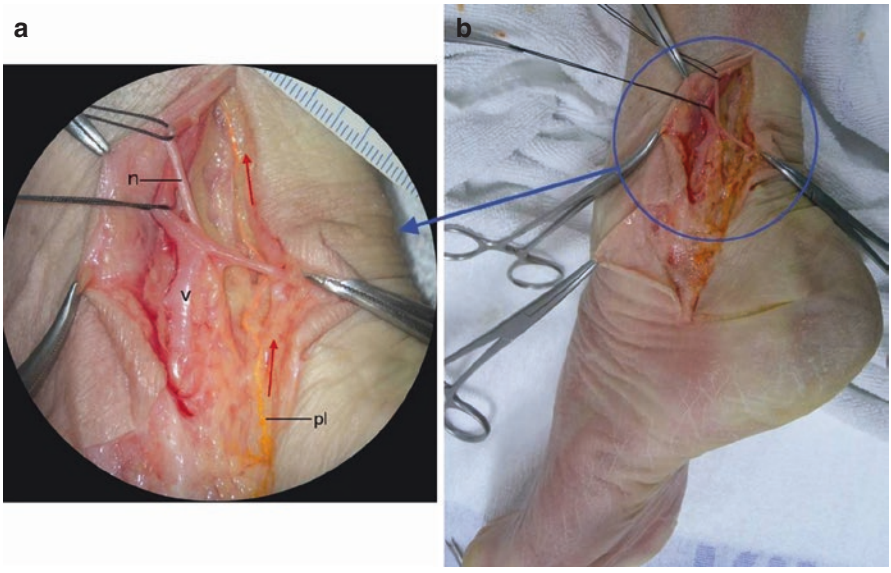

Fig. 3.110 The posterolateral (*pl*) lymph vessel (filled by a barium sulphate mixture) travels next to GSV (*v*) and the sural nerve (*n*). A magnified image (**a**) captured from the circled area in image (**b**)

6.4 Leg

An average of 13 (ranging from 12 to 16) collecting lymph vessels were distributed in the subcutaneous tissue of the leg (Figs. 3.102, 3.103 and 3.111). The mean vessel diameter was 1.0 mm (ranging from 0.2 to 1.8 mm). They were divided into anteromedial, anterolateral and posterior groups. The largest vessels were mostly situated in the anteromedial and posterior groups.

6.4.1 Anteromedial Group

Arising from the foot and ankle, the anteromedial lymph vessels were denser with a straighter path, following the adjacent great saphenous vein (GSV) and its tributaries (Figs. 3.103 orange and yellow vessels, 3.111 and 3.112).

6.4.2 Anterolateral Group

Arising from the foot, ankle and the superior half of the lateral aspect of the leg, the anterolateral lymph vessels were relatively sparse, following a curving path tending towards to the anteromedial aspect of the proximal third of the leg and the thigh (Figs. 3.103 green vessels and 3.111).

6.4.3 Posterior Group

There were only one or two large lymph vessels (mean diameter of 1 mm, ranging from 0.7 to 1.4 mm) in the posterior aspect of the leg accompanying the small saphenous vein (SSV). Two vessels were presented in the area; the posterolateral and posteromedial lymph vessels were noticed on each side of SSV (Figs. 3.102, 3.103 aqua blue vessels, 3.111, 3.113, 3.114, 3.115, 3.116 and 3.117).

Clinical Implication
Any injury or infection in the lower extremity, especially in the foot and toes, may cause lymphangitis. Besides systemic symptoms such as chills, fever, malaise, headache, loss of appetite and throbbing pain along the affected area, local signs appear in the affected extremity; thin red lines may be observed running along the course of the lymph vessels especially in the anteromedial aspect of the lower extremity associated with lymphadenitis.

Clinical Implication

Procedures of lymphaticovenous anastomosis and lymphatic grafting have been performed for treating secondary lymphoedema (Baumeister and Siuda 1990; Weiss et al. 2003; Demirtas et al. 2009; Narushima et al. 2010). Results from this section have shown that one or two large lymph vessels were presented in the posterior aspect of the leg accompanying the small saphenous vein (Figs. 3.111, 3.113, 3.114, 3.115, 3.116 and 3.117) that may be a potential site for lymphaticovenous anastomosis and harvesting the lymphatic graft in the clinic.

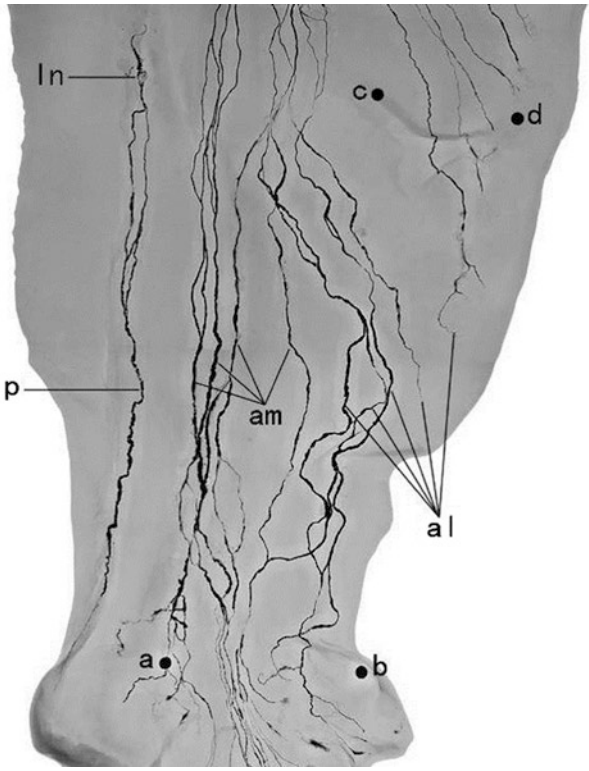

Fig. 3.111 Inverted radiograph of the lymphatic distribution in the integument of the leg. *am.* anteromedial group, *al.* anterolateral group, *p.* posterior group, *a.* medial malleolus, *b.* lateral malleolus, *c.* medial epicondyle, *d.* lateral epicondyle, *ln.* superficial popliteal lymph node

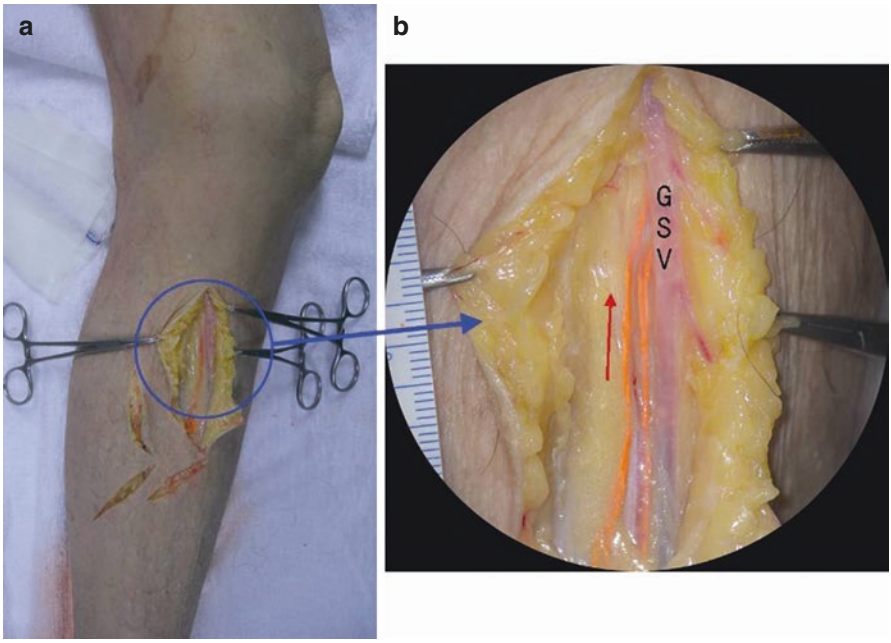

Fig. 3.112 The anteromedial lymph vessels of the left leg travelling with GSV. A magnified image (**b**) captured from the circled area in image (**a**)

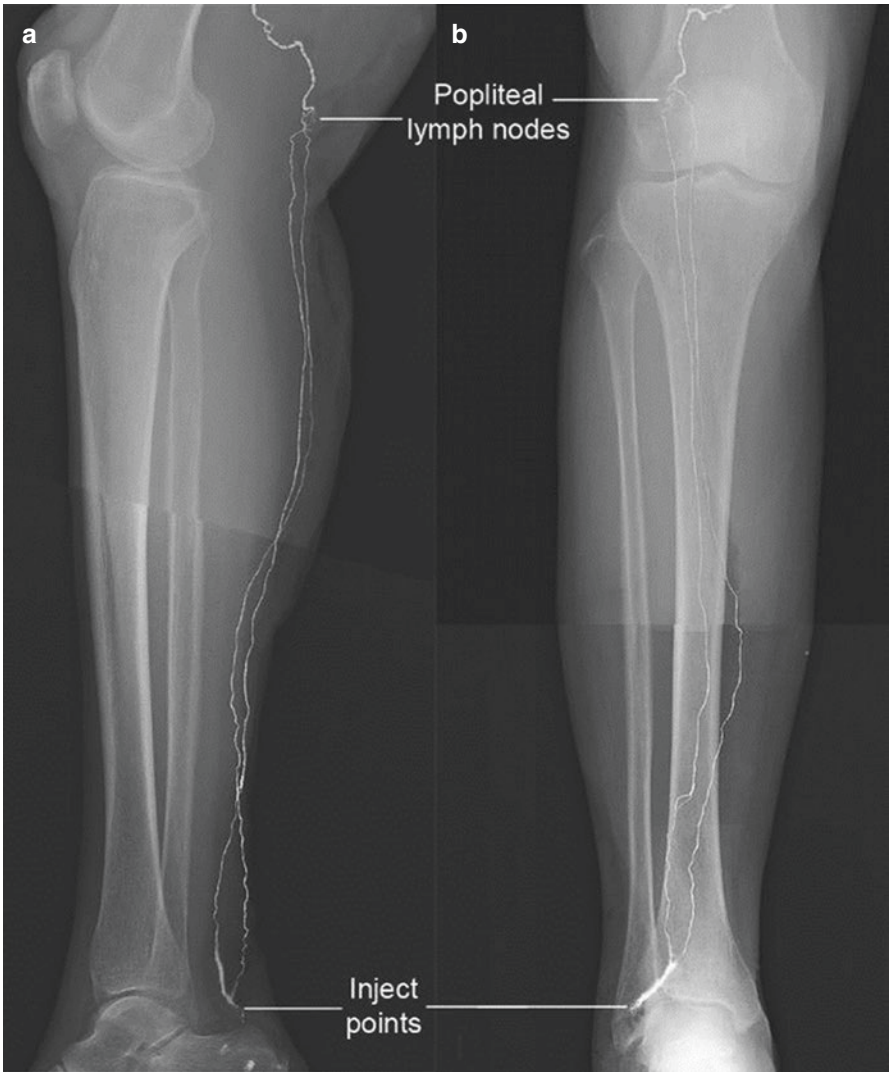

Fig. 3.113 Radiographs of the posterior group of lymph vessels in the right leg after a lead oxide mixture injection. (**a**) Lateral view; (**b**) Anteroposterior view

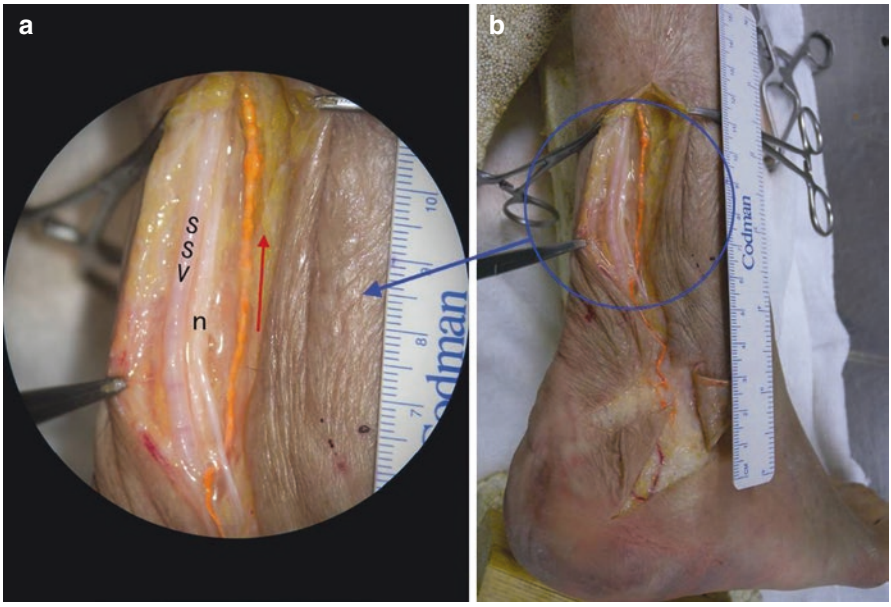

Fig. 3.114 The posterolateral lymph vessel (filled by a lead oxide mixture) of the posterior group travelling with the SSV and the sural nerve (*n*). A magnified image (**a**) captured from the circled area in image (**b**)

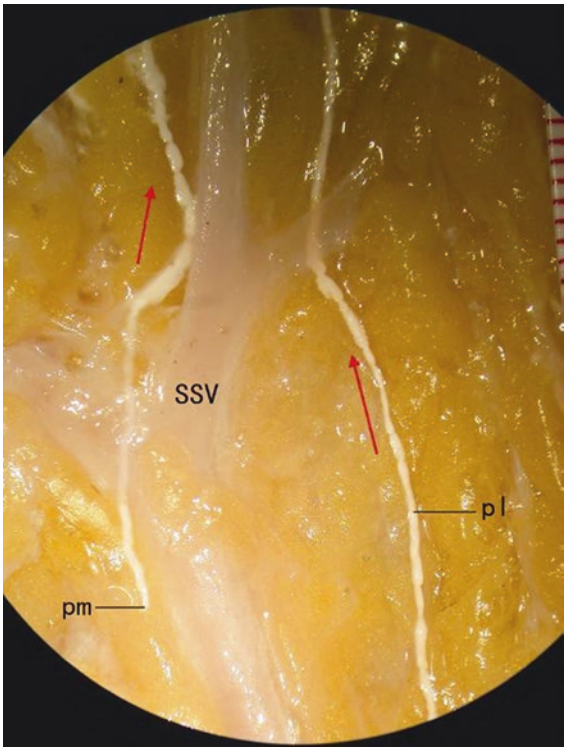

Fig. 3.115 The posterolateral (*pl*) and posteromedial (*pm*) lymph vessels (filled by a barium sulphate mixture) in the lower part of the right leg

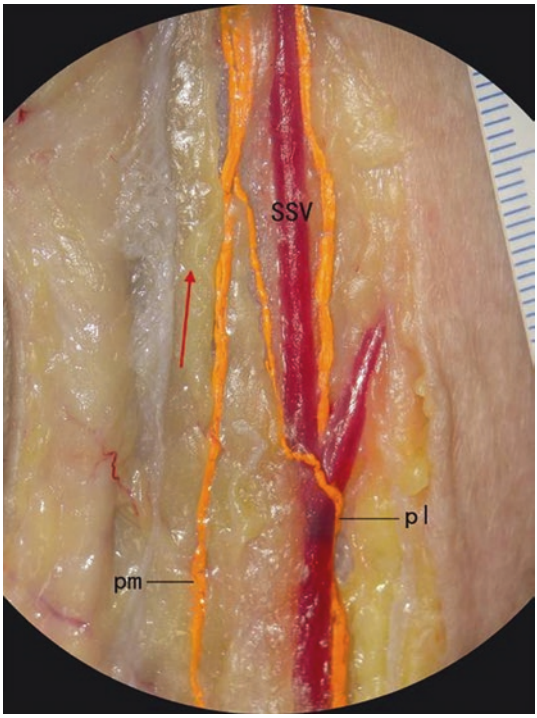

Fig. 3.116 The posterolateral (*pl*) and posteromedial (*pm*) lymph vessels (filled by a lead oxide mixture) in the middle part of the right leg

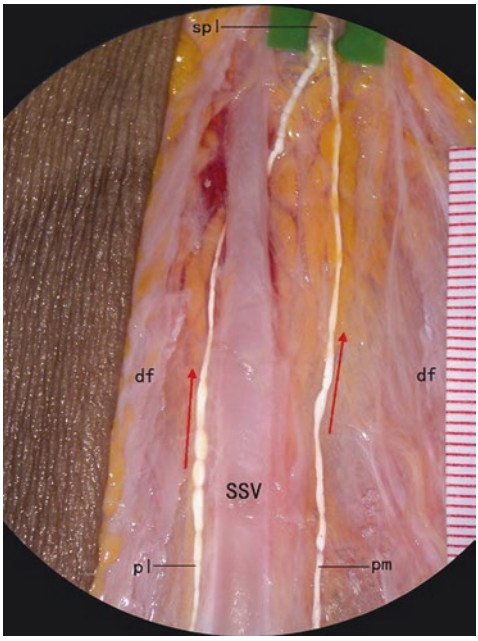

Fig. 3.117 The posterior group of lymph vessels (filled by a barium sulphate mixture) travels with the SSV in the upper part of the leg. *spl*. Superficial popliteal lymph node, *df*. Deep fascia, *pl*. Posterolateral lymph vessel, *pm*. posteromedial lymph vessel

6.5 *Knee*

An average of 15 (ranging from 11 to 17) collecting lymph vessels were found in the subcutaneous tissue around the knee region (Figs. 3.102 and 3.103). The mean vessel diameter was 0.8 mm (ranging from 0.3 to 1.6 mm).

6.5.1 Anterior Group

Extending from the superolateral (part of the anterolateral group) aspect of the leg, lymph vessels formed the anterior group in the knee. They were relatively sparse and travelled obliquely towards the medial aspect of the thigh (Fig. 3.103 green vessels).

6.5.2 Medial Group

Extending from the anteromedial and anterolateral groups of the leg, lymph vessels formed the medial group in the knee. They were denser and travelled around the GSV and its tributaries (Figs. 3.103 orange vessels, 3.118 and 3.119).

6.5.3 Posterior Group

Extending from the posterior group of the leg, one or two larger lymphatic vessels paralleled with the SSV in the popliteal fossa and drained to the superficial popliteal and/or then the deep lymph node(s) (Figs. 3.103 aqua blue vessels and 3.120). Two vessels were presented in the area; the posterolateral and posteromedial lymph vessels were noticed (Figs. 3.120 and 3.121).

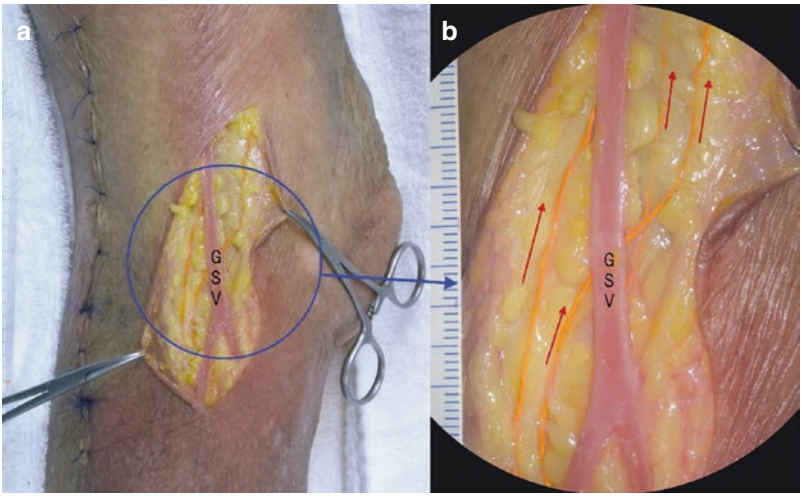

Fig. 3.118 The medial group of lymph vessels of the left knee travels next to the GSV. A magnified image (**b**) captured from the circled area in image (**a**)

Fig. 3.119 The medial group of lymph vessels of the right knee travels around the GSV and its tributaries

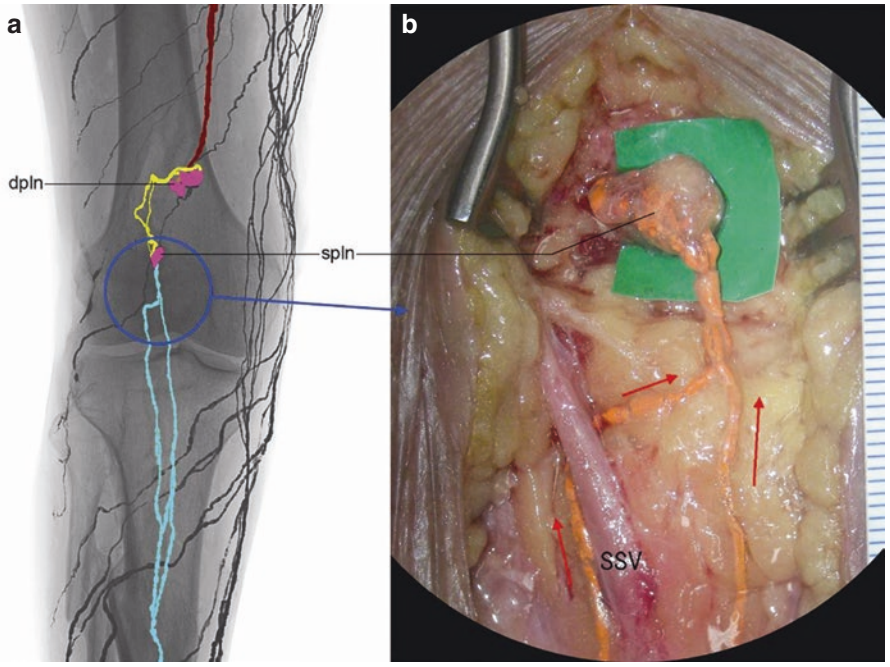

Fig. 3.120 The posterior group of lymph vessels of the left knee travelling next to the SSV. (**a**) Anterolateral view of the radiograph. (**b**) Photograph. *dpln*. Deep popliteal lymph nodes, *spln*. Superficial popliteal lymph node. *Red arrows* indicate the direction of flow

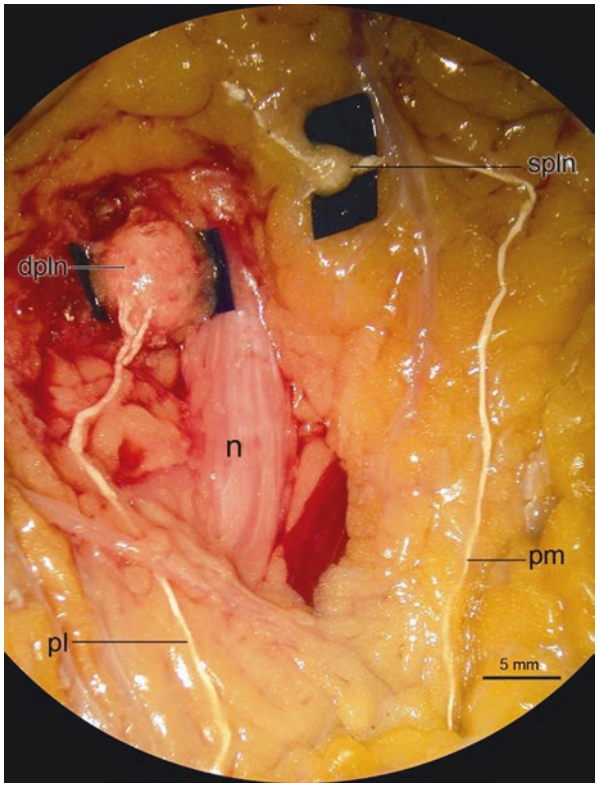

Fig. 3.121 The posterior group of lymph vessels in the left popliteal fossa. The posterolateral vessel (*pl*) drains into the deep popliteal lymph node (*dpln*). The posteromedial vessel (*pm*) drains into the superficial popliteal lymph node (*spln*). Tibial nerve in the popliteal fossa

6.6 Thigh

An average of 29 (ranging from 27 to 31) collecting lymph vessels were found in the thigh. The mean vessel diameter was 0.8 mm (ranging from 0.3 to 1.7 mm). Vessels were dense on the medial side and sparse on the lateral side. Three superficial and two deep groups were present in the thigh (Figs. 3.102, 3.103, 3.122, 3.123, 3.124, 3.125, 3.126, 3.127, 3.128 and 3.129).

6.6.1 Anterior Group

Originating from the anterolateral aspect of the thigh, vessels travelled obliquely in the subcutaneous tissue before entering the lateral group of the superficial inguinal lymph nodes (Figs. 3.102, 3.103 and 3.122 pink vessels).

6.6.2 Medial Group

Extending from the anterior and medial groups of the knee, collecting lymph vessels formed the medial group on the medial aspect of the thigh. They ascended proximally in the subcutaneous tissue around the GSV and its tributaries and entered the centre group of the superficial inguinal lymph nodes (Figs. 3.102, 3.103 and 3.122 orange and green vessels).

6.6.3 Posterior Group

Originating from the posterolateral side of the thigh, vessels ran obliquely in the subcutaneous tissue of the posterior aspect of the thigh and entered the medial group of the superficial inguinal lymph nodes (Figs. 3.102, 3.103 and 3.122 blue vessels).

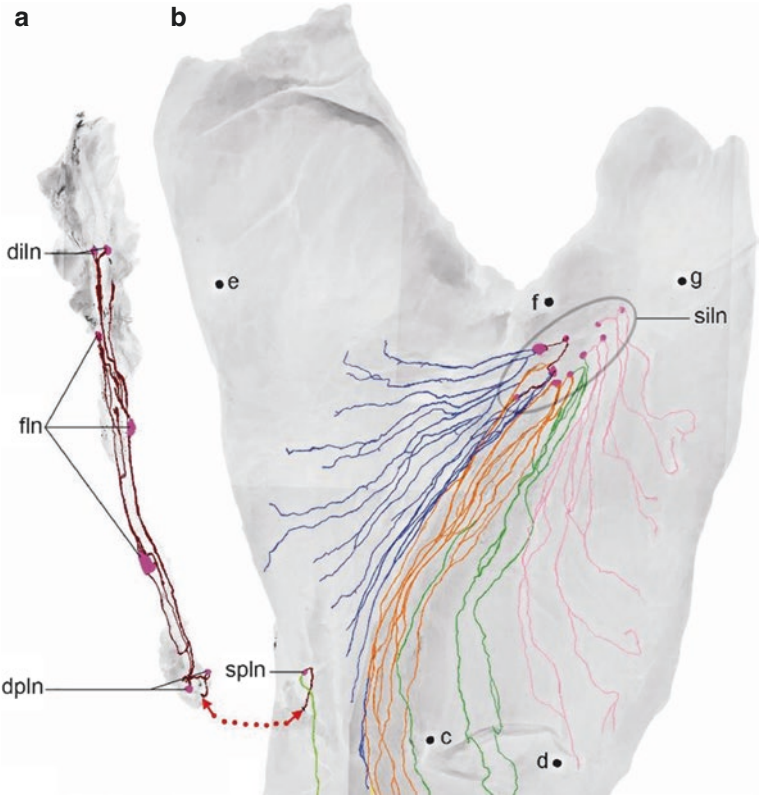

Fig. 3.122 Lymphatic distribution of the left thigh. (**a**) Lymphatics in the femoral neurovascular bundle. (**b**) The lymphatic distribution in the integument of the left thigh. Groups of lymph vessels are highlighted by different colours. *diln*. Deep inguinal lymph nodes, *fln*. Femoral lymph nodes, *dpln*. Deep popliteal lymph nodes, *spln*. Superficial popliteal lymph node, *siln*. Superficial inguinal lymph nodes, *c*. medial epicondyle, *d*. lateral epicondyle, *e*. ischial tuberosity, *f*. pubic tubercle, *g*. anterosuperior iliac spine

Fig. 3.123 The medial group of lymphatic vessels of the thigh travels around the GSV. *siln*. Superficial inguinal lymph nodes

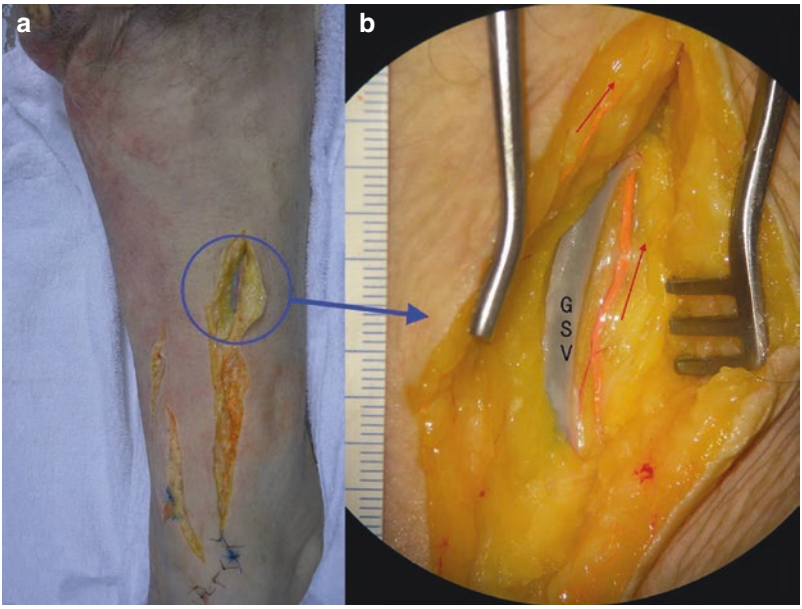

Fig. 3.124 The medial group of lymphatic vessels of the thigh travels in different depths (lymphatic vessels next to rad *arrows*) of the subcutaneous tissue next to the GSV. A magnified image (**b**) captured from the circled area in image (**a**)

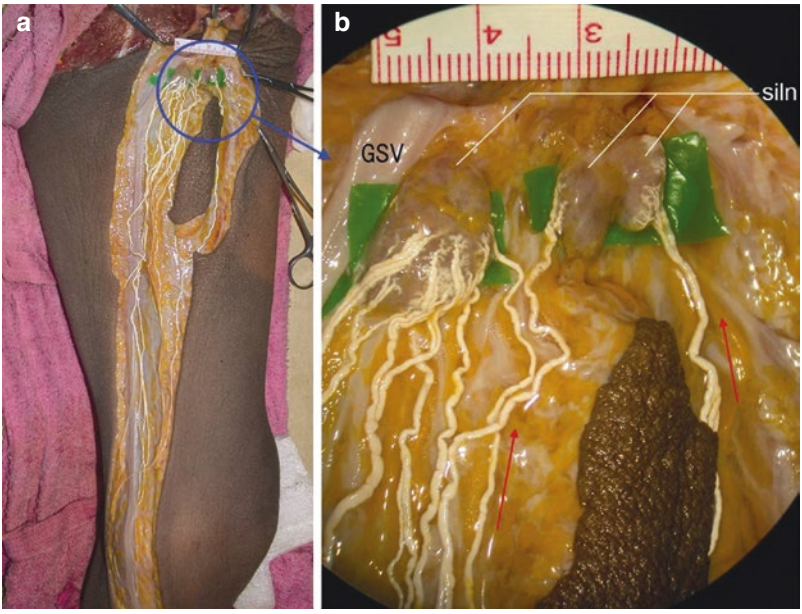

Fig. 3.125 The medial group of lymphatic vessels of the thigh travels around the GSV and drains into the superficial inguinal lymph nodes (*siln*). A magnified image (**b**) captured from the circled area in image (**a**)

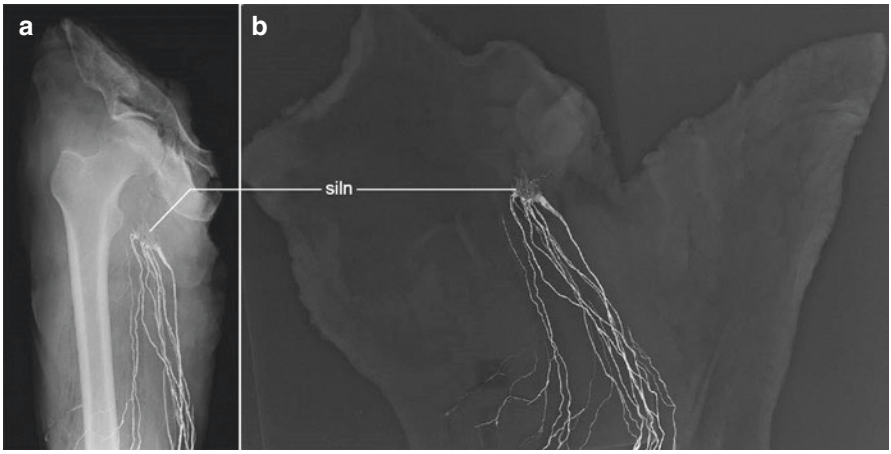

Fig. 3.126 The medial group of lymphatic vessels enters the superficial inguinal lymph nodes (*siln*)

6.7 *Alternative Lymphatic Routes from the Popliteal to Inguinal Lymph Nodes*

After the posterior group of lymph vessels in the popliteal fossa drained into the superficial popliteal lymph node, the efferent vessels ascended to reach the inguinal lymph nodes via three routes.

6.7.1 Superficial Route

Originating from the superficial popliteal lymph node, the efferent lymph vessel ascended obliquely in the subcutaneous tissue to the medial side of the thigh and then turned towards the anteromedial side in the upper part of the thigh to join the medial group of vessels before entering the superficial inguinal lymph node (Fig. 3.127).

6.7.2 Femoral Route

Originating from the superficial popliteal lymph node, internodal lymph vessels drain to the deep popliteal lymph node (Fig. 3.120a yellow vessels), from which the efferent lymph vessel (Figs. 3.103, 3.122 brown vessels and 3.129) coursed with the femoral vascular bundle (Figs. 2.121 and 3.128) before entering the deep inguinal lymph nodes.

6.7.3 Profunda Route

The efferent lymph vessel, from the deep popliteal lymph node, was running on the anterior side of the tibial nerve at the superior margin of the popliteal fossa and then between the sciatic nerve and the profunda femoral vessels and thereafter between the sciatic nerve and the common femoral vessels before entering the external iliac lymph node (Fig. 3.129).

Clinical Implication
Lymphaticovenous anastomosis has been performed for treating secondary lymphoedema in the lower extremities (Weiss et al. 2003; Demirtas et al. 2009; Narushima et al. 2010). Accurate anatomical awareness of the lymphatic distribution in the lower extremity may assist in the preoperative preparation and intraoperative management of these patients, thus affecting the postoperative outcome. It has been mentioned that, in order to obtain the best result, lymphaticovenous anastomosis should be performed as many as possible in each case (Huang et al. 1985). Information in this section provides a roadmap for surgeons when searching for potential lymphaticovenous anastomotic sites in the lower extremity where lymph vessels are situated close to the major veins in the subcutaneous tissue.

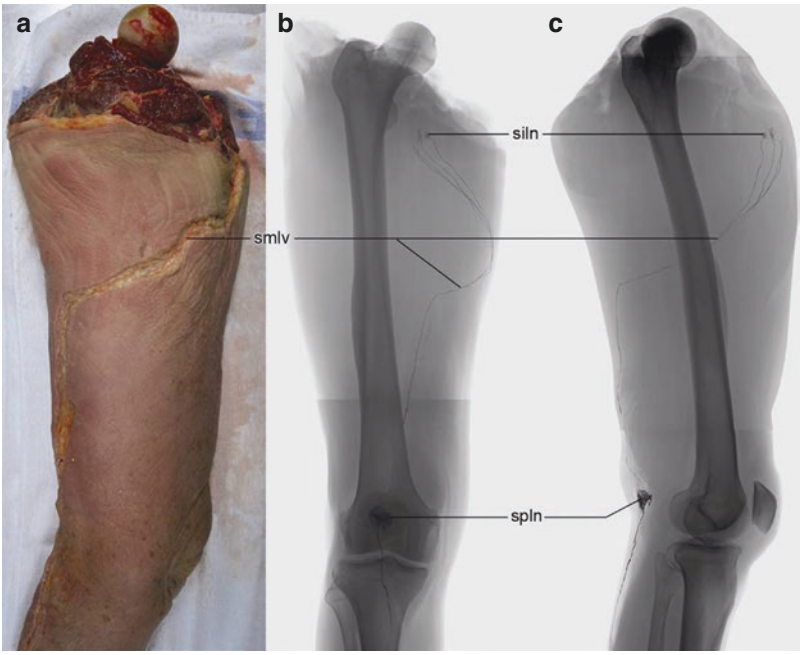

Fig. 3.127 The superficial lymphatic route from the popliteal to the inguinal lymph nodes. *siln*. Superficial inguinal lymph nodes, *smlv*. Superficial medial group of lymph vessels. A photograph (**a**) and radiograph (**c**) of the medial view of the left thigh; (**b**) a posterior-anterior view of radiograph of the left thigh

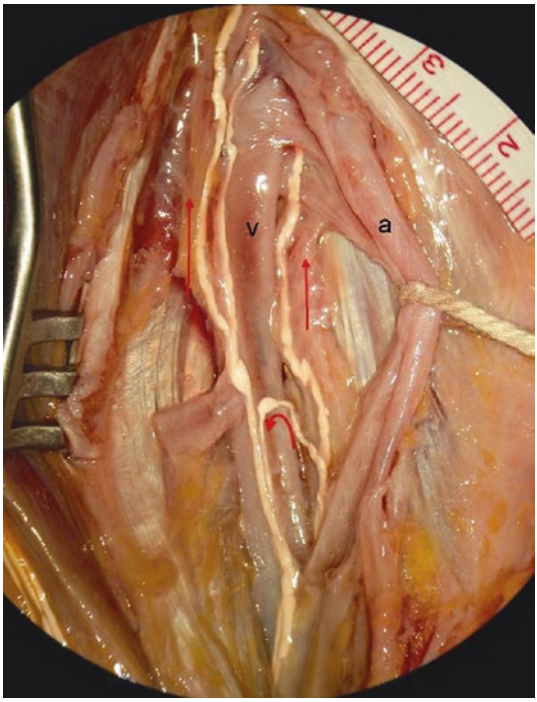

Fig. 3.128 Femoral lymph vessels (filled by a barium sulphate mixture) travelling with the femoral artery (*a*) and vein (*v*)

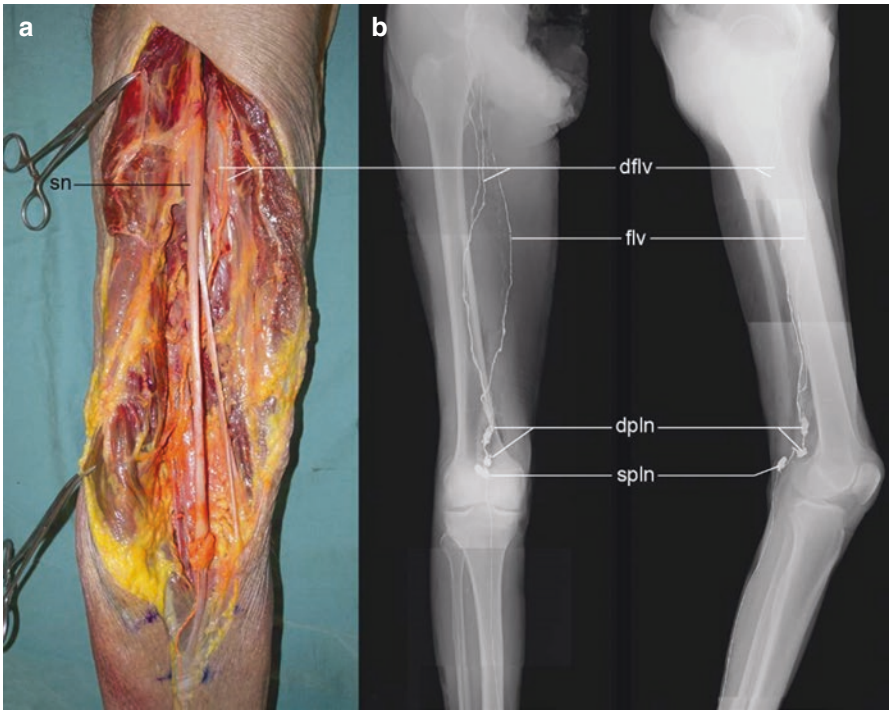

Fig. 3.129 The femoral and deep lymphatic routes in the left thigh. (**a**) A photograph of the posterior view of the left thigh. The deep femoral lymph vessels travel on the anterior side of the tibial and sciatic nerves. (**b**) Posteroanterior and lateral views of the thigh. The femoral and deep lymphatic routes between the popliteal and inguinal lymph nodes. *sn*. Sciatic never. *dflv*. Deep femoral lymph vessels, *flv*. Femoral lymph vessels, *dpli*. Deep popliteal lymph nodes, *splln*. Superficial popliteal lymph node

Chapter 4
Lymphatic Anatomy and Clinical Implications

Anatomical uncertainties of the human lymphatic system are often discordant with clinical experience, especially in the head and neck region. Since a new technique for lymphatic study was established (Suami et al. 2005a), a series of articles related to the lymphatic distribution, morphology and drainage pattern have been published in the last decade. Thus, lymphatic vessels in the head and neck were recorded precisely by radiographs and photographs for the first time since Aselli (1627) discovered the "lymphatic vessels"; the lymphatic capillary plexus has been found and recorded in the galea layer of the scalp for the first time; the lymphatic "ampullae" and "diverticula" structures on the lymph vessels were found and described for the first time; lymph vessels and their drainage directions above the platysma of the anterior neck were found and described (Pan et al. 2008a and b) for the first time. These results have led to a fundamental re-evaluation of the "classic" theory, as the drainage varies from the traditional predictions of Sappey (1874) and others in many cases.

1 Superficial Lymphatic Distribution and Drainage of the Head and Neck

Lymphatic pathways of the head and neck were complex. In the scalp region, a rich avalvular lymph capillary plexus was located, originating from both the dermis and galea, which converged to form precollecting lymph vessels and then drained to the collecting lymph vessels that distributed densely in the subcutaneous tissue. The double structure of the lymph capillaries is a characteristic that may relate to the strong immunity present in the scalp. In the facial and cervical regions, lymph capillaries were found, arising from a single layer of the dermis, linked to precollecting lymph vessels and then drained to the collecting lymph vessels that distributed sparsely in the subcutaneous tissue. The lymphatic drainage patterns of the

W.-R. Pan, *Atlas of Lymphatic Anatomy in the Head, Neck, Chest and Limbs*,
DOI 10.1007/978-981-10-3749-8_4

head and neck were different from person to person and even asymmetrical on each side of the same body (Fig. 4.1). Due to the unpredictable drainage pattern in individuals, it may confuse clinicians during the sentinel lymph node biopsy for treating head and neck cancer patients.

The term "sentinel node" was first described by Braithwaite (1923). Gould et al. (1960) suggested that during routine excision of the "sentinel node", a frozen section assay should be completed before deciding whether or not to perform a radical neck dissection in parotid tumour patients. Morton et al. (1992) introduced an invasive method of intraoperative lymphatic mapping for treating early stage melanoma, which was the first time the concept to localize the sentinel nodes in skin cancer patients was employed. Alex and Kraig (1993) introduced a non-invasive technique by using a handheld gamma probe to localize radiolabelled sentinel lymph nodes for patients with melanoma in the head and neck. Currently techniques of lymphoscintigraphy and sentinel lymph node biopsy have become routine procedures to identify cancer spread and determine the need for lymph node ablation, especially with melanoma and breast cancer surgery.

After analysing nearly 1000 cases with melanomas in the head and neck, Uren et al. (2004) found that results of lymphoscintigraphy were often discordant with clinical predictions based on our "classic" knowledge of the lymphatic system. They found a false negative rate of sentinel node biopsy to be as high as 30%. This figure indicated that the surgeon would fail to remove nodes potentially containing metastatic disease in one of three patients.

Although this book demonstrates static anatomical images rather than in the dynamic physiological state, it updates the anatomical knowledge of the lymphatic system and may help explain the unexpected findings of lymphoscintigraphy (Pan et al. 2008a, b). The following points should always be of concern to surgeons when performing lymphoscintigraphy and were emphasized by Thompson et al. (1999, 2004) and Uren et al. (1999):

1. If an injection is placed at the frontal-parietal junction of the scalp, it might drain to the buccinator lymph node by crossing the forehead, or retroauricular and cervical lymph nodes by crossing the mid-coronal line, or all of them. It has shown that one injection at this site may reach two or more sentinel nodes (Fig. 4.2a).
2. If an injection is placed at the parietal-occipital junction, it might bypass the expected first-tier node (Fig. 4.2).
3. If an injection is placed on the inferior part of the neck, it might drain to the submandibular or submental lymph nodes (Figs. 4.2b and 4.3).

Besides a site where a lymphaticovenous shunt was found in the superficial tissue of the left head and neck in Chap. 2. The efferent lymph vessels of the superficial occipital lymph nodes formed a lymphatic network from which two small lymphatic vessels emerged to drain to a superficial occipital vein in the subcutaneous layer (Fig. 2.122). This confirmed the clinical findings of Wallace et al. (1964). It should be noted that anastomosis may provide a systemic route for metastatic disease.

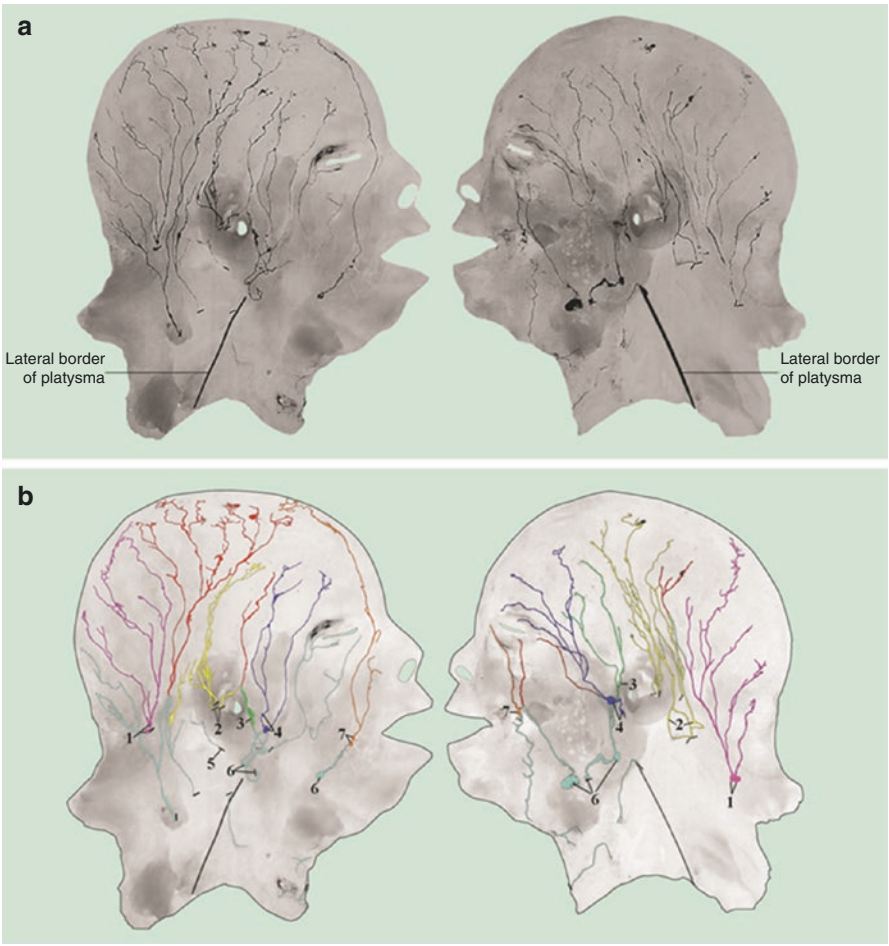

Fig. 4.1 Asymmetrical lymphatic drainage pattern on bilateral sides of the superficial tissue of the head and neck in the same subject. (**a**) Radiographs. (**b**) Lymph vessels have been colour coded to match their perspective first-tier lymph nodes. (*1*) Superficial and deep occipital lymph nodes, (*2*) retroauricular lymph node, (*3*) preauricular lymph nodes, (*4*) parotid lymph nodes, (*5*) infra-auricular lymph nodes (*6*) submandibular lymph nodes, (*7*) buccinator lymph node

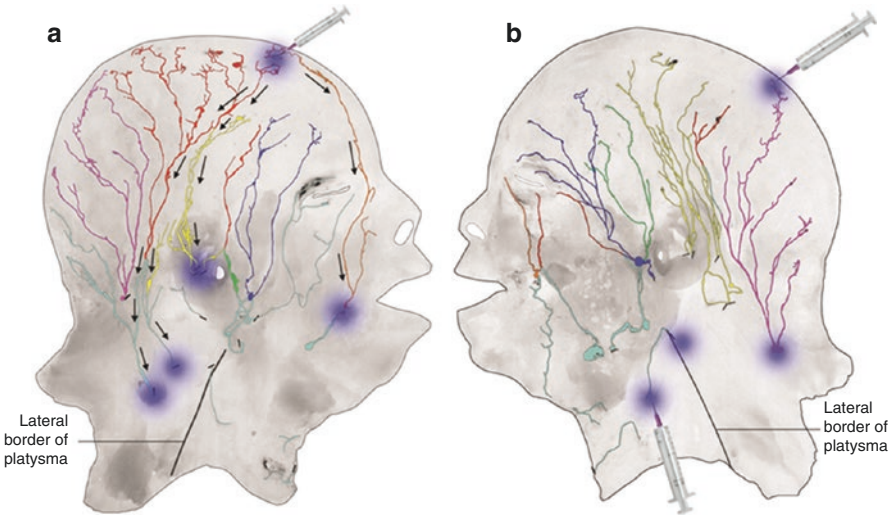

Fig. 4.2 Diagrams showing the various directions the lymphatic pathways travel from different injection sites in the superficial tissue of the scalp. (**a**) The right side. (**b**) The *left side*

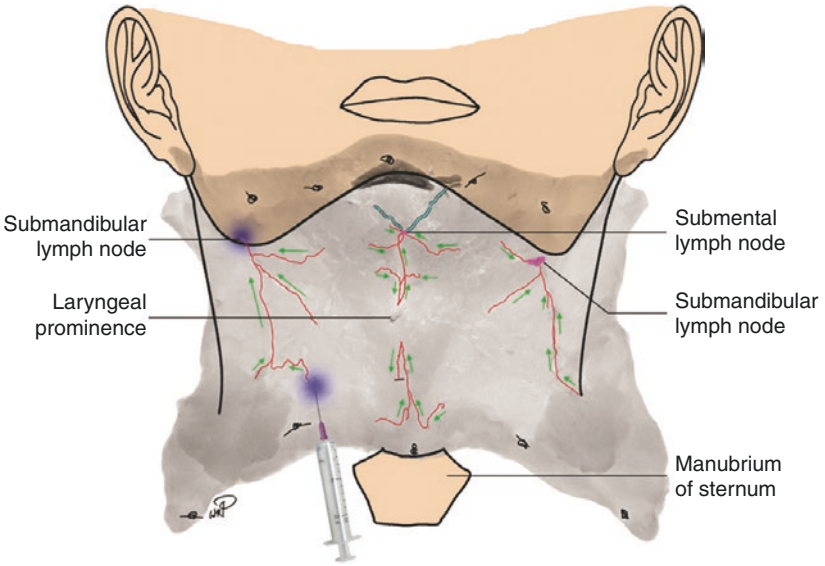

Fig. 4.3 Diagrams showing the direction of the lymphatic pathway from one injection point in the superficial tissue of the suprasternal area in the neck. *Red lines* indicate lymphatic vessels. *Green arrows* indicate the direction of the lymph flow. *Purple dots* indicate lymph nodes

2 Superficial Lymphatic Distribution and Drainage of the Face

The incidence of postoperative prolonged oedema after rhytidectomy procedures is very low, but remains a frustrating complication for the surgeons and patients alike. After Baker et al. (1977) reviewed 1500 cases, they found five cases where the patient suffered from prolonged oedema after rhytidectomy. The correlation between lymphatic drainage and prolonged oedema was not mentioned. Guy et al. (1977) stated that the postoperative persistent oedema associated with rhytidectomy was rare and presumably related to lymph stasis. They did not provide any further discussion due to inadequate details of the lymphatic anatomy in this region. The anatomical details of the lymphatic drainage patterns in the superficial tissue of the head, face and neck have been provided in Chap. 5 of the book. Drainage patterns were different between individuals. Therefore, occasionally lymph vessels gathering in the preauricular area might be cut off by a crossing incision of rhytidectomy and result in the frustrating complication of oedema (Fig. 4.4). Besides, if over-dissecting were performed in the subcutaneous tissue of the facial region, extensive lymph vessels might be damaged and lead to oedema (Figs. 4.1, 4.4 and 4.5). This information may help surgeons avoid damaging lymphatic vessels in the region for preventing the lymphoedema during rhytidectomy.

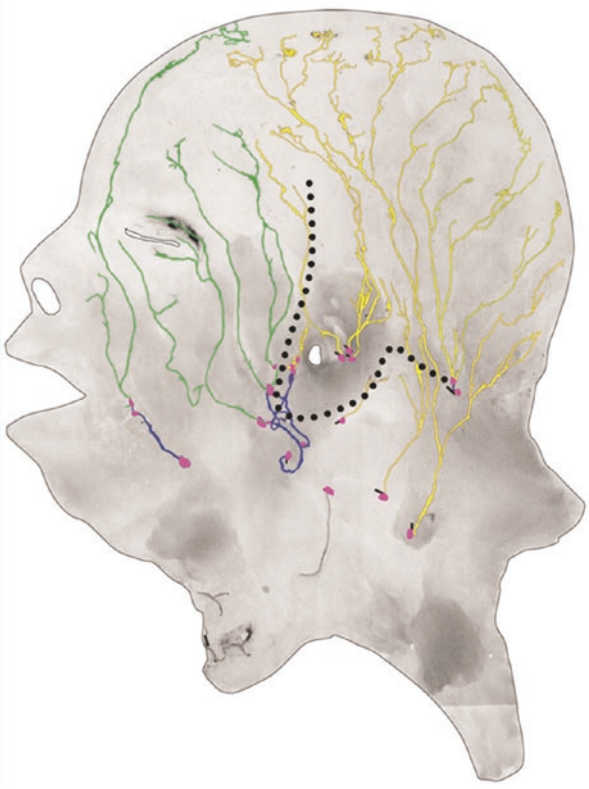

Fig. 4.4 The relationship between the incision (*black dotted line*) of the rhytidectomy and lymphatic vessels (*coloured in green*) in the facial region. Lymphatic vessels in the scalp are coloured in *yellow*, and intermodal vessels are coloured in *blue* and lymph nodes in *purple*

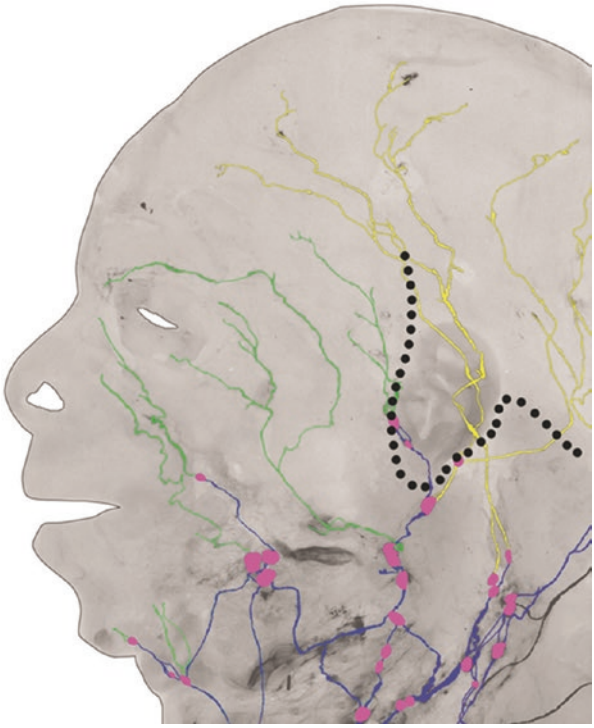

Fig. 4.5 The relationship between the incision (*black dotted line*) of the rhytidectomy and lymphatic vessels (*coloured in green*) in the facial region. Note the lymphatic drainage pattern of the face differ from those in Fig.4.4. Lymphatic vessels in the scalp are coloured in *yellow*, intermodal vessels are coloured in *blue* and lymph nodes in *purple*

3 Lymphatic Distribution and Drainage of Eyelids

The avalvular lymph capillary plexus arose in the upper and lower eyelids where lymph returned via the inner canthus, outer canthus and inferior eyelid lymph vessels (Fig. 4.6 left). If one of those vessels was destroyed or blocked, the others could still perform the function (Fig. 4.6 right). Eyelid oedema is one of the postoperative complications after blepharoplasty. It was believed that if over-dissecting were performed in the subcutaneous tissue of the outer canthal area during surgery, a majority of lymph vessels could be damaged which leads to eyelid oedema (Klapper and Patrinely 2007) (Fig. 4.7). Common oedema might be greatly subsided as the lymph might return via the inner canthus or inferior eyelid lymph vessels (Fig. 4.6 right).

Chronic lymphoedema of the eyelid is an uncommon condition presenting in many cases as a chronic form related to acne rosacea, irradiation and ocular surgery (Chalasani and McNab 2010). However acute eyelid lymphoedema is even rarer. Aveta et al. (2011) reported a case of acute eyelid lymphoedema after a major reconstruction of the medial canthus treating a recurrent basal cell carcinoma in the upper third of the nasal dorsum and the left medial canthus. Extended resection including a wide skin excision (the upper two-thirds of the nasal dorsum, medial third of both eyelids, the glabella and the head of the left eyebrow) was performed. Reconstruction was achieved by using a right forehead flap and a rotational cheek flap with lateral cantholysis and tarsoconjunctival sliding. After 10 days, a severe acute lymphoedema occurred in the left upper eyelid but not in the lower eyelid. It was likely, according to the description given by Pan et al. (2011a and b), that the medial lymphatic pathway was destroyed by the radical excision and the lateral path was interrupted as a consequence of the rotational cheek flap, while the inferior eyelid remained unaffected because of the inferior eyelid lymph vessel (Fig. 4.8).

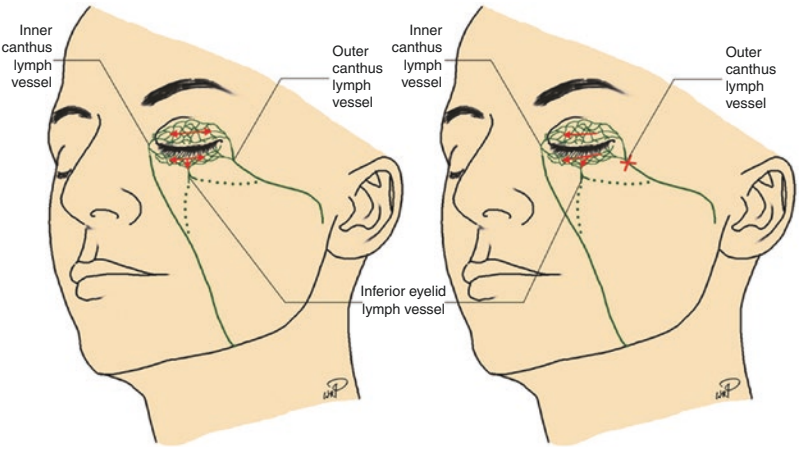

Fig. 4.6 Lymphatic pathways of the eyelids. *Green lines* and *dotted lines* indicate lymph vessels; *red arrows* indicate the direction of the lymph flow; *red cross* indicates the blockage of the lymph vessel

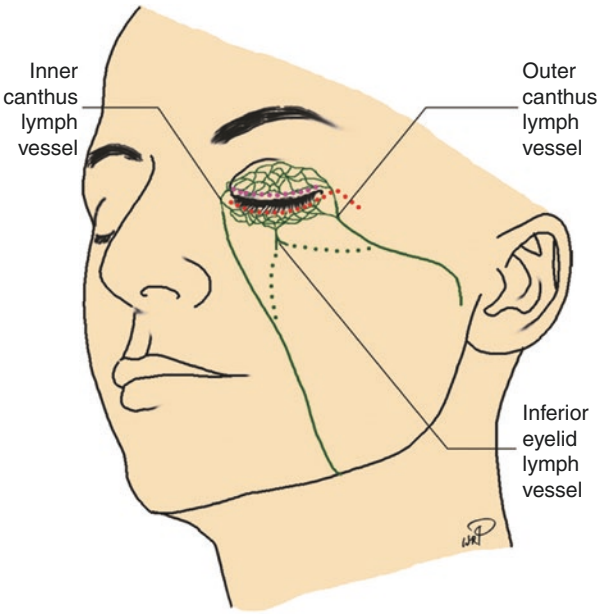

Fig. 4.7 Sketch of incisions (*red* and *purple dotted lines*) of eyelids in blepharoplasty

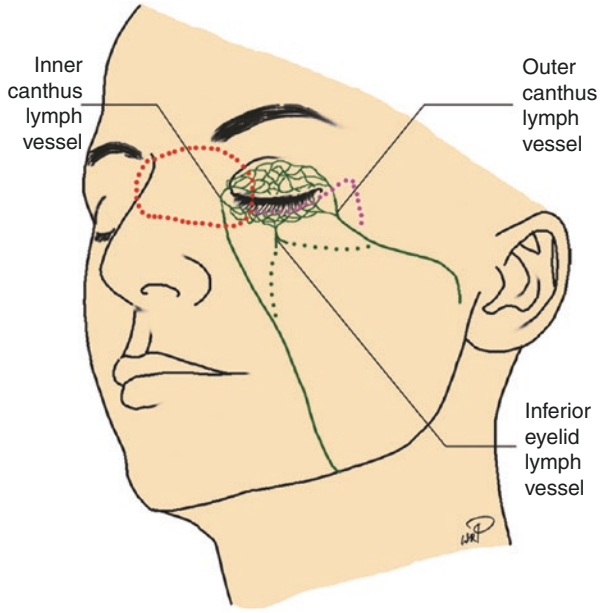

Fig. 4.8 The relationship between eyelid lymph vessels (*green lines* and *dotted lines*) and incisions (*red* and *purple dotted lines*) on a recurrent basal cell carcinoma of the nasal dorsum. Diagram was sketched according to the description of Aveta et al. (2011)

4 Lymphatic Distribution and Drainage of the Auricle

There are several published articles regarding the lymphatic drainage of the ear, but most of them, except Sappey's work (1874) (Fig. 4.9), provide simple sketches rather than actual lymphatic pathways (Figs. 4.10 and 4.11).

Results from Chaps. 2 and 3 of this book have revealed some differences, as shown through photographs and radiographs of actual lymphatic pathways (Figs. 2.55, 2.56, 3.31, 3.32, 3.33, and 3.34). Lymphatic vessels of the auricle were sparse when compared with the rich lymphatic vessels of the auricle seen in Sappey's diagram (Fig. 4.9). This was probably due to (1) the different ages of the cadavers, (2) Sappey used mercury for the injection that could perfuse to the tiny lymphatic capillaries and (3) his drawings might be based on multiple cadaveric studies.

Regarding lymphatic pathways in different regions of the auricle, the conchal branches presented by Sappey correspond well to the anterior branch identified in this book, which both drained to preauricular lymph nodes. Lymphatic vessels of the lobule (inferior) identified by Sappey and in this book also concur well with both draining into infra-auricular lymph nodes (Sappey referred to these as parotid lymph nodes). However, differences were noted in the lymphatic vessels of the superior and middle regions (referred to as helical and antihelical branches by Sappey). In Chap. 4, these vessels are identified to drain to the infra-auricular lymph nodes (Figs. 3.31, 3.32, 3.33, and 3.34) that are consistent with the description by Haagensen et al. (1972) (Fig. 4.8), while Sappey found that these vessels drained to the retroauricular or mastoid lymph nodes (Fig. 4.9).

Based on Rouvière's (1938) anatomical study, the lymphatic drainage area of the auricle can be divided into three principal territories (Fig. 4.10). He described lymphatic vessels in the anteromedial part of the anterior aspect of the auricle draining into the preauricular lymph node, the vessels of the lobule draining into the infra-auricular (parotid) lymph nodes. He stated that the lymph from the superiolateral part of the auricle could drain into either infra-auricular (parotid) or retroauricular lymph nodes. Haagensen et al. (1972) also divided the lymphatic drainage of the auricle into three regions based on their clinical investigation (Fig. 4.11), but they stated that lymph from the superiolateral part of the auricle would mostly drain into the infra-auricular lymph nodes. Based on lymphoscintigraphic studies in vivo, Aydin et al. (2005) divided the lymphatic drainage area of the auricle into two possible territories. The lobule portion was excluded due to a design blemish with the technique, where the target site (infra-auricular node) was always overlapped by the injection site in the lobule.

In Chap. 3 of this book, four lymphatic drainage territories are described based on four lymphatic vessels in the auricle (Figs. 3.31, 3.32, 3.33, and 3.34). It also shows that lymphatic vessels from the upper two-thirds of the anterolateral aspect and upper two-thirds of the posterior aspect drain to the infra-auricular lymph nodes. Sometimes these vessels diverge into two, one drains to the nearest node and one bypassing it to continue its course.

Primary malignant melanoma of the external ear is rare, but the prognosis is poor (Ward and Acquarelli 1967; Byers et al. 1980). Previous studies have reported a 5-year survival rate of >74% after the treatment, while a downtrend of the rate was noticed in patients after 5 years (Cole et al. 1992; Davidsson et al. 1993; Ravin et al. 2006). It was mentioned that the prognosis directly correlates to the thickness, stage and topography of melanoma (Mondin et al. 2005). While others hold a different view, it was discussed whether the location of melanoma on the auricle would significantly affect survival rates (Byers et al. 1980; Ravin et al. 2006). Variable relationship between the primary site of the auricular melanoma and the sentinel node has been revealed through lymphoscintigraphic studies that used mapping the sentinel lymph node in the treatment (Morton et al. 1992; Uren et al. 1999; Thompson et al. 2004). Thompson et al. (1999) reported a case that the lymphatic drainage from the tragus passed directly to a submental node but also to the ipsilateral upper cervical chain. Cole et al. (2003) stated the proportional location of auricular melanomas as the helix (47%), lobule (21%), ear-scalp junction (10.5%), posterior ear (10.5%), concha (5%) and tragus (5%). They found 24 sentinel lymph nodes in 19 patients. The sentinel lymph nodes were summarized as level II cervical lymph nodes ($n = 10$), mastoid ($n = 1$), parotid ($n = 6$), lower jugular chain ($n = 2$), supraclavicular ($n = 1$) and nonspecified neck ($n = 4$). It was concluded that the lymphatic drainage of the auricle was variable and unpredictable.

Shown in Fig. 4.12, the lymphatic vessels from the auricular apex drain to either the infra-auricular or sternocleidomastoid lymph nodes. While vessels from the lateral middle part of the auricle drain to infra-auricular lymph node or bypass the node and may drain into a distant node, which explains some anomalies seen in lymphoscintigraphy and update the knowledge of the lymphatic anatomy in the auricle for performing sentinel node biopsy in the treatment of melanoma.

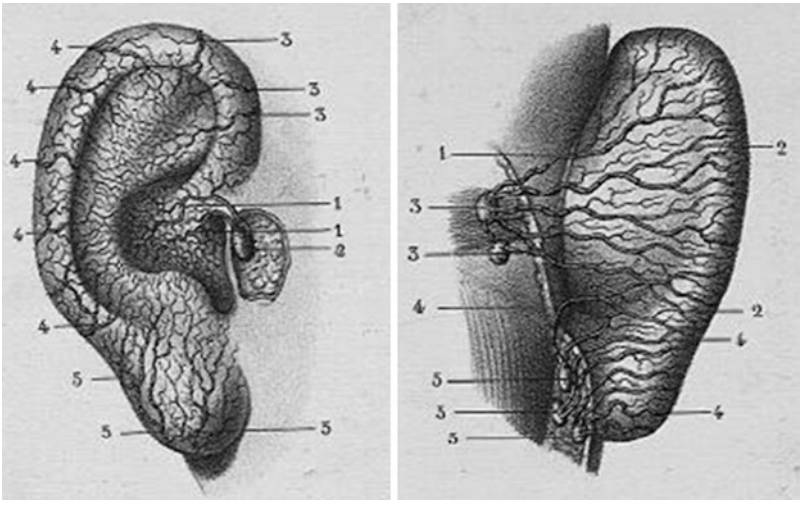

Fig. 4.9 Sappey's drawings of the lymphatic drainage in the anterior (*left*) and posterior (*right*) aspects of the auricle (Source: http://web2.bium.univparis5.fr/livanc/?cote=01562&do=chapitre)

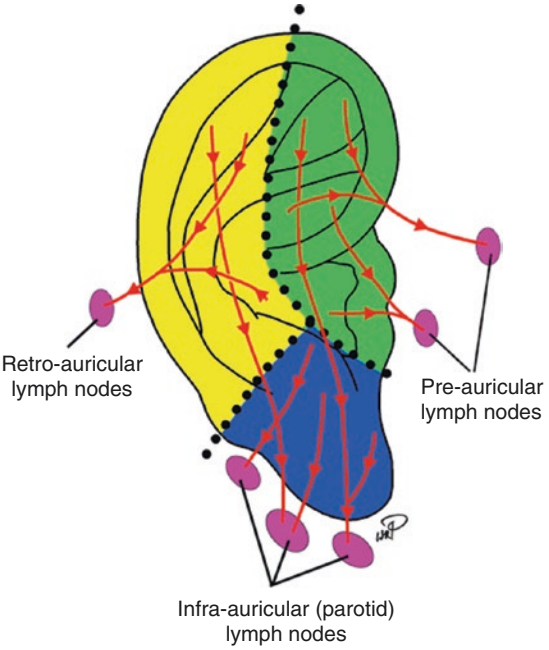

Fig. 4.10 A redrawing of Rouvière's (1938) result showing the lymphatic pathways of the auricle

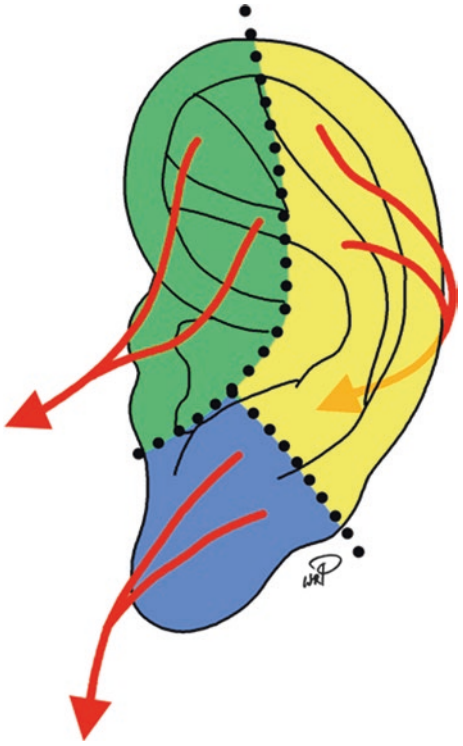

Fig. 4.11 A redrawing of Haagensen et al.'s result (1972) showing the lymphatic pathways of the auricle

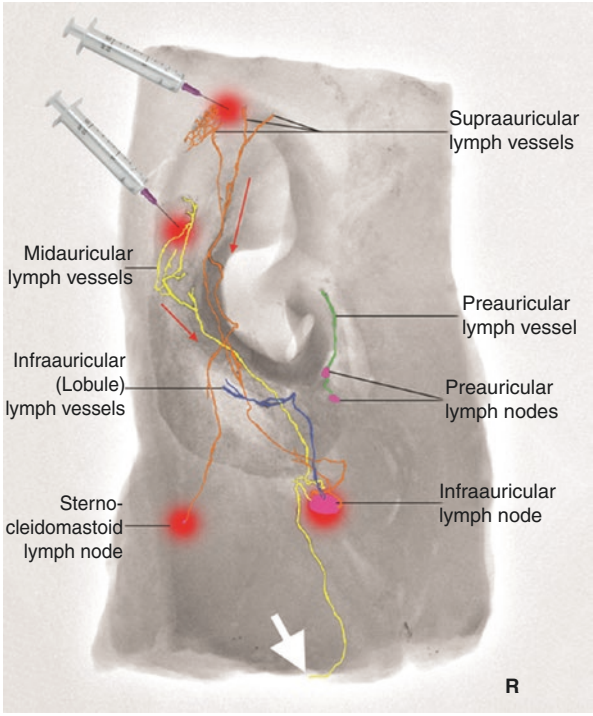

Fig. 4.12 Diagram showing directions of the lymphatic pathways from injection sites in the auricle. Each group of lymph vessels are coloured differently: *green*, preauricular vessel; *orange*, supraauricular vessels; *yellow*, midauricular vessels; *blue*, infra-auricular (lobule) vessels. *Red arrows* indicate the direction of the lymph flow. A *white arrow* indicates that a branch of the midauricular lymph vessel bypasses the infra-auricular node and continues its course to the edge of the specimen in the cervical area

5 Lymphatic Distribution and Drainage of the Nose, Pharynx, Larynx and Soft Palate

Knowledge regarding the lymphatic anatomy of the nasal fossae, nasopharynx, soft palate and oropharynx from previous studies are still vague.

Sappey's (1874) original diagrams have shown an abundant lymphatic network on the wall of the nasal fossae and the nasopharynx (Figs. 4.13 and 4.14). The radiographic and photographic images in previous chapters of this book have presented the lymphatic pathways of this region in detail, from the lymphatic capillaries to the precollecting vessels and from collecting vessels to lymph nodes (Figs. 2.57, 2.58, 2.59, 2.60, 2.61, 2.62, 2.75, 2.76, 2.100, 3.36, 3.37, 3.38, 3.39, 3.40, 3.41, 3.42, 3.43, 3.44, 3.45, and 3.46).

Based on Sappey's work, Delamère and Cunéo (1913) also described the lymphatic drainage in this area. They reported that the *collecting trunks* network of the nasal fossae formed *anterior and posterior* groups. According to their description, it is assumed that their *anterior* trunks were equivalent to the precollecting lymph vessels arising from three turbinates that are presented in Figs. 2.57, 2.58, 2.100, 3.36, 3.38, 3.39, 3.40, and 3.41. The basis for this assumption is (1) they are situated in the mucous membrane; (2) there are no valves between these vessels and lymphatic capillaries where the injectant can flow back to; and (3) they are connected to both lymphatic capillaries in the mucosa and collecting lymph vessels in the paranasopharyngeal fat tissue. The *posterior* trunks described by Delamere and Cunéo were that collecting lymph vessels were actually situated in the paranasopharyngeal fat tissue.

The retropharyngeal lymph nodes were first discovered by Rouvière (1938), also named as Rouvière nodes, and discussed in previous studies (Delamère et al. 1913; Ballantyne et al. 1964; Watanabe et al. 1985; Batsakis et al. 1989; Hasegawa et al. 1994; Okumura et al. 1998; Saito et al. 2002; Földi et al. 2003; Standring 2005). However, in these reports the anatomical lymphatic pathways in this area were not seen. Images in Chap. 5 have shown the entire lymphatic pathway, from lymphatic capillaries in the nasal fossa to the retropharyngeal and lateral pharyngeal lymph nodes in the parapharyngeal space. There are two major groups of collecting lymph vessels. One is running along the outside of the lateral pharyngeal wall and the other one more posteriorly. The collecting lymph vessel on the lateral side of the wall divides several times and then crosses over the external carotid artery medially and the internal carotid artery laterally, before finally reaching multiple first-tier nodes: the lateral pharyngeal node, the subdigastric node and the third and fifth nodes of the retropharyngeal group (Figs. 3.40 and 3.41). Therefore, the third- and fifth-tier nodes of the retropharyngeal group could be multiple first-tier nodes for the lateral pharyngeal lymphatic vessels. These findings may guide clinical management of cancer treatment in this region.

Primary malignant melanoma in the mucosa of the nasal cavity is rare, but the prognosis is poor, despite the advances in radical neck surgery, postoperative radiotherapy and chemotherapy (Bhattacharyya 2002; Martin et al. 2004; Huang et al.

2007). Local recurrence may have an anatomical base. The abundance of avalvular lymph capillaries on the wall of the nasal fossa and the nasopharynx reaches *multiple* first-tier lymph nodes by passing three precollecting lymph vessels and two groups of collecting vessels. Meanwhile, there are numerous bypassing connections between nodes and pathways permitting cells to take alternative pathways particularly if the main path is blocked. In Fig. 4.15, if an injection is inserted in any of the three nasal turbinates, the lymphatic drainage could reach multiple lymph nodes in the parapharyngeal space.

According to *neck dissection classification* (Robbins et al. 2002), the lateral pharyngeal lymph nodes were included in the level II group, but the retropharyngeal nodes were excluded. This result suggests that for the treatment of patients with cancer in the nasal fossae or nasopharynx, multiple lymph nodes should be included.

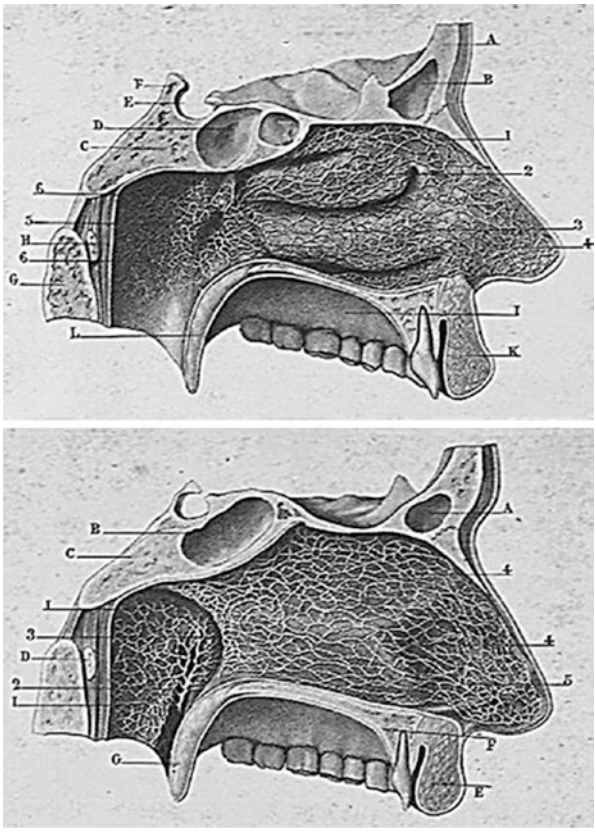

Fig. 4.13 Sappey's drawings of the lymphatic capillary network in the nasal fossae and nasopharynx (Source: http://web2.bium.univparis5.fr/livanc/?cote=01562&do=chapitre)

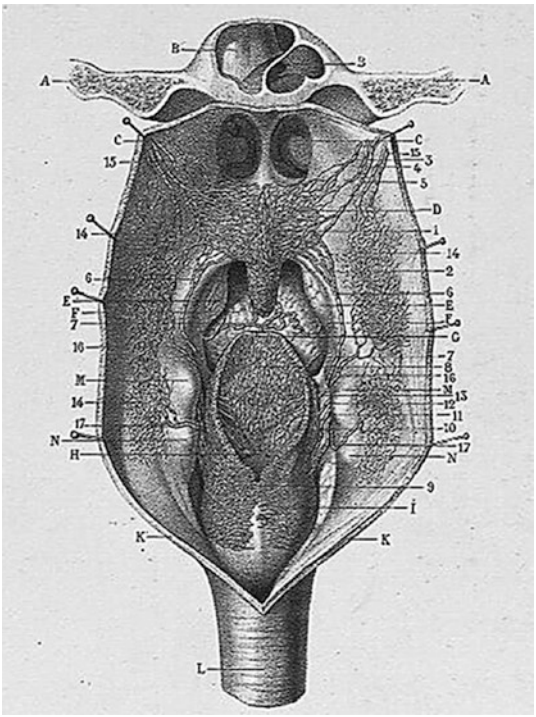

Fig. 4.14 Sappey's drawings of the lymphatic capillary network in the nasal, pharyngeal and laryngeal cavities and soft palate (Source: http://web2.bium.univparis5.fr/livanc/?cote=01562&do=chapitre)

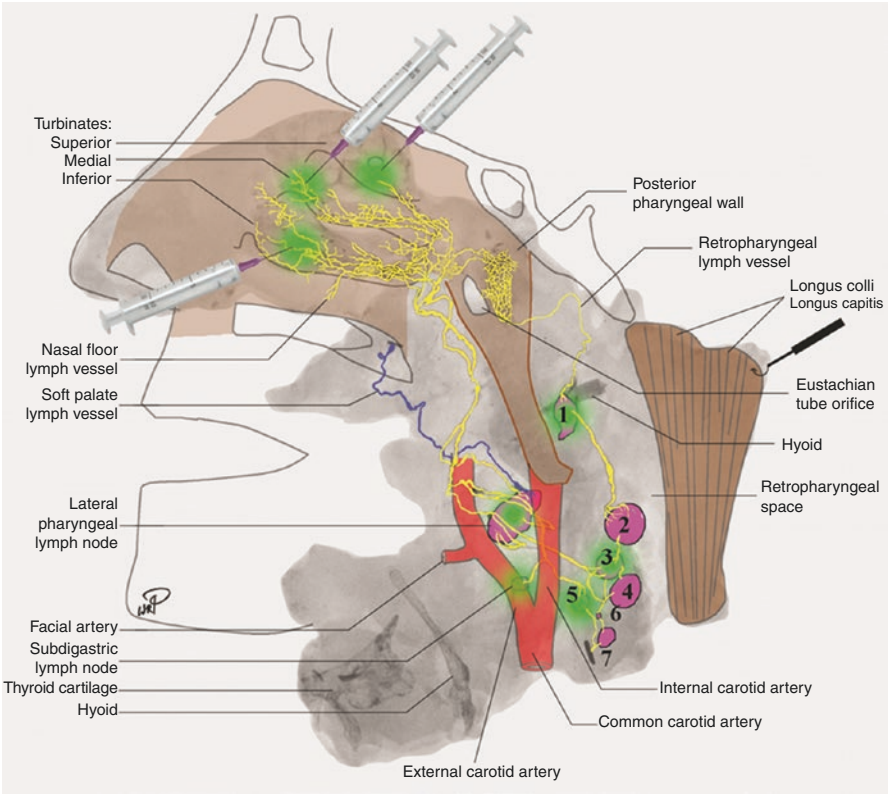

Fig. 4.15 Lymphatic pathways (*yellow vessels*) from lymphatic capillaries in the nasal fossa to the retropharyngeal and lateral pharyngeal lymph nodes (*purple*) in the parapharyngeal space. *Green dots* indicate injection sites and their multiple first-tier nodes

6 Lymphatic Distribution and Drainage of the Tongue

The lymphatic anatomy of the tongue has been widely studied (Sappey 1874; Jamieson and Dobson 1920; Rouvière 1938; Haagensen et al. 1972; Moore 1992; Standring 2005). Most reports, except Sappey's original drawings, which are based on results using a mercury injection, have only provided text and sketches rather than accurate radiographs and photographs.

The lymphatic distribution and pathways of the tongue have been presented as radiographs and photographs in Chaps. 2 and 3 of the book (Figs. 2.20, 2.74, 3.47, 3.48, 3.49, 3.50, 3.51, and 3.52). The difference between results of sparse lingual vessels in the book and drawings with numerous lymphatic vessels seen in Sappey's work (Fig. 4.16) is probably due to (1) the different ages of cadavers, (2) mercury was used for injections which are able to fill more tiny lymph vessels and (3) Sappey's drawings might be based on multiple results from different cadavers. In his book, a rich lymphatic network was shown on the dorsal tongue and the lymph-collecting vessels on the inferior aspect of the tongue mostly drained to the upper internal jugular lymph nodes. He did not include the submandibular lymph nodes in his diagrams.

The lymphatic drainage of the tongue involving the contralateral lymph node was reported by Jamieson and Dobson (1920) after analysing 268 clinical cases. The report was based on the clinical results, but did not include any anatomical study.

Rouvière (1938) has mentioned lymph vessels crossing the midline in his book: "*the lymph from one side of the tongue may be drained by nodes of the opposite side via four routes: (1) By the intermediation of the mucous network which covers without interruption the entire extent of the lingual surface; (2) By the apical collecting trunks, which, may cross the median line and terminate in a node of the opposite side; (3) By the median basal vessels which quite often bifurcate in such manner as to divert their contents into the nodes of both sides: (4) By the central collecting trunks which occasionally pierce the interstice between the geniohyoglossus and geniohyoid muscles of the opposite side*". He also found, only in some newborn and young cadavers, that one of the apical lymph vessels might drain into the submental lymph node on one side or the other. He also pointed out that this vessel was hard to find in adult cadavers. While images in this book were based on cadaveric studies in the elderly, the midline crossing of the apical lymph vessel can be still observed (Figs. 3.47 and 3.50).

Haagensen et al. (1972) conducted a clinical study of 138 patients with carcinoma of the tongue and summarized that (1) the tip of the tongue drained into the submental and internal jugular node chains, (2) the middle of the tongue drained into the internal jugular chain from the level of the omohyoid muscle to the posterior belly of the digastric muscle and (3) the base of the tongue drained to the upper internal jugular chain. They confirmed that carcinoma of the tongue could spread to the contralateral lymph nodes in the anterior, middle or posterior parts of the tongue.

The tongue is a common site of primary squamous cell carcinoma (SCC) in the oral cavity. Successful treatment of SCC is based largely on a thorough knowledge of the lymphatic anatomy. Clinical information has been utilized to map the lymphatic drainage of the tongue for guiding neck dissection with glossectomy (Droulias and Whitehurst 1976; Ozeki et al. 1985; Werner et al. 2003; De Cicco et al. 2006; Wang et al. 2007). Neck dissection classification is the key for the procedure (Robbins et al. 2002), but only provides the anatomical location of the cervical lymph node levels (areas). Recently, lymphoscintigraphy has been used for locating the sentinel lymph node; it minimizes the extent of the operation and reduces surgically related morbidity through the selection of neck nodes that are potentially at risk of harbouring cancer (Thompson et al. 2004).

Radiologic and photographic images in this book have revealed in detail three groups of the lingual lymph vessels. The outcome of these new observations expanded the traditional predictions of Sappey (1874) and many others (Rouvière 1938, Jamieson and Dobson 1920, Haagensen et al. 1972) and will be a guide for clinicians with cancer management.

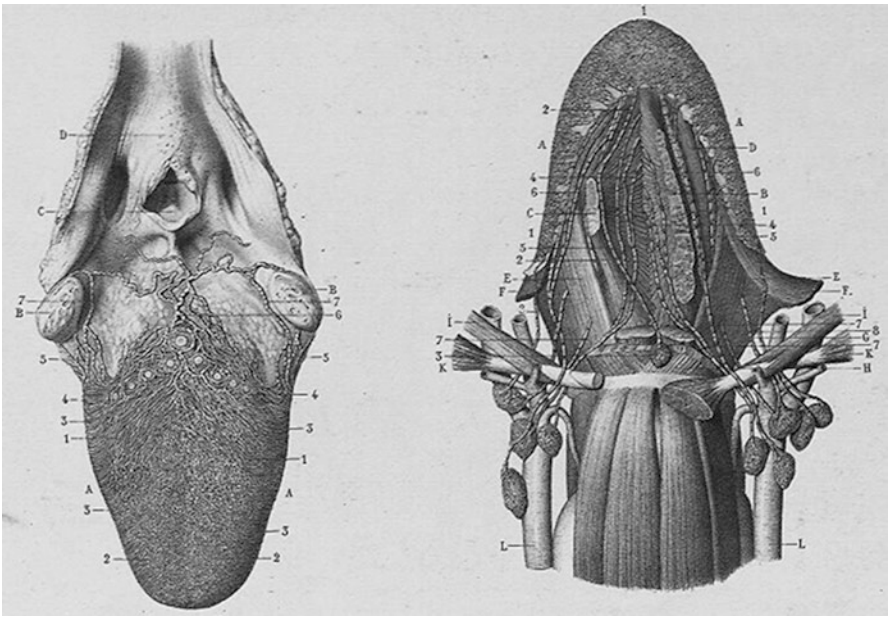

Fig. 4.16 Sappey's drawings of the lymphatic distribution and drainage of the tongue (Source: http://web2.bium.univ-paris5.fr/livanc/?cote=01562&do=chapitre)

7 Lymphatic Distribution and Drainage of the Anterior Chest

It is very important to understand the entire lymphatic anatomy of the anterior torso, especially the lymphatic drainage of the female breast for the management of breast cancer. The earliest description regarding the lymphatics of the breast and the chest was reported by Cruikshank (1786) in his book, whose techniques comprised of injecting mercury through the nipple. Cooper (1840) described in detail lymphatic routes from the nipple and breast tissue to the axilla and lymphatic ducts by using the mercury injection method with female cadavers in pregnancy and lactation. Using the same technique, Sappey (1874) revealed the lymphatic distribution of the breast and chest wall and pointed out that the lymphatic vessels from female breast directly drained to the axilla on the same side. Delamère et al. (1913) produced a composite diagram displaying the lymphatics of the breast after reviewing and combining previous anatomical and clinical findings. Their illustration is still referred to in anatomical and clinical textbooks. Bartel (1909), using an ink injection, in his results presented that the lymphatic vessels arose from the breast and the anterior upper torso and drained into different lymph nodes in the axilla. But his results were deficient on the details concerning the adult female breast due to the fact that the cadavers he used were of fetuses and young children.

A recent study by Suami et al. (2008) revealed the lymphatic drainage of one breast by using radiographic injection techniques. It demonstrated the lymphatic anatomy in significantly greater detail than previous works. However, due to the limitations of tissue putrefaction, the study was unable to present the anatomy of the contralateral side. In Chap. 3 an analysis of the lymphatic anatomy of a bilateral breast and anterior torso specimen by using new preservation techniques was reported. Meanwhile, a series of cross-sections and CT scans have enabled us to complete three-dimensional images of the lymphatic anatomy. The final results emphasize the preferential superficial drainage patterns of the lymphatics and the asymmetrical lymphatic drainage patterns in breasts (Pan et al. 2009a, b).

Developments in the concept of the sentinel lymph node biopsy are now widely applied for the treatment of patients with breast cancer, especially in the early stages (Uren et al. 1999; Thompson et al. 2004). The information provided from this book is pertinent for breast cancer research and clinical applications (Fig. 4.17). The outcome highlights several key points regarding the utilization of sentinel lymph node mapping and biopsy: (1) patterns of lymphatic drainage vary between sides and thus require an individualized approach to each breast; (2) intraparenchymal lymphatics course superficially and thus are amenable to surgical approaches; and (3) lymphatics coalesce at the nipple; however, many lymphatics bypass the nipple, and thus a periareolar injection rather than peritumoral injection of nuclear tracer or dye may not map the appropriate lymphatics and nodes.

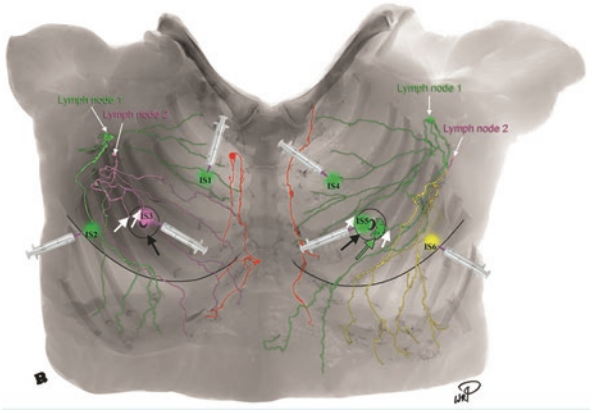

Fig. 4.17 Note the asymmetrical lymphatic pattern of the anterior upper torso, with the lymphatics of each breast highlighted. *White arrows* indicate two collecting lymph vessels arising from each side of the nipple-areola complex. The *green arrow* indicates the lymphatic plexus in the periareolar region. *Black arrows* indicate the nipple-areola complex. *Green highlights* lymphatic vessels draining to lymph node 1; *purple highlights* lymphatic vessels draining to lymph node 2; *yellow highlights* lymphatic vessels draining to both lymph nodes 1 and 2; *red highlights* the internal mammary lymphatic system. Right region: if nuclear tracer or dye was injected into injection site 1 (*IS1*) or 2 (*IS2*) (supposed tumour site), lymph node 1 will be detected. Lymph node 2 will be detected if injecting into *IS3* (periareolar injection site). On the left side, injection into either *IS4* (supposed tumour site) or *IS5* (periareolar injection site) will drain to lymph node 1, from the *IS6* (supposed tumour site) to both lymph nodes 1 and 2

8 Lymphatic Distribution and Drainage of the Upper Extremity

Numerous previous studies have revealed the lymphatic anatomy of the upper extremity, but some details, such as the number and size of lymph vessels in each section, the site easiest to locate and is most suitable for lymphaticovenous anastomosis and so on, still needed to be discovered. In the preceding chapters of this book, an accurate lymphatic map in the superficial tissue of the upper extremity has been revealed quantitatively and morphologically assisting clinicians to predict cancer spread and plan operative procedures to relieve lymphatic obstruction.

Secondary lymphoedema of the upper extremity is one of the complications after breast cancer surgery. It is an unsolved iatrogenic complication with a progressive pathologic condition, in which there is interstitial accumulation of protein-rich lymphatic fluid, recurrent cellulitis, adipose tissue hypertrophy and fibrosis resulting in an increase of volume and chronic oedema in the affected region. Reports have shown that an average of 20% (ranging from 9 to 41%) breast cancer patients developed secondary lymphoedema in the upper extremity after surgery with axillary clearances (Mazeron et al. 1985; Suami and Chang 2010; Kambhampati and Rockson 2015), and 7% (0–23%) of them developed secondary lymphoedema in the upper extremity with sentinel node dissection (Fleissig et al. 2006; langer et al. 2007; Lucci et al. 2007).

Several surgical procedures have been designed for reducing the oedema of the affected extremity. In the early twentieth century, Sir Gillies (1935) performed a replacement transplantation using a long strip of pedicled skin flap from the medial aspect of the upper extremity and the same sized flap from the ipsilateral abdominal-thigh region when treating a patient with lymphoedema in the lower extremity. The flap of the upper extremity contained rich lymph vessels that connected the obstructed lymphatics in the groin and normal lymphatics in the abdomen, thus diverting the lymph flow to the axilla via the chest (Fig. 4.18). In recent years, Lin et al. (2009) transferred a vascularized groin lymph node flap to the wrist to relieve the lymphoedema in the upper extremity of a postmastectomy patient. Also, a free or pedicled lymph "wick" flap transfer was suggested for treating obstructive lymphoedema by bridging the site of the obstruction to divert the lymph flow (Suami et al. 2005a, b; Taylor and Pan 2014) (Fig. 4.19).

Lymphovenous anastomosis is one of the existing options for treating secondary lymphoedema in surgery (O'Brien et al. 1990). Detailed lymphatic awareness of the upper extremity may help in locating the collecting lymph vessels for the proposed procedure. It was suggested that multiple lymphovenous anastomoses should be performed rather than a single one in order to obtain better results in each case (Huang et al. 1985). Information from previous chapters provided the details of the lymphatic pathways in the upper extremity and is summarized as follows:

1. Collecting lymph vessels are dense in the dorsal hand, forearm and medial side of the upper arm surrounding the basilic and cephalic veins with their accessories except the cephalic vein in the upper arm (Figs. 3.80, 3.81, 3.82, 3.83, 3.84, 3.85. 3.86, 3.87, 3.88, 3.89, 3.91, 3.92, 3.93, 3.94, 3.95, 3.96, 3.97, 3.98, 3.99, and 3.100).
2. The largest vessels are located in the medial aspect of the upper arm (Fig. 4.20).
3. The characteristics of different sizes of lymph vessels have been presented that may help the performer find them in the site.
4. The larger vessels have stronger walls than the smaller ones according to the author's dissecting experience that may be conducive to suture.

Replantation is one of the surgical treatments after a finger amputation injury. A variety of factors can influence the survival rate after surgery. The patency of the digital artery and vein is an important factor for the preservation of the replanted finger (Morrison et al. 1977; Cheng et al. 1997; Yang et al. 2003; Morrison and McCombe 2007; Sebastin and Chung 2011). General clinical indicators, such as examination of the skin tone and temperature, tension of the replanted finger, capillary refill test and so on, are able to judge the vascular patency (Yang et al. 2003). It has been proposed (Cheng et al. 1997) that the skin of the replanted finger occasionally turned to a wax-whitish colour with constant tension in the postoperative period, while the outflow of the fresh red blood was observed from a small dermic incision cutting on the side of the replanted finger, which indicated that the vascular patency and the blood supply were satisfactory. It was believed that the appearance of the phenomenon was mainly due to ischemia of the severed finger, as some of the cells had begun to denature so that capillary permeability increased. Once the blood flow re-perfused, cell (tissue) oedema occurred, peripheral circulatory obstructed and finally oedema in the replanted finger took place. However, we believe that this phenomenon should be regarded as lymphoedema. The reason is that the lymph vessels in the digit were unable to anastomose in the surgery. The lymph (cellular waste) was unable to be removed and remained in the tissue.

The establishment of the thumb or finger reconstruction with the microsurgical technique has brought benefit to those patients (Cheng et al. 1997; Hou et al. 2005; Buncke et al. 2007), while the development of the techniques using tissue engineering and 3D organ (tissue) bioprint (Mironov et al. 2003; Lovett et al. 2009) will provide further benefit to these patients. If the defective thumb or fingers could be printed using the 3D bioprint method according to special needs of each individual patient, it will exempt the surgical trauma caused to the toe. It is assumed that blood vessels should be included as well as the lymph vessels in order to avoid the occurrence of lymphoedema when using this technique.

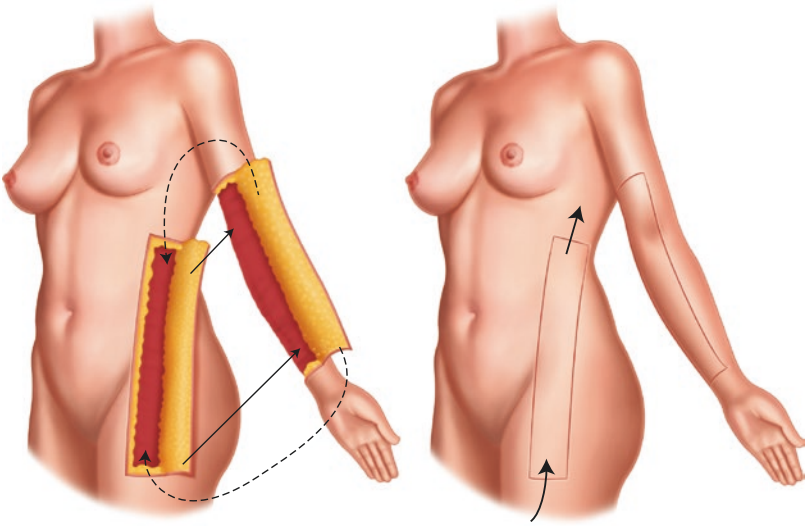

Fig. 4.18 Drawings of Gillies operation

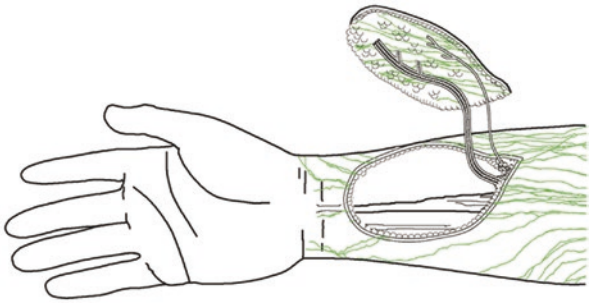

Fig. 4.19 Sketches of potential radial forearm lymphatic flap

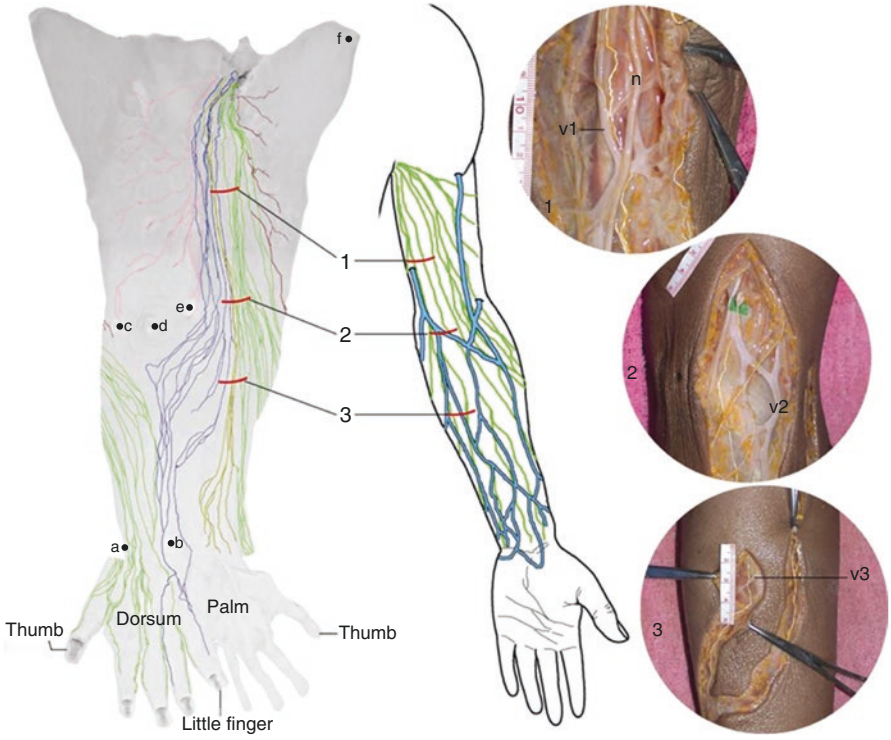

Fig. 4.20 The relationship of the superficial lymphatic vessels and veins in the upper extremity for selecting the possible site of lymphovenous anastomosis. (*a*) Styloid process of the radius; (*b*) styloid process of the ulna; (*c*) lateral epicondyle of the humerus; (*d*) olecranon; (*e*) medial epicondyle of the humerus; (*f*) acromion of the scapula; (*n*) medial cutaneous nerve; (*v1*) basilic vein; (*v2*) median cubital vein; (*v3*) tributary of the basilic vein

9 Lymphatic Distribution and Drainage of the Lower Extremity

In early 1874, Sappey described two lymphatic trunks within the posterior leg that accompanied the small saphenous vein and terminated in the popliteal lymph nodes. In the twentieth century, similar results were reported by Bartel (1909) and Rouvière (1938) based on cadaveric studies of children and/or adults by using Gerota's method (Gerota 1896). But they did not describe the course of these vessels beyond the popliteal lymph nodes. With the development of imaging technology, single or partial groups of lymphatic vessels of the lower limb were also found and reported by using dye injection, lymphangiography and clinical techniques in vivo (Málek et al. 1959; Haagensen et al. 1972; Viamonte and Rüttimann 1980). However, this knowledge does not explain some of the unexpected findings of lymphoscintigraphy seen clinically (Uren et al. 1999; Thompson et al. 2004; Reynolds et al. 2007). Recent studies (Pan et al. 2010a, b and c, 2011a and b, 2013) have shown, through radiograph photographs, the entire lymphatic drainage pattern of the superficial tissues in the lower extremity, the individual variation of lymphatic distribution, the nutrient blood vessels in the lymphatic wall and lymphatic pathways accompanying the small saphenous vein.

The lymphatic distribution of the lower extremity is complex (Figs. 3.102 and 3.103). Most lymphatic vessels drained into their first-tier lymph nodes in the groin (superficial inguinal lymph nodes). In contrast, there were one or two lymph-collecting vessels arising from the lateral side of the Achilles tendon in the subcutaneous tissue above the heel that travelled with the small saphenous vein. These vessels drained through superficial and deep popliteal lymph nodes (Figs. 3.111, 3.113, 3.114, 3.115, 3.116, and 3.117), femoral lymph vessels and nodes (Figs. 3.122 and 3.127) before finally entering the deep inguinal lymph nodes (Figs. 3.122 and 4.21).

The depth of lymph vessels depends on the thickness of the surrounding subcutaneous tissue. Lymph vessels ran within a very thin layer of tissue on the dorsal foot, whereas a great number of collecting lymph vessels were packed within the entire layer of tissue in the groin. It has been reported (Kubik and Manestar 1995) that lymph vessels of the thigh formed three layers: the first layer located immediately below the surface of the subcutaneous fat, the second layer situated between the first and third layers and the third layer lay on the deep fascia. But it has been found (Pan et al. 2013) that the lymph vessels were distributed in close association with the great and small saphenous vein, travelling tortuously in different depths of the subcutaneous tissue.

Lymphatic pathways from the lateral heel to the popliteal fossa, passing through the subcutaneous tissue in the calf region, are constant. There are three lymphatic pathways from the popliteal fossa to the groin area: (1) via the superficial tissue on the medial side of the thigh (Fig. 3.129), (2) travelling with the femoral blood vessels (Figs. 3.103a, 3.122a, and 3.127) and (3) travelling between the sciatic nerve and the profunda femoral vessels (Fig. 3.128). In addition to three routes, other pathways have been described by Viamonte and Rüttimann (1980): the deep lymphatic vessels accompanying the obturator artery drained into the internal iliac

lymph node; vessels accompanying the sciatic nerve drained into the inferior gluteal lymph node. These findings may help to explain those patients who have not suffered from lymphoedema after lymph clearance in the groin. But on the other hand, it could be an alternative lymph pathway for cancer metastases in those patients.

Lymphaticovenous anastomoses have been performed to treat secondary lymphoedema in the lower extremities (Gloviczki et al. 1988; O'Brien et al. 1990; Koshima et al. 2003; Demirtas et al. 2009). Accurate anatomical understanding of the lymphatic routes involved may assist in the preoperative preparation and intraoperative management of these patients, thus affecting their postoperative outcome. It has been mentioned that as many anastomoses as possible should be created in order to obtain the best result in this procedure (Huang et al. 1985). Usually, anastomosis sites were mostly selected in the medial side of the lower extremity (Fig. 4.22). Moore et al. (2010) described a simple method to locate the great saphenous vein in the medial side of the knee region as the superficial lymph vessels converged towards and accompanied the vein that passes anterior to the medial malleolus and posterior, approximately a four fingerbreadth, to the patella. Images from this book provide a lymphatic roadmap for surgeons when searching for sites intended for potential lymphaticovenous anastomoses in the lower extremity where lymph vessels are situated close to the veins: (1) the dorsal foot, rich lymphatic vessels are present in the same plane as the dorsal metatarsal veins; (2) the medial side of the lower extremity, abundant lymph vessels travel with or cross the great saphenous vein and its branches in the anterior tibial region adjacent to the medial malleolus, the medial leg, knee and thigh; and (3) the posterior side of the leg, one or two large lymph vessels always accompany the small saphenous vein. Therefore, the larger and stronger lymph vessels next to the small saphenous vein could be considered for lymphaticovenous anastomoses in obstruct lymphoedema patients.

Lymphatic grafting procedures for treating secondary lymphoedema have been reported (Baumeister and Siuda 1990). These procedures involve the harvest of a single or multiple lymphatic vessels from the ventromedial bundle (medial group in the thigh) in the contralateral thigh (healthy limb). The distal ends of these vessels from the donor were anastomosed to vessels in the affected limb through a subcutaneous tunnel above the pubic symphysis. Alternatively, the vessels were harvested as free grafts for transfer to the upper limb (Weiss et al. 2003). Results from this book have provided details of the lymphatic distribution in the thigh. If one or more vessels were harvested from the ventromedial bundle of the thigh, the remaining lymphatic vessels could probably still perform the required drainage function. Furthermore, the vessels were constant and easily located, travelling on both sides of the small saphenous vein in the same depth of tissue in the posterior aspect of the leg. This could act as an additional donor site for harvesting lymphatic graft tissue for treatment.

The lower extremity is a common donor site for flap harvesting, especially on the thigh. The details of the neurovascular supplies of these flaps have been well documented, but their lymphatic supply was not well understood (Taylor and Razaboni 1994; Mathes and Nahai 1997; Strauch and Yu 2006; Pan et al. 2009a, b). Information from this book provides identification of the afferent and efferent lymphatic pathways, the direction and quantitative distribution of lymph vessels within flaps in the

lower extremity to assist surgeons in designing flaps (lymphatic bridging flaps) for the treatment of lymphoedema patients (Gillies 1935; Thompson 1970; Tanaka et al. 1996; Salvin et al. 1997; Becker and Hidden 1988). For example, a flap harvested from the medial aspect of the thigh would contain rich vertical lymphatic vessels, whereas a flap from the lateral side of the thigh would contain fewer and obliquely oriented vessels. Finally, it is believed that these results have provided additional information regarding superficial lymphatic distribution to complete the entire neurovasculature (arteries, veins, lymphatics and nerves) of the superficial tissue in the lower extremity to complement previous studies.

Lymphatic fistula is a complication after vascular surgery in the lower extremity (Yuan et al. 2006; Liu et al. 2010; Twine et al. 2013). Several treatment options for lymphatic fistulas have been described but remain controversial. Detailed information of the neurovascular anatomy including the lymphatics in the lower extremity have been discussed previously, which may facilitate clinicians to preventing and assisting treatment of this disease.

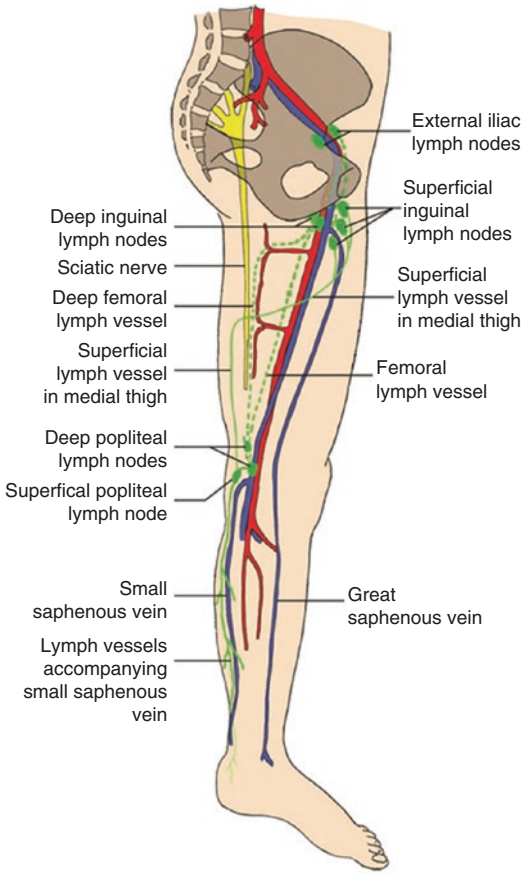

Fig. 4.21 Lymphatic pathways from the lateral heel to the inguinal region

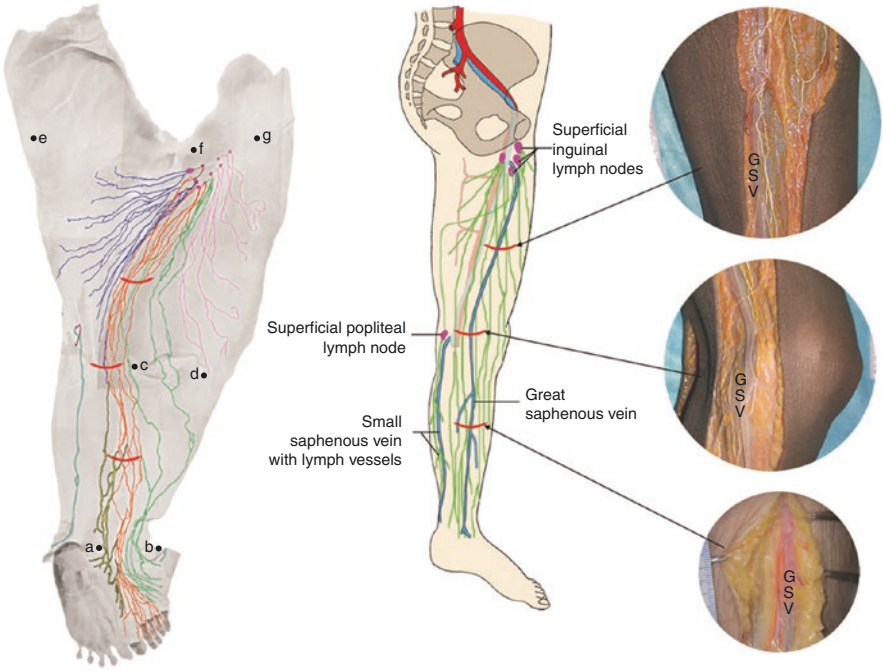

Fig. 4.22 The relationship of the superficial lymphatic vessels and veins in the lower extremity for selecting the possible site for lymphovenous anastomosis. (*a*) Medial malleolus; (*b*) lateral malleolus; (*c*) medial epicondyle; (*d*) lateral epicondyle; (*e*) ischial tuberosity; (*f*) pubic tubercle; (*g*) anterosuperior iliac spine. *Red lines* indicate incision of the anastomosis sites; *GSV* great saphenous vein

Chapter 5
Materials and Methods

Lymphatic vessels are difficult to be found in the embalmed cadavers during anatomical dissection as they have a transparent thin wall; however, if contrast media have been perfused, they become visible. In the early stages, there were only two major injection techniques for lymphatic studies in unembalmed cadavers, direct and indirect injections. In the former, mercury was utilized as an injectant for identifying lymphatic vessels, but it was abandoned due to its toxicity afterwards. In the latter, the mixture of Prussian blue, turpentine and ether was the injection media for the study, but satisfactory results were not always obtained. Other materials such as coloured dye, iodine or milk and so on were used for injection, which were described in many previous articles and will not get into detail here.

Details of materials and methods for obtaining results in this book are described in the following.

1 Materials

1.1 Specimens

The investigation was performed with appropriate institutional ethics approval. Acquired from deceased people who had donated their bodies, unembalmed (fresh) cadavers were separated to parts that were kept in a deep freezer. Each part of the cadaver was then ready for lymphatic study.

W.-R. Pan, *Atlas of Lymphatic Anatomy in the Head, Neck, Chest and Limbs*,
DOI 10.1007/978-981-10-3749-8_5

1.2 Materials for Injection

Hydrogen peroxide (6%) (Orion Laboratories Pty Ltd., Australia; Zhonglian Chemical Co., Ltd., Suzhou, China) or mixed with Indian ink (Encre de chine, Pebeo, France) or Prussian blue ink (Code 134010.318 Emb22278J, Le Géant des Beaux-Arts, Saverne Cédex, France) was applied for finding the lymphatic vessels in the tissues. The ratio was 20:1. Both inks did not leak from the vessels into the surrounding tissue if they were injected in lymphatic vessels. Lead oxide mixture was utilized as an injectant for revealing lymphatic vessels. It contained lead oxide (Pb_3O_4) (Ajax Chemicals P/L NSW Australia), milk powder (Heinz Ltd., Qingdao, China) and water.

Methods for mixture: Put 5 g of milk powder into a pestle and mortar with 3–5 drops of water and mix them well; add 3–4 ml of water to dilute it; add 15 g of lead oxide, mix well and then put in 15 ml of water; mix them very well for use (Fig. 5.1).

As lead oxide contains a low level of toxic material, it could be replaced by barium sulphate (Shanghai Silian Industry Co. Ltd., China) (Fig. 5.2).

Fig. 5.1 A lead oxide mixture

Fig. 5.2 A barium sulphate mixture

1.3 Instruments and Equipment

Instruments include general and microsurgical instruments, such as scalpels, scissors, forcipes, vascular clips, different sizes of needles, syringes and connecting tubes.

If the diameter of the lymph vessel was smaller than 0.3 mm, then a glass needle was used for injection. The glass needle is made of a micro glass tube (Micro Pipets: Fisher Scientific, Pittsburgh, PA, USA) pulled by a glass tube puller (Model PP-830: Narishige Co., Tokyo, Japan) (Fig. 5.3).

A micromanipulator (MN-153, Narishige Scientific Instrument Laboratory Tokyo, Japan) was used for holding and adjusting the needle during the injection (Fig. 5.4).

Surgical microscope (Zeiss, Nano Technology Systems Division, Oberkochen, Germany), microscope (Olympus BH2, Tokyo, Japan), radiological diagnostic machines and accessories (Model Diamond-150TH High-Frequency X-ray Generator, North American Imaging Inc., Camarillo, CA, USA; Fuji FCR IP Cassette: Fujifilm Corporation, Tokyo, Japan; Fuji Computed Radiography Processor: Fujifilm Corporation, Tokyo, Japan), computer (Optiplex 745, Dell, Australia), software (FCR Cr Console Lite, Fuji Photo Film Co., Ltd., Tokyo, Japan), digital camera and so on were utilized for obtaining images, data processing and analysis.

Fig. 5.3 Micro glass tubes and glass tube puller

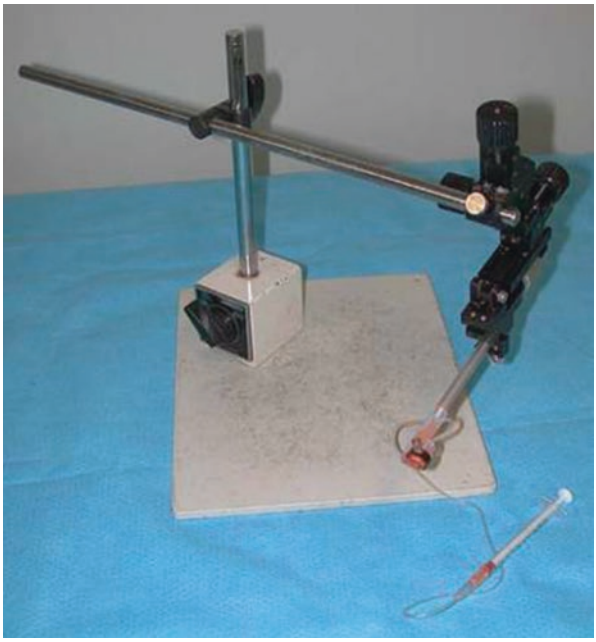

Fig. 5.4 A micromanipulator for holding the needle

2 Methods

Two steps were included in the technique for finding and perfusing lymphatic vessels. Then specimens were radiographed and photographed for final results. In some cases, a CT scan and histological study were included for acquiring additional information.

2.1 Finding the Lymphatic Vessel

In the head and neck region, a small amount of the 6% hydrogen peroxide and dye (Indian ink or Prussian blue ink) mixture was injected into the dermis and the subcutaneous tissue in the midline of the head. The superficial tissue of the head and neck including the galea, muscles of facial expression, platysma, deep fascia on the temporalis and masseter muscles was removed with a midline sagittal incision. The specimen was examined both macroscopically and microscopically, and collecting lymph vessels were detected in the subcutaneous tissue when viewed from the undersurface of the galea layer (Fig. 5.5). The mixture was also applied for finding lymph vessels around the nipple and in bilateral sides of the digits (Figs. 5.6, 5.7, and 5.8). As ink could taint the surrounding tissue to haze lymph vessel, a single solution of 6% hydrogen peroxide was applied for detection (Fig. 5.9a, b).

Lymphatic vessels in the superficial tissue of the head and face travelled radially towards lymph nodes in the neck. Collecting lymph vessel arose approximately 2 cm from the midline of the scalp where the initial injection commenced. The lymphatic dissection was performed on the galeal side (undersurface) of the scalp and on the skin side of the face (the canthi of eyelids, the nose and the corner of the mouth) and neck. In the auricle, the dissection commenced in the scaphoid fossa area and extended to the dorsal auricle from superior to inferior and then to the lobule.

Lymphatic vessels in the superficial tissue of the anterior chest and breasts ran radially towards lymph nodes in the axilla. The dissection process initiated from the parasternal and costal margins. For examining the internal thoracic lymph vessels, the dissection began beneath the parietal pleura of the infrasternal angle area in the inner surface of the anterior chest wall (Fig. 5.10).

In the exploration of lymphatic vessels in the mucosa and submucosa, a small amount of 6% hydrogen peroxide was smeared directly onto the mucosa. Excess bubbles were then gently rinsed off; lymphatic vessels were revealed in the mucosa and submucosa (Fig. 5.11a).

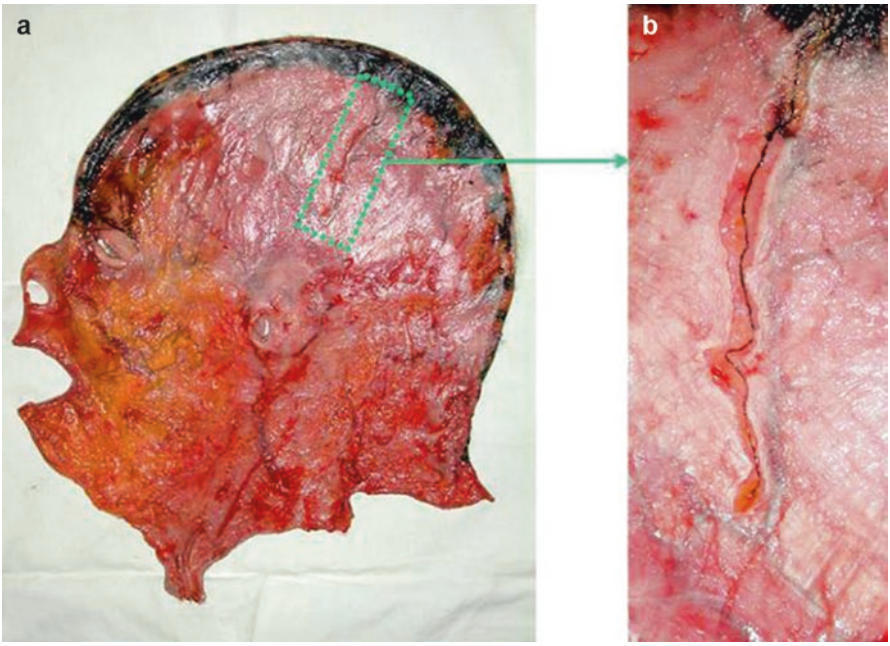

Fig. 5.5 Lymphatic vessel is filled by a mixture of hydrogen peroxide and ink in the scalp. (**a**) The collecting lymph vessel is visible from the undersurface of the galea (*green rectangle*). (**b**) An image magnified from the green-boxed area in (**a**) shows the lymph collecting vessel filled with the mixture

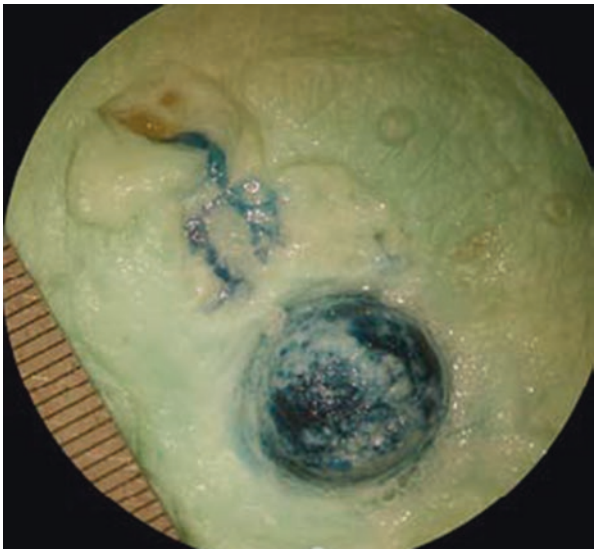

Fig. 5.6 Lymphatic vessels were detected in the subareolar area after the nipple was injected by a mixture of hydrogen peroxide and ink

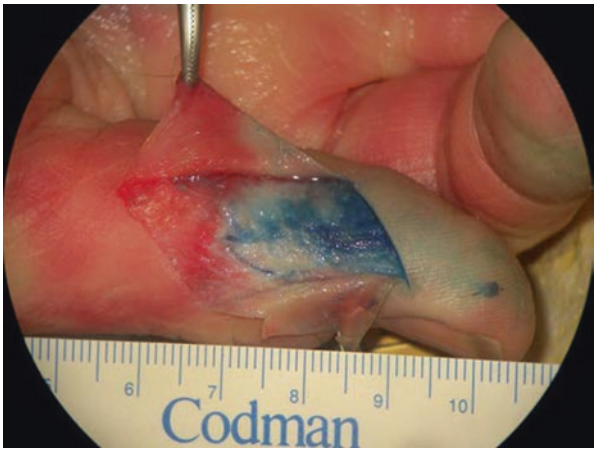

Fig. 5.7 A digital lymphatic vessel was detected in the lateral side of the right thumb after a mixture of hydrogen peroxide and *ink* was applied

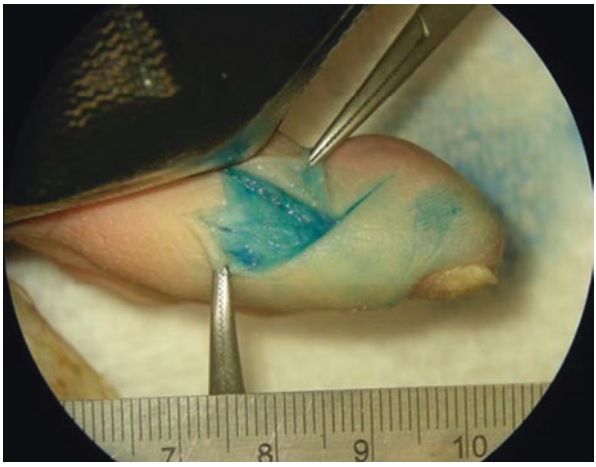

Fig. 5.8 Digital lymphatic vessels were detected in the medial side of the second right toe after a mixture of hydrogen peroxide and *ink* was applied

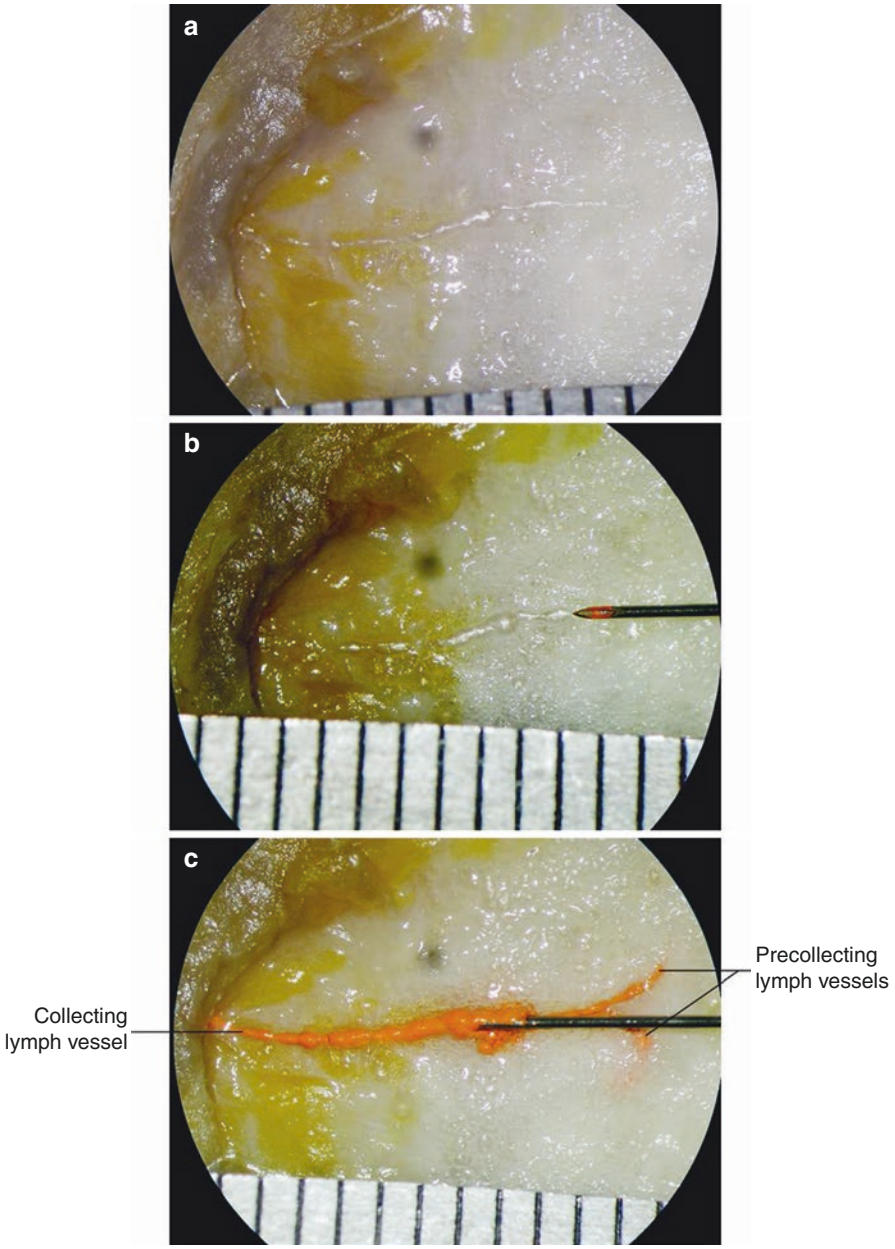

Fig. 5.9 Steps of the lymphatic injection in the subcutaneous tissue. (**a**) The inflated lymph vessels were found in the galea and the subcutaneous tissue. (**b**) A 30 gauge 1 in. needle was inserted into the vessel. (**c**) A lead oxide mixture was injected. The lymph collecting vessel is lying in the *yellowish* subcutaneous tissue, and the precollecting vessels filled with backflow are lying in the *whitish* galeal layer

Fig. 5.10 Lymphatic vessel in the adipose tissue near to the left costal margin of the inner surface of the anterior chest wall

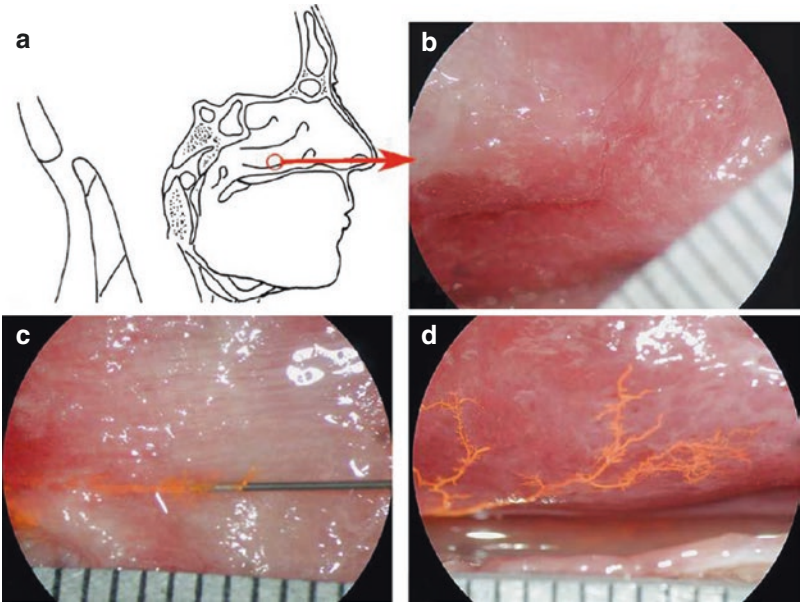

Fig. 5.11 (**a**) Sketch of the inner view of the head and neck. (**b**) Lymphatic vessels have been dilated after using hydrogen peroxide. (**c**) A 30 gauge 1 in. needle was inserted in the vessel, and a lead oxide mixture was beginning to inject. (**d**) Lymphatic vessels have been filled with a lead oxide mixture

2.2 *Lymphatic Injection*

Under a surgical microscope, the inflated lymph vessels were found (Figs. 5.5, 5.6, 5.7, 5.8, 5.9, 5.10, and 5.11). A suitable vessel was selected, a 30 gauge 1 in. needle, and connected to an extension tube linked to a 1 ml syringe that was fixed on a micromanipulator (Fig. 5.4); it was then inserted carefully into the lumen of the vessel. A suspension of radio-opaque mixture was slowly and gently infused by hand into the vessel (Figs. 5.9b, c and 5.11c). Any resistance from the syringe or leakage at the injection point indicated the end of the injection. Following the injection, the specimen was radiographed, and that acted as a guide for the next injection. If the vessel was not filled completely, the procedure was repeated at the distal point of the injection as many times as necessary until the injectant reached the lymph node and/or the edge of the specimen (Fig. 5.12). If the diameter of the lymph vessel was smaller than 0.3 mm, a glass needle was used for injection (Fig. 5.13).

Each specimen contained many lymph vessels, thus requiring numerous injections that required more than 20 days to be completed. In some larger specimens, it needed 6–8 weeks to be accomplished. Therefore, areas not under study were cooled with ice packs that were changed every 3 h to delay putrefaction.

During the dissection, a digital camera under a surgical microscope was used to capture fundamental views. After the completion of the injection process, each specimen was radiographed and photographed macroscopically and microscopically again for the final results (Fig. 5.12).

Fig. 5.12 The superficial lymphatic distribution of the head and neck after a lead oxide mixture injection

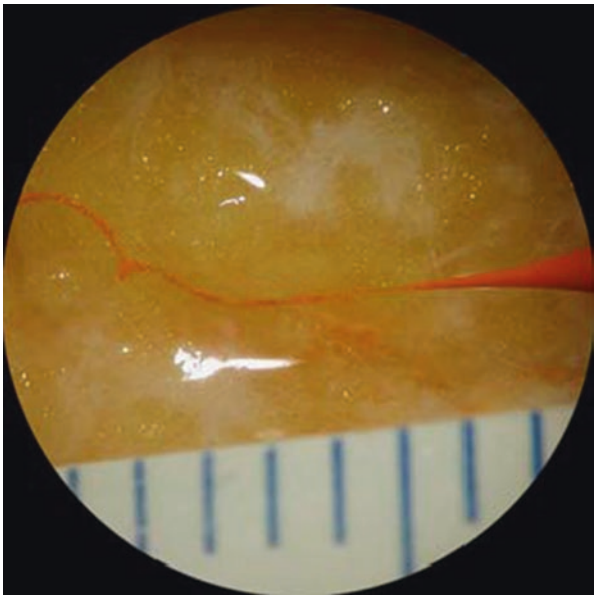

Fig. 5.13 A glass needle was used for injection

2.3 Auxiliary Examinations

(a) *CT lymphangiography and cross-section examination*

A larger specimen was studied by a series of cross-sections and CT scans to complete three-dimensional images of the lymphatic anatomy (Figs. 3.67, 3.68, 3.70–3.73).

(b) *Histological examination*

It is a necessary means for understanding the detailed structure of lymph vessels and nodes.

(c) *Data processing and analysis*

The photographs and radiographs were transferred into a computer for analysis. Each lymphatic vessel was traced and colour coded to match their related lymph nodes for mapping territories of the lymphatic distribution on each specimen (Fig. 5.14).

Fig. 5.14 The lymphatic distribution of the superficial tissue of the head and neck

References

Aglianò M, Sacchi G, Weber E, et al. Vasa vasorum of superficial collecting lymphatics of human thigh. Lymphology. 1997;30:116–21.

Alex JC, Krag DN. Gamma-probe guided localization of lymph nodes. Surg. Oncol. 1993;2:137–43.

Aselli G. Lactibus sine lacteis venis. Milan: Italy; 1627.

Aveta A, Tenna S, Segreto F, et al. Acute lymphedema of the eyelid after major reconstruction of the medial cantus: the role of the lymphatic drsinsge pattern. Plast Reconstr Surg. 2011;128(4):370e–2e.

Aydin MA, Okudan B, Aydin ZD, Ozbek FM, Nasir S. Lymphoscintigraphic drainage patterns of the auricle in healthy subjects. Head Neck. 2005;27:893–900.

Baker TJ, Gordon HL, Molienko P. Rhytidectomy. Plast Reconstr Surg. 1977;59:24–30.

Ballantyne AJ. Significance of retropharyngeal nodes in cancer of the head and neck. Am J Surg 1964;108:500–4.

Bartel B. Das Lymphgefasssystem. In: Bardeleben KV, editor. Handbuch der Anatomie des Menschen. Jene: Gustav Fischer; 1909. p. 1–250.

Batsakis J, Sneige N. Parapharyngeal and retropharyngeal space disease. Ann Otol Rhinol Laryngol 1989;98:320–1.

Baumeister R, Siuda S. Treatment of lymphedemas by microsurgical lymphatic grafting: what is proved? Plast Reconstr Surg. 1990;85:64–74.

Becker C, Hidden G. Transfer of free lymphatic flaps: microsurgery and anatomical study (in French). J Mal Vasc. 1988;13:119–22.

Bhattacharyya N. Cancer of the nasal cavity–survival and factors influencing prognosis. Arch Otolaryngol Head Neck Surg. 2002;128:1079–83.

Braithwaite LR. The flow of lymph from the ileocaecal angle, and its possible bearing on the cause of duodenal and gastic ulcer. Br J Surg. 1923;11:7–26.

Buncke GM, Buncke HJ, Lee CK. Great toe-to-thumb microvascular transplantation after traumatic amputation. Hand Clin. 2007;23(1):105–15.

Byers RM, Smith JL, Russell N, Rosenberg V. Malignant melanoma of the external ear. Review of 102 cases. Am J Surg. 1980;140(4):518–21.

Cao YL, Vacanti P, Paige KT, Upton J, et al. Transplantation of chondrocytes utilizing a polymer-cell construct to produce tissue-engineered cartilage in the shape of a human ear. Plast Reconstr Surg. 1997;100(2):297–302.

Cascinelli N, Morabito A, Santinami M, et al. Immediate or delayed dissection of regional nodes in patients with melanoma of the trunk: a randomised trial. WHO Melanoma Programme. Lancet. 1998;351:793–6.

Chalasani R, McNab A. Chronic lymphedema of the eyelid: case series. Orbit. 2010;29:222–6.

W.-R. Pan, *Atlas of Lymphatic Anatomy in the Head, Neck, Chest and Limbs*,
DOI 10.1007/978-981-10-3749-8

Cheng GL, Pan HD. Replantation and reconstruction of fingers. Beijing: People's Health Publishing House. 1997. p. 1–3, 118–27, 227–8.
Cole DJ, Mackay GJ, Walker BF, et al. Melanoma of the external ear. J Surg Oncol. 1992;50(2):110–4.
Cole MD, Jakowatz J, Evans GR. Evaluation of nodal patterns for melanoma of the ear. Plast Reconstr Surg. 2003;112(1):50–6.
Cooper AP. The anatomy of the breast. London: Longman, Orme, Green, Brown and Longmans; 1840.
Cowdry EVA. textbook of histology. Philadelphia: Lea and Febiger; 1950.
Cruikshank W. The anatomy of the absorbing vessels of the human body. London: G. Nicol; 1786.
Davidsson A, Hellquist HB, Villman K, et al. Malignant melanoma of the ear. J Laryngol Otol. 1993;107(9):798–802.
De Cicco C, Trifiro G, Calabrese L, et al. Lymphatic mapping to tailor selective lymphadenectomy in cN0 tongue carcinoma: beyond the sentinel node concept. Eur J Nucl Med Mol Imaging. 2006;33(8):900–5.
de Gier HH, Balm AJ, Bruning PF, et al. Systematic approach to treatment of chylous leakage after neck dissection. Head Neck. 1996;18(4):347–51.
Delamère G, Poirier P, Cunéo B. The lymphatics-general anatomy of the lymphatic system. London: Constable & Company Ltd; 1903.
Delamère G, Poirier P, Cunéo B. The lymphatics (English translated by Leaf CH). London: Constable & Company Ltd; 1913. pp. 283–6.
Demirtas Y, Ozturk N, Yapici O, et al. Supermicrosurgical lymphaticovenular anastomosis and lymphaticovenous implantation for treatment of unilateral lower extremity lymphedema. Microsurgery. 2009;29(8):609–18.
Denz F. Age changes in lymph nodes. J Pathol Bacteriol. 1947;59:575–91.
Drinker CK, Yoffey JM. Lymphatics, lymph and lympoid tissue. Cambridge: Harvard University Press; 1941.
Droulias C, Whitehurst JO. The lymphatics of the tongue in relation to cancer. Am Surg. 1976;42(9):670–4.
Fleissig A, Fallowfield LJ, Langridge CI, et al. Post-operative arm morbidity and quality of life: results of the ALMANAC randomised trial comparing sentinel node biopsy with standard axillary treatment in the management of patients with early breast cancer. Breast Cancer Res Treat. 2006;95:279–93.
Földi M, Földi E, Kubik SE. Textbook of lymphology. San Francisco: Urban & Fischer; 2003.
Forkert PG, Thliveris J, Bertalanffy F. Structure of sinuses in the human lymph node. Cell Tissue Res. 1977;183:115–30.
Fujita T, Miyoshi M, Murakami T. Scanning electron microscope observation of the dog mesenteric lymph node. Zellforsch. 1972;133:147–62.
Furuta WJ. An experimental study of lymph node regeneration in rabbits. Am J Anat 1947;80:437.
Gillies HD. Treatment of lymphoedema by plastic operation. Br Med J. 1935;1:96.
Gloviczki P, Fisher J, Holloer LH, et al. Microsurgical lymphovenous anastomosis for treatment of lymphedema: a critical review. J Vasc Surg. 1988;7(5):647–52.
Gould EA, Winship T, Philbin PH, et al. Observation on a "sentinel node" in cancer of the parotid. Cancer. 1960;13:77–8.
Gulland G. The development of lymphatic glands. J Pathol Bacteriol. 1894;1:447–85.
Guy CL, Converse JM, Morello DC. Esthetic surgery for the aging face. In: Converse JM, McCarthy JG, Littler JW, editors. Reconstructive plastic surgery. 2nd ed. Philadelphia: WB Saunders Company; 1977.
Guyton A, Hall J. Textbook of medical physiology. 11th ed. Philadelphia: Elsevier Saunders; 2006.
Haagensen CD, Feind CR, Herter FP, et al. The lymphatics in cancer. Philadelphia: WB Saunders; 1972.
Hall BJ, Hall JC. Skin infections: diagnosis and treatment. New York: Cambridge University Press; 2009.

Hasegawa Y, Matsuura H. Retropharyngeal node dissection in cancer of the oropharynx and hypopharynx. Head Neck 1994;16:173–80.
Hou SJ, Cheng GL, Fang GR, Wang ZJ, Zhang YX, Zhang YF, Teng GD. Etiology and management of vascular compromise in toe-to-hand transfer (an analysis of 164 cases). Chinese J Microsurg, 2005;28(2):130–2.
Houseman ND, Taylor GI, Pan WR. The angiosomes of the head and neck: anatomic study and clinical applications. Plast Reconstr Surg. 2000;105:2287–313.
Huang SF, Liao CT, Kan CR, Chen IH. Primary mucosal melanoma of the nasal cavity and paranasal sinuses— 12 years of experience. J Otolaryngol. 2007;36:124–9.
Hudack S, McMaster PD. The lymphatic participation in human cutaneous phenomena. J Exp Med. 1933;57:751.
Huang GK, Hu RQ, Liu ZZ, et al. Microlymphaticovenous anastomosis in the treatment of lower limb obstructive lymphedema: analysis of 91 cases. Plast Reconstr Surg. 1985;76:671–85.
Jamieson JK, Dobson JF. The lymphatics of the tongue: with particular reference to the removal of lymphatic glands in cancer of the tongue. Br J Surg. 1920;8(29):80–7.
Junqueira L, Carneiro J. Basic histology-text & atlas. 10th ed. New York: Lange Medical Books McGraw-Hill; 2003.
Kambhampati S, Rockson S. Lymphedema risk factors in breast cancer. In: Neligan PC, Masia J, Piller NB, editors. Lymphedema: complete medical and surgical management; 2015. p. 255–62.
Klapper SR, Patrinely JR. Management of cosmetic eyelid surgery complications. Semin Plast Surg. 2007;21(1):80–93.
Koshima I, Nanba Y, Tsutsui T, et al. Long-term follow-up after lymphaticovenular anastomosis for lymphedema in the leg. J Reconstr Microsurg. 2003;19(4):209–15.
Krag DN. Minimal access surgery for staging regional lymph nodes: the sentinel-node concept. Curr Probl Surg. 1998;35:951–1016.
Krstić R. Human microscopic anatomy. Berlin: Springer; 1991.
Kubik S, Manestar M. Topographic relationship of the ventromedial lymphatic bundle and the superficial inguinal nodes to the subcutaneous veins. Clin Anat. 1995;8(1):25–8.
Langer I, Guller U, Berclaz G, et al. Morbidity of sentinel lymph node biopsy (SLN) alone versus SLN and completion axillary lymph node dissection after breast cancer surgery: a prospective Swiss multicenter study on 659 patients. Ann Surg. 2007;245:452–61.
Lin CH, Ali R, Chen SC, et al. Vascularized groin lymph node transfer using the wrist as a recipient site for management of postmastectomy upper extremity lymphedema. Plast Reconstr Surg. 2009;123(4):1265–75.
Liu D, Fang HL, Liu H. Analysis and review of literature to lymphatic fistula in groin incision after great saphenous vein high ligation and stripping. Chin J Bases Clin Gener Surg. 2010;17(12):1312–3.
Liu NF. Lymphedema: diagnosis and treatment. Beijing: Science Press; 2013. p. 142–8.
Lord RSA. The white veins: conceptual difficulties in the history of lymphatics. Med Hist. 1967;12:174–84.
Lovett M, Lee K, Edwards A, et al. Vascularization strategies for tissue engineering. Tissue Eng Part B Rev. 2009;15(3):353–70.
Lucci A, McCall LM, Beitsch PD, et al. Surgical complications associated with sentinel lymph node dissection (SLND) plus axillary lymph node dissection compared with SLND alone in the American College of Surgeons Oncology Group Trial Z0011. J Clin Oncol. 2007;25:3657–63.
Ludwig V. Über Kurzschlußwege der Lymphbahnen und ihre Beziehungen zur lymphogenen Krebsmetastasierung. Pathol Microbiol. 1962;25:329–34.
Lutz BS, Wei FC. Basic principles on toe-to-hand transplantation. Chang Gung Med J. 2002;25(9):568–76.
Male D, Brostoff J, Roth DB, et al. Immunology. 7th ed. Philadelphia: Mosby Elsevier; 2006.
Málek P, Kolc J, Belán A. Lymphography of the deep lymphatic system of the thigh. Acta Radiol. 1959;51(6):422–8.

Mannoor MS, Jiang Z, James T, et al. 3D printed bionic ears. Nano Lett. 2013;13(6):2634–9.
Martin JM, Porceddu S, Weih L, Corry J, Peters LJ. Outcomes in sinonasal mucosal melanoma. ANZ J Surg. 2004;74:838–42.
Martini L, Brandani P, Chiarugi C, et al. First recurrence analysis of 840 cutaneous melanomas: a proposal for a follow-up schedule. Tumori. 1994;80:188–97.
Mascagni P. Vas lymphaticorum corporis humani historia et ichnographia. Sienne: P. Carli; 1787.
Mathes SJ, Nahai F. Reconstructive surgery: principles, anatomy & technique. New York: Churchill Livingstone, Quality Medical Publishing Inc; 1997.
Mazeron JJ, Otmezguine Y, Huart J, et al. Conservative treatment of breast cancer: Results of management of axillary lymph node area in 3353 patients. Lancet. 1985;1:1387.
Mironov V, Boland T, Trusk T, et al. Organ printing: computer-aided jet-based 3D tissue engineering. Trends Biotechnol. 2003;21(4):157–61.
Mondin V, Rinaldo A, Shaha AR, et al. Malignant melanoma of the auricle. Acta Otolaryngol. 2005;125(11):1140–4.
Moore K, Persaud T. The developing human-clinically oriented embryology. 6th ed. Philadelphia: WB Saunders; 1998.
Morrison WA, McCombe D. Digital replantation. Hand Clin. 2007;23(1):1–12.
Moore KL. Clinically oriented anatomy, 3rd ed. Williams & Wilkins, Baltimore, 1992.
Moore KL, Dalley AF, Agur AM. Clinically oriented anatomy, 6rd ed. Williams & Wilkins, Baltimore, 2010.
Morrison WA, O'Brien BM, MacLeod AM. Evaluation of digital replantation–a review of 100 cases. Orthop Clin North Am. 1977;8(2):295–308.
Morton DL, Wen DR, Wong JH, et al. Technical details of intraoperative lymphatic mapping for early stage melanoma. Arch Surg. 1992;127:392–9.
Narushima M, Mihara M, Yamamoto Y, Iida T, Koshima I, Mundinger GS. The intravascular stenting method for treatment of extremity lymphedema with multiconfiguration lymphaticovenous anastomoses. Plast Reconstr Surg. 2010;125(3):935–43.
O'Brien BM, Mellow CG, Khazanchi RK, et al. Long-Term results after microlymphaticovenous anastomoses for the treatment of obstructive lymphedema. Plast Reconstr Surg. 1990;85(4):562–72.
Okumura K, Fujimoto Y, Hasegawa Y, Matsuura H, Nakayama B, Komura T, et al. Retropharyngeal node metastasis in cancer of the oropharynx and hypopharynx: analysis of retropharyngeal node dissection regarding preoperative radiographic diagnosis. Nihon Jibiinkoka Gakkai Kaiho. 1998;101(5):573–7.
Ozeki S, Tashiro H, Okamoto M, et al. Metastasis to the lingual lymph node in carcinoma of the tongue. J Maxillofac Surg. 1985;13(6):277–81.
Pan W-R, le Roux CM, Briggs CA. Reply: acute lymphedema of the eyelid after major reconstruction of the medial cantus: the role of the lymphatic drsinsge pattern. Plast Reconstr Surg. 2011a;128(4):372e.
Pan W-R, le Roux CM, Levy SM. Alternative lymphatic drainage routes from the lateral heel to the inguinal lymph nodes: anatomic study and clinical implicationsans. ANZ J Surg. 2010a;81(6):431–5.
Pan W-R, le Roux CM, Levy SM, et al. Lymphatic drainage of the external ear. Head Neck. 2011b;33(1):60–4.
Pan W-R, le Roux CM, Levy SM, et al. Lymphatic drainage of the tongue and the soft palate: anatomic study and clinical implications. Eur J Plast Surg. 2010b;33(5):251–7.
Pan W-R, le Roux CM, Levy SM, et al. The morphology of the human lymphatic vessels in the head and neck. Clin Anat. 2010c;23(6):654–61.
Pan W-R, Rozen WR, Stella D, et al. A three-dimensional analysis of the lymphatics of a bilateral breast specimen: a human cadaveric study. Clin Breast Cancer. 2009a;9(2):86–91.
Pan W-R, Suami H, Corlett RJ, et al. Lymphatic drainage of the nasal fossae and nasopharynx: preliminary anatomical and radiological study with clinical implications. Head Neck. 2009b;31(1):52–7.
Pan W-R, Suami H, Taylor GI. Senile changes in human lymph nodes. Lymphat Res Biol. 2008a;6(2):77–83.

Pan W-R, Suami H, Taylor GI. The superficial lymphatic drainage of the head and neck: an anatomical study and clinical implication. Plast Reconstr Surg. 2008b;121(5):1614–24.
Pan W-R, Wang D-G, Levy SM, et al. Superficial lymphatic drainage of the lower extremity: anatomic study and clinical implications. Plast Reconstr Surg. 2013;132(3):696–707.
Pizza G, Vizza D, De Vinci C, Vich I, Pascuchi JM, Busutti L, Bergami T. Intra-lymphatic administration of interleukin-2 (IL-2) in cancer patients: a pilot study. Lymphokine Res. 1988;7(1):45–8.
Ravin AG, Pickett N, Johnson JL, et al. Melanoma of the ear: treatment and survival probabilities based on 199 patients. Ann Plast Surg. 2006;57(1):70–6.
Reynolds HM, Dunbar PR, Uren RF, Blackett SA, Thompson JF, Smith NP. Three-dimensional visualisation of lymphatic drainage patterns in patients with cutaneous melanoma. Lancet Oncol. 2007;8(9):806–12.
Robbins KT, Clayman G, Levine PA, Medina J, Sessions R, Shaha A, et al. Neck dissection classification update: revisions proposed by the American Head and Neck Society and the American Academy of Otolaryngology-Head and Neck Surgery. Arch Otolaryngol Head Neck Surg. 2002;128(7):751–8.
Roitt I, Brostoff J, Male D. Immunology. 6th ed. Oxford: Alden Group; 2003. p. 7–12.
Rollon A, Salazar C, Mayorga F, et al. Severe cervical chyle fistula after radical neck dissection. Int J Oral Maxilofac Stag. 1996;25(5):363–5.
Rouvière H. Anatomy of the human lymphatic system. Edwards Brothers: Michigan; 1938.
Rubin E, Gorstein F, Rubin R, et al. Rubin's pathology-clinicopathologic foundations of medicine. 4th ed. Philadelphia: Lippincott Williams & Wilkins; 2005.
Ruysch F. Dilucidatio Valvularum in Vasis Lymphaticis et Lacteis. The Hague: Netherlands; 1665.
Saito H, Sato T, Yamashita Y, Amagasa T. Topographical analysis of lymphatic pathways from the meso- and hypopharynx based on minute cadaveric dissections: possible application to neck dissection in pharyngeal cancer surgery. Surg Radiol Anat 2002;24:38–49.
Salvin SA, Upton J, Kaplan WD, Van den Abbeele AD. An investigation of lymphatic function following free-tissue transfer. Plast Reconstr Surg. 1997;99(3):730–43.
Sappey PC. Anatomie, Physiologie, Pathologie des vaisseaux lymphatiques. Paris: Adrien Delahaye; 1874.
Sebastin SJ, Chung KC. A systemic review of the outcomes of replantation of distal digital amputation. Plast Reconstr Surg. 2011;128(3):723–37.
Shayan R, Achen MG, Stacker SA. Lymphatic vessels in cancer metastasis: bridging the gaps. Carcinogenesis. 2006;27(9):1729–38.
Standring S. Gray's anatomy. Edinburgh: Elsevier Churchill Livingstone; 2005.
Strauch B, Yu H-L. Atlas of microvascular surgery: anatomy and operative approaches. 2nd ed. New York: ThiemeMedical Publishers Inc; 2006.
Strigel G. Lymphangiomas and hemangiomas. In: Ashcraft KW, Holder TM, editors. Pediatric surgery. 2nd ed. Philadelphia: Saunders; 1996. p. 802–22.
Suami H, Chang DW. Overview of surgical treatments for breast cancer-related lymphedema. Plast Reconstr Surg. 2010;126(6):1853–63.
Suami H, Pan W-R, Mann GB, et al. The lymphatic anatomy of the breast and its implications for sentinel lymph node biopsy: a human cadaver study. Ann Surg Oncol. 2008;15(3):863–71.
Suami H, Taylor GI, Pan WR. A new radiofraohic cadaver injection technique for investigating the lymphatic system. Plast Reconstr Surg. 2005a;115(7):2008–13.
Suami H, Taylor GI, Pan WR. The lymphatic territories of the upper limb: anatomical study and clinical implications. Plast Reconstr Surg. 2007;119(6):1813–22.
Tanaka Y, Tajima S, Imai K, Tsujiguchi K, Ueda K, Yabu K. Experience of a new surgical procedure for the treatment of unilateral obstructive lymphedema of the lower extremity: adipolymphatico venous transfer. Microsurgery. 1996;17(4):209–16.
Taylor GI, Pan W-R. The angiosome concept and tissue transfer. St Louis/Missouri: QMP; 2014.
Taylor GI, Razaboni RM. Michel salmon anatomic studies: arteries of the muscles of the extremities and the trunk: arterial anastomotic pathways of the extremities. 1st ed. St. Louis: Quality Medical Publishinhg; 1994.

Thompson N. Buried dermal flap operation for chronic lymphoedema of the extremities: ten-year survey of results on 79 cases. Plast Reconstr Surg. 1970;45(6):541–8.
Thompson JF, McCarthy WH, Bosch CM, et al. Sentinel lymph node status as an indicator of the presence of metastatic melanoma in regional lymph nodes. Melanoma Res. 1995;5:255–60.
Thompson JF, Morton DL, Kroon BBR. Textbook of melanoma. London: Martin Dunitz; 2004.
Thompson JF, Uren RF. Lymphatic mapping in management of patients with primary cutaneous melanoma. Lancet Oncol. 2005;6:877–85.
Thompson JF, Uren RF, Shaw HM, et al. Location of sentinel lymph nodes in patients with cutaneous melanoma: new insights into lymphatic anatomy. J Am Coll Surg. 1999;189:195–204.
Twine CP, Lane IF, Williams IM. Management of lymphatic fistulas after arterial reconstruction in the groin. Ann Vasc Surg. 2013;27(8):1207–15.
Uren RF, Howman-Giles RB, Thompson JF, et al. Interval nodes: the forgotten sentinel nodes in patients with melanoma. Arch Surg. 2000a;135:1168–72.
Uren RF, Howman-Giles R, Chung D, Thompson JF. Nuclear medicine aspects of melanoma and breast lymphatic mapping. Semin Oncol. 2004;31(3):338–48.
Uren RF, Thompson JF, Howman-Giles RB. Lymphatic drainage of the skin and breast. Sydney, Australia: Harwood Academic Publishers; 1999.
Uren RF, Thompson JF, Howman-Giles RB. Sentinel nodes. Interval nodes, lymphatic lakes, and accurate sentinel node identification. Clin Nucl Med. 2000b;25:234–6.
van den Brekel MW, Castelijns JA, Snow GB. The size of lymph nodes in the neck on sonograms as a radiologic criterion for metastasis: how reliable is it? AJNR. 1998;19:695–700.
Viamonte MJ, Rüttimann A. Atlas of lymphography. New York: Thieme-Stuttgart; 1980.
Wallace S, Jackson L, Dodd GD, et al. Lymphatic dynamics in certain abnormal states. Am J Roentgenol Radium Ther Nucl Med. 1964;91:1187–206.
Wang SL, Guo ZM, Zhang Q, et al. Sentinel lymph node radiolocalization in squamous cell carcinoma of the oral tongue. Ai Zheng. 2007;26(5):533–6.
Ward NO, Acquarelli MJ. Malignant melanoma of the external ear. Cancer. 1967;21(2):226–3.
Watanabe H, Komiyama S, Soh N, Kudoh S. Metastases to the Rouviere nodes and headache. Auris Nasus Larynx. 1985;12:53–6.
Weiss M, Baumeister RG, Hahn K. Dynamic lymph flow imaging in patients with oedema of the lower limb for evaluation of the functional outcome after autologous lymph vessel transplantation: an 8-year follow-up study. Eur Nucl Med Mol Imaging. 2003;30(2):202–6.
Werner JA, Dunne AA, Myers JN. Functional anatomy of the lymphatic drainage system of the upper aerodigestive tract and its role in metastasis of squamous cell carcinoma. Head Neck. 2003;25(4):322–32.
Wey PD, De La Cruz C, Goydos JS, Choi ML, Borah GL. Sentinel lymph node mapping in melanoma of the ear. Ann Plast Surg. 1998;40(5):506–9.
Yang FC, Zhao JM, Yang Z, et al. Explorate the factors affecting the survival of replantation: analysis of 167 cases with 111 fingers. Guangxi Medi J. 2003;25(2):195–7.
Ying ZP. Cervical chylorrhea (review). Chin J ENT & HN Surg. 1997;4(5):315–7.
Young B, Heath JW. Wheater's functional histology: a text and colour atlas. 4th ed. Edinburgh: Churchill Livingstone; 2000.
Yuan B, Zhao S, Hunag CJ, Zhao Z, Zhu XY. Application and histological assess of endoscopic saphenous vein harvesting. Chin J Throac Cardiovasc Surg. 2006;22(2):99–101.
Zezula-Szpyra A, Gawrońska B, Skipor J. Vasa vasorum of blood and lymph vessels in the broad ligament of the sheep uterus analyzed by scanning electron microscopy. Rocz Akad Med Bialymst. 1997;42(Suppl 2):134–46.
Zhang QF, Jing CH, Miao JL, Lu XH, Yang S, Xu LB. Trans – Lymphatic infusion of immunochemical drugs in the treatment of lymphatic metastases. J Intervent Radio. 1998;7:25–8.
Zhang ZX. Lymphatic surgery, vol. 75. Beijing: People's Health Publishing House; 1984. p. 176–80.